

DISSERTATION

REACTION DEVELOPMENT AND MECHANISTIC INVESTIGATION OF RHODIUM-  
CATALYZED PYRIDINE SYNTHESIS VIA C-H ACTIVATION

Submitted by

Jamie M. Neely

Department of Chemistry

In partial fulfillment of the requirements

For the Degree of Doctor of Philosophy

Colorado State University

Fort Collins, Colorado

Fall 2014

Doctoral Committee:

Advisor: Tomislav Rovis

Andrew McNally

John D. Fisk

James R. Neilson

Julia M. Inamine

## ABSTRACT

### REACTION DEVELOPMENT AND MECHANISTIC INVESTIGATION OF RHODIUM– CATALYZED PYRIDINE SYNTHESIS VIA C–H ACTIVATION

Described herein are two complementary rhodium–catalyzed methods for the synthesis of substituted pyridines from unsaturated oxime derivatives and alkenes. In the first, formal [4+2] cycloaddition of *O*–pivaloyl  $\alpha,\beta$ –unsaturated oxime esters and activated terminal alkenes was discovered to proceed in high yields and with excellent selectivity for 6–substituted pyridine products. Mechanistic experiments were found to be consistent with a reversible C–H activation step and a C–N bond forming, N–O bond cleaving process en route to pyridine formation. Rhodium–catalyzed coupling using unactivated alkene substrates was shown to present important information regarding the influence of the alkene component on product distribution. In a second method, access to 5–substituted pyridine derivatives was achieved by decarboxylative annulation of  $\alpha,\beta$ –unsaturated oxime esters and  $\beta$ –substituted acrylic acid derivatives. In this case, carboxylic acids were found to serve as traceless activating groups for selective alkene incorporation. A wealth of mechanistic insight was gained by identification of and decomposition studies regarding catalytically relevant rhodium complexes.

## ACKNOWLEDGEMENT

I would like to sincerely thank Professor Tomislav Rovis for his guidance during my graduate career. Tom, your critical and incredibly insightful perception of chemistry along with your patience and enthusiasm as a mentor create a motivating environment for your students to reach their full potential as scientists. Thank you for giving me freedom to tackle problems my own way, for providing direction when I needed help finding my footing, and for always being on my team.

It has been a true privilege to work with all of the talented and hard-working individuals in the Rovis group, past and present. Thank you all for helpful discussions and for your friendship. I would especially like to thank Stephen Lathrop, Derek Dalton and Kevin Oberg for bringing me up to speed in the beginning and their advice throughout the years. Todd and Oz, it was a pleasure to navigate graduate school together with you two. Darrin, thank you for reminding me to not take things too seriously. Thank you Nick, for your consistent support and comic relief. Tiffany, thank you for sharing your intuition and opinions about chemistry and for keeping me entertained. Clairebear, I cannot explain how grateful I am to have met you. Thank you for being by my side during this tumultuous experience and for carrying me through it when I was unable to do it alone.

Finally, I would like to thank my family for their unconditional love and support during these and all of my years. You all keep me grounded and help me remember what is really important in life. Thank you Daddy, for keeping me calm and rational; Mamabear, for always lifting me up; Tommy, for giving me perspective; Jason, for truly understanding me; and Melissa, for reminding me to be myself. None of this would have been possible without you.

## TABLE OF CONTENTS

CHAPTER ONE: Rhodium(III)–Catalyzed Coupling of $\alpha,\beta$ –Unsaturated Oxime Esters and Alkenes: Selective Synthesis of 6–Substituted Pyridines.....	1
1.1 Introduction.....	1
1.1.1 Nitrogen Heterocycles in Medicinal Chemistry .....	1
1.1.2 Directed Transition Metal–Catalyzed C–H Activation.....	2
1.1.3 Pyridine Synthesis by Transition Metal–Catalyzed Formal [4+2] Cycloaddition.....	4
1.1.4 Rhodium–Catalyzed Coupling of 1–Azadiene Derivatives and Alkynes.....	5
1.1.5 Nitrogen–Directed C–H Functionalization with Alkenes.....	8
1.2 Results.....	9
1.2.1 Reaction Optimization .....	9
1.2.2 $\alpha,\beta$ –Unsaturated Oxime Ester Scope .....	14
1.2.3 Activated Alkene Scope.....	17
1.2.4 Mechanistic Studies .....	22
1.2.5 Discussion of Product Selectivity .....	27
1.2.6 Unexpected Selectivity with Secondary Alkyl Alkene Substrates .....	29
1.3 Conclusion .....	31
1.4 References.....	33
CHAPTER TWO: Rhodium(III)–Catalyzed Decarboxylative Coupling of $\alpha,\beta$ –Unsaturated Oxime Esters and Acrylic Acids: Selective Synthesis of 5–Substituted Pyridines .....	40
2.1 Introduction.....	40
2.1.1 Product Selectivity in Synthetic Methodology .....	40

2.1.2 Removable Directing Groups in Transition Metal–Catalyzed C–H Functionalization .....	41
2.1.3 Rhodium–Catalyzed Decarboxylative Coupling with $\beta$ –Substituted Acrylic Acids..	42
2.2 Results.....	44
2.2.1 Reaction Optimization .....	44
2.2.2 Substrate Scope.....	51
2.2.3 Mechanistic Studies .....	54
2.3 Conclusion .....	63
2.4 References.....	65
Appendix One .....	69
Appendix Two .....	143

## CHAPTER ONE

### Rhodium(III)–Catalyzed Coupling of $\alpha,\beta$ –Unsaturated Oxime Esters and Alkenes: Selective Synthesis of 6–Substituted Pyridines

#### 1.1 Introduction

##### 1.1.1 Nitrogen Heterocycles in Medicinal Chemistry

Nitrogen heterocycles are incredibly important scaffolds in medicinal chemistry. A recent study found 59% of United States FDA approved pharmaceutical drugs,<sup>1</sup> including many of the most lucrative (Figure 1.1),<sup>2</sup> contain a nitrogen heterocycle (*N*–heterocycle). In a general sense, the prevalence of these scaffolds may be attributed to advantages associated with both the nitrogen atom and the cyclic structure (Figure 1.2). Specifically, nitrogen polarizes the molecule and provides a lone pair for hydrogen bonding: two favorable properties in terms of aqueous solubility. As a result, an *N*–heterocyclic pharmaceutical drug likely exhibits better bioavailability than its carbocyclic counterpart.<sup>3</sup> On the other hand, the cyclic structure of an *N*–heterocycle restricts bond rotations, therefore eliminating potential conformers available to the

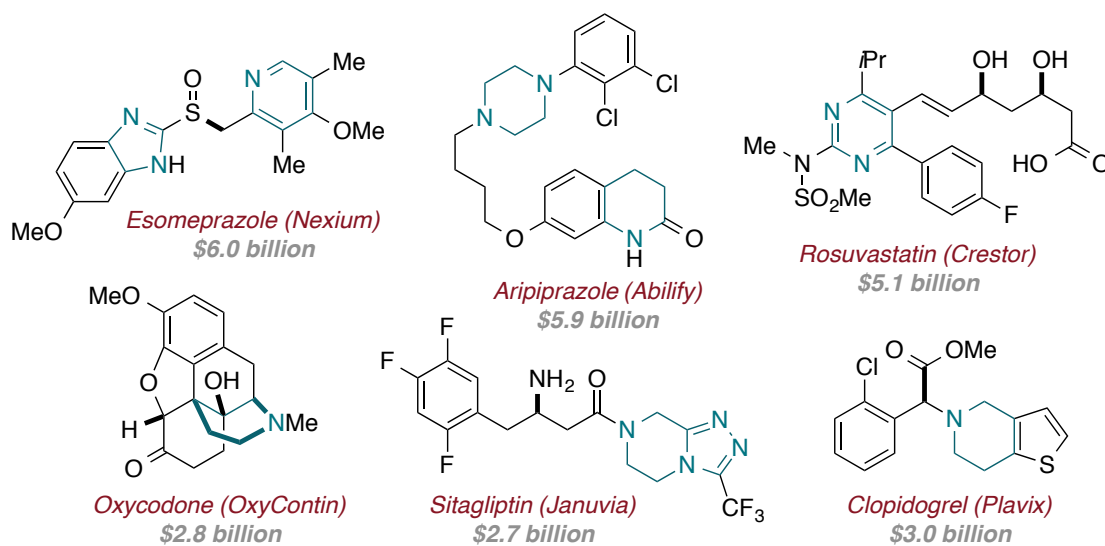


**Figure 1.1** Top *N*–heterocyclic pharmaceutical drugs by retail sales in 2012.

corresponding acyclic framework.

This difference is especially significant

as it relates to binding of a

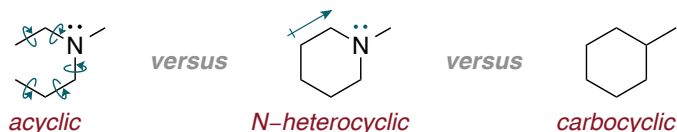


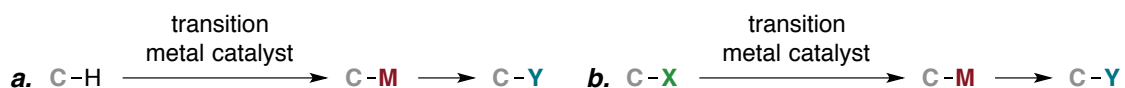
**Figure 1.2** Comparison of pharmaceutical scaffolds.

pharmaceutical drug to its biological target, an interaction that carries a large entropic cost due to conformational constraints in both components.<sup>3a</sup> For an *N*-heterocyclic drug, the conformational degrees of freedom lost upon binding are fewer compared to the acyclic analog, resulting in a more entropically favorable interaction.<sup>3b</sup>

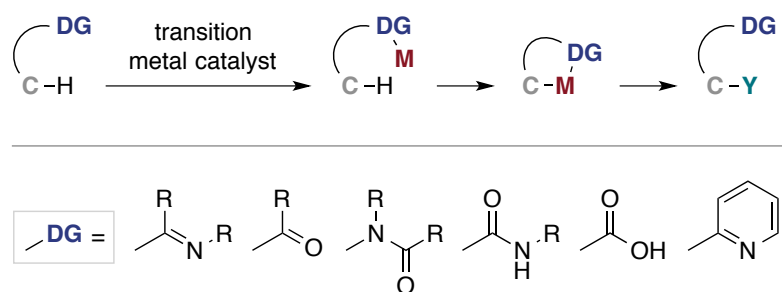
### 1.1.2 Directed Transition Metal–Catalyzed C–H Activation

Transition metal–catalyzed C–H bond activation represents a particularly powerful approach to constructing complex molecules from simple starting materials.<sup>4</sup> By the generally accepted definition,<sup>5</sup> the process is characterized by direct interaction of a transition metal catalyst and a carbon–hydrogen bond, most often resulting in formation of a carbon–metal bond (Scheme 1.1a). In this way, simple starting materials (C–H) are converted to reactive intermediates (C–M) that may undergo a variety of transformations to afford value–added products (C–Y). This reactivity, herein referred to as C–H functionalization, offers an attractive alternative to cross coupling strategies (Scheme 1.1b) by circumventing the need for activated substrates (C–X).

Carbon–hydrogen bonds are ubiquitous in organic compounds. Therefore, a significant challenge in transition metal–catalyzed C–H functionalization is site selectivity. Steric repulsion, hybridization of the carbon atom, and acidity of the C–H bond are all factors that may



**Scheme 1.1** Approaches to functionalized products by transition metal catalysis.



**Scheme 1.2** Directed C–H functionalization.

through the use of a directing group (DG, Scheme 1.2).<sup>7</sup> In this case, a coordinating group within the substrate engages the transition metal catalyst to bring a particular C–H bond in proximity to the metal center. As a result, directed C–H functionalization reactions typically exhibit predictable and reliable site selectivity. Common directing groups for transition metal–catalyzed C–H activation are given in Scheme 1.2.

In addition to imparting selectivity during the C–H activation step, a directing group may be incorporated to afford a cyclic product: a popular concept in *N*–heterocycle synthesis.<sup>8</sup> Nitrogen–containing substrates often serve as 4–atom components with the generic structure illustrated in Scheme 1.3. Here, nitrogen–directed C–H activation affords a 5–membered *aza*–metalacycle that may incorporate a 1– or 2–carbon component, ultimately resulting in annulation by C–C and C–N bond formation. These formal cycloaddition reactions are powerful strategies for *N*–heterocycle synthesis, as multiple bonds of the cyclic core are generated in a single step. A variety of *N*–heterocyclic scaffolds have been accessed by transition metal–catalyzed formal cycloaddition including phthalimides,<sup>9</sup> isoindolones,<sup>10</sup> isoquinolones,<sup>11</sup> dihydroisoquinolones,<sup>12</sup> pyridones,<sup>13</sup> isoquinolines,<sup>14</sup> and pyridines (*vide infra*).



**Scheme 1.3** *N*–heterocycle synthesis by formal cycloaddition.

contribute variable levels of selectivity in the C–H activation step.<sup>6</sup> Rather, one of the most effective ways to ensure selectivity in a C–H functionalization reaction is



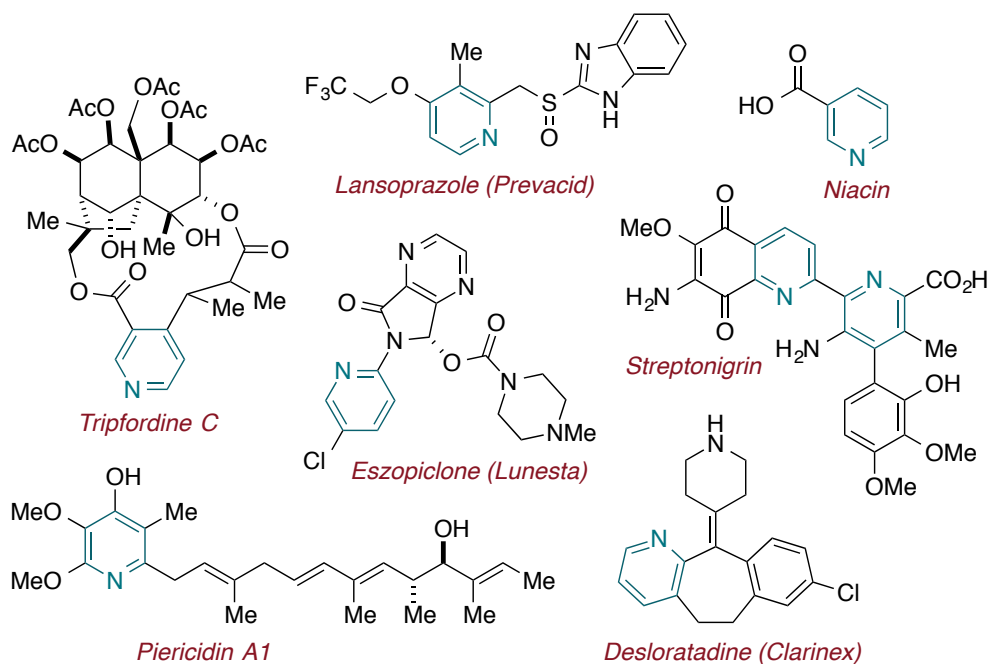
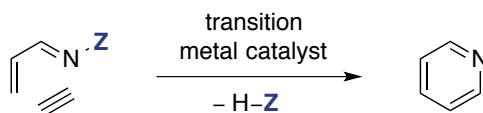


**Figure 1.3** Selected biologically active pyridines.

### 1.1.3 Pyridine Synthesis by Transition Metal–Catalyzed Formal [4+2] Cycloaddition

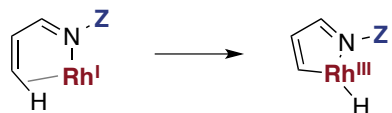
Substituted pyridines are an especially significant class of nitrogen heterocycles (Figure 1.3). A recent analysis of the ring systems encountered in all FDA approved pharmaceutical drugs determined the pyridine ring to be the most prevalent.<sup>15</sup> Indeed, the development of methods to access pyridine derivatives is a topic of continued interest for synthetic chemists, illustrated by the wealth of elegant examples that have recently contributed to this field.<sup>16,17</sup>

Using the general concept shown in Scheme 1.3, we can devise a



route to pyridine products from 1-azadiene derivatives and alkynes (Scheme 1.4). Several reports have taken advantage of such formal [4+2] cycloaddition approaches for the synthesis of substituted pyridines.<sup>18</sup> Transition metal catalysts in these examples are typically rhodium–based.<sup>19</sup> Pyridine formation may be accomplished using either rhodium(I) or rhodium(III) catalysis, a difference that is perhaps most

**a. Oxidative addition**



**b. Concerted metalation deprotonation**



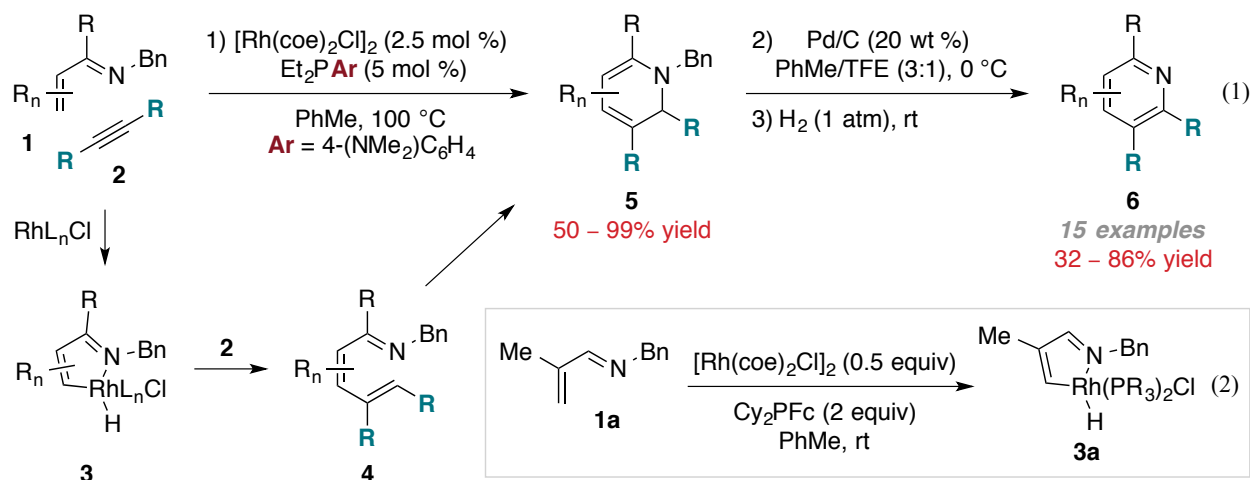
**Scheme 1.5** Mechanisms proposed for Rh-catalyzed C–H activation.

relevant to the mechanism of the C–H activation step (Scheme 1.5).<sup>20</sup> In

general, C–H activation is proposed to proceed by oxidative addition to the C–H bond in rhodium(I)-catalyzed methods (Scheme 1.5a), while rhodium(III) catalysts are thought to operate by base-assisted deprotonation or concerted metalation deprotonation<sup>21</sup> (Scheme 1.5b, shown for a carboxylate base).

#### 1.1.4 Rhodium-Catalyzed Coupling of 1-Azadiene Derivatives and Alkynes

In their longstanding contribution to the field of C–H functionalization,<sup>7b</sup> Bergman and Ellman have shown *N*-alkyl imines provide suitable directing groups for rhodium-catalyzed C–H bond activation.<sup>22</sup> They applied this insight to the synthesis of substituted pyridines by Rh(I)-catalyzed annulation of  $\alpha,\beta$ -unsaturated *N*-benzyl imines (*N*-benzyl 1-azadienes, **1**) and alkynes (**2**, eq 1, Scheme 1.6).<sup>23</sup> In this study, the authors found the stoichiometric reaction of imine **1a** leads to formation of rhodium hydride complex **3a** (eq 2), providing evidence for C–H activation by an oxidative addition mechanism. They propose pyridine formation proceeds by imine-directed C–H activation to access *aza*-metacycle **3**, followed by migratory insertion of the alkyne substrate (**2**) and reductive elimination to afford azatriene intermediate **4**. Subsequent  $6\pi$ -electrocyclization provides an *N*-benzyl dihydropyridine derivative **5** that is isolable by chromatography. Rather, oxidation and removal of the benzyl group may be conducted in the same flask to provide pyridine products (**6**) in a three step, one pot sequence.

**Bergman and Ellman:<sup>23</sup>****Scheme 1.6** Rh(I)-catalyzed coupling of  $\alpha,\beta$ -unsaturated *N*-benzyl imines and alkynes.

As illustrated in Scheme 1.4, pyridine formation by formal [4+2] cycloaddition of 1-azadienes and alkynes requires overall loss of H-Z. Compared to an *N*-alkyl 1-azadiene, this process is simplified in the case of an unsubstituted (*N*-H) 1-azadiene. Indeed, Jun and coworkers demonstrated Rh(III)-catalyzed annulation of  $\alpha,\beta$ -unsaturated *N*-H imine derivatives and alkynes accesses pyridine products (**6**) directly in the presence of a copper(II) acetate oxidant ( $\text{Cu}(\text{OAc})_2$ , eq 3).<sup>24</sup> In this method, unstable *N*-H imine substrates are generated *in situ* by condensation of the corresponding ketones (**7**) and ammonium acetate ( $\text{NH}_4\text{OAc}$ ).

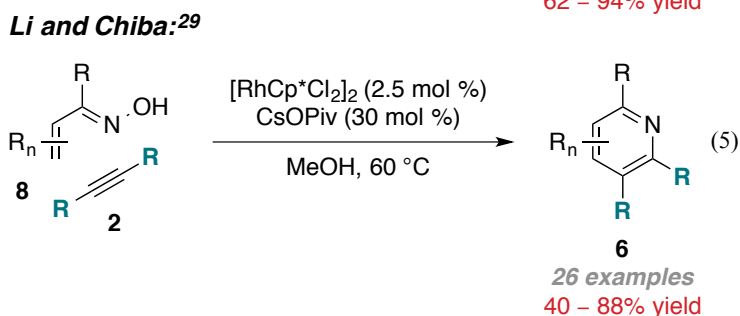
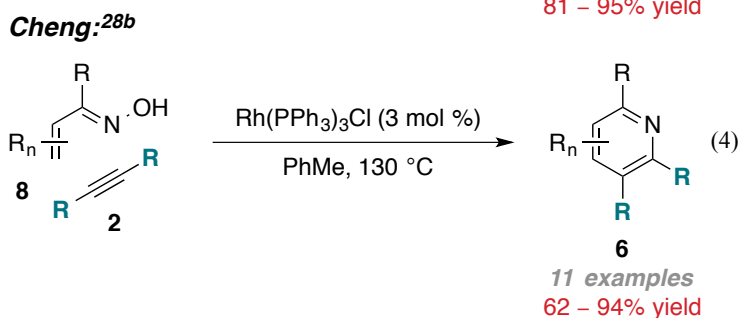
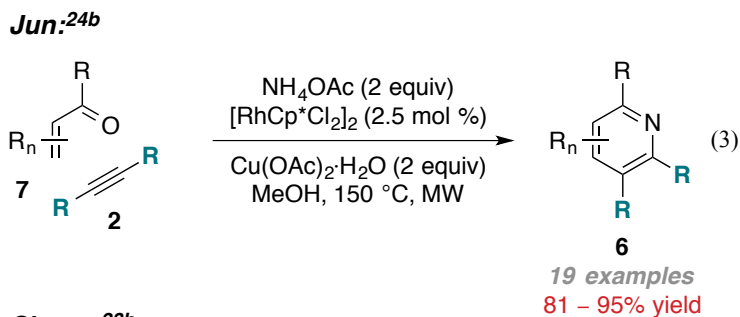
When the *N*-substituent (*Z* in Scheme 1.4) of a 1-azadiene is a leaving group, the nitrogen directing group can provide an ‘internal’ oxidant.<sup>25</sup> The most commonly encountered oxidizing directing groups in pyridine synthesis by formal [4+2] cycloaddition are oxime derivatives (*Z* = OR).<sup>26</sup> In their seminal report, Cheng and coworkers demonstrated the Rh(I)-catalyzed intermolecular<sup>27</sup> coupling of  $\alpha,\beta$ -unsaturated oximes (**8**) and alkynes (eq 4).<sup>28</sup> In this case, loss of H-Z (Scheme 1.4) is accomplished by elimination of water, obviating the need for an external oxidant. Li and Chiba reported the analogous transformation using rhodium(III)

catalysis (eq 5).<sup>29</sup> In both examples, reactions of unsymmetrical alkynes afford regioisomeric mixtures with little selectivity (shown for the Rh(III)-catalyzed reaction, conditions A, eq 7), presumably the reason nearly all alkyne substrates are symmetrical.

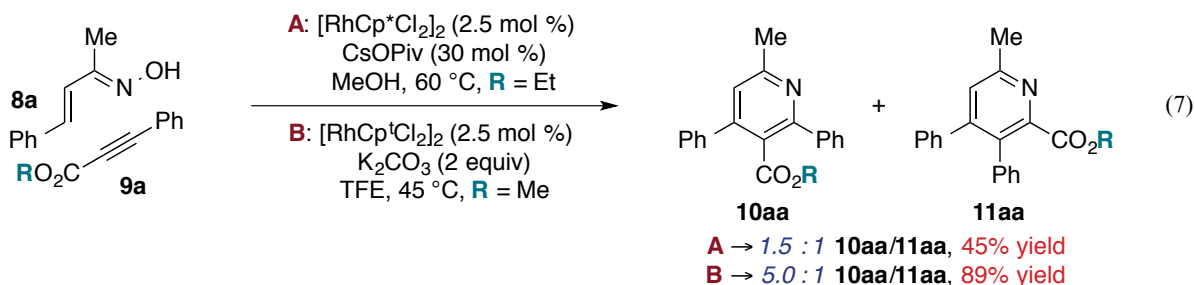
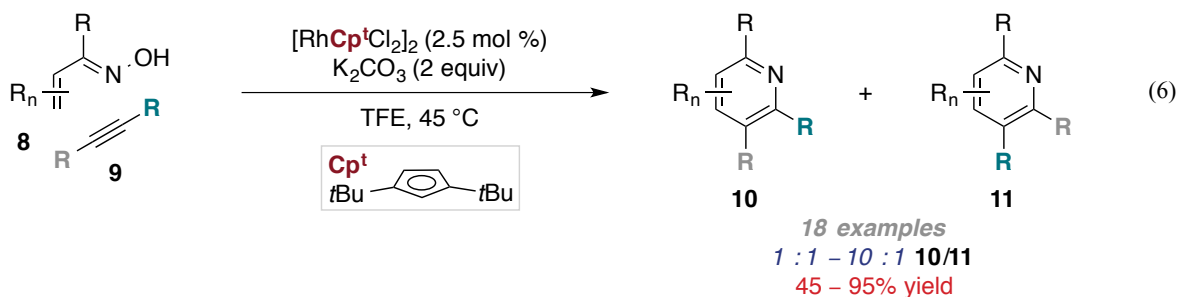
Hyster and Rovis explored a ligand modification strategy for enhancing selectivity in Rh(III)-catalyzed coupling of  $\alpha,\beta$ -

unsaturated oximes (**8**) and unsymmetrical alkynes (**9**, eq 6).<sup>30</sup> They identified a bulky di-*tert*-butylcyclopentadienyl ligand ( $\text{Cp}^t$ ) that results in substantial improvements in selectivity and reactivity (eq 7). Furthermore, mechanistic studies support a concerted metalation deprotonation pathway for C-H activation in this case.

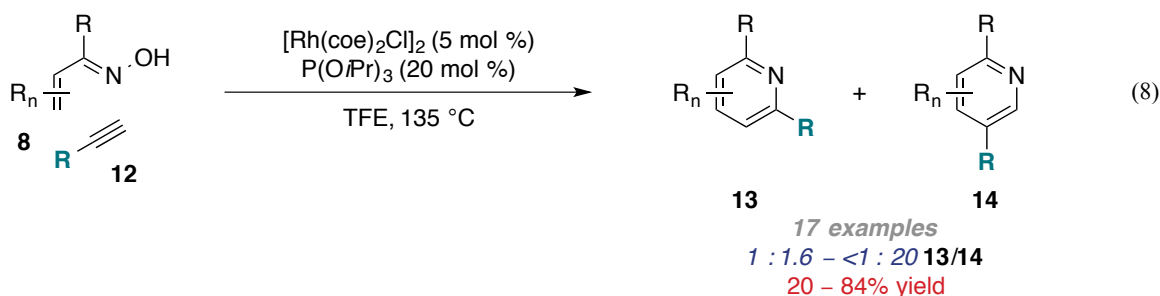
Terminal alkyne substrates are often problematic in transition metal-catalyzed reactions, including the examples discussed thus far, since they are susceptible to a variety of side reactions.<sup>31</sup> Bergman and Ellman addressed this issue in their report of Rh(I)-catalyzed formal [4+2] cycloaddition of  $\alpha,\beta$ -unsaturated oximes and terminal alkynes (**12**, eq 8).<sup>32</sup> In the presence of a phosphite ligand ( $\text{P}(\text{O}i\text{Pr})_3$ ), reactions afford mixtures of pyridine isomers **13** and **14** with selectivities that range from 1:1.6 to <1:20 **13/14** (eq 8).



**Rovis:**<sup>30</sup>

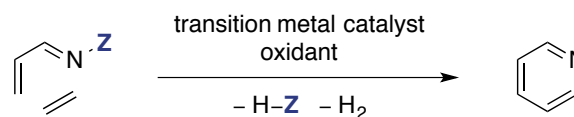


**Bergman and Ellman:**<sup>32</sup>



### 1.1.5 Nitrogen-Directed C–H Functionalization with Alkenes

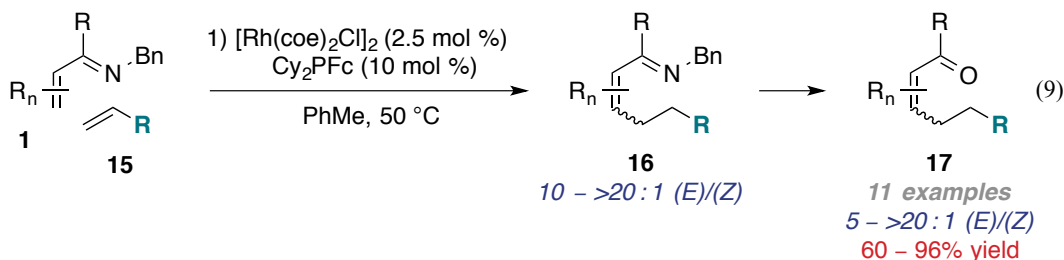
One possible alternative to the alkyne component in rhodium-catalyzed coupling with 1-azadienes



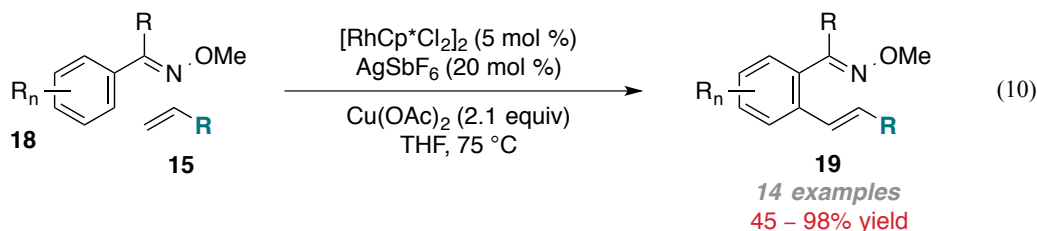
**Scheme 1.7** Pyridines from 1-azadienes and alkenes.

is use of an alkene substrate in combination with a stoichiometric oxidant (Scheme 1.7). The numerous reports of alkene incorporation by rhodium-catalyzed, nitrogen-directed C–H functionalization reactions support the feasibility of this approach to pyridine synthesis.<sup>33</sup> In one relevant example, Bergman and Ellman showed Rh(I)-catalyzed coupling of  $\alpha,\beta$ -unsaturated *N*-benzyl imines (**1**) and terminal alkenes (**15**) affords  $\beta$ -alkylated products **16**, isolated after

**Bergman and Ellman:<sup>34</sup>**



**Bergman and Ellman:<sup>35</sup>**

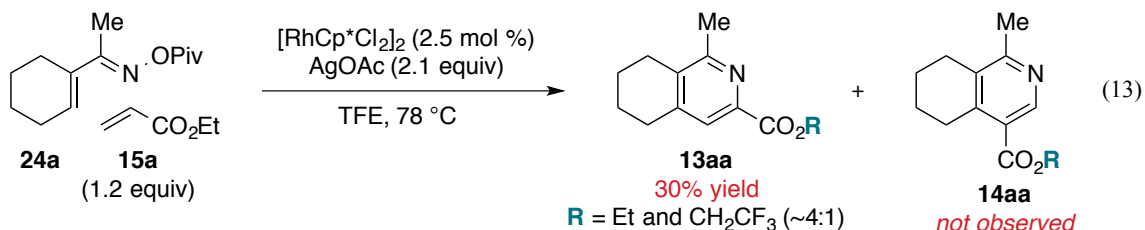
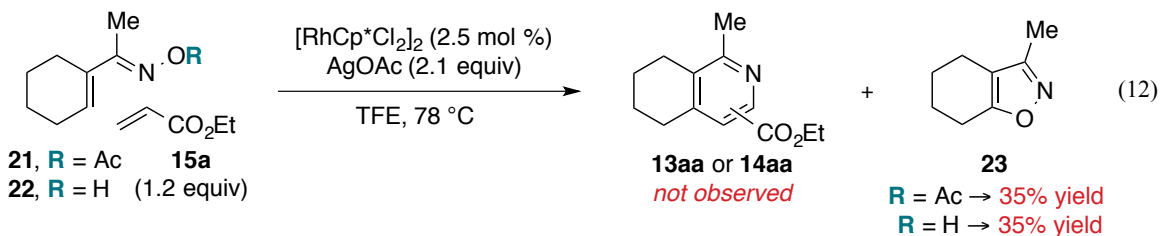
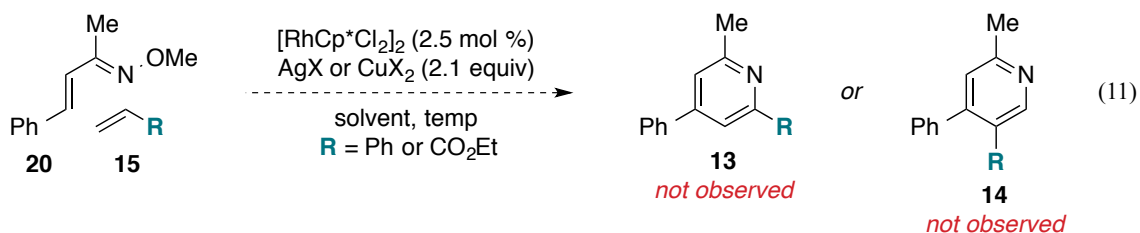


hydrolysis upon purification by chromatography (eq 9).<sup>34</sup> The same authors demonstrated oxime ethers (**18**) are effective directing groups for Rh(III)–catalyzed C–H functionalization with alkenes (eq 10).<sup>35</sup> The reaction is conducted in the presence of an oxidant ( $\text{Cu}(\text{OAc})_2$ ) to provide unsaturated products **19**. Notably, in both cases, alkene substrates incorporate selectively to afford only linear products (eqs 9 and 10).

## 1.2 Results<sup>36</sup>

### 1.2.1 Reaction Optimization

Limitations associated with pyridine synthesis by formal [4+2] cycloaddition of  $\alpha,\beta$ -unsaturated oximes and alkynes, as well as the established reactivity of alkenes in C–H functionalization reactions, prompted our investigation of rhodium–catalyzed annulation of  $\alpha,\beta$ -unsaturated oxime derivatives and alkenes. We began with *O*-methyl  $\alpha,\beta$ -unsaturated oxime ether **20** (eq 11), an alkenyl analog of the aryl oxime ether substrates employed by Bergman and Ellman (**18**, eq 10). Using  $[\text{RhCp}^*\text{Cl}_2]_2$ <sup>37</sup> ( $\text{Cp}^*$  = pentamethylcyclopentadienyl) as the catalyst,



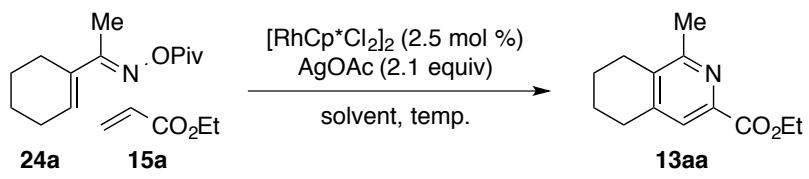
the desired reaction of **20** does not proceed under a variety of conditions (eq 11). We turned our attention to *O*-acetyl oxime ester **21** (Ac = C(O)Me, eq 12), since oxime esters are also known to be effective directing groups for rhodium-catalyzed C–H activation.<sup>14b,g,i</sup> Reaction of **21** and ethyl acrylate (**15a**) in 2,2,2-trifluoroethanol (TFE) with 2.1 equivalents silver(I) acetate (AgOAc) as the external oxidant affords no pyridine products **13aa** or **14aa**; rather, isoxazole **23** is observed (eq 12). Formation of **23** may proceed by ester solvolysis to release unsubstituted derivative **22** (eq 12), followed by intramolecular cyclization. The reaction of **22** also affords isoxazole **23** in 35% yield, consistent with this proposed pathway.

We hypothesized the bulky *tert*-butyl substituent of *O*-pivaloyl oxime ester **24a** (Piv = C(O)*t*Bu, eq 13) would suppress isoxazole formation by preventing decomposition to unsubstituted oxime **22**. We were delighted to find desired annulation of **24a** and ethyl acrylate (**15a**) proceeds to 30% yield (eq 13). Importantly, alkene incorporation is selective for formation

of 6-substituted pyridine **13aa** and no 5-substituted isomer **14aa** is observed. Partial transesterification of **13aa** with the solvent also occurs, leading to an approximately 4:1 mixture of ethyl and trifluoroethyl esters (eq 13).

The interaction of pyridine **13aa** and TFE prompted a screen of reaction solvents (Table 1.1). Little or no product formation occurs in a range of media including nonpolar (entry 2), polar aprotic (entries 3–7), and polar protic (entries 8–10) systems. Only use of perfluorinated alcohol solvents TFE and

**Table 1.1.** Optimization of the reaction solvent.<sup>a</sup>



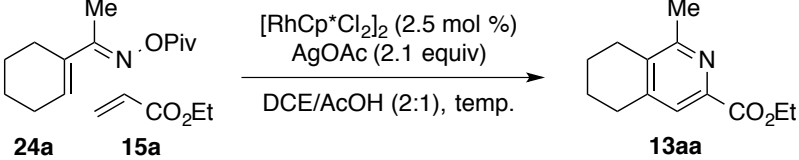
entry	solvent	temperature (°C)	yield <b>13aa</b> (%) <sup>b</sup>
1	TFE	74	30 <sup>c</sup>
2	PhMe	110	0
3	1,4-dioxane	110	0
4	THF	68	0
5	acetone	68	<5
6	DCE	85	<5
7	MeCN	90	<5
8	EtOH	90	<5
9	<i>t</i> AmOH	90	0
10	<i>i</i> PrOH	68	0
11	HFIP	68	20
12	AcOH	85	35
13	DCE/AcOH (20:1)	85	25
14	DCE/AcOH (10:1)	85	35
15	DCE/AcOH (2:1)	85	45

<sup>a</sup>Conditions: 1.2 equiv **15a**, 0.15 M. <sup>b</sup>Determined by <sup>1</sup>H NMR.

<sup>c</sup>~4:1 mixture of Et and CH<sub>2</sub>CF<sub>3</sub> esters.

1,1,1,3,3,3-hexafluoroisopropanol (HFIP) results in observable amounts of pyridine formation (entries 1 and 11). We speculated the substantial difference in reactivity between alcohol solvents ethanol (EtOH) and isopropanol (*i*PrOH) compared to their perfluorinated analogs TFE and HFIP could be attributed to the difference in acidity. Specifically, the pK<sub>a</sub>'s of TFE and HFIP are 23.5 and 18.2 in DMSO, respectively, and those of EtOH and *i*PrOH are 29.8 and 30.3 in DMSO, respectively.<sup>38</sup> With this in mind, we evaluated more acidic solvent systems. Indeed, the yield of **13aa** increases to 45% in an acetic acid (AcOH) reaction solvent (entry 12).



**Table 1.2.** Optimization of concentration and temperature.<sup>a</sup>

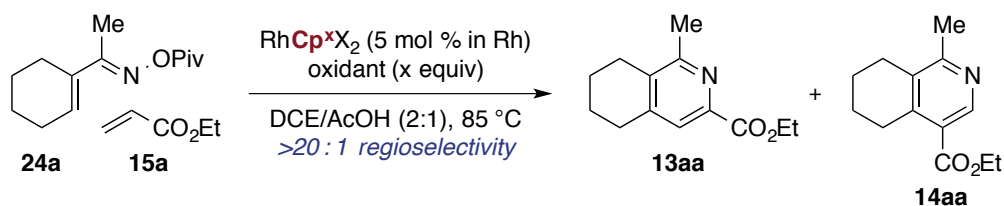
entry	concentration (M)	temperature (°C)	yield <b>13aa</b> (%) <sup>b</sup>
1	0.075	85	50
2	0.15	85	45
3	0.3	85	65
4	0.6	85	60
5	0.3	23	0
6	0.3	60	30
7	0.3	100	50

<sup>a</sup>Conditions: 1.2 equiv **15a**. <sup>b</sup>Determined by <sup>1</sup>H NMR.

Employing AcOH as a mixture with 1,2-dichloroethane (DCE) lessens decomposition of the oxime substrate (**24a**), and pyridine **13aa** forms in 45% yield using a 2:1 DCE/AcOH solvent system (entry 15). Increasing reaction concentration favors pyridine formation (Table 1.2), accessing **13aa** in 65% yield at the optimal concentration of 0.3 molar (M, entry 3). Rh(III)-catalyzed coupling of **24a** and **15a** does not proceed at room temperature (entry 5) and decreasing reaction temperature to 60 °C results in lower yield (entry 6). Substrate decomposition occurs at elevated temperature, leading to 50% yield of **13aa** (entry 7).

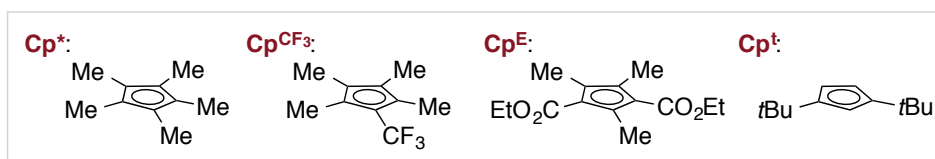
Previous work in the Rovis group showed the substituents of a cyclopentadienyl ligand can have significant effects in Rh(III)-catalyzed annulation of unsaturated oximes and alkynes.<sup>30</sup> With this in mind, we examined the reaction of **24a** and alkene substrate **15a** in the presence of various [RhCp<sup>x</sup>Cl<sub>2</sub>]<sub>2</sub> complexes (Table 1.3). Use of electron-deficient catalysts containing Cp<sup>CF<sub>3</sub></sup> or Cp<sup>E</sup> ligands leads to significantly lower reactivity (entries 2 and 3). Interestingly, 6-substituted pyridine **13aa** still forms with >20:1 selectivity when bulky *tert*-butyl-substituted [RhCp<sup>t</sup>Cl<sub>2</sub>]<sub>2</sub> is employed, but in slightly lower yield (entry 4).

Finally, we evaluated potential oxidizing reagents (Table 1.3). It is worth noting, in addition to its role as an oxidant, AgOAc is presumably responsible for *in situ* generation of a

**Table 1.3.** Catalyst and oxidant screen.<sup>a</sup>

entry	RhCp <sup>*</sup> X <sub>2</sub>	oxidant (x equiv)	yield <b>13aa</b> (%) <sup>b</sup>
1	[RhCp <sup>*</sup> Cl <sub>2</sub> ] <sub>2</sub>	AgOAc (2.1 equiv)	65
2	[RhCp <sup>CF<sub>3</sub></sup> Cl <sub>2</sub> ] <sub>2</sub>	AgOAc (2.1 equiv)	20
3	[RhCp <sup>E</sup> Cl <sub>2</sub> ] <sub>2</sub>	AgOAc (2.1 equiv)	5
4	[RhCp <sup>t</sup> Cl <sub>2</sub> ] <sub>2</sub>	AgOAc (2.1 equiv)	50
5	[RhCp <sup>*</sup> Cl <sub>2</sub> ] <sub>2</sub> <sup>c</sup>	AgOAc (2.1 equiv)	65
6	RhCp <sup>*</sup> (OAc) <sub>2</sub>	AgOAc (2.1 equiv)	60
7	RhCp <sup>*</sup> (OAc) <sub>2</sub>	Cu(OAc) <sub>2</sub> ·H <sub>2</sub> O (2.1 equiv)	0
8	RhCp <sup>*</sup> (OAc) <sub>2</sub>	CAN (2.1 equiv)	0
9	RhCp <sup>*</sup> (OAc) <sub>2</sub>	benzoquinone (1.05 equiv)	0
10	RhCp <sup>*</sup> (OAc) <sub>2</sub>	anthraquinone (1.05 equiv)	10
11	RhCp <sup>*</sup> (OAc) <sub>2</sub>	TEMPO (2.1 equiv)	20
12	RhCp <sup>*</sup> (OAc) <sub>2</sub>	NMO (1.05 equiv)	10

<sup>a</sup>Conditions: 1.2 equiv **15a**, 0.3 M. <sup>b</sup>Determined by <sup>1</sup>H NMR. <sup>c</sup>5 mol % [RhCp<sup>\*</sup>Cl<sub>2</sub>]<sub>2</sub>.

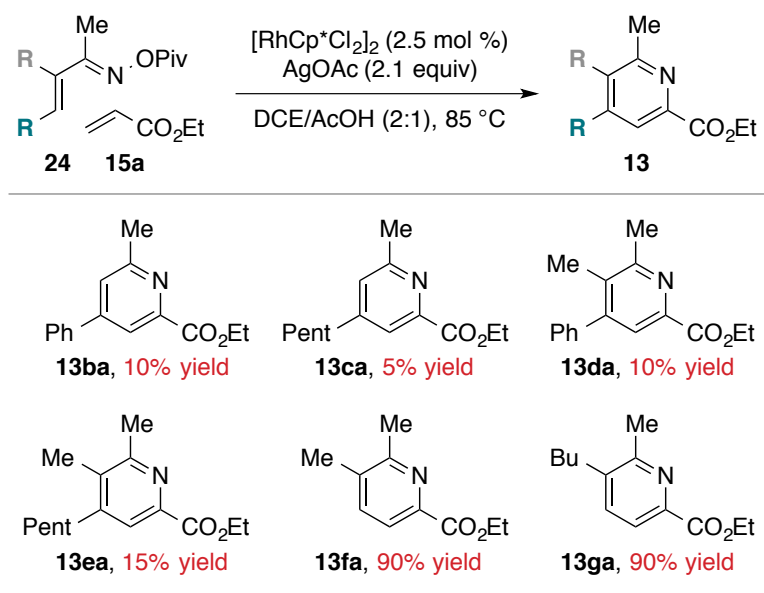


rhodium acetate complex by halide abstraction from [RhCp<sup>\*</sup>Cl<sub>2</sub>]<sub>2</sub>.<sup>39</sup> Therefore, screening of other external oxidants was conducted using preformed rhodium acetate catalyst RhCp<sup>\*</sup>(OAc)<sub>2</sub>. Copper(II) acetate (Cu(OAc)<sub>2</sub>) is a common oxidant for rhodium-catalyzed *N*-heterocycle synthesis *via* C–H activation,<sup>11g,j,13a,c</sup> however, reaction of **24a** and **15a** with 2.1 equivalents Cu(OAc)<sub>2</sub> affords no desired product (entry 7). Use of ceric ammonium nitrate (CAN) results in complete decomposition of the oxime substrate (entry 8). Pyridine formation proceeds in the presence of organic oxidants anthraquinone (entry 10), 2,2,6,6-tetramethylpiperidine 1-oxyl (TEMPO, entry 11), and *N*-methylmorpholine *N*-oxide (NMO, entry 12). However, yields of **13aa** are lower in these cases.

### 1.2.2 $\alpha,\beta$ -Unsaturated Oxime Ester Scope

We explored the scope of the reaction using AgOAc as the external oxidant, beginning with the oxime substrate (**24**, Chart 1.1). *O*-Pivaloyl  $\alpha,\beta$ -unsaturated oxime esters are easily accessed from the corresponding ketones by condensation with hydroxylamine hydrochloride

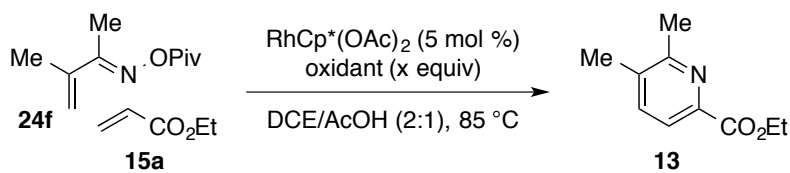
**Chart 1.1.** Initial examination of oxime substrates **24**.<sup>a,b</sup>



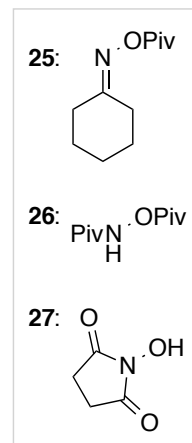
<sup>a</sup>Conditions: 1.2 equiv **15a**, 0.3 M. <sup>b</sup>Yields determined by  $^1\text{H}$  NMR.

and subsequent acylation with pivaloyl chloride (see Appendix 1.3). Reactions of  $\beta$ -aryl and  $\beta$ -alkyl substrates **24b** and **24c** result in little product formation. We wondered if the diminished reactivity compared to **24a** could be due to lack of  $\alpha$ -substitution, so  $\alpha$ -methyl derivatives **24d** and **24e** were prepared. However, coupling with ethyl acrylate (**15a**) proceeds with similarly low conversion in both cases. We were delighted to find the reaction of  $\beta$ -H  $\alpha,\beta$ -unsaturated oxime ester **24f** affords pyridine **13fa** with >20:1 selectivity and in 90% isolated yield. The related substrate **24g** also undergoes formal [4+2] cycloaddition to provide **13ga** in 90% yield.

At this point in our study, we chose to reevaluate alternative external oxidants using the more reactive substrate **24f** (Table 1.4). Similar to the reaction of **24a** (Table 1.3), low conversion is observed in the presence of anthraquinone or NMO (entries 1 and 2). Employing 2.1 equivalents of organic oxidant TEMPO, on the other hand, leads to formation of **13fa** in 80% yield (entry 3). Increasing the amount of TEMPO to 3.2 equivalents proves detrimental for

**Table 1.4.** Alternative oxidants for the reaction of **24f**.<sup>a</sup>

entry	oxidant (x equiv)	yield <b>13fa</b> (%) <sup>b</sup>
1	anthraquinone (1.05 equiv)	25
2	NMO (1.05 equiv)	35
3	TEMPO (2.1 equiv)	80
4	TEMPO (3.2 equiv)	60
5	$\text{Cu}(\text{OAc})_2 \cdot \text{H}_2\text{O}$ (2.1 equiv)	0
6	$\text{Cu}(\text{OAc})_2 \cdot \text{H}_2\text{O}$ (0.2 equiv) + air <sup>c</sup>	0
7	air <sup>c</sup>	50
8	none	45 <sup>d</sup>
9	<b>25</b> (1.05 equiv)	45
10	<b>26</b> (1.05 equiv)	35
11	<b>27</b> (1.05 equiv)	30



<sup>a</sup>Conditions: 1.2 equiv **15a**, 0.3 M. <sup>b</sup>Determined by <sup>1</sup>H NMR.

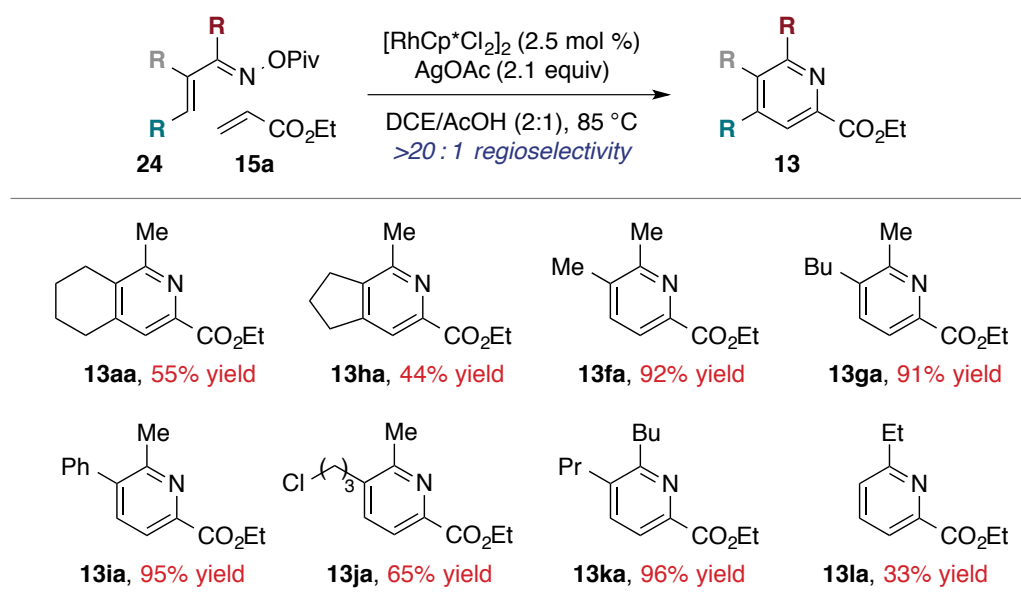
<sup>c</sup>Reaction vial not flushed with Ar. <sup>d</sup>Isolated yield.

reactivity (entry 4). In the case of a  $\text{Cu}(\text{OAc})_2$  oxidant, <sup>1</sup>H NMR data suggests polymerization of the alkene substrate occurs, likely precluding pyridine formation (entry 5).

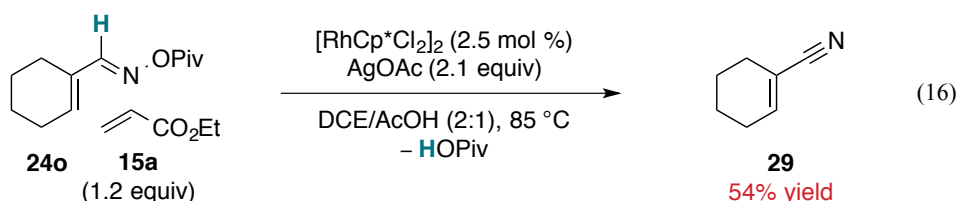
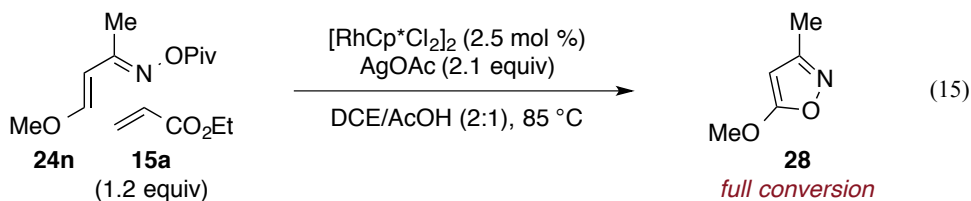
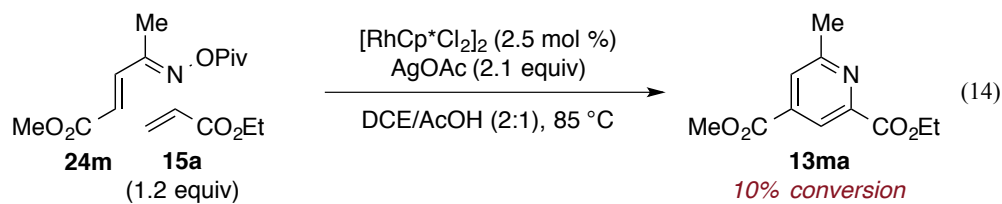
Several studies have investigated the use of atmospheric oxygen as a terminal oxidant for Rh(III)-catalyzed C–H functionalization reactions,<sup>40</sup> typically in the presence of catalytic copper(II) reagents.<sup>13a,33a</sup> Reaction of **24f**, **15a**, and 20 mol %  $\text{Cu}(\text{OAc})_2$  under air, however, leads to decomposition (entry 6). Surprisingly, the same reaction without  $\text{Cu}(\text{OAc})_2$  affords pyridine **13fa** in 50% yield (entry 7). Moreover, complete conversion of **24f** is observed in the reaction conducted under an atmosphere of argon, and pyridine **13fa** is isolated in 45% yield (entry 8). These observations are consistent with a pathway in which the N–O bond of **24f** acts as both the internal *and* external oxidant for pyridine formation. With this in mind, other potential oxidants containing N–O bonds were examined (**25**, **26** and **27**); however, diminished reactivity is observed these cases (entries 9–11).

Since other oxidizing reagents provided no improvement to the reaction of **24f** and **15a**, we continued our investigation of the reaction scope using AgOAc as the oxidant. Results of Rh(III)-catalyzed coupling of various *O*-pivaloyl  $\alpha,\beta$ -unsaturated oxime esters **24** and ethyl acrylate (**15a**) are provided in Chart 1.2. Importantly, 6-substituted products are formed with >20:1 selectivity in all cases.  $\alpha$ -Alkyl and  $\alpha$ -aryl substrates undergo the desired annulation to access 2,3,6-trisubstituted pyridines **13f,g** and **13i** in excellent yields. The primary alkyl chloride functionality in **24j** is tolerated in the presence of the Ag(I) reagent, and the slightly larger butyl substituent of oxime **24k** does not diminish reactivity. Pyridine formation also proceeds with vinyl oxime substrate **24l** to afford disubstituted pyridine **13la**, but in lower yield. Use of electron deficient substrate **24m** results in low conversion (eq 14), while electron rich substrate **24n** undergoes cyclization to isoxazole **28** (eq 15). Reaction of aldoxime ester **24o** does not provide the pyridine product; rather, elimination of PivOH occurs under the reaction conditions to generate nitrile **29** in 54% yield (eq 16).

**Chart 1.2.** *O*-Pivaloyl  $\alpha,\beta$ -unsaturated oxime ester scope.<sup>a</sup>



<sup>a</sup>Conditions: 1.2 equiv **15a**, 0.3 M, 14 h.



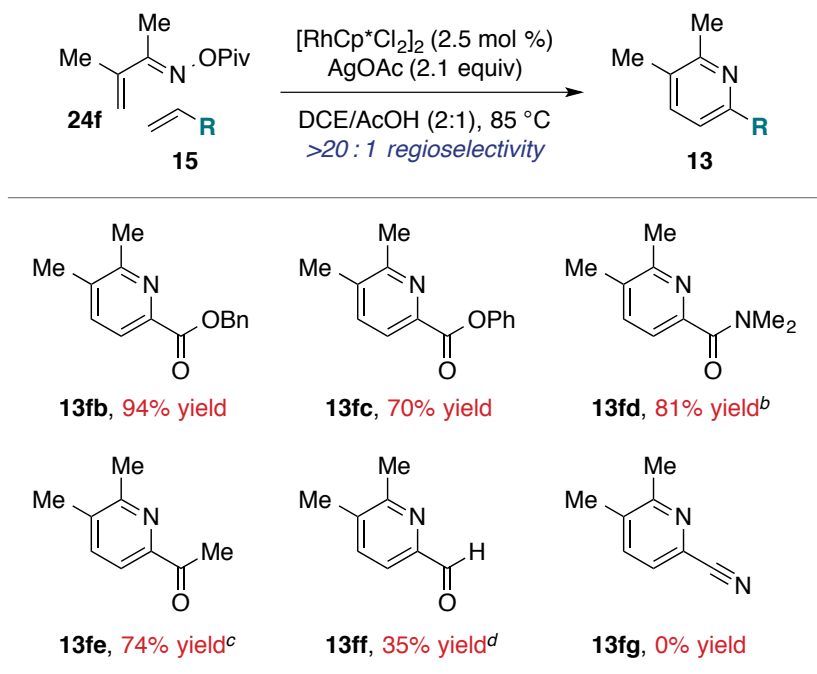
### 1.2.3 Activated Alkene Scope

A variety of electron deficient terminal alkenes undergo Rh(III)-catalyzed formal [4+2] cycloaddition with  $\alpha,\beta$ -unsaturated oxime ester **24f** (Chart 1.3). Reactions of benzyl and phenyl acrylate (**15b** and **15c**), *N,N*-Dimethylacrylamide (**15d**) and methyl vinyl ketone (**15e**) all provide 6-substituted pyridine products with >20:1 selectivity and in good yield. It is worth mentioning that an observed byproduct in the case of *N,N*-dimethylacrylamide (**15d**) is alkyl acetate **30** (eq 17), a compound that inseparable from the pyridine product **13fd** by chromatography. Fortunately, use of excess oxime substrate **24f** suppresses formation of **30**, allowing isolation of **13fd** in 81% yield. Alkene decomposition competes with pyridine formation in the case of acrolein (**15f**), and pyridine **13ff** forms with a maximum yield of 35% in the presence of 3 equivalents **15f**. Interestingly, Rh(III)-catalyzed annulation does not proceed with acrylonitrile (**15g**). To test for inhibition of pyridine formation by the nitrile group, perhaps by coordination to the catalyst, the control reaction in equation 18 was performed. Consistent

with this hypothesis, addition of 1.2 equivalents **15g** to the standard reaction of **24f** and **15a** leads to a significantly decreased yield of **13fa** (32% versus 92% yield, Chart 1.2).

Rh(III)-catalyzed coupling of oxime **24f** and styrene (**15h**) or 2-vinyl anisole (**15i**) proceeds with

**Chart 1.3.** Electron deficient alkene scope.<sup>a</sup>



<sup>a</sup>Conditions: 1.2 equiv **15a**, 0.3 M, 14 h. <sup>b</sup>1.2 equiv **24f**. <sup>c</sup>75 °C. <sup>d</sup>3 equiv **15f**, 5 mol %  $[\text{RhCp}^*\text{Cl}_2]_2$ .

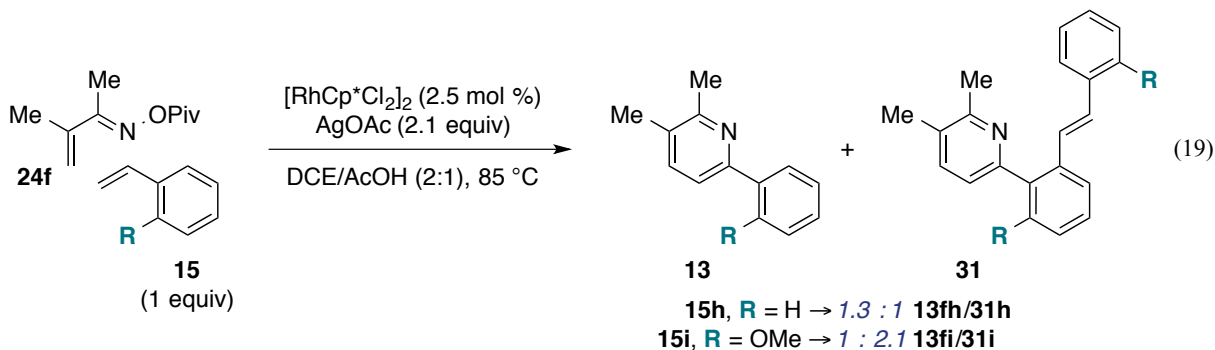
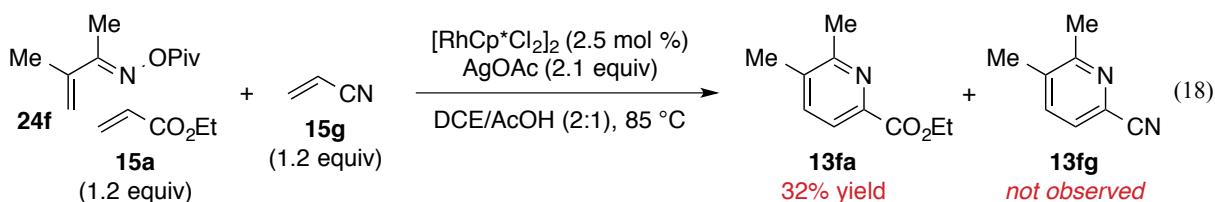
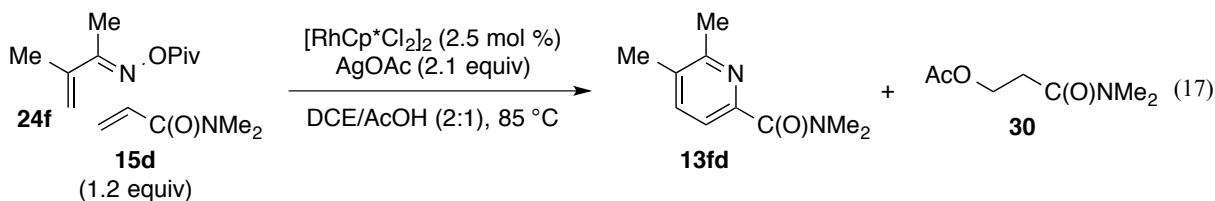


**Table 1.5.** Optimization of Rh(III)–catalyzed coupling with styrene (**15h**).<sup>a</sup>

entry	oxime	R	R	concentration (M)	yield <b>13</b> (%) <sup>b</sup>	<b>13/31</b> <sup>b</sup>
1	<b>24f</b>	Me	Me	0.3	35	1.3 : 1
2	<b>24f</b>	Me	Me	0.15	30	2.1 : 1
3	<b>24f</b>	Me	Me	0.075	35	4.3 : 1
4 <sup>c</sup>	<b>24f</b>	Me	Me	0.15	20	4.1 : 1
5	<b>24k</b>	Bu	Pr	0.3	61 <sup>d</sup>	>20 : 1

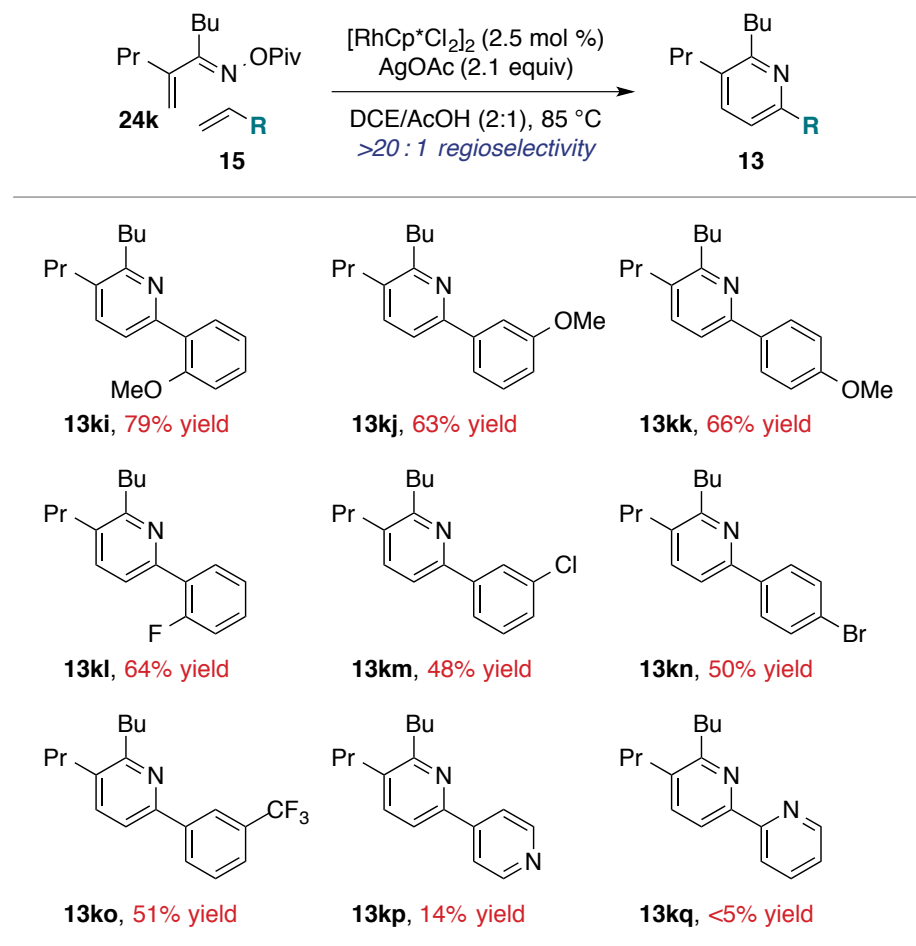
<sup>a</sup>Conditions: 1 equiv **15h**. <sup>b</sup>Determined by <sup>1</sup>H NMR. <sup>c</sup>**15h** added over 7 h. <sup>d</sup>Isolated yield.

complete conversion and >20:1 selectivity for 6–substituted isomers (eq 19). However, 2–aryl pyridine products (**13**) are capable substrates for directed C–H activation;<sup>41</sup> therefore, **13fh** and **13fi** are generated as mixtures with olefinated products **31h** and **31i**. We investigated strategies for suppressing the second C–H activation event in the reaction of **15h** (Table 1.5). Less olefinated product **31i** is observed at lower concentrations, but reactivity is also diminished (entries 2 and 3). Similarly, slow addition of **15h** disfavors olefination but pyridine **13fh** forms in lower yield (entry 4). Fortunately, pyridine **13kh** is the only observed product in the reaction of butyl–substituted oxime **24k**, isolated in 61% yield (entry 5).

We explored the scope of aryl alkene substrates using oxime **27k** (Chart 1.4). The desired annulation of 2–, 3–, and 4–vinyl anisole (**15i–k**) generates 6–aryl pyridine products selectively in good yields. The fluoride, chloride, and bromide substituents of alkenes **15l–n** are tolerated under the reaction conditions. Electron deficient 3–(trifluoromethyl)styrene (**15o**) participates to afford **13ko** in 56% yield, while little or no conversion is observed in reactions of 2– and 4–vinyl pyridine (**15p** and **15q**).

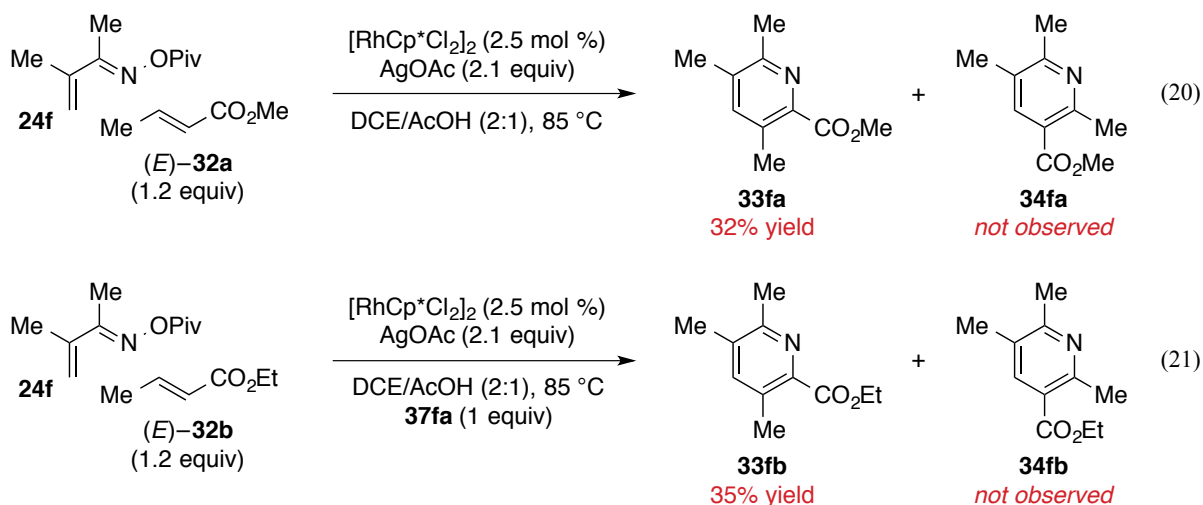


**Chart 1.4.** Aryl alkene scope.<sup>a</sup>



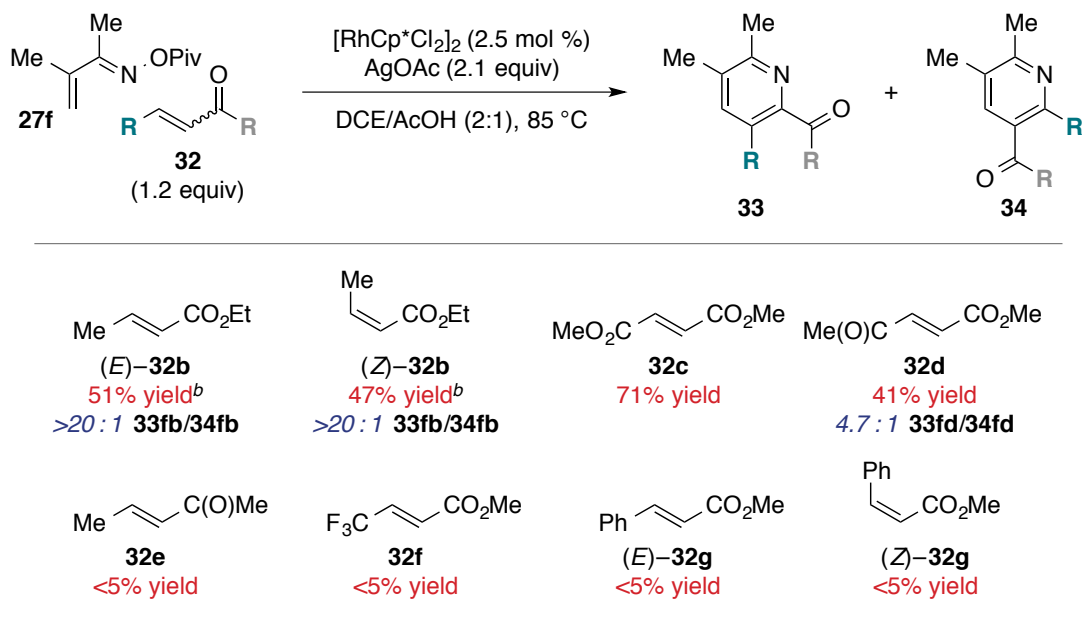
<sup>a</sup>Conditions: 1.05 equiv **15**, 0.3 M, 14 h.

We investigated the incorporation of internal alkene substrates, beginning with methyl crotonate ((*E*)-**32a**). Reaction of **24f** and (*E*)-**32a** under the optimized conditions affords 6-carboxymethyl pyridine **33fa** as the only observed product in 32% yield (eq 20). A control experiment was performed to probe potential product inhibition (eq 21), perhaps by coordination of the slightly more electron rich pyridine **33fa** to rhodium. In fact, reaction of **24f** and (*E*)-**32b** affords **33fb** in 35% yield in the presence of 1 equivalent pyridine **33fa**, suggesting product inhibition does not occur in this case.



Reactions of oxime **24f** and various internal alkene substrates **32** were examined (Chart 1.5). Interestingly, (*E*)- and (*Z*)-isomers of ethyl crotonate (**32b**) participate with similar reactivity, affording pyridine **33fb** in 51% and 47% yield, respectively. Methyl fumarate (**32c**) is a particularly reactive substrate, and **33fc** forms in 71% yield. Acetyl methyl acrylate (**32d**) incorporates with a surprisingly high level of selectivity for 6-carboxymethyl pyridine **33fd**. Changing the activating group to a ketone in **32e** or inclusion of a trifluoromethyl substituent in **32f** or inclusion of a phenyl substituent in **32g** results in low yields.

**Chart 1.5.** Internal alkene scope.<sup>a</sup>



<sup>a</sup>Conditions: 1.2 equiv **32**, 0.3 M, 14 h. <sup>b</sup>5 mol %  $[\text{RhCp}^*\text{Cl}_2]_2$ .

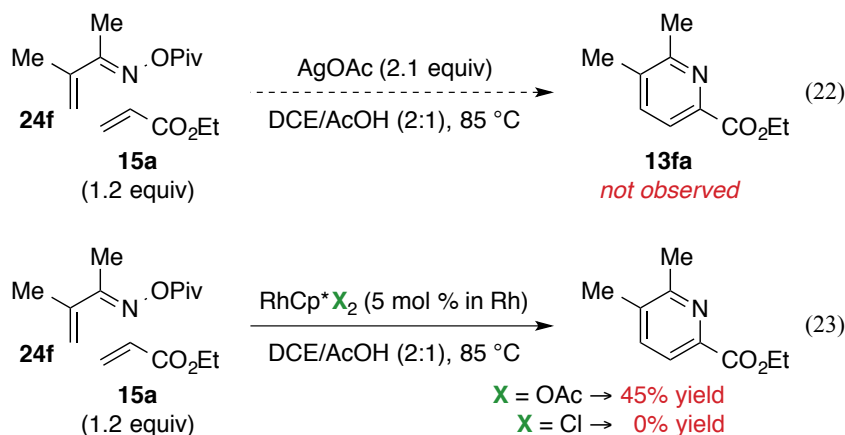
**32f** diminishes reactivity. Both (*E*)- and (*Z*)-methyl cinnamate (**32g**) are unreactive under these conditions.

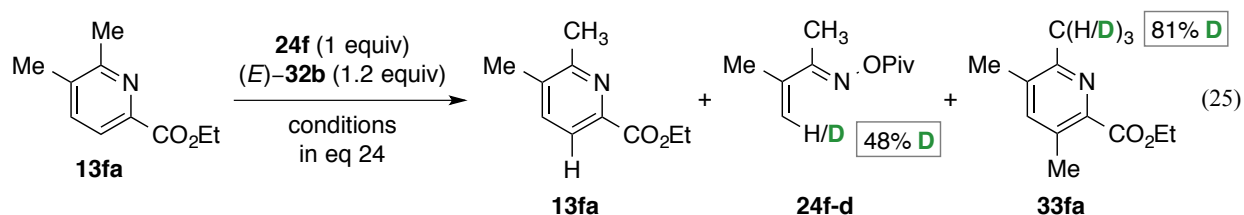
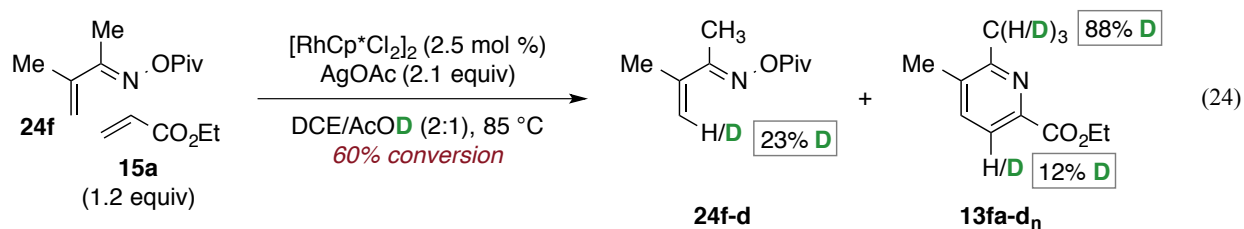
#### 1.2.4 Mechanistic Studies

Several observations contributed to our current understanding of the reaction mechanism. The control reaction of **24f** and **15a** without rhodium catalyst results in no conversion to the pyridine product (eq 22), providing evidence against annulation by *thermal* [4+2] cycloaddition.<sup>42</sup> Prior observations indicate coupling of **24f** and **15a** proceeds in the absence of added oxidant when the catalyst is acetate complex  $\text{RhCp}^*(\text{OAc})_2$  (Table 1.4 and eq 23). On the other hand, use of chloride complex  $[\text{RhCp}^*\text{Cl}_2]_2$  in the analogous reaction completely suppresses product formation (eq 23). That reactivity hinges upon the presence of a carboxylate is consistent with C–H activation by a concerted metalation deprotonation mechanism.<sup>21a</sup>

Isotope experiments provided further insight regarding the mechanism of pyridine formation. Reaction of **24f** and **15a** using acetic acid-*d* ( $\text{AcOD}$ ) results in significant deuterium incorporation at the  $\beta$ -position in **24f-d** after 60% conversion (eq 24), an observation consistent with reversible C–H activation at this site. In the same reaction, near complete deuteration of the

2-methyl substituent in pyridine **13fa-d<sub>n</sub>** occurs, implicating reversible deprotonation at this position at some point in the reaction. The control reaction of **24f**, (*E*)-**32b**



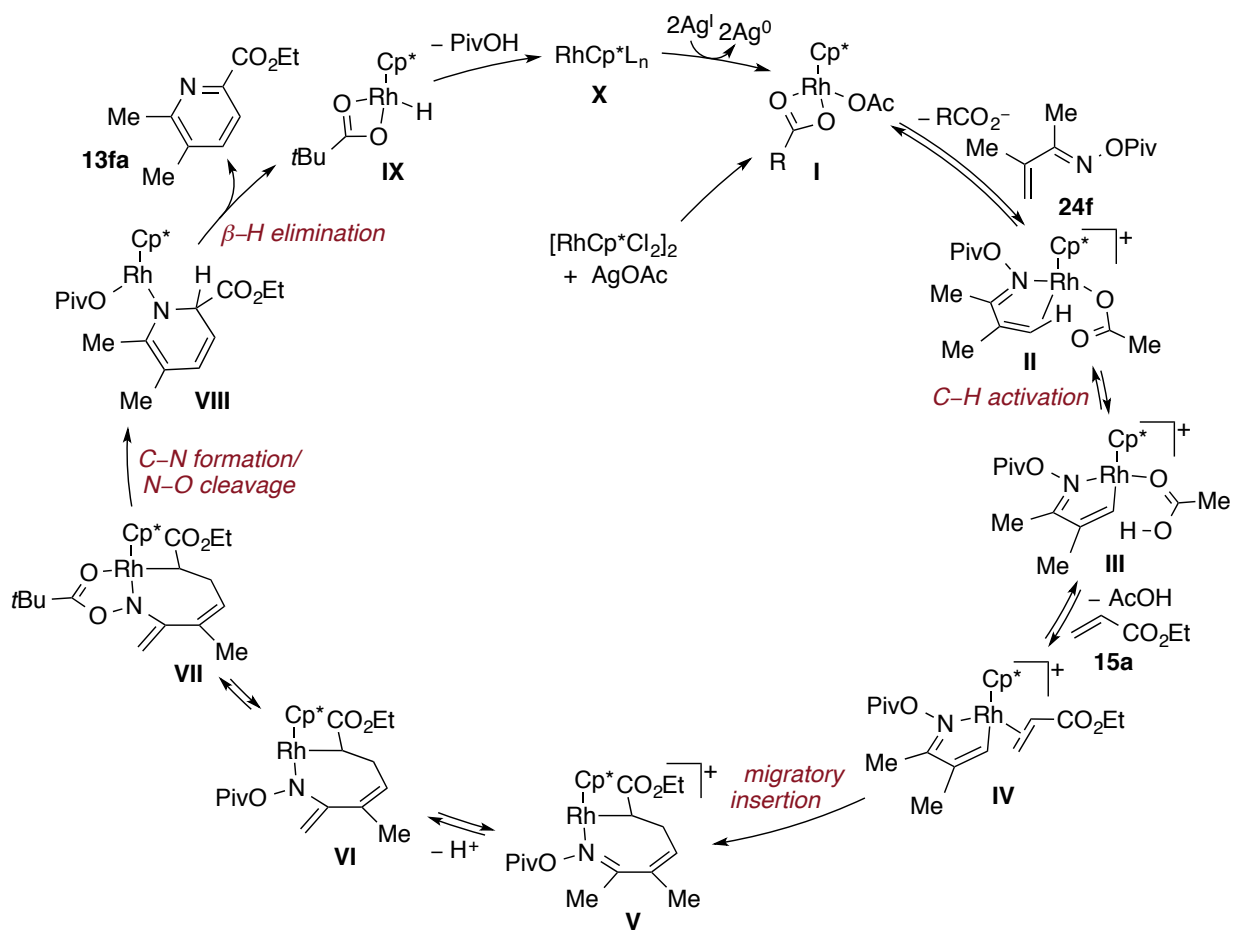


and 1 equivalent **13fa** leads to no deuterium incorporation in **13fa** (eq 25), ruling out deuteration by background deprotonation of the pyridine product. Instead, deprotonation likely takes place en route to the pyridine product. Since no deuterium incorporation at the corresponding site in oxime **24f-d** is observed, the deprotonation step is likely preceded by the first irreversible step of the reaction mechanism.

Based on these and forthcoming observations, we propose Rh(III)–catalyzed annulation of  $\alpha,\beta$ –unsaturated oxime ester **24f** and alkene **15a** proceeds by the mechanism depicted in Figure 1.4. Silver(I)–promoted ligand exchange generates active rhodium acetate catalyst **I**. Carboxylate dissociation provides an available site for coordination by **24f** to form intermediate **II**. Reversible C–H activation by carboxylate–assisted concerted metalation deprotonation at the  $\beta$ –position of **24f** affords rhodacycle **III**. Alkene coordination and migratory insertion to the Rh–C bond provides cationic intermediate **V**. Deprotonation of the 2–methyl group accesses neutral complex **VI**.

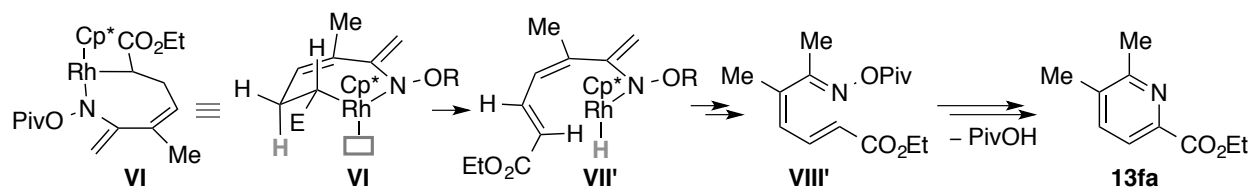
Two distinct pathways to pyridine **13fa** from 7–membered rhodacycle **VI** are feasible. In the first,  $\beta$ –hydride elimination affords azatriene intermediate **VIII'** (Scheme 1.8). Subsequent  $6\pi$ –electrocyclization<sup>43</sup> and elimination of PivOH access the pyridine product **13fa**. If pyridine

**Figure 1.4.** Proposed mechanism for formation of pyridine **13fa**.

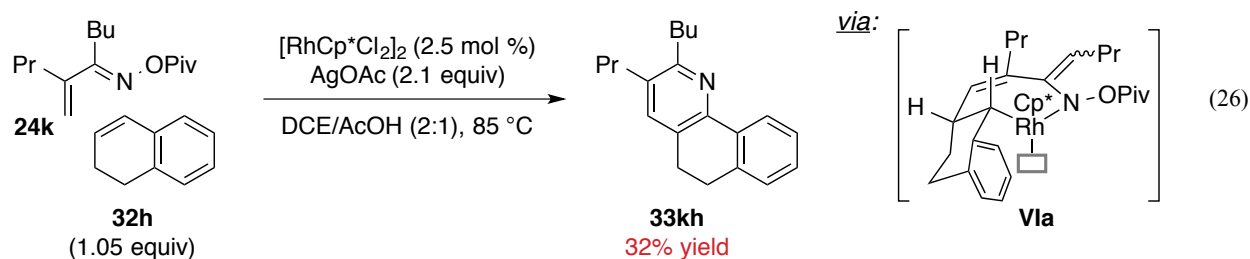


formation occurred by this mechanism, then reaction of a *cis*-fused alkene like 1,2-dihydronaphthalene (**32h**) should not proceed, since the *trans* relationship between rhodium and hydride substituents in intermediate **VIa** (eq 26) would preclude the *cis*-coplanar geometry required for elimination.<sup>6</sup> In fact, Rh(III)-catalyzed coupling of **24k** and **32h** affords pyridine **33kh** in 32% yield (eq 26), implying a different pathway.

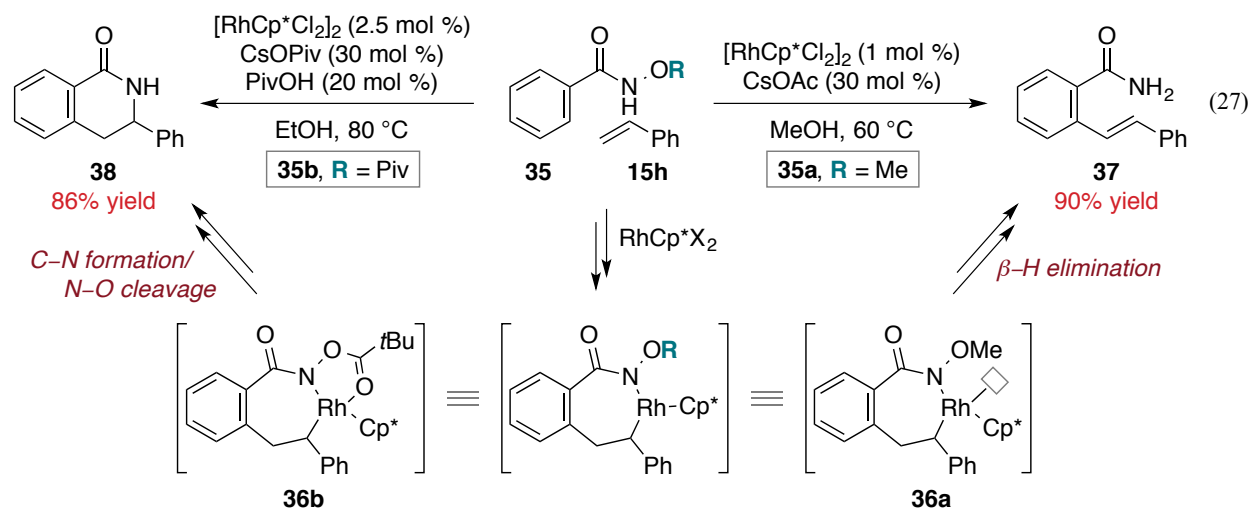
Glorius and coworkers' report of C-H functionalization in hydroxamic acid derivatives (**35**, Scheme 1.9)<sup>12g</sup> provides insight regarding the mechanism of pyridine formation from intermediate **VI** in Figure 1.4. During the course of their study, the authors discovered the outcome of Rh(III)-catalyzed functionalization with alkenes depends critically on the



**Scheme 1.8.** Alternate pathway to **13fa** from **VI**.

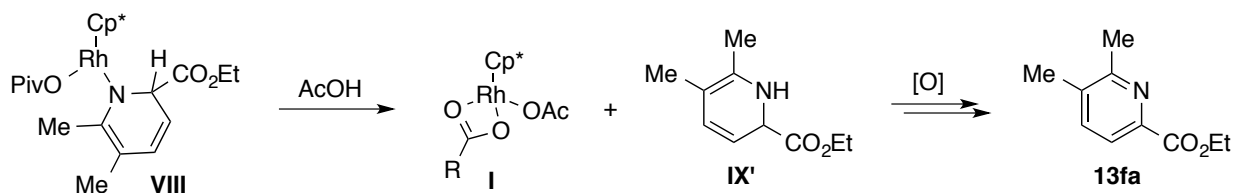


**Glorius:<sup>12g</sup>**

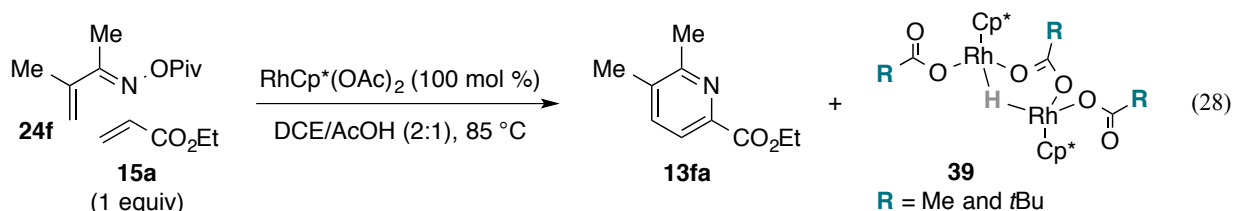


**Scheme 1.9.** Rh(III)-catalyzed C–H functionalization of hydroxamic acid derivatives **35**.

hydroxamic acid *O*-substituent (eq 27). Specifically, *O*-methyl ether **35a** couples with styrene (**15h**) to afford olefinated product **37**, presumably *via*  $\beta$ -hydride elimination from rhodium complex **36a** (eq 27, right). On the other hand, the analogous reaction of *O*-pivaloyl ester **35b** produces dihydroisoquinolone **38** (eq 27, left). The authors suggest chelation by the pivalate group in intermediate **36b** prevents  $\beta$ -hydride elimination, since **36b** is a coordinatively



**Scheme 1.10.** Alternate pathway to **13fa** from **VIII**.



saturated complex.<sup>6</sup> Instead, an N–O bond cleaving, C–N bond forming event occurs, ultimately leading to cyclized product **38**.<sup>12g</sup>

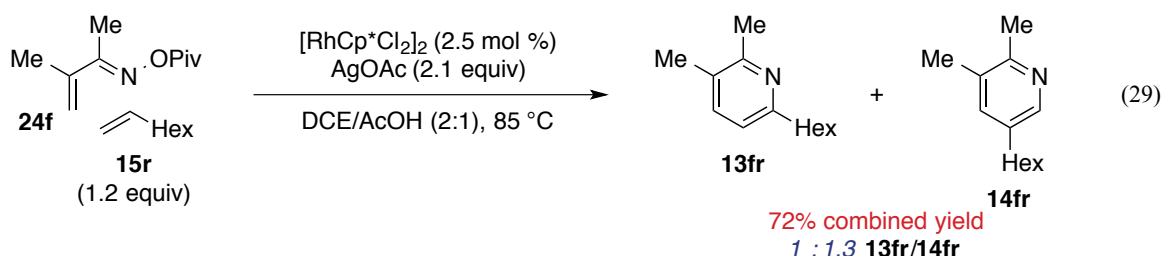
We propose coordination of the pivalate group in **VI** generates saturated complex **VII** that undergoes a C–N bond forming, N–O bond cleaving process to provide rhodium amide **VIII** (Figure 1.4). From **VIII**, protonolysis of the Rh–N bond with AcOH is possible (Scheme 1.10), regenerating active catalyst **I** and accessing 1,2–dihydropyridine intermediate **IX'** that is oxidized by the external oxidant to afford pyridine **13fa**. However, experimental observations are not fully consistent with the pathway shown in Scheme 1.10. For one, Ag(I) reagents are not common in methods for pyridine synthesis by oxidation of dihydropyridines.<sup>44</sup> In fact, oxidative aromatization reactions of 1,2–dihydropyridine derivatives analogous to **IX'** are often conducted using relatively weak oxidants.<sup>45</sup> In the present study, on the other hand, examination of several oxidizing reagents (Table 1.3) found only AgOAc to be effective for accessing pyridine **13aa**, a distinction that suggests the role of the oxidant is not aromatization of a 1,2–dihydropyridine intermediate (**XI'**). Furthermore, reaction **24f**, **15a** and 100 mol % RhCp\*(OAc)<sub>2</sub> results in formation of **13fa** and a rhodium hydride species (eq 28), tentatively assigned as **39** based on <sup>1</sup>H NMR data (see Appendix 1.5), an observation not easily explained by the pathway illustrated in

Scheme 1.10. Rather, we propose  $\beta$ -hydride elimination from intermediate **VIII** affords pyridine **13fa** and rhodium hydride complex **IX** (Figure 1.4). Reductive elimination of PivOH from **IX** provides a Rh(I) species **X** that is oxidized by Ag(I) to regenerate active catalyst **I**.

### 1.2.5 Discussion of Product Selectivity

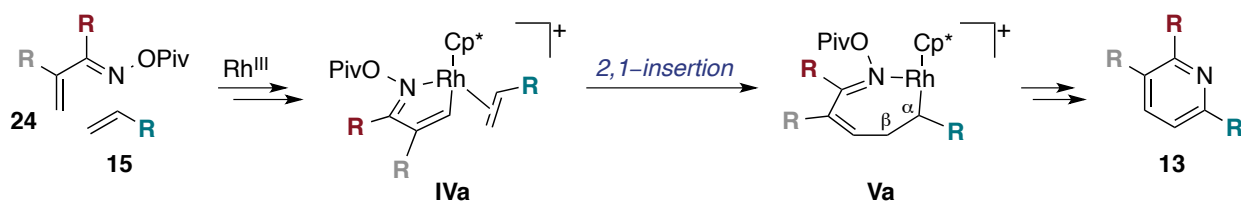
Unactivated terminal alkenes are also reactive substrates for Rh(III)-catalyzed formal [4+2] cycloaddition with *O*-pivaloyl  $\alpha,\beta$ -unsaturated oxime esters. For example, coupling of oxime **24f** and 1-octene (**15r**) proceeds with complete conversion under the optimized conditions (eq 29). However, approximately equal amounts of 6- and 5-substituted products **13fr** and **14fr** are observed in this case. The difference in selectivity between reactions of activated terminal alkenes **15a–q** (>20:1 **13/14**, *vide supra*) and unactivated substrate **15r** may be explained in terms of the selectivity-determining step of the mechanism proposed in Figure 1.4: migratory insertion (**IV**  $\rightarrow$  **V**).

In general, migration insertion of a terminal alkene installs the substituent (R) at either an  $\alpha$ - or  $\beta$ -position relative to the metal center (Scheme 1.11), processes termed 2,1- and 1,2-insertion, respectively.<sup>6</sup> With respect to the present study, 2,1-insertion from complex **IVa** leads to **Va** and, ultimately, 6-substituted pyridines **13** (Scheme 1.11a), while 1,2-insertion results in rhodacycle **Vb** and 5-substituted products **14** (Scheme 1.11b). Electron deficient and aryl terminal alkenes (i.e. **15a–g** and **15h–q**, respectively) are known to favor 2,1-insertion,<sup>6</sup> offering

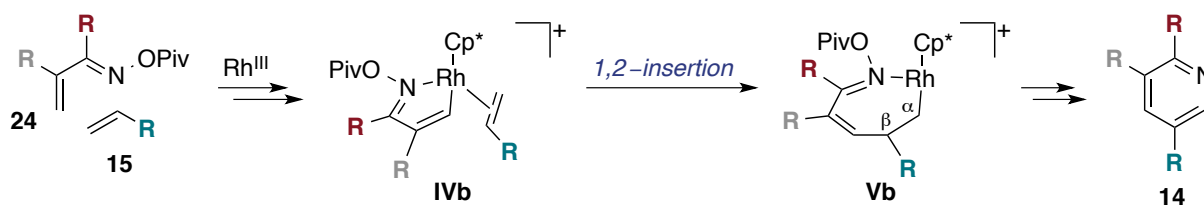




**a. 2,1-Insertion**



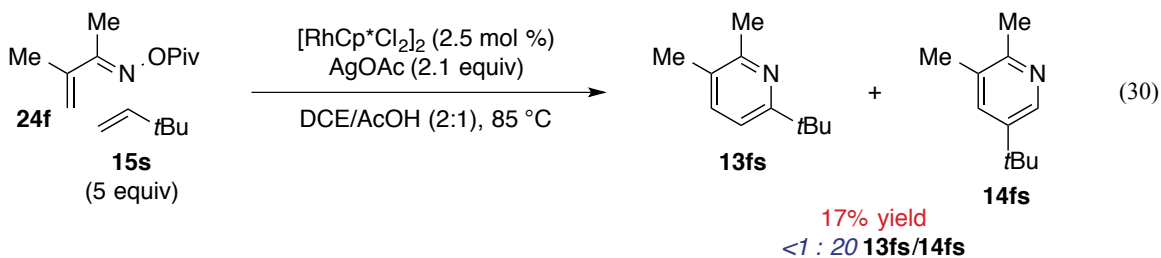
**b. 1,2-Insertion**



**Scheme 1.11.** Migratory insertion of alkenes in Rh(III)-catalyzed coupling with oximes **24**.

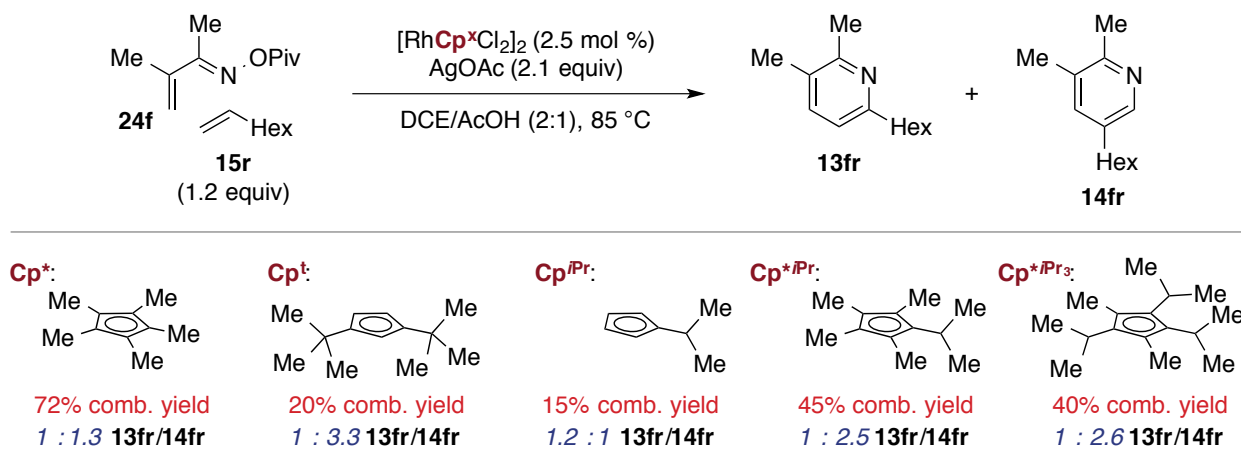
an explanation for the selective incorporation of these substrates to afford 6-substituted pyridines **13** (*vide supra*). On the other hand, alkyl alkenes often participate by both 2,1- and 1,2-insertion pathways,<sup>6</sup> consistent with formation of a mixture of **13fr** and **14fr** in the reaction of 1-octene (**15r**).

We can also discuss steric effects on the migratory insertion step using the model provided in Scheme 1.11. If the alkene substituent (R) is large, steric repulsion between the substituent and the environment around the metal center presumably favors orientation of the alkene as illustrated in **IVb** (Scheme 1.11b). Therefore, use of a bulky terminal alkene substrate should lead to selective 1,2-insertion and formation of 5-substituted pyridine **14**. Indeed, reaction of **24f** and 3,3-dimethyl butene (**15s**) affords **14fs** with >20:1 selectivity, albeit in low



yield (eq 30). By the same logic, modification of the steric environment through the use of a cyclopentadienyl ligand with bulky substituents should also favor formation of 5-substituted products **14** (Chart 1.6).<sup>46</sup> Consistent with this hypothesis, reaction of oxime **24f** and 1-octene (**15r**) in the presence of  $[\text{RhCp}^t\text{Cl}_2]_2$  affords a mixture of products with 3.3:1 selectivity for 5-substituted pyridine **14fr**. However, only 20% combined yield is observed in this case. Use of monosubstituted ligand  $\text{Cp}^{i\text{Pr}}$  leads to similarly low conversion. Reactivity is recovered in the presence of  $[\text{RhCp}^{*i\text{Pr}}\text{Cl}_2]_2$ , implying pentasubstitution of the cyclopentadienyl ligand is important for reactivity. Additional *iso*-propyl groups in  $\text{Cp}^{*i\text{Pr}_3}$  do not significantly affect the reaction of **24f** and **15r**, resulting in a 1:2.6 mixture of **13fr** and **14fr** in 40% combined yield.

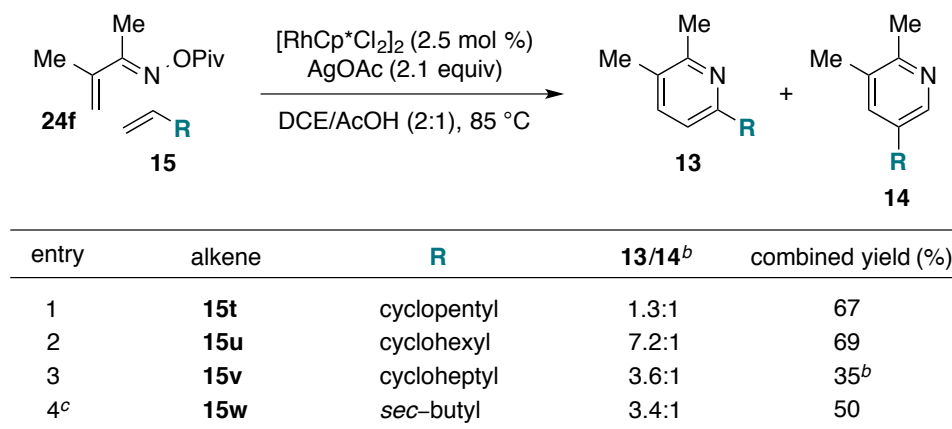
**Chart 1.6.** Investigation of the cyclopentadienyl ligand.<sup>a,b</sup>



<sup>a</sup>Conditions: 1.2 equiv **15r**, 0.3 M. <sup>b</sup>Yields and ratios determined by <sup>1</sup>H NMR.

### 1.2.6 Unexpected Selectivity with Secondary Alkyl Alkene Substrates

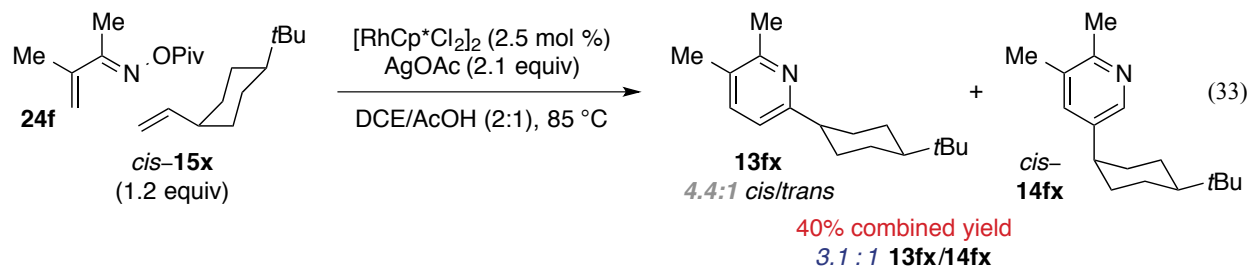
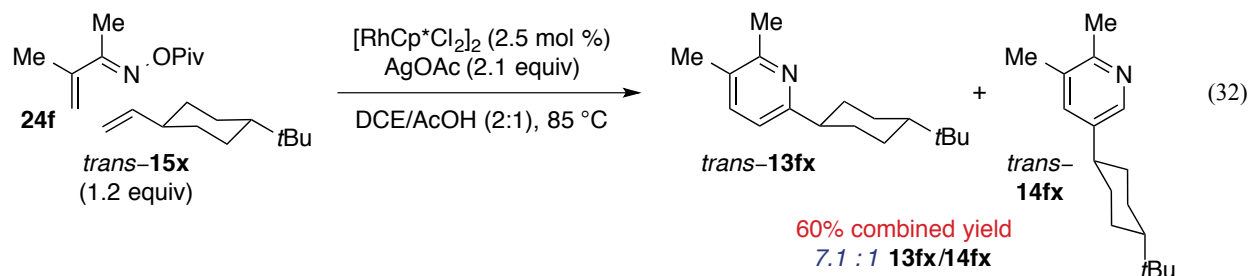
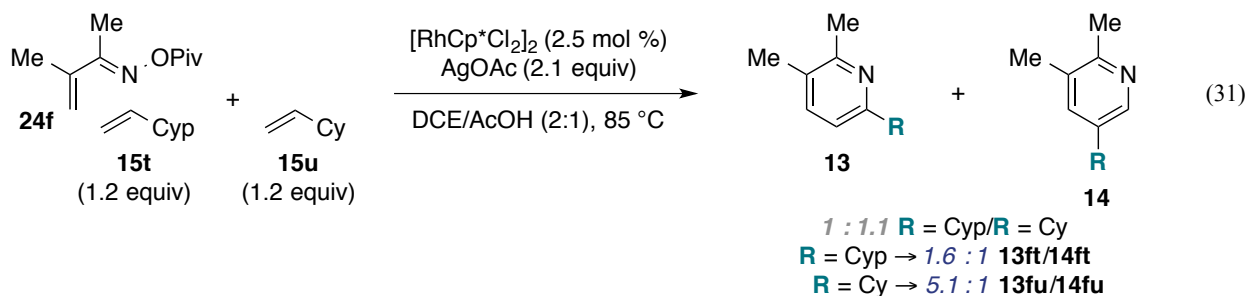
It is reasonable to predict, based on the observations in equations 29 and 30, Rh(III)-catalyzed coupling of oxime **24f** and a secondary alkyl alkene will generate a mixture of products with a level of selectivity for 5-substituted product **14**. In fact, 6-substituted pyridines **13** are major products in reactions of all secondary alkyl alkene substrates examined in this study

**Table 1.6.** Secondary alkyl alkene scope.<sup>a</sup>

<sup>a</sup>Conditions: 1.2 equiv **15**, 0.3 M, 14 h. <sup>b</sup>Determined by <sup>1</sup>H NMR. <sup>c</sup>5 equiv **15**.

(Table 1.6). Perhaps the most striking of these results is the significant difference in selectivity between reactions of vinyl cyclopentane (**15t**, 1.3:1 selectivity) and vinyl cyclohexane (**15u**, 7.2:1 selectivity). The control reaction of **24f** and 1.2 equivalents **15t** and **15u** leads to incorporation of both alkene substrates with selectivities that are similar to those observed in the standard reaction (eq 31), suggesting a contaminant in either reagent is not responsible for the difference.

One property that varies among secondary alkyl alkenes **15t–w** is conformation. In this respect, cyclohexane is unique, since it exists predominantly in one conformation: the chair form. Furthermore, in vinyl cyclohexane (**15u**), the conformer in which the vinyl substituent occupies an equatorial position is favored by 1.5–1.7 kcal/mol compared to the axial isomer.<sup>47</sup> As a result, vinyl cyclohexane (**15u**) likely exhibits higher conformational rigidity compared to other secondary alkyl alkene substrates. To probe conformational effects in Rh(III)-catalyzed coupling of **24f** and alkyl alkenes, *tert*-butyl-substituted derivatives **15x** were prepared (eqs 32 and 33). Preference for an equatorial *tert*-butyl group (favored by 4.7–4.9 kcal/mol in *tert*-butylcyclohexane)<sup>47</sup> presumably dictates conformation in both *trans*-**15x** and *cis*-**15x**, such that



the vinyl substituent is equatorial in *trans*-**15x** and axial in *cis*-**15x**. Reaction of **24f** and *trans*-**15x** favors formation of 6-substituted pyridine *trans*-**13fx** with 7.1:1 selectivity (eq 32). On the other hand, reaction of **24f** and *cis*-**15x** leads to a 3.1:1 mixture of **13fx** (4.4:1 *cis/trans* isomers) and *cis*-**14fx**. These results suggest Rh(III)-catalyzed coupling of alkyl alkenes is influenced by conformation; however, the reason for this effect is not fully understood at this time.

### 1.3 Conclusion

In conclusion, we developed a synthetic method for accessing substituted pyridines by Rh(III)-catalyzed annulation of  $\alpha,\beta$ -unsaturated *O*-pivaloyl oxime esters and alkenes. Reactions of activated alkene substrates afford 6-substituted pyridines with exquisite selectivity and in

excellent yields. Mechanistic studies support pyridine formation by reversible C–H activation, selective 2,1–insertion and a C–N bond forming/N–O bond cleaving process. Both ligand and alkene substituents influence product distribution in reactions of unactivated alkene substrates.

## REFERENCES

1. Vitaku, E.; Smith, D. T.; Njardarson, J. T. *J. Med. Chem.* **2014**, doi: 10.1021/jm501100b.
2. McGrath, N. A.; Brichacek, M.; Njardarson, J. T. *J. Chem. Educ.* **2010**, *87*, 1348.
3. Silverman, R. B. *The Organic Chemistry of Drug Design and Drug Action*, 2<sup>nd</sup> ed.; Elsevier: Burlington, MA, 2004. a) “Drug–Receptor Interactions,” pp 123–158. b) “Lead Modification: Drug Design and Development,” pp. 17–86.
4. a) Rousseaux, S.; Liégault, B.; Fagnou, K. “C–H Functionalization: A New Strategy for the Synthesis of Biologically Active Natural Products” in *Modern Tools for the Synthesis of Complex Bioactive Molecules*; Cossy, J.; Arseniyadis, S. Eds.; Wiley: New Jersey, 2012; pp 1–32. b) Tomin, A.; Bag, S.; Török, B. “Catalytic C–H Bond Activation Reactions” in *Green Techniques for Organic Synthesis and Medicinal Chemistry*; Zhang, W.; Cue, B. W. Eds.; Wiley: Chichester, UK, 2012; pp 69–98. c) Kakiuchi, F.; Kochi, T. *Synthesis* **2008**, 3013. d) Alberico, D.; Scott, M. E.; Lautens, M. *Chem. Rev.* **2007**, *107*, 174.
5. Sezen, B.; Sames, D. “What is C–H activation?” in *Handbook of C–H Transformations*; Dyker, G., Ed.; Wiley: Weinheim, Germany, 2005, pp 3–10.
6. Hartwig, J. F. *Organotransition Metal Chemistry: From Bonding to Catalysis*; University Science Books: Sausalito, CA, 2010.
7. For reviews of directed, transition metal–catalyzed C–H functionalization, see: a) Neufeldt, S. R.; Sanford, M. S. *Acc. Chem. Res.* **2012**, *45*, 936. b) Colby, D. A.; Tsai, A. S.; Bergman, R. G.; Ellman, J. A. *Acc. Chem. Rev.* **2012**, *45*, 814. c) Engle, K. M.; Mei, T.–S.; Wasa, M.; Yu, J.–Q. *Acc. Chem. Res.* **2012**, *45*, 788. d) Yoshikai, N. *Synlett* **2011**, 1047. e) Lyons, T. W.; Sanford, M. S. *Chem. Rev.* **2010**, *110*, 1147. f) Colby, D. A.; Bergman, R. G.; Ellman, J. A. *Chem. Rev.* **2010**, *110*, 624.

8. a) Ackermann, L. *Acc. Chem. Res.* **2014**, *47*, 281. b) Satoh, T.; Miura, M. *Chem. Eur. J.* **2010**, *16*, 11212. c) Thansandote, P.; Lautens, M. *Chem. Eur. J.* **2009**, *15*, 5874.
9. a) Du, Y.; Hyster, T. K.; Rovis, T. *Chem. Commun.* **2011**, *47*, 12074. b) Wrigglesworth, J. W.; Cox, B.; Lloyd-Jones, G. C.; Booker-Milburn, K. I. *Org. Lett.* **2011**, *13*, 5326. c) Inoue, S.; Shiota, H.; Fukumoto, Y.; Chatani, N. *J. Am. Chem. Soc.* **2009**, *131*, 6898.
10. a) Ye, B.; Cramer, N. *Angew. Chem. Int. Ed.* **2014**, *53*, 7896. b) Hyster, T. K.; Ruhl, K. E.; Rovis, T. *J. Am. Chem. Soc.* **2013**, *135*, 5364. c) Zhu, C.; Xie, W.; Falck, J. R. *Chem. Eur. J.* **2011**, *17*, 12591.
11. a) Webb, N. J.; Marsden, S. P.; Raw, S. A. *Org. Lett.* **2014**, *16*, 4718. b) Huckins, J. R.; Bercot, E. A.; Thiel, O. R.; Hwang, T.-L.; Bio, M. M. *J. Am. Chem. Soc.* **2013**, *135*, 14492. c) Wang, H.; Grohmann, C.; Nimphius, C.; Glorius, F. *J. Am. Chem. Soc.* **2012**, *134*, 19592. d) Shiota, H.; Ano, Y.; Aihara, Y.; Fukumoto, Y.; Chatani, N. *J. Am. Chem. Soc.* **2011**, *133*, 14952. e) Guimond, N.; Gorelsky, S. I.; Fagnou, K. *J. Am. Chem. Soc.* **2011**, *133*, 6449. f) Li, B.; Feng, H.; Xu, S.; Wang, B. *Chem. Eur. J.* **2011**, *17*, 12573. g) Hyster, T. K.; Rovis, T. *J. Am. Chem. Soc.* **2010**, *132*, 10565. h) Guimond, N.; Gouliaras, C.; Fagnou, K. *J. Am. Chem. Soc.* **2010**, *132*, 6908. i) Song, G.; Chen, D.; Pan, C.-L.; Crabtree, R. H.; Li, X. *J. Org. Chem.* **2010**, *75*, 7487. j) Mochida, S.; Umeda, N.; Hirano, K.; Satoh, T.; Miura, M. *Chem. Lett.* **2010**, *39*, 744.
12. a) Hyster, T. K.; Dalton, D. M.; Rovis, T. *Chem. Sci.* **2014**, doi: 10.1039/C4SC02590C. b) Tang, Q.; Xia, D.; Jin, X.; Zhang, Q.; Sun, X.-Q.; Wang, C. *J. Am. Chem. Soc.* **2013**, *135*, 4628. c) Davis, T. A.; Hyster, T. K.; Rovis, T. *Angew. Chem. Int. Ed.* **2013**, *52*, 14181. d) Ye, B.; Cramer, N. *Science* **2012**, *338*, 504. e) Hyster, T. K.; Knorr, L.; Ward, T. R.; Rovis, T. *Science* **2012**, *338*, 500. f) Li, B.; Ma, J.; Wang, N.; Feng, H.; Xu, S.; Wang, B. *Org. Lett.*

- 2012**, *14*, 736. g) Rakshit, S.; Grohmann, C.; Besset, T.; Glorius, F. *J. Am. Chem. Soc.* **2011**, *133*, 2350. h) References 11b and 11e.
13. a) Hyster, T. K.; Rovis, T. *Chem. Sci.* **2011**, *2*, 1606. b) Ackermann, L.; Lygin, A. V.; Hofmann, N. *Org. Lett.* **2011**, *13*, 3278. c) Su, Y.; Zhao, M.; Han, K.; Song, G.; Li, X. *Org. Lett.* **2010**, *12*, 5462.
14. a) He, R.; Huang, Z.-T.; Zheng, Q.-Y.; Wang, C. *Angew. Chem. Int. Ed.* **2014**, *53*, 4950. b) Zhao, D.; Lied, F.; Glorius, F. *Chem. Sci.* **2014**, *5*, 2869. c) Chuang, S.-C.; Gandeepan, P.; Cheng, C.-H. *Org. Lett.* **2013**, *15*, 5750. d) Villuendas, P.; Urriolabeitia, E. P. *J. Org. Chem.* **2013**, *78*, 5254. e) Chinnagolia, R. K.; Pimparkar, S.; Jeganmohan, M. *Org. Lett.* **2012**, *14*, 3032. f) Zheng, L.; Ju, J.; Bin, Y.; Hua, R. *J. Org. Chem.* **2012**, *77*, 5794. g) Too, P. C.; Chua, S. H.; Wong, S. H.; Chiba, S. *J. Org. Chem.* **2011**, *76*, 6159. h) Zhang, X.; Chen, D.; Zhao, J.; Jia, A.; Li, X. *Adv. Synth. Catal.* **2011**, *353*, 719. i) Too, P. C.; Wang, Y.-F.; Chiba, S. *Org. Lett.* **2010**, *12*, 5688. j) Guimond, N.; Fagnou, K. *J. Am. Chem. Soc.* **2009**, *131*, 12050. k) Parthasarathy, K.; Cheng, C.-H. *J. Org. Chem.* **2009**, *74*, 9359. l) Lim, S. G.; Lee, J. H.; Moon, C. W.; Hong, J. B.; Jun, C. H. *Org. Lett.* **2003**, *5*, 2759.
15. Taylor, R. D.; MacCoss, M.; Lawson, A. D. G. *J. Med. Chem.* **2014**, *57*, 5845.
16. For reviews, see: a) Bull, J. A.; Mousseau, J. J.; Pelletier, G.; Charette, A. B. *Chem. Rev.* **2012**, *112*, 2642. b) Nakao, Y. *Synthesis* **2011**, 3209. c) Hill, M. D. *Chem. Eur. J.* **2010**, *16*, 12052. d) Schlosser, M.; Mongin, F. *Chem. Soc. Rev.* **2007**, *36*, 1161. e) Henry, G. D. *Tetrahedron* **2004**, *60*, 6043. f) Varela, J. A.; Saá, C. *Chem. Rev.* **2003**, *103*, 3787. g) Joule, J. A.; Mills, K. *Heterocyclic Chemistry*, 4<sup>th</sup> ed.; Blackwell Science: Malden, MA, 2000.
17. For recent examples, see: a) Jiang, Y.; Park, C.-M.; Loh, T.-P. *Org. Lett.* **2014**, *16*, 3432. b) Londregan, A. T.; Burford, K.; Conn, E. L.; Hesp, K. D. *Org. Lett.* **2014**, *16*, 3336. c) Chen,



Q.; Mollat du Jourdin, X.; Knochel, P. *J. Am. Chem. Soc.* **2013**, *135*, 4958. d) Lei, C.-H.; Wang, D.-X.; Zhao, L.; Zhu, J.; Wang, M.-X. *J. Am. Chem. Soc.* **2013**, *135*, 4708. e) Wei, Y.; Yoshikai, N. *J. Am. Chem. Soc.* **2013**, *135*, 3756. f) Stark, D. G.; Morrill, L. C.; Yeh, P.-P.; Slawin, A. M. Z.; O’Riordan, T. J. C.; Smith, A. D. *Angew. Chem. Int. Ed.* **2013**, *52*, 11642. g) Michlik, S.; Kempe, R. *Angew. Chem. Int. Ed.* **2013**, *52*, 6326. h) Andou, T.; Saga, Y.; Komai, H.; Matsunaga, S.; Kanai, M. *Angew. Chem. Int. Ed.* **2013**, *52*, 3213. i) Loy, N. S. Y.; Singh, A.; Xu, X.; Park, C.-M. *Angew. Chem. Int. Ed.* **2013**, *52*, 2212. j) Hoshikawa, T.; Inoue, M. *Chem. Sci.* **2013**, *4*, 3118. k) He, Z.; Dobrovolsky, D.; Trinchera, P.; Yudin, A. K. *Org. Lett.* **2013**, *15*, 334. l) Satoh, Y.; Obora, Y. *J. Org. Chem.* **2013**, *78*, 7771. m) Gati, W.; Rammah, M. M.; Rammah, M. B.; Couty, F.; Evano, G. *J. Am. Chem. Soc.* **2012**, *134*, 9078. n) Chen, M. Z.; Micalizio, G. C. *J. Am. Chem. Soc.* **2012**, *134*, 1352. o) Yamamoto, S.-I.; Okamoto, K.; Murakoso, M.; Kuninobu, Y.; Takai, K. *Org. Lett.* **2012**, *14*, 3182. p) Ye, M.; Gao, G.-L.; Edmunds, A. J. F.; Worthington, P. A.; Morris, J. A.; Yu, J.-Q. *J. Am. Chem. Soc.* **2011**, *133*, 19090. q) Ohashi, M.; Takeda, I.; Ikawa, M.; Ogoshi, S. *J. Am. Chem. Soc.* **2011**, *133*, 18018. r) Ye, M.; Gao, G.-L.; Yu, J.-Q. *J. Am. Chem. Soc.* **2011**, *133*, 6964. s) Wang, Y.-F.; Toh, K. K.; Ng, E. P. J.; Chiba, S. *J. Am. Chem. Soc.* **2011**, *133*, 6411. t) Wang, C.; Li, X.; Wu, F.; Wan, B. *Angew. Chem. Int. Ed.* **2011**, *50*, 7162. u) Kral, K.; Hapke, M. *Angew. Chem., Int. Ed.* **2011**, *50*, 2434. v) Li, B.-J.; Shi, Z.-J. *Chem. Sci.* **2011**, *2*, 488.

18. For a review of pyridine synthesis by formal [4+2] cycloaddition of 1-azadienes, see: Neely, J. M.; Rovis, T. *Org. Chem. Front.* **2014**, *1*, 1010.

19. For methods catalyzed by other transition metals, see: a) Yoshida, Y.; Kurahashi, T.; Matsubara, S. *Chem. Lett.* **2012**, *41*, 1498. b) Liu, S.; Liebeskind, L. S. *J. Am. Chem. Soc.* **2008**, *130*, 6918.
20. Kapdi, A. R. *Dalton Trans.* **2014**, *43*, 3021.
21. a) Ackermann, L. *Chem. Rev.* **2011**, *111*, 1315. For selected early studies regarding C–H activation by concerted metalation deprotonation, see: b) Gorelsky, S. I.; Lapointe, D.; Fagnou, K. *J. Am. Chem. Soc.* **2008**, *130*, 10848. c) García–Cuadrado, D.; de Mendoza, P.; Braga, A. A. C.; Maseras, F.; Echavarren, A. M. *J. Am. Chem. Soc.* **2007**, *129*, 6880. d) García–Cuadrado, D.; Braga, A. A. C.; Maseras, F.; Echavarren, A. M. *J. Am. Chem. Soc.* **2006**, *128*, 1066.
22. a) Thalji, R. K.; Ahrendt, K. A.; Bergman, R. G.; Ellman, J. A. *J. Org. Chem.* **2005**, *70*, 6775. b) Thalji, R. K.; Ellman, R. G.; Ellman, J. A. *J. Am. Chem. Soc.* **2004**, *126*, 7192. c) Thalji, R. K.; Ahrendt, K. A.; Bergman, R. G.; Ellman, J. A. *J. Am. Chem. Soc.* **2001**, *123*, 9692.
23. Colby, D. A.; Bergman, R. G.; Ellman, J. A. *J. Am. Chem. Soc.* **2008**, *130*, 3645.
24. a) Lee, H.; Sim, Y.–K.; Park, J.–W.; Jun, C.–H. *Chem. Eur. J.* **2013**, *20*, 323. b) Sim, Y.–K.; Lee, H.; Park, J.–W.; Kim, D.–S.; Jun, C.–H. *Chem. Commun.* **2012**, *48*, 11787.
25. For a review of oxidizing directing groups, see: Patureau, F. W.; Glorius, F. *Angew. Chem. Int. Ed.* **2011**, *50*, 1977.
26. Dong and coworkers recently demonstrated the use of *N*–sulfonyl imines as oxidizing directing groups for pyridine synthesis. See: Zhang, Q.–R.; Huang, J.–R.; Zhang, W.; Dong, L. *Org. Lett.* **2014**, *16*, 1684.

27. For the Rh(I)-catalyzed intramolecular reaction of  $\epsilon$ -alkynyl  $\alpha,\beta$ -unsaturated oxime ethers, see: Saito, A.; Hironaga, M.; Oda, S.; Hanzawa, Y. *Tetrahedron Lett.* **2007**, *48*, 6852.
28. a) Parthasarathy, K.; Cheng, C.-H. *Synthesis* **2009**, 1400. b) Parthasarathy, K.; Jegannathan, M.; Cheng, C.-H. *Org. Lett.* **2008**, *10*, 325.
29. Too, P. C.; Noji, T.; Lim, Y. J.; Li, X.; Chiba, S. *Synlett* **2011**, 2789.
30. Hyster, T. K.; Rovis, T. *Chem. Commun.* **2011**, *47*, 11846.
31. a) Ritleng, V.; Sirlin, C.; Pfeffer, M. *Chem. Rev.* **2002**, *102*, 1731. b) Reference 23.
32. Martin, R. M.; Bergman, R. G.; Ellman, J. A. *J. Org. Chem.* **2012**, *77*, 2501.
33. a) Han, S.; Shin, Y.; Sharma, S.; Mishra, N. K.; Park, J.; Kim, M.; Kim, M.; Jang, J.; Kim, I. *S. Org. Lett.* **2014**, *16*, 2494. b) Xie, W.; Yang, J.; Wang, B.; Li, B. *J. Org. Chem.* **2014**, *79*, 8278. c) Zhang, Y.; Zheng, J.; Cui, S. *J. Org. Chem.* **2014**, *79*, 6490. d) Mishra, N. K.; Park, J.; Sharma, S.; Han, S.; Kim, M.; Shin, Y.; Jang, J.; Kwak, J. H.; Jung, Y. H.; Kim, I. S. *Chem. Commun.* **2014**, *50*, 2350. e) Suzuki, C.; Morimoto, K.; Hirano, K.; Satoh, T.; Miura, M. *Adv. Synth. Catal.* **2014**, *356*, 1521. f) Liu, B.; Fan, Y.; Gao, Y.; Sun, C.; Xu, C.; Zhu, J. *J. Am. Chem. Soc.* **2013**, *135*, 468. g) Kwak, J.; Ohk, Y.; Jung, Y.; Chang, S. *J. Am. Chem. Soc.* **2012**, *134*, 17778. h) Zhao, P.; Wang, F.; Han, K.; Li, X. *Org. Lett.* **2012**, *14*, 3400. i) Zhu, C.; Falck, J. R. *Chem. Commun.* **2012**, *48*, 1674. j) Li, X.; Gong, X.; Zhao, M.; Song, G.; Deng, J.; Li, X. *Org. Lett.* **2011**, *13*, 5808. k) Besset, T.; Kuhl, N.; Patureau, F. W.; Glorius, F. *Chem. Eur. J.* **2011**, *17*, 7167. l) Willwacher, J.; Rakshit, S.; Glorius, F. *Org. Biomol. Chem.* **2011**, *9*, 4736. m) Reference 12. n) Wang, F.; Song, G.; Du, Z.; Li, X. *J. Org. Chem.* **2011**, *76*, 2926 and references cited therein.
34. Colby, D. A.; Bergman, R. G.; Ellman, J. A. *J. Am. Chem. Soc.*, **2006**, *128*, 5604.
35. Tsai, A. S.; Brasse, M.; Bergman, R. G.; Ellman, J. A. *Org. Lett.* **2011**, *13*, 540.

36. Neely, J. M.; Rovis, T. *J. Am. Chem. Soc.* **2013**, *135*, 66.
37. For a review of  $[\text{RhCp}^*\text{Cl}_2]_2$  in C–H functionalization, see: Patureau, F. W.; Wencel–Delord, J.; Glorius, F. *Aldrichim. Acta* **2012**, *45*, 31.
38. a) Bordwell, F. G. *Acc. Chem. Res.* **1988**, *21*, 456. b) Olmstead, W. N.; Margolin, Z.; Bordwell, F. G. *J. Org. Chem.* **1980**, *45*, 3295.
39. Boyer, P. M.; Roy, C. P.; Bielski, J. M.; Merola, J. S. *Inorg. Chim. Acta* **1996**, *245*, 7.
40. Zhang, G.; Yang, L.; Wang, Y.; Xie, Y.; Huang, H. *J. Am. Chem. Soc.* **2013**, *135*, 8850.
41. a) Reference 33g. b) Umeda, N.; Hirano, K.; Satoh, T.; Miura, M. *J. Org. Chem.* **2009**, *74*, 7094.
42. a) Lu, J.–Y.; Keith, J. A.; Shen, W.–Z.; Schürmann, M.; Preut, H.; Jacob, T.; Arndt, H.–D. *J. Am. Chem. Soc.* **2008**, *130*, 13219. b) Lu, J.–Y.; Arndt, H.–D. *J. Org. Chem.* **2007**, *72*, 4205.
43. For an example of  $6\pi$ –electrocyclization of a 1–azatriene derivative, see: Trost, B. M.; Gutierrez, A. C. *Org. Lett.* **2007**, *9*, 1473.
44. Eisner, U.; Kuthan, J. *Chem. Rev.* **1972**, *72*, 1.
45. For examples of 1,2–dihydropyridine oxidation by atmospheric oxygen, see: a) Palacios, F.; Alonso, C.; Rubiales, G.; Ezpeleta, J. M. *Eur. J. Org. Chem.* **2001**, 2115. b) Palacios, F.; Herrán, E.; Rubiales, G. *J. Org. Chem.* **1999**, *64*, 6239.
46. A portion of this work was accomplished by Kassandra Sedillo.
47. Anslyn, E. V.; Dougherty, D. A. *Modern Physical Organic Chemistry*; University Science Books: Sausalito, CA, 2006.

## CHAPTER TWO

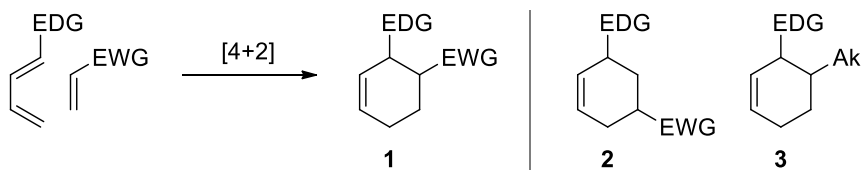
### Rhodium(III)–Catalyzed Decarboxylative Coupling of $\alpha,\beta$ –Unsaturated Oxime Esters and Acrylic Acids: Selective Synthesis of 5–Substituted Pyridines

#### 2.1 Introduction

##### 2.1.1 Product Selectivity in Synthetic Methodology

In any synthetic method, selectivity for the desired product is just as important as reactivity.<sup>1</sup> If a reaction is complete but multiple products are generated, starting materials incorporated into undesired isomers go to waste. Fortunately, chemical transformations often exhibit remarkable sensitivity to the steric and electronic nature of substrates. In a classic example, appropriately activated  $\pi$ –components undergo Diels Alder cycloaddition selectively based on favorable orbital interactions,<sup>2</sup> providing a reliable route to compounds like **1** (Scheme 2.1, EDG = electron–donating group, EWG = electron–withdrawing group). However, a synthetic target may require a substitution pattern contrary to what is dictated by inherent substrate bias (as in **2**) or one involving substrates that lack necessary properties for selectivity, for instance, Diels Alder cycloaddition of an unactivated alkene to afford **3** (Ak = alkyl). If so, access to the synthetic target necessitates either an alternate method or a means of encouraging selectivity.

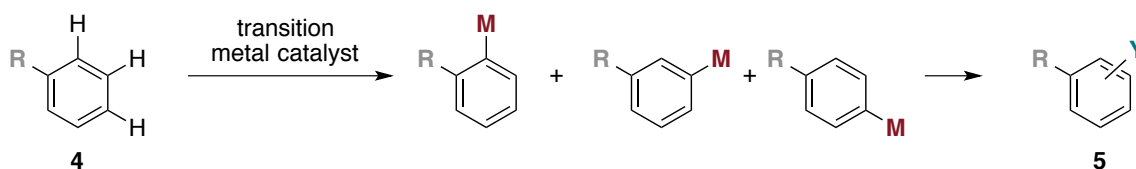
Synthetic chemists have devised a variety of clever strategies for promoting selectivity in otherwise unselective transformations. One such strategy is the use of a directing group for



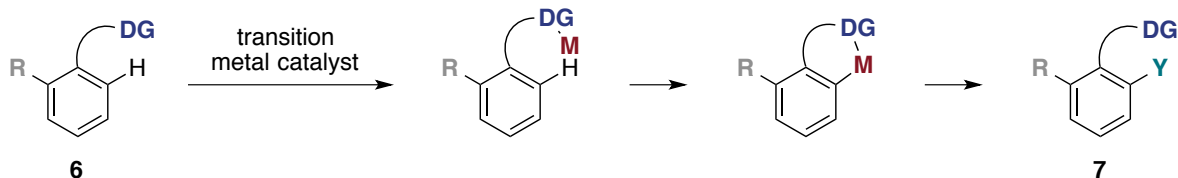
**Scheme 2.1.** Diels Alder cycloaddition.

site selectivity in transition metal–catalyzed C–H functionalization (Scheme 2.2).<sup>3</sup> As an illustration, ignoring any steric or electronic influence of the substituent (R), C–H activation of benzene derivative **4** presumably affords a mixture of isomeric products **5** (Scheme 2.2a). In the case of substrate **6**, on the other hand, coordination of the catalyst by the directing group (DG) brings the adjacent C–H bond in proximity to the metal center, resulting in selective C–H activation and formation of functionalized product **7** (Scheme 2.2b).

**a. Not directed**



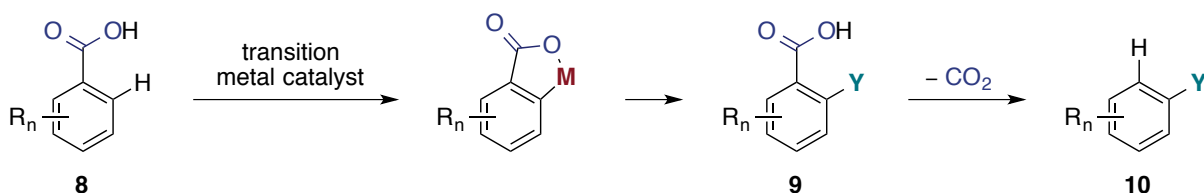
**b. Directed**



**Scheme 2.2.** Selectivity in C–H functionalization.

**2.1.2 Removable Directing Groups in Transition Metal–Catalyzed C–H Functionalization**

One potential caveat in directed C–H functionalization reactions is inclusion of directing groups within products. With this in mind, considerable research effort has targeted incorporation of synthetically useful directing groups.<sup>4</sup> Conversely, several studies have identified directing groups that may be removed either *in situ* or in a subsequent step.<sup>5,6</sup> In these



**Scheme 2.3.** Carboxylic acids as removable directing groups.

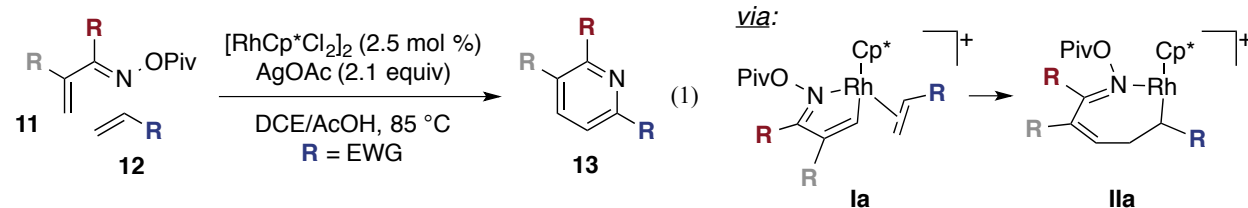
examples, C–H activation proceeds selectively without requiring directing groups in the functionalized products.

Carboxylic acids are effective directing groups for C–H activation in a variety of functionalization reactions (**8** → **9**, Scheme 2.3).<sup>7</sup> Furthermore, several reports have demonstrated decarboxylation processes<sup>8</sup> that result in carboxylic acid removal from a variety of (hetero)aryl substrates (**9** → **10**).<sup>9</sup> Indeed, these two modes of reactivity have been combined for selective C–H functionalization reactions in which carboxylic acids serve as removable directing groups (**8** → **10**, Scheme 2.3) for C–H alkenylation,<sup>10</sup> arylation<sup>11</sup> and etherification.<sup>12</sup>

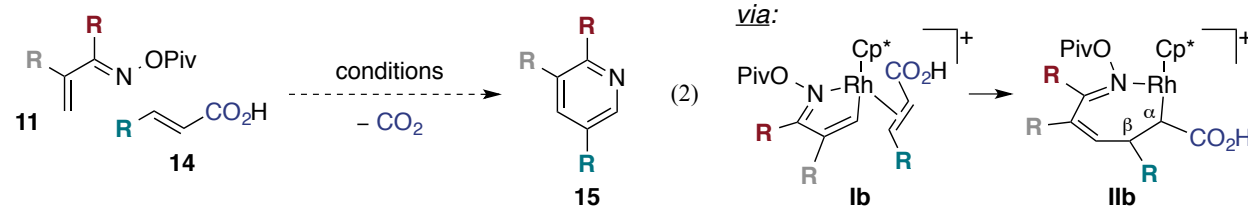
### 2.1.3 Rhodium–Catalyzed Decarboxylative Coupling with $\beta$ -Substituted Acrylic Acids

We envisioned a related decarboxylation strategy for pyridine synthesis by Rh(III)–catalyzed annulation of *O*-pivaloyl  $\alpha,\beta$ -unsaturated oxime esters (**11**) and acrylic acid derivatives (**14**, Scheme 2.4). Our previous research showed electron deficient terminal alkenes (**12**) incorporate with exquisite selectivity to access 6-substituted pyridines (**13**, eq 1).<sup>13</sup> These results can be explained by preferred 2,1-insertion of the alkene substrate in **Ia**, favored by a

#### Prior work:<sup>13</sup>



#### Proposed:



**Scheme 2.4.** Synthesis of 6- and 5-substituted pyridines from unsaturated oximes and alkenes.

stronger, more polar Rh–C bond in intermediate **IIa**.<sup>14</sup> Likewise, complex **IIb** should undergo migratory insertion to favor installation of the carboxylic acid moiety  $\alpha$  to the metal center (thus placement of the substituent  $\beta$ ) in rhodacycle **IIb**. Ideally, subsequent decarboxylation would proceed *in situ* to afford pyridine products directly.<sup>15</sup> In this way, Rh(III)–catalyzed coupling of  $\alpha,\beta$ –unsaturated oxime esters (**11**) and acrylic acid derivatives (**15**) should access 5–substituted pyridine products (**15**, eq 2) selectively,<sup>16,17</sup> complementing our prior work in this area.<sup>13</sup>

The reaction of oxime substrate **11a** and acrylic acid (**16**, eq 3) provided inspiration for the proposed decarboxylative method for pyridine synthesis. In the presence of catalytic  $[\text{RhCp}^*\text{Cl}_2]_2$  ( $\text{Cp}^*$  = pentamethylcyclopentadienyl) and 2.1 equivalents silver(I) acetate ( $\text{AgOAc}$ ), the expected picolinic acid product **18a** is not observed. Instead, the reaction affords dialkyl pyridine **17a**, the result of overall loss of  $\text{CO}_2$ , in 60% yield. An initial survey of reaction

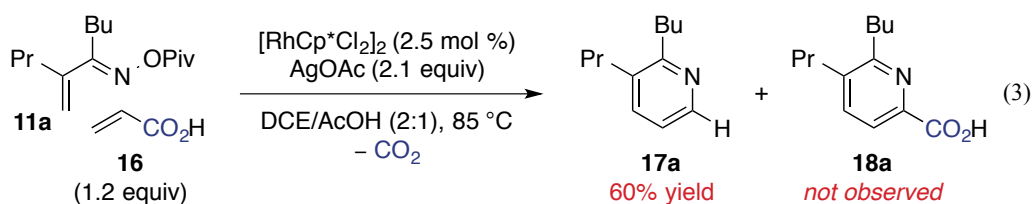
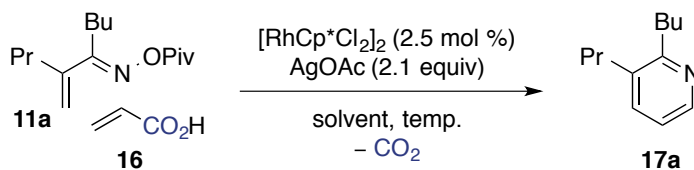


**Table 2.1.** Initial optimization with acrylic acid (**16**).<sup>a</sup>



entry	solvent	temperature ( $^\circ\text{C}$ )	concentration (M)	yield <b>17a</b> (%) <sup>b</sup>
1	DCE/AcOH (2:1)	85	0.3	60
2	DCE/AcOH (9:1)	85	0.3	45
3	AcOH	85	0.3	50
4	TFE	78	0.3	85
5	TFE	78	0.15	80
6	TFE	78	0.6	85

<sup>a</sup>Conditions: 1.2 equiv **16**. <sup>b</sup>Determined by  $^1\text{H}$  NMR.



solvents and concentrations (Table 2.1) found a 0.3 M solution of 2,2,2-trifluoroethanol (TFE) to be optimal for reactivity, providing **17a** in 85% yield (entry 4).

## 2.2 Results<sup>18</sup>

### 2.2.1 Reaction Optimization

We turned our attention to the synthesis of 5-substituted pyridines **15**, beginning with the reaction of oxime **11b** and crotonic acid (**14a**, eq 4). To our delight, pyridine **15ba** is the only observed product in this case, indicating both selective alkene incorporation and complete removal of the carboxylic acid group under the reaction conditions. We began optimizing

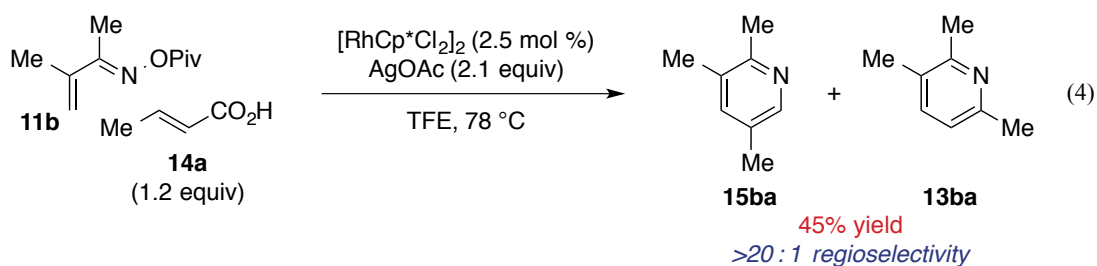
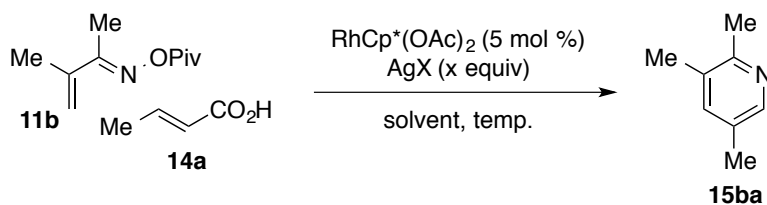


**Table 2.2.** Initial optimization with crotonic acid (**14a**).<sup>a</sup>



entry	AgX (x equiv)	solvent	temp. (°C)	yield <b>15ba</b> (%) <sup>b</sup>
1	AgOAc (2.1 equiv)	TFE	78	45
2	AgOAc (2.1 equiv)	HFIP	78	50
3 <sup>c</sup>	AgOAc (2.1 equiv)	HFIP	58	30
4	AgO (1.05 equiv)	TFE	78	40
5	Ag <sub>2</sub> O (1.05 equiv)	TFE	78	15
6	AgO (2.1 equiv)	TFE	78	20
7	AgO (1.05 equiv)	HFIP	78	45
8	AgO (1.05 equiv)	TFE	100	25
9	AgO (1.05 equiv)	HFIP	100	40

<sup>a</sup>Conditions: 1.2 equiv **14a**, 0.3 M, 12 h. <sup>b</sup>Determined by <sup>1</sup>H NMR. <sup>c</sup>With 2.5 mol % [RhCp\*Cl<sub>2</sub>]<sub>2</sub>.

conditions for Rh(III)-catalyzed decarboxylative coupling of **11b** and **14a** by evaluating silver reagents and fluorinated alcohol solvents (Table 2.2). In addition to TFE, 1,1,1,3,3,3-hexafluoroisopropanol (HFIP) is a competent solvent for the reaction at 78 °C (entry 2); decreased reactivity is observed at 58 °C (entry 3). Use of silver(II) oxide (AgO) as the stoichiometric oxidant results in 40% yield **15ba** (entry 4), while the reaction with silver(I) oxide (Ag<sub>2</sub>O) affords **15ba** in 15% yield (entry 5). In fact, the reagent labeled silver(II) oxide or AgO likely exists as a 1:1 mixture of silver(I) and silver(III) species.<sup>19</sup> Since Ag<sub>2</sub>O (silver(I)) is a less efficient oxidant for decarboxylative coupling of **11b** and **14a**, we wondered if addition of 2.1 equivalents AgO (thus, 2.1 equivalents silver(III)) would benefit reactivity. Actually, pyridine **15ba** forms in only 20% yield under these conditions (entry 6). Finally, reactions conducted in both TFE and HFIP at 100 °C lead to decreased product yields (entries 8 and 9).

One major difference between the current transformation and our prior work is the stoichiometric amount of carboxylic acid (RCO<sub>2</sub>H). Acid dissociation (RCO<sub>2</sub>H → RCO<sub>2</sub><sup>-</sup> + H<sup>+</sup>) results in a negatively charged alkene component as well as a more acidic reaction medium: two changes that certainly could affect the desired reaction. For this reason, we investigated the addition of acidic or basic reagents to the reaction of **11b** and **14a**, using high throughput experimentation (HTE) as an efficient means for screening additives (Figure 2.1). Concentrating on the two effective catalyst/oxidant systems ([RhCp\*Cl<sub>2</sub>]<sub>2</sub>/AgOAc and RhCp\*(OAc)<sub>2</sub>/AgO) and two competent solvents (TFE and HFIP), twelve different additives were employed in both catalytic and stoichiometric amounts, constituting 96 different combinations. General conclusions from the data shown in Figure 2.1 include: a) use of acidic additives benefits reactivity and b) higher product yields are observed when HFIP is the solvent. Specifically, addition of 1 equivalent *p*-toluenesulfonic acid (TsOH) to reactions in HFIP results in the

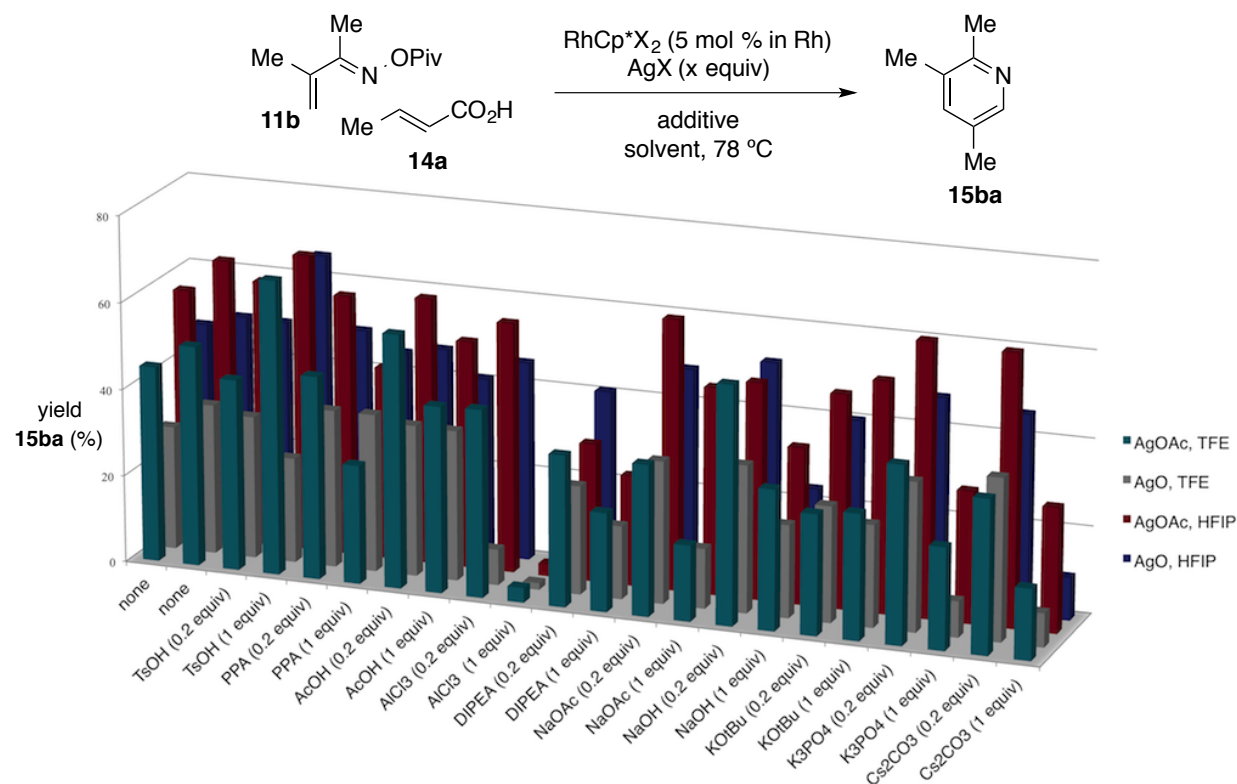
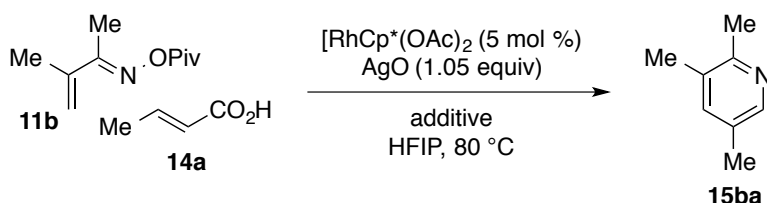


**Figure 2.1.** Screening of acid and base additives using HTE.

highest yields of **15ba** observed in this screen. AgO is as effective as AgOAc in this system, so we chose to continue our investigation using the less expensive reagent, AgO. The benefit of adding 1 equivalent TsOH to the reaction of **11b** and **14a** on the small scale needed for HTE was confirmed using standard reaction setup on 0.12 mmol scale (entry 1, Table 2.3). Since oxidation by AgO theoretically generates water, hygroscopic agents were also examined. Addition of 3Å molecular sieves or magnesium sulfate (MgSO<sub>4</sub>) under the previous conditions (entries 2 and 3) or in combination with 1 equivalent TsOH (entries 4 and 5) lends no improvement to the reaction. Replacing TsOH with Amberlyst 15, a polymeric sulfonic acid, results in decreased reactivity (entry 6). Addition of 1 equivalent methanesulfonic acid (MeSO<sub>3</sub>H) leads to formation of pyridine **15ba** in 75% yield (entry 7), while complete decomposition of oxime substrate **11b** occurs in the presence of excess MeSO<sub>3</sub>H (entry 8).

The positive effect of sulfonic acid additives has a few potential explanations, apart from acidity of the reaction medium. For one, ligand exchange could afford a rhodium tosylate complex *in situ*, which may be more reactive. To test this possibility, RhCp\*(OTs)<sub>2</sub> was prepared and employed in the otherwise standard reaction. In this case, pyridine **15ba** forms in 45% yield (entry 3, Table 2.4), suggesting the enhanced reactivity is not due to generation of

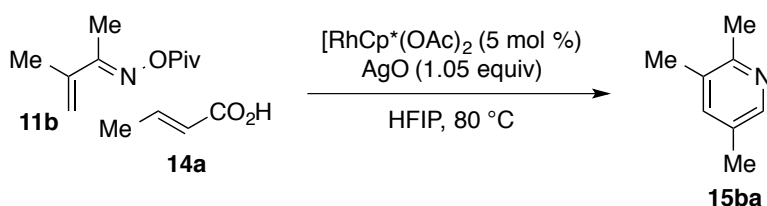
**Table 2.3.** Sulfonic acid and hygroscopic additives.<sup>a</sup>



entry	additive	yield <b>15ba</b> (%) <sup>b</sup>
1	TsOH (1 equiv)	75
2	3Å mol sieves	30
3	MgSO <sub>4</sub>	45
4	TsOH (1 equiv) + 3Å mol sieves	65
5	TsOH (1 equiv) + MgSO <sub>4</sub>	65
6	Amberlyst 15 (1 equiv)	30
7	MeSO <sub>3</sub> H (1 equiv)	75
8	MeSO <sub>3</sub> H (2 equiv)	0

<sup>a</sup>Conditions: 1.2 equiv **14a**, 0.3 M, 12 h. <sup>b</sup>Determined by <sup>1</sup>H NMR.

**Table 2.4.** The effect of sulfonic acid additives.<sup>a</sup>



entry	change	yield <b>15ba</b> (%) <sup>b</sup>
1	none	45
2	TsOH (1 equiv) additive	75
3	RhCp*(OTs) <sub>2</sub> (5 mol %)	45
4	AgOTs (2.1 equiv)	75

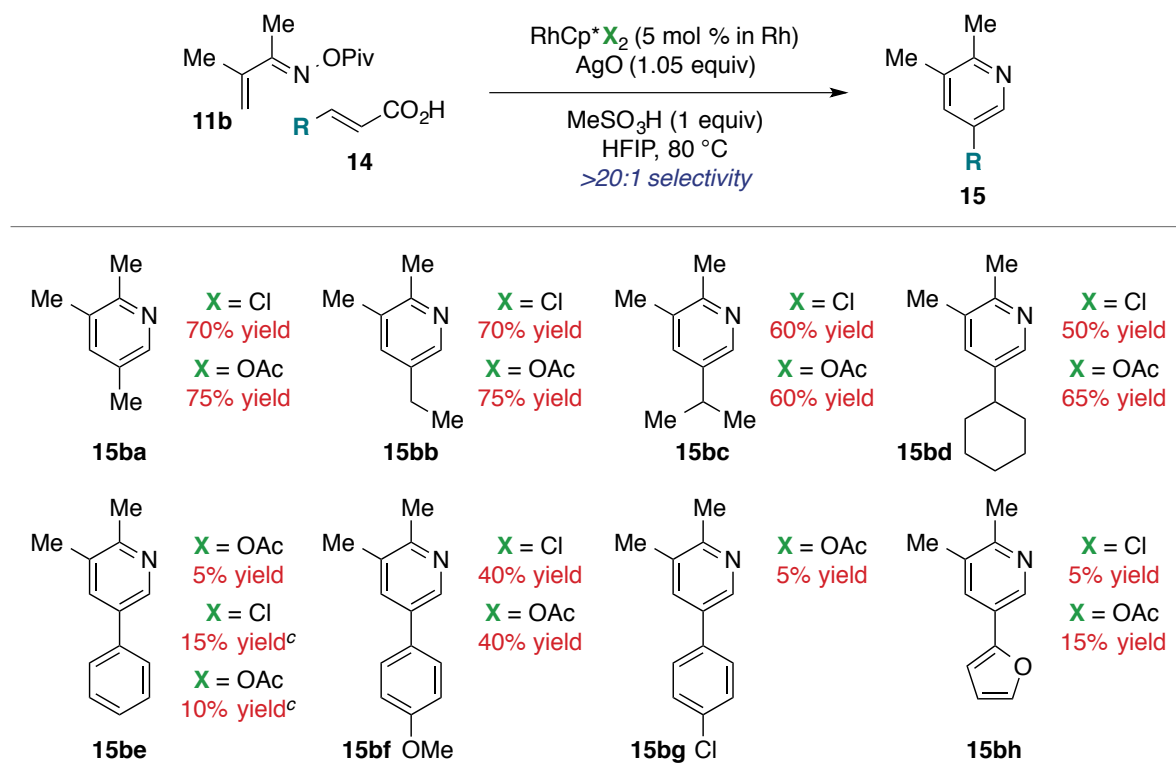
<sup>a</sup>Conditions: 1.2 equiv **14a**, 0.3 M, 12 h. <sup>b</sup>Determined by <sup>1</sup>H NMR.

rhodium tosylate complex.

Alternately, combination of AgO and TsOH could produce AgOTs *in situ*, perhaps providing a more effective oxidizing reagent. Indeed, reaction of **11b** and **14a** in the presence of 2.1 equivalents AgOTs affords pyridine **16ba** in 75% yield (entry 4). The greater solubility of AgOTs compared to AgO in the reaction medium offers one potential explanation for this difference in reactivity.

We explored the scope of Rh(III)-catalyzed annulation of oxime **11b** and various

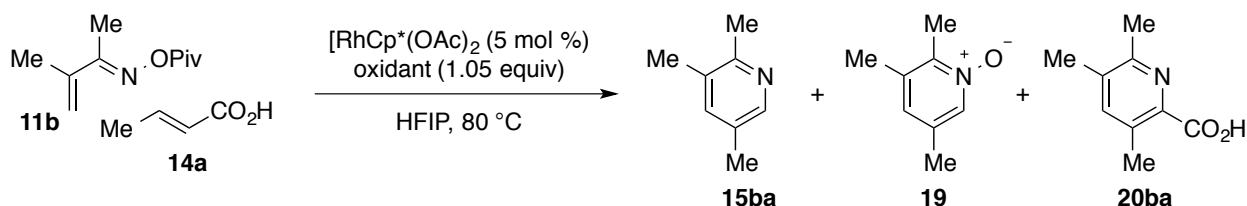
**Chart 2.1.** Initial examination of the reaction scope.<sup>a,b</sup>



<sup>a</sup>Conditions: 1.2 equiv **14**, 0.3 M, 12 h. <sup>b</sup>Yields determined by <sup>1</sup>H NMR. <sup>c</sup>With (Z)-cinnamic acid.

acrylic acid derivatives (**14**) in the presence of 1.05 equivalents AgO and 1 equivalent MeSO<sub>3</sub>H (Chart 2.1). For each substrate, both [RhCp\*Cl<sub>2</sub>]<sub>2</sub> and RhCp\*(OAc)<sub>2</sub> precatalysts were evaluated, although no significant differences were observed. Decarboxylative coupling of a variety of alkyl-substituted acrylic acids proceeds to complete conversion with >20:1 selectivity for 5-alkyl pyridines (**15ba–15bd**). Reactions of aryl-substituted acrylic acids also favor formation of 5-substituted products (**15be–15bh**), but in lower yields. In fact, significant decomposition of furyl substrate **14h** occurs under the standard conditions as well as in control reactions. For these reasons, a second examination of stoichiometric oxidants was conducted.

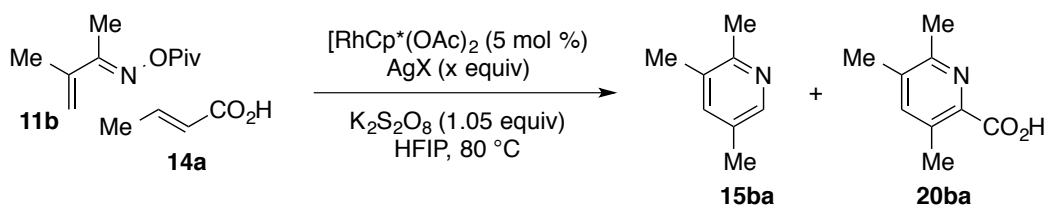
Inspired by a recent report in which rhodium(I) precatalysts were activated by oxidation with benzoyl peroxide,<sup>20</sup> we evaluated potential peroxy-type oxidants (Table 2.5). Various organic peroxides effect the desired annulation (entries 1–4); however, the decarboxylation

**Table 2.5.** Investigation of peroxy-type oxidants.<sup>a</sup>

entry	oxidant	yield <b>15ba</b> (%) <sup>b</sup>	yield <b>19</b> (%) <sup>b</sup>	yield <b>20ba</b> (%) <sup>b</sup>
1	BzOOBz	<5	15	10
2	<i>t</i> BuOO <i>t</i> Bu	<5	10	10
3	BzOO <i>t</i> Bu	<5	15	20
4	<i>t</i> BuOOH	<5	5	15
5	KHSO <sub>5</sub> <sup>c</sup>	20	<5	10
6	K <sub>2</sub> S <sub>2</sub> O <sub>8</sub>	15	<5	15

<sup>a</sup>Conditions: 1.2 equiv **14a**, 0.3 M, 12h. <sup>b</sup>Determined by <sup>1</sup>H NMR. <sup>c</sup>As 2KHSO<sub>5</sub>·KHSO<sub>4</sub>·K<sub>2</sub>SO<sub>4</sub> (Oxone).

process is incomplete and picolinic acid **20ba** is observed in these cases. Furthermore, pyridine products undergo additional oxidation to pyridine *N*-oxides **19** under these conditions. On the other hand, over-oxidation to **19** does not occur in the presence of potassium peroxymonosulfate (KHSO<sub>5</sub>, entry 5) or potassium persulfate (K<sub>2</sub>S<sub>2</sub>O<sub>8</sub>, entry 6). These reactions afford mixtures of the desired pyridine **15ba** and picolinic acid **20ba**. We elected to continue our study using

**Table 2.6.** Silver additive screen.<sup>a</sup>

entry	AgX (x equiv)	yield <b>15ba</b> (%) <sup>b</sup>	yield <b>20ba</b> (%) <sup>b</sup>
1	AgOTs (0.25 equiv)	50	5
2	AgOTs (0.5 equiv)	70	5
3	AgOTs (0.7 equiv)	75	<5
4	AgOTs (0.8 equiv)	80	<5
5	AgOTs (1 equiv)	75	<5
6	AgOTf (0.8 equiv)	70	<5
7	AgSbF <sub>6</sub> (0.8 equiv)	60	<5
8 <sup>c</sup>	AgOTs (0.8 equiv)	70	<5

<sup>a</sup>Conditions: 1.2 equiv **14a**, 0.3 M, 12h. <sup>b</sup>Determined by <sup>1</sup>H NMR. <sup>c</sup>With 1.5 equiv K<sub>2</sub>S<sub>2</sub>O<sub>8</sub>.

$K_2S_2O_8$  as the stoichiometric oxidant since less substrate decomposition is observed in this case.

We hypothesized combination of  $K_2S_2O_8$  and substoichiometric silver reagents would favor the desired decarboxylative process (Table 2.6). Indeed, addition of 0.25 equivalents AgOTs enhances selectivity for pyridine **15ba**, resulting in a 10:1 mixture of **15ba** and **20ba** (entry 1); however, conversion is incomplete in this case. The yield of **15ba** increases with greater amounts of silver additive, and use of 0.8 equivalents AgOTs proves optimal (entry 4). Reactions employing other silver(I) salts with non-coordinating counterions afford **15ba** in slightly lower yields (entries 6 and 7) and use of excess  $K_2S_2O_8$  is not beneficial (entry 8).

These newly optimized conditions proved unsatisfactory for Rh(III)-catalyzed annulation of oxime **11b** and

(hetero)aryl acrylic acids **14h** and **14i** (eq 5). We

evaluated the effects of modifying the

cyclopentadienyl ligand of the rhodium catalyst in the reaction of oxime

**11b** and 3-(methoxy)cinnamic acid

(**14i**, Chart 2.2).

Fortunately, use of electron deficient

$[RhCp^{CF_3}Cl_2]_2$  results in

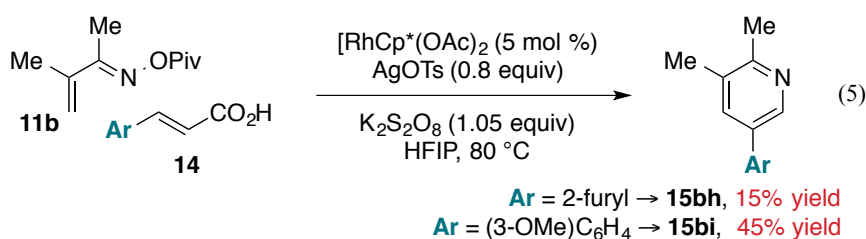
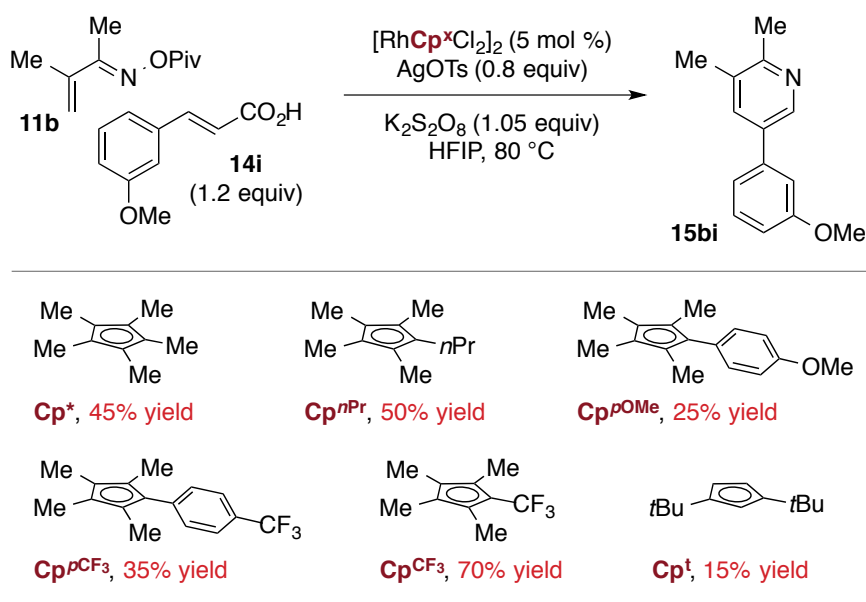


**Chart 2.2.** Catalyst screen with alkene **14i**.<sup>a,b</sup>



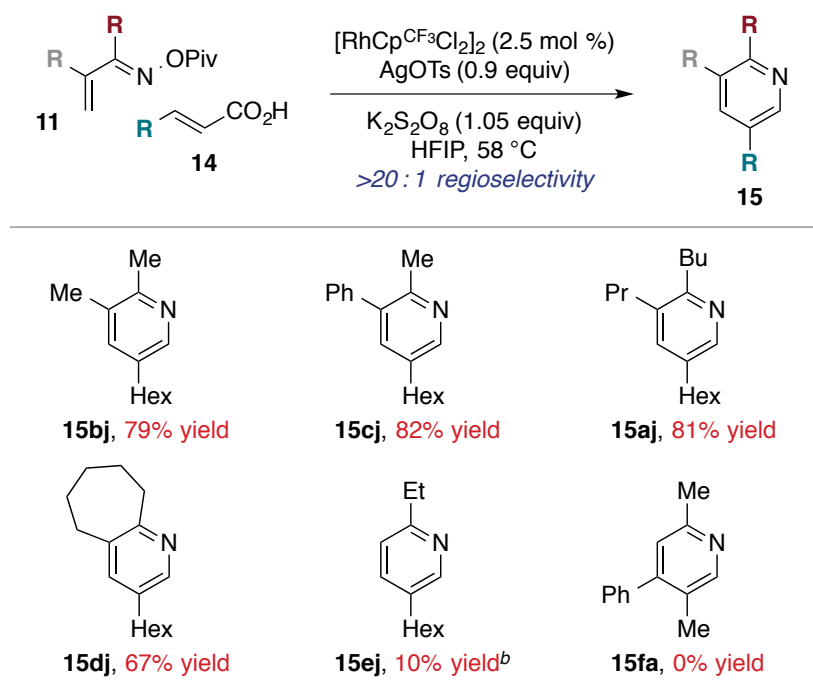
<sup>a</sup>Conditions: 1.2 equiv **14i**, 0.3 M, 12 h. <sup>b</sup>Yields determined by  $^1H$  NMR.

70% yield of 5-aryl pyridine **15bi**. Furthermore, employing  $[\text{RhCp}^{\text{CF}_3\text{Cl}_2}]_2$  in reactions of various oxime substrates **11** and substituted acrylic acids **14** leads to full conversion at 58 °C (Charts 2.3 and 2.4).

### 2.2.2 Substrate Scope

With optimized conditions in hand, we explored the scope of oxime substrates **11** in the reaction of non-2-enoic acid (**14j**, Chart 2.3).  $\alpha,\beta$ -Unsaturated oxime esters containing  $\alpha$ -alkyl and  $\alpha$ -aryl substitution undergo decarboxylative coupling to afford 5-substituted pyridines (**15**) with >20:1 selectivity and good yield. As in the analogous reaction of terminal alkenes, reactivity decreases in the case of ethyl vinyl oxime ester **11e**, and use of  $\beta$ -substituted oxime substrate **11f** leads to no desired product. Furthermore, elimination of PivOH affords nitrile **21** in the reaction of aldoxime ester **11g** (eq 6).

**Chart 2.3.** Unsaturated oxime ester scope.<sup>a</sup>



<sup>a</sup>Conditions: 1.2 equiv **14**, 0.3 M, 12 h. <sup>b</sup>Determined by  $^1\text{H}$  NMR.

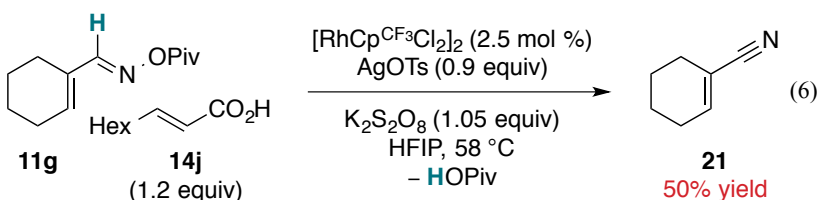
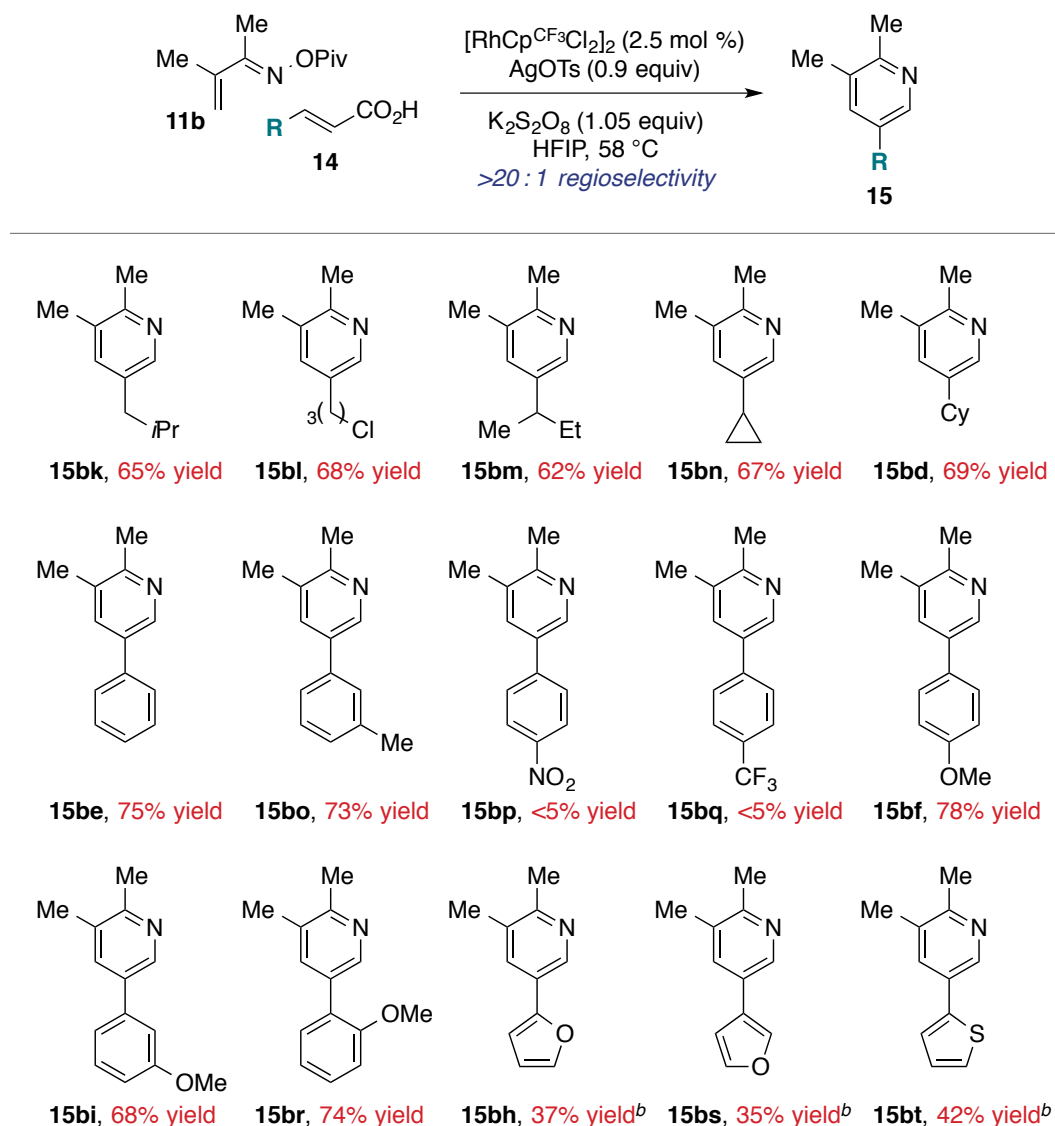


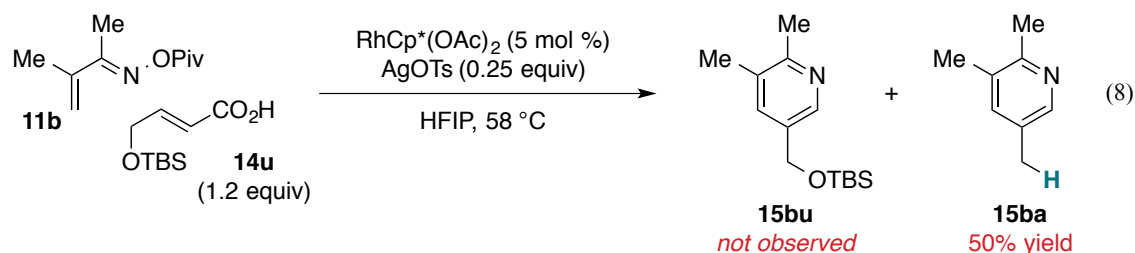
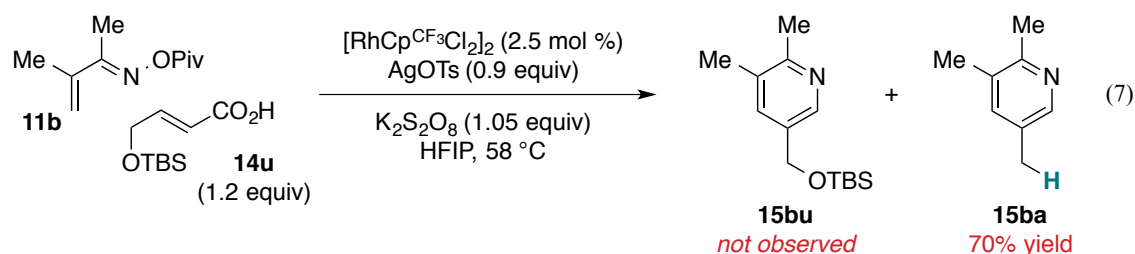


**Chart 2.4.** Substituted acrylic acid scope.<sup>a</sup>



<sup>a</sup>Conditions: 1.2 equiv **14**, 0.3 M, 12 h. <sup>b</sup>0.5 equiv AgOTs.

Rh(III)-catalyzed annulation of **11b** proceeds with a variety of acrylic acid derivatives (**14**, Chart 2.4), conveniently accessed by Knoevenagel condensation of the appropriate aldehyde and malonic acid.<sup>21</sup> Both primary and secondary alkyl-substituted derivatives participate to access 5-alkyl pyridines **15** in good yield and with >20:1 selectivity. The acrylic acid substrate may also bear aryl or heteroaryl substitution. While the alkene component contains two activating groups in these cases, 5-substituted products **15** still form with >20:1 selectivity.

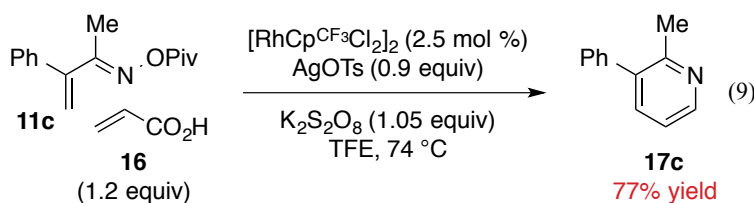


Reactions of cinnamic acid (**15e**) as well as 3-(methyl) and 2-, 3-, and 4-(methoxy)cinnamic acid derivatives proceed with complete conversion to 5-aryl pyridine products. On the other hand, electron deficient 4-(nitro) and 4-(trifluoromethyl)cinnamic acids (**14p** and **14q**) are

**Table 2.7.** Decarboxylative coupling of acrylic acid (**16**).<sup>a</sup>

entry	change from standard conditions	yield <b>17a</b> (%) <sup>b</sup>
1	none	35
2	AgOTs (2.1 equiv), no $\text{K}_2\text{S}_2\text{O}_8$	15
3	AgOAc (2.1 equiv), no $\text{K}_2\text{S}_2\text{O}_8$	25
4	$[\text{RhCp}^*\text{Cl}_2]_2$ (2.5 mol %)	<5
5	HFIP, 80 °C	50
6	TFE, 74 °C	65

<sup>a</sup>Conditions: 1.2 equiv **16**, 0.3 M. <sup>b</sup>Determined by  $^1\text{H}$  NMR.



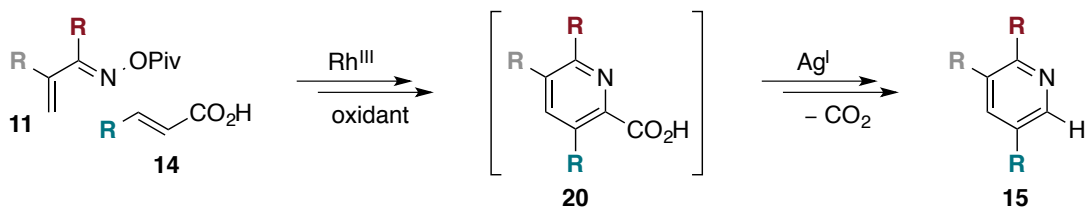
unreactive substrates. Use of 0.5 equivalent AgOTs is optimal for decarboxylative coupling of **10b** and heteroaryl acrylic acid substrates **15h**, **15s**, and **15t**, although yields are lower in these cases. Interestingly, reaction of **11b** and **14u** does not afford pyridine **15bu** but reduced product **15ba** in 70% yield (eq 7). This overall redox-neutral process does not require an

external oxidant, and **15ba** forms in 50% yield in the absence of  $K_2S_2O_8$  using catalytic AgOTs (eq 8).

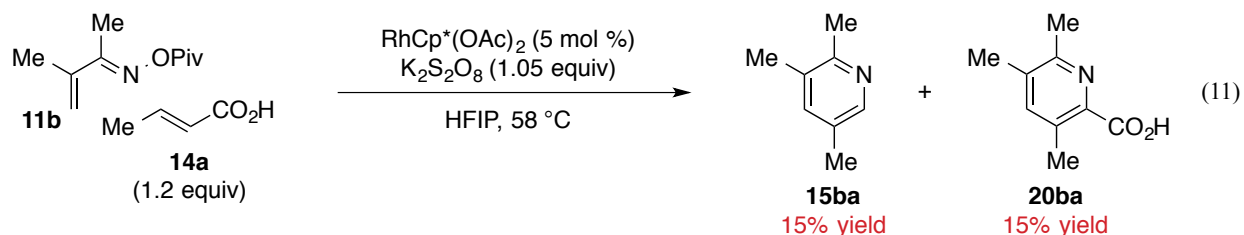
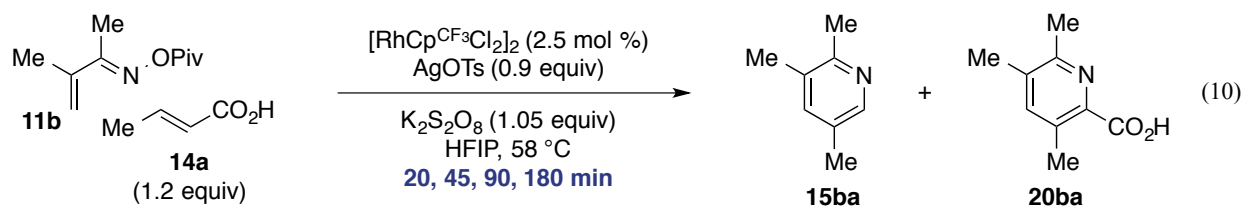
Surprisingly, optimization of conditions for Rh(III)–catalyzed coupling of oximes **11** and  $\beta$ –substituted acrylic acids **14** proved detrimental in the reaction of acrylic acid (**16**, entry 1, Table 2.7). We investigated this change by alternating several reaction parameters separately (Table 2.7). That is, use of the previous oxidant (AgOAc, entry 3) or catalyst ( $[RhCp^*Cl_2]_2$ , entry 4) leads to similarly low yields of pyridine **17a**. On the other hand, performing the reaction at elevated temperature (entry 5) and in TFE (entry 6) recovers reactivity. Using these conditions, decarboxylative coupling of oxime **11c** and acrylic acid (**16**) affords disubstituted pyridine **17c** in 77% isolated yield (eq 9).

### 2.2.3 Mechanistic Studies

Early mechanistic experiments aimed to elucidate the mechanism of the decarboxylation step. We considered a pathway involving initial Rh(III)–catalyzed annulation of **11** and **14** to access picolinic acid intermediate **20**, followed by *in situ* decarboxylation, perhaps assisted by the silver(I) reagent, to afford observed pyridine product **15** (Scheme 2.5). Indeed, silver(I)–catalyzed decarboxylation is an established process that has been demonstrated for both aromatic and heteroaromatic carboxylic acid substrates.<sup>9b–d</sup> However, preliminary observations were not completely consistent with the pathway shown in Scheme 2.5. For instance, monitoring the

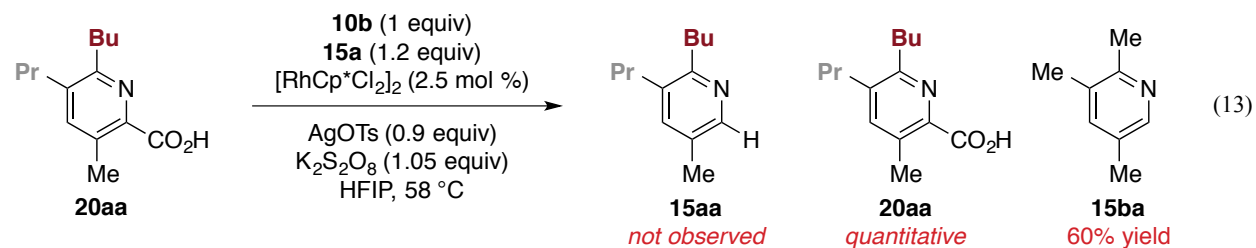
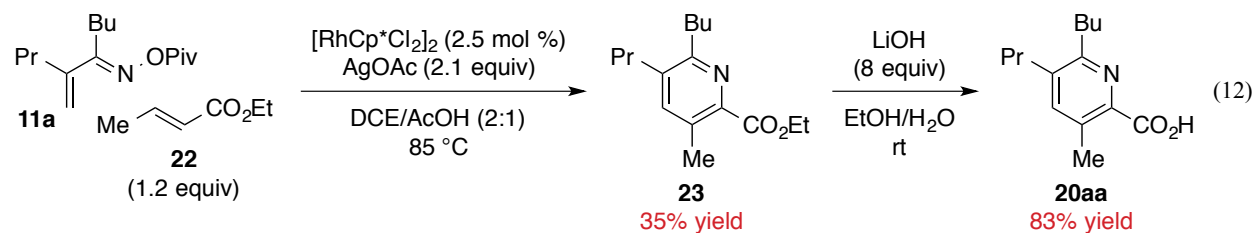


**Scheme 2.5.** Decarboxylation of a picolinic acid intermediate.



reaction of **11b** and **14a** by  $^1\text{H}$  NMR spectroscopy indicates picolinic acid **20ba** is not present in observable amounts at 20, 45, 90, or 180 minutes (eq 10). Furthermore, pyridine **15ba** forms alongside picolinic acid **20ba** in the absence of Ag(I) reagent (eq 11), implying Ag(I) is not a prerequisite for decarboxylation.

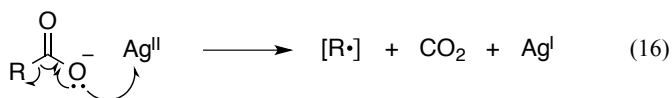
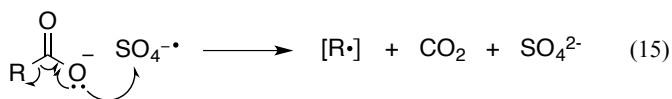
To confirm Rh(III)-catalyzed decarboxylative coupling does not involve the process illustrated in Scheme 2.5, potential intermediate **20aa** was prepared (eq 12). In fact, we took advantage of our previously developed conditions for Rh(III)-catalyzed coupling of oxime **11a** and ethyl crotonate (**22**), as these were the only reported conditions for accessing picolinate



esters like **23**. Subsequent basic hydrolysis provides the desired picolinic acid **20aa**. In the reaction of **11b** and **14a** in the presence of 1 equivalent **20aa**, decarboxylation of the picolinic acid does not occur and a quantitative amount of **20aa** is recovered. This result provides strong evidence that decarboxylative coupling does not proceed *via* a picolinic acid intermediate **20** (Scheme 2.5).

We also considered decarboxylation by a single electron transfer mechanism.  $K_2S_2O_8$  is often used in combination with Ag(I) catalysts for decarboxylative coupling reactions of carboxylic acid derivatives (Scheme 2.6).<sup>22</sup> The decarboxylation process is proposed to proceed by single electron transfer from Ag(I) to  $S_2O_8^{2-}$ , generating Ag(II) and persulfate radical ( $SO_4^{\cdot-}$ , eq 14).<sup>23</sup> Either species may abstract an electron from the carboxylate group, resulting in loss of  $CO_2$  to form a radical species  $[R\cdot]$  (eq 15 and 16) that undergoes functionalization. Actually,  $S_2O_8^{2-}$  may gain an electron from a variety of sources, so a Ag(I) catalyst is not necessarily required for reactivity. In Ag(I)/ $S_2O_8^{2-}$ -catalyzed decarboxylative coupling, aryl carboxylic acids are typically less reactive than alkyl substrates, a difference that presumably results from stability of the radical intermediate

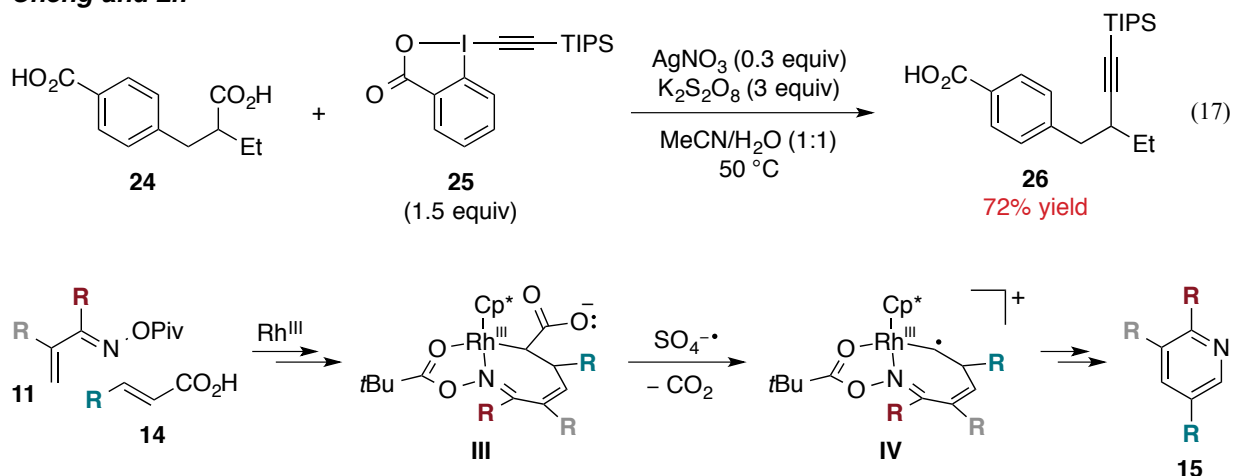
( $[R\cdot]$ ). For example, Cheng and Li demonstrated Ag(I)/ $S_2O_8^{2-}$ -catalyzed decarboxylative alkylation only proceeds with the alkyl carboxylic acid group in substrate **24**, resulting in exclusive formation of **26** (eq 17).<sup>22</sup>



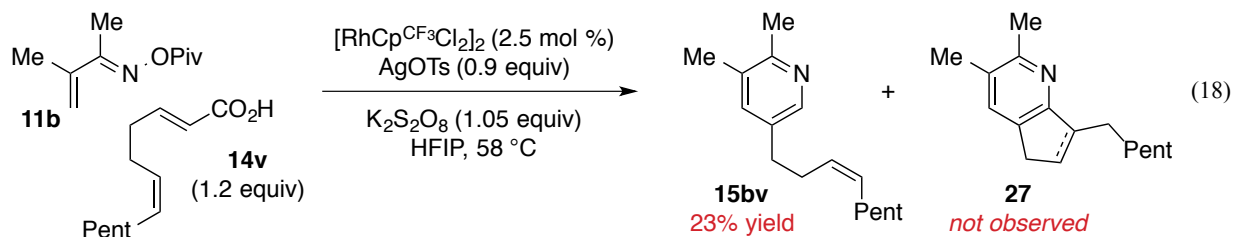
**Scheme 2.6.** Ag(I)/ $S_2O_8^{2-}$ -assisted decarboxylation.

Decarboxylation by a single electron transfer pathway could explain the amount of pyridine **15ba** produced in the absence of Ag(I) (eq 11), as well as the enhanced selectivity for

Cheng and Li:<sup>22</sup>

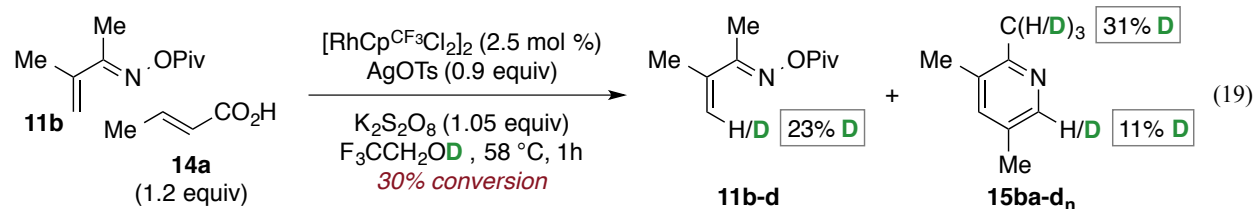


Scheme 2.7. Decarboxylation by a single electron transfer pathway.



**15ba** in the presence of Ag(I) additives (Table 2.6). A possible decarboxylation pathway is illustrated in Scheme 2.7. Here, single electron abstraction from alkyl carboxylate **III** and loss of  $\text{CO}_2$  affords radical species **IV**. If this pathway were operative, then decarboxylative coupling of **11b** and alkene-tethered **14v** (eq 18) could generate bicyclic product **27** via 5-*exo*-trig radical cyclization from the corresponding intermediate **IV**. In fact, pyridine **15bv** is the only product observed in the reaction of **11b** and **14v** (eq 18). This result, however, does not conclusively rule out decarboxylation by the pathway shown in Scheme 2.7.

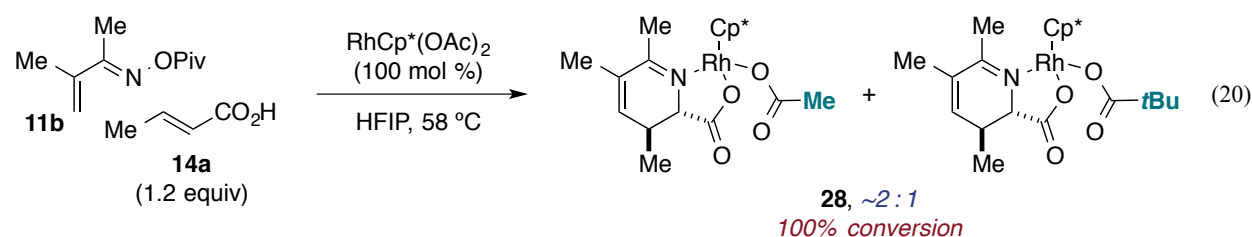
We gained further insight regarding the mechanism of pyridine formation from isotope studies. Specifically, reaction of **11b** and **14a** conducted in TFE-*d* ( $\text{F}_3\text{CCH}_2\text{OD}$ ) leads to deuterium incorporation at the  $\beta$ -position in **11a-d** after 30% conversion, providing evidence for a reversible C-H activation step (eq 19). Deuteration also occurs at the 2-methyl substituent of



**15ba-d<sub>n</sub>** but not at the corresponding position in **11b-d**. Our prior mechanistic work showed deuterium incorporation does not occur by reversible deprotonation of the pyridine product (Chapter 1, eq 25). These observations are consistent with reversible deprotonation en route to the pyridine product, after the first irreversible step of the reaction mechanism. Furthermore, the relatively lower amount of deuterium incorporation at the 2-methyl substituent in the reaction of crotonic acid (**14a**, 31% D) versus ethyl acrylate (**23a**, Chapter 1, eq 24, 88% D) suggests the carboxylic acid moiety is present during the deprotonation step.

Stoichiometric reactions provided a wealth of information regarding the mechanism of pyridine formation by Rh(III)-catalyzed decarboxylative coupling of unsaturated oxime esters and substituted acrylic acids. After 90 minutes at 58 °C, the reaction of **11b**, **14a**, and 1 equivalent  $\text{RhCp}^*(\text{OAc})_2$  affords not the pyridine product, but a mixture of rhodium carboxylate complexes **28** (eq 20). Structures of **28** were tentatively assigned based on NMR, IR, and mass spectroscopy.

Purification of rhodium complexes **28** proved difficult, so alternate strategies were explored. We hypothesized exchange of carboxylate ligands for chloride would provide a more crystalline compound, allowing isolation by precipitation (Scheme 2.8). Indeed, addition of



excess LiCl to a solution of crude complexes **28** in Et<sub>2</sub>O affords an insoluble pale orange solid. Dissolving in CH<sub>2</sub>Cl<sub>2</sub> and separation from LiCl by filtration leads to pure rhodium chloride complex **29** (eq 21). However, conversion is low in this case, even during prolonged reaction times. On the other hand, rapid ligand exchange occurs in the presence of excess trimethylsilyl chloride (TMSCl); in fact, both carboxylate ligands are replaced to afford precatalyst [RhCp\*Cl<sub>2</sub>]<sub>2</sub> (eq 22). Use of 1 equivalent TMSCl allows selective exchange with the non-tethered carboxylate ligand, affording rhodium chloride **29** in 68% yield (eq 23). The pure complex **29** was characterized by NMR, IR, and mass spectroscopy. A few data points were troubling: a) Coupling between 5-H and 6-H (eq 23) has a particularly large *J* value (15.6 Hz). b) 4-H does not couple to 5-H. Fortunately, slow evaporation from a concentrated solution of **29** in CH<sub>2</sub>Cl<sub>2</sub> afforded red orange crystals suitable for X-ray analysis. The crystal structure of

**29** (Figure 2.2)

confirms the structure shown in Scheme 2.8

and, by analogy, the

structure of **28** given in

eq 20. Furthermore,

crystallographic data

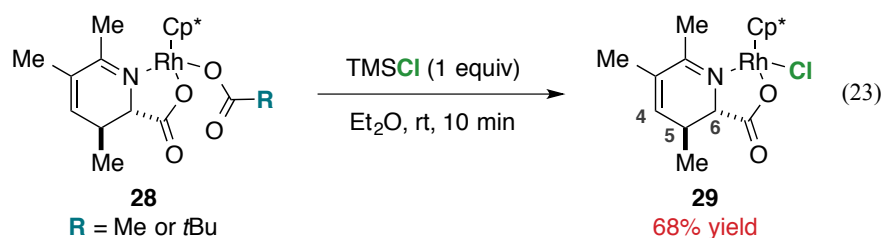
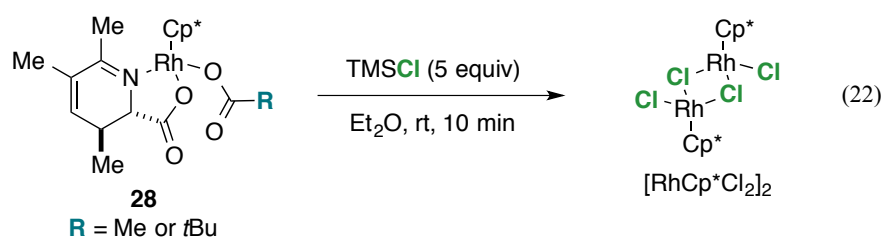
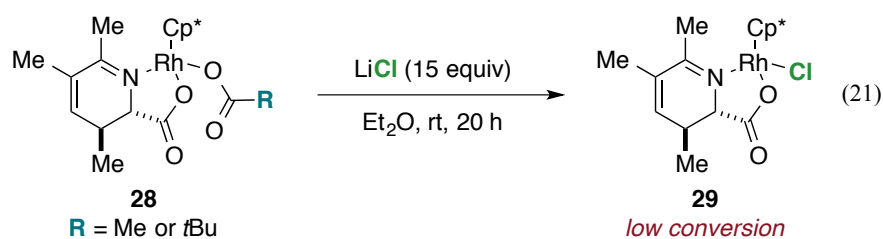
indicates a dihedral

angle between C5-H

and C6-H bonds close

to 180°, explaining the

large *J* value, as well as



**Scheme 2.8.** Synthesis of rhodium chloride complex **29**.



a dihedral angle between C4–H and C5–H bonds near 90°, consistent with a small (in this case, unobservable) coupling constant. Importantly, in **29**, C–N bond formation has taken place but decarboxylation has not yet occurred, lending insight to the timing of the decarboxylation step in the reaction mechanism (*vide infra*).

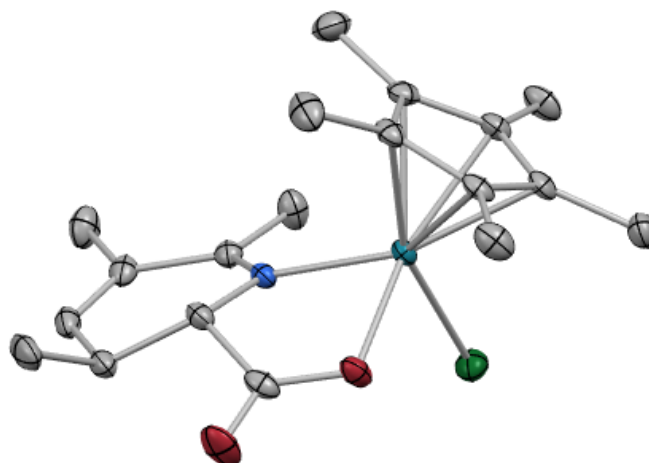
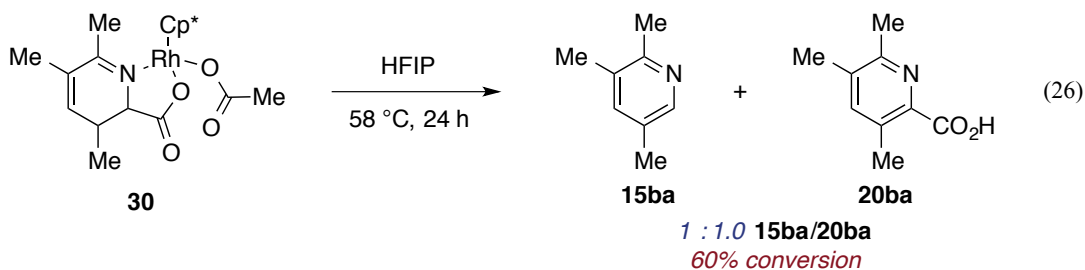
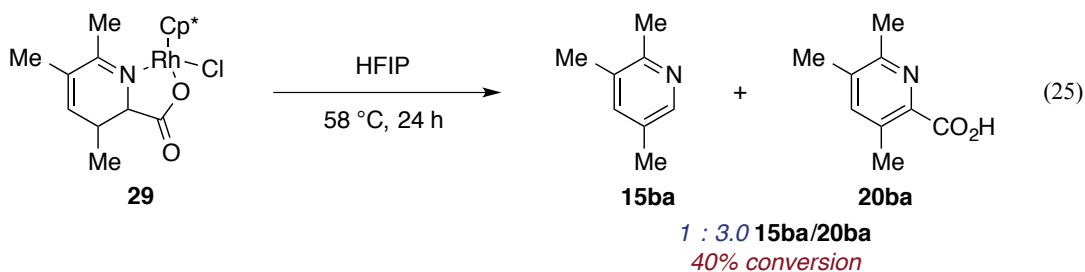
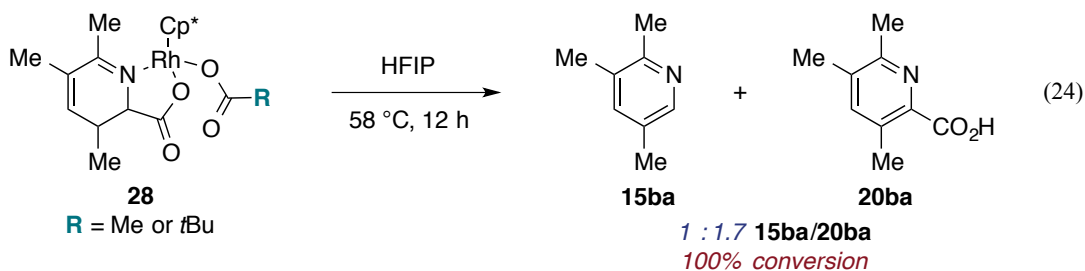


**Figure 2.2.** X-ray crystal structure of **29**.<sup>24</sup>

Metalacycle decomposition studies contributed further mechanistic insight (Scheme 2.9). Crude carboxylate complexes **28** are stable in solution at room temperature, but heating to 58 °C results in complete conversion to a 1:1.7 mixture of pyridine **15ba** and picolinic acid **20ba** after 12 hours (eq 24). This observation suggests a complex analogous to **28** is a common intermediate of both observed products. Contrastingly, conversion of pure chloride complex **29** is sluggish, reaching only 40% conversion after 24 hours (eq 25). Furthermore, decomposition of **29** favors formation of picolinic acid **20ba**, leading to a 1:3 mixture of **15ba** and **20ba**. To rule out any influence of impurities in the decomposition of crude carboxylate complexes **28**, we targeted the synthesis of pure rhodium acetate **30**. Silver(I)-promoted ligand exchange of rhodium chloride **29** with AgOAc proved to be the easiest strategy, affording acetate complex **30** in 80% yield (see Appendix 2). Like the reaction of **29**, decomposition of **30** is slow, resulting in 60% conversion after 24 hours (eq 26). Importantly, pyridine and picolinic acid products **15ba** and **20ba** form as a 1:1 mixture in this case. The difference in product distributions in decomposition reactions of rhodium chloride **29** compared to acetate complex **30** suggests

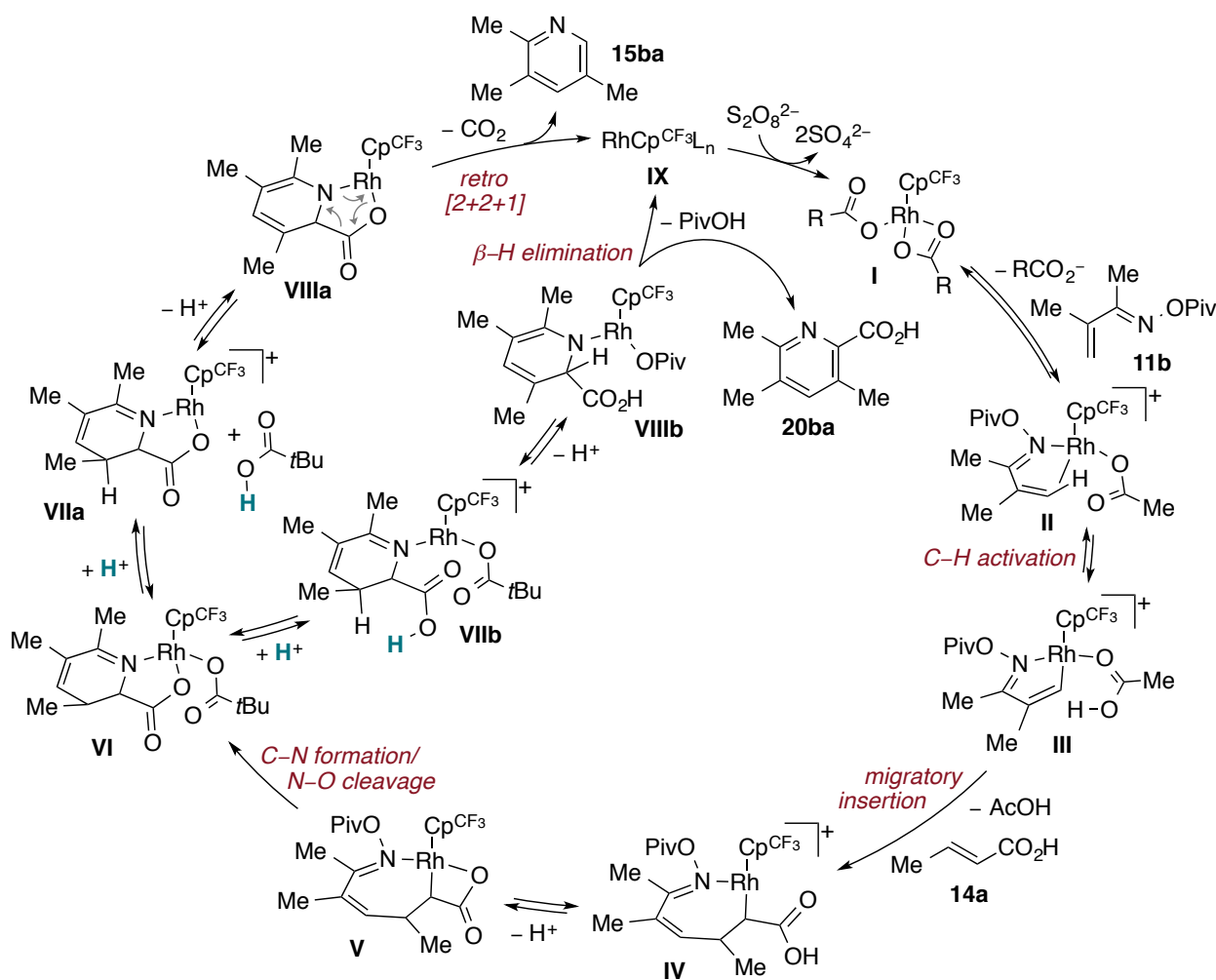


**Scheme 2.9.** Decomposition of complexes **28**, **29**, and **30**.

identity of the X-type ligand at this stage in the mechanism influences the divergence of reaction pathways to the two observed products.

We propose formation of pyridine **15ba** and picolinic acid **20ba** by Rh(III)-catalyzed decarboxylative coupling of **11b** and **14a** in the absence of Ag(I) proceeds by the mechanism shown in Figure 2.3. After generation of active carboxylate catalyst **I**, dissociation of an acetate ligand opens a site for coordination by the oxime substrate **11b**, resulting in cationic complex **II**. Reversible C–H activation at the  $\beta$ -position affords metalacycle **III**. Coordination and migratory insertion of **14a** installs the electron-withdrawing carboxylic acid moiety  $\alpha$  to the metal center in 7-membered rhodacycle **IV**. Deprotonation of the carboxylic acid and chelation provides neutral complex **V**. C–N bond formation/N–O bond cleavage affords rhodium carboxylate **VI**

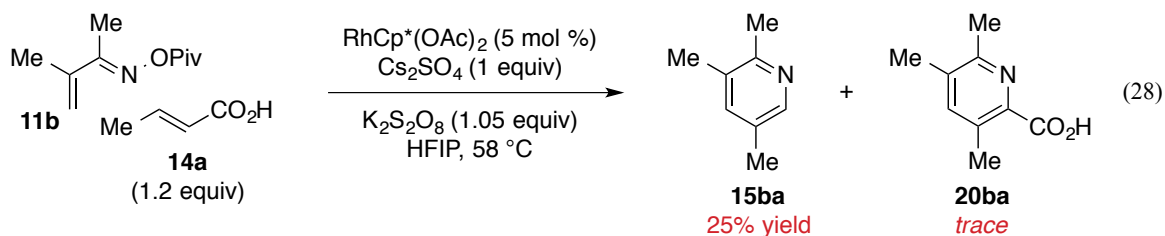
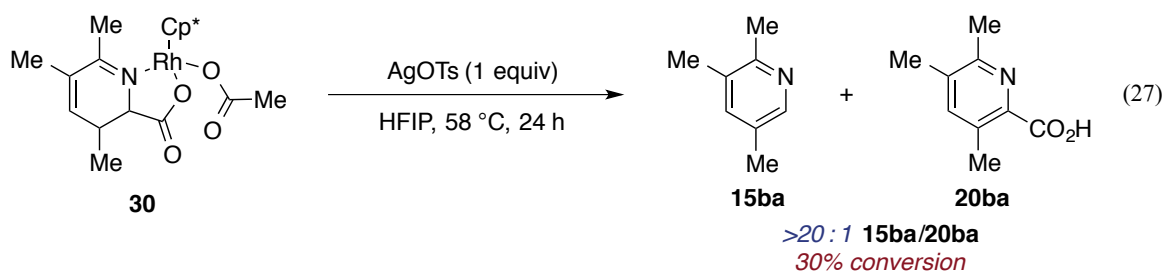
**Figure 2.3.** Proposed mechanism for formation of **15ba** and **20ba**.



that is related to complexes **28**, **29**, and **30**. At this point, protonation and ligand dissociation may occur to liberate either of the two carboxylate ligands, accessing cationic complex **VIIa** or **VIIIb**. From **VIIa**, deprotonation leads to intermediate **VIIIa** that may undergo *retro*-[2+2+1] cycloaddition to extrude CO<sub>2</sub> and pyridine product **15ba**. Alternatively, from **VIIIb**, deprotonation and subsequent  $\beta$ -hydride elimination provides picolinic acid **20ba** and Rh(I) species **IX** that is oxidized to regenerate active catalyst **I**.

It is clear the Ag(I) reagent plays a major part in both selectivity and reactivity in Rh(III)-catalyzed decarboxylative coupling of  $\alpha,\beta$ -unsaturated oxime esters and  $\beta$ -substituted

acrylic acids (Table 2.6). The exact role of Ag(I) in the reaction mechanism is not fully understood at this time, but the following observations have provided some insight. Reaction of acetate complex **30** in the presence of 1 equivalent AgOTs leads to exclusive formation of pyridine **15ba** (eq 27). This result suggests Ag(I) becomes involved after formation of an intermediate analogous to **30** (i.e. **VI** in Figure 2.3). Additionally, selective decarboxylative coupling is not limited to Ag(I) additives. Specifically, only a trace amount of picolinic acid **20ba** is observed in the reaction of **11b** and **14a** in the presence of 1 equivalent Cs<sub>2</sub>SO<sub>4</sub> (eq 28).



### 2.3 Conclusion

In conclusion, we developed a complementary method for pyridine synthesis by rhodium(III)-catalyzed decarboxylative coupling of  $\alpha,\beta$ -unsaturated *O*-pivaloyl oxime esters and acrylic acid derivatives. Carboxylic acids function as traceless activating groups, allowing selective formation of 5-substituted pyridine products. Mechanistic studies strongly suggest pyridine formation does not proceed *via* a picolinic acid intermediate. Stoichiometric experiments allow characterization of catalytically relevant rhodium complexes that provide

evidence for C–N bond formation before the decarboxylation step. Metalacycle decomposition studies lend valuable insight regarding the divergence of reaction pathways leading to the observed products.

## REFERENCES

1. Trost, B. M. *Science* **1983**, *219*, 245.
2. Fleming, I. *Frontier Orbitals and Organic Chemical Reactions*; Wiley: Chichester, U. K., 1976.
3. For reviews of directed, transition metal–catalyzed C–H functionalization, see: a) Neufeldt, S. R.; Sanford, M. S. *Acc. Chem. Res.* **2012**, *45*, 936. b) Colby, D. A.; Tsai, A. S.; Bergman, R. G.; Ellman, J. A. *Acc. Chem. Rev.* **2012**, *45*, 814. c) Yoshikai, N. *Synlett* **2011**, 1047. d) Lyons, T. W.; Sanford, M. S. *Chem. Rev.* **2010**, *110*, 1147. e) Colby, D. A.; Bergman, R. G.; Ellman, J. A. *Chem. Rev.* **2010**, *110*, 624.
4. For reviews, see: a) De Sarkar, S.; Liu, W.; Kozhushkov, S. I.; Ackermann, L. *Adv. Synth. Catal.* **2014**, *356*, 1461. b) Zheng, Q.–Z.; Jiao, N. *Tetrahedron Lett.* **2014**, *55*, 1121. c) Engle, K. M.; Mei, T.–S.; Wasa, M.; Yu, J.–Q. *Acc. Chem. Res.* **2012**, *45*, 788. d) Reference 3.
5. For reviews of removable directing groups, see: a) Wang, C.; Huang, Y. *Synlett* **2013**, *24*, 145. b) Rousseau, G.; Breit, B. *Angew. Chem. Int. Ed.* **2011**, *50*, 2450.
6. For selected recent examples, see: a) Shang, M.; Sun, S.–Z.; Dai, H.–X.; Yu, J.–Q. *J. Am. Chem. Soc.* **2014**, *136*, 3354. b) Lahm, G.; Opatz, T. *Org. Lett.* **2014**, *16*, 4201. c) Li, X.; Liu, Y.–H.; Gu, W.–J.; Li, B.; Chen, F.–J.; Shi, B.–F. *Org. Lett.* **2014**, *16*, 3904. d) Schinkel, M.; Wang, L.; Bielefeld, K.; Ackermann, L. *Org. Lett.* **2014**, *16*, 1876. e) Boultadakis–Arapinis, M.; Hopkinson, M. N.; Glorius, F. *Org. Lett.* **2014**, *16*, 1630. f) Uhlig, N.; Li, C.–J. *Chem. Eur. J.* **2014**, *20*, 12066. g) Lee, S.; Lee, H.; Tan, K. L. *J. Am. Chem. Soc.* **2013**, *135*, 18778. h) Preshlock, S. M.; Plattner, D. L.; Maligres, P. E.; Krska, S. W.; Maleczka, R. E.; Smith, M. R. *Angew. Chem. Int. Ed.* **2013**, *52*, 12915. i) Smout, V.; Peschiulli, A.; Verbeeck, S.; Mitchell, E. A.; Herrebout, W.; Bultinck, P.; Vande Velde, C. M. L.; Berthelot, D.;

- Meerpoel, L.; Maes, B. U. W. *J. Org. Chem.* **2013**, *78*, 9803. j) Ma, W.; Ackermann, L. *Chem. Eur. J.* **2013**, *19*, 13925. k) Wang, C.; Chen, H.; Wang, Z.; Chen, J.; Huang, Y. *Angew. Chem. Int. Ed.* **2012**, *51*, 7242.
7. For a review, see: a) Shi, G.; Zhang, Y. *Adv. Synth. Catal.* **2014**, *356*, 1419. Selected recent examples: b) Ng, F.-N.; Zhou, Z.; Yu, W.-Y. *Chem. Eur. J.* **2014**, *20*, 4474. c) Thuy-Boun, P. S.; Villa, G.; Dang, D.; Richardson, P.; Su, S.; Yu, J.-Q. *J. Am. Chem. Soc.* **2013**, *135*, 17508. d) Gallardo-Donaire, J.; Martin, R. *J. Am. Chem. Soc.* **2013**, *135*, 9350. e) Dai, H.-X.; Li, G.; Zhang, X.-G.; Stepan, A. F.; Yu, J.-Q. *J. Am. Chem. Soc.* **2013**, *135*, 7567. f) Cheng, X.-F.; Li, Y.; Su, Y.-M.; Yin, F.; Wang, J.-Y.; Sheng, J.; Vora, H. U.; Wang, X.-S.; Yu, J.-Q. *J. Am. Chem. Soc.* **2013**, *135*, 1236. g) Li, Y.; Ding, Y.-J.; Wand, J.-Y.; Su, Y.-M.; Wang, X.-S. *Org. Lett.* **2013**, *15*, 2574. h) Yang, M.; Jiang, X.; Shi, W.-J.; Zhu, Q.-L.; Shi, Z.-J. *Org. Lett.* **2013**, *15*, 690. i) Frasco, D. A.; Lilly, C. P.; Boyle, P. D.; Ison, E. A. *ACS Catal.* **2013**, *3*, 2421.
8. Transition metal-catalyzed decarboxylative coupling is also an established method for substitution at the *ipso*-position of carboxylic acid substrates. For reviews, see: a) Dzik, W. I.; Lange, P. P.; Gooßen, L. J. *Chem. Sci.* **2012**, *3*, 2671. b) Rodríguez, N.; Goossen, L. J. *Chem. Soc. Rev.* **2011**, *40*, 5030.
9. a) Dupuy, S.; Nolan, S. P. *Chem. Eur. J.* **2013**, *19*, 13034. b) Lu, P.; Sanchez, C.; Cornella, J.; Larrosa, I. *Org. Lett.* **2009**, *11*, 5710. c) Cornella, J.; Sanchez, C.; Banawa, D.; Larrosa, I. *Chem. Commun.* **2009**, 7176. d) Gooßen, L. J.; Linder, C.; Rodríguez, N.; Lange, P. P.; Fromm, A. *Chem. Commun.* **2009**, 7173.

10. a) Mochida, S.; Hirano, K.; Satoh, T.; Miura, M. *J. Org. Chem.* **2011**, *76*, 3024. b) Mochida, S.; Hirano, K.; Satoh, T.; Miura, M. *Org. Lett.* **2010**, *12*, 5776. c) Maehara, A.; Tsurugi, H.; Satoh, T.; Miura, M. *Org. Lett.* **2008**, *10*, 1159.
11. a) Morimoto, K.; Itoh, M.; Hirano, K.; Satoh, T.; Shibata, Y.; Tanaka, K.; Miura, M. *Angew. Chem. Int. Ed.* **2012**, *51*, 5359. b) Cornella, J.; Righi, M.; Larrosa, I. *Angew. Chem. Int. Ed.* **2011**, *50*, 9429.
12. Bhadra, S.; Dzik, W. I.; Goossen, L. J. *Angew. Chem. Int. Ed.* **2013**, *52*, 2959.
13. Neely, J. M.; Rovis, T. *J. Am. Chem. Soc.* **2013**, *135*, 66.
14. Hartwig, J. F. *Organotransition Metal Chemistry: From Bonding to Catalysis*; University Science Books: Sausalito, CA, 2010.
15. For related decarboxylative coupling strategies, see: a) Yang, Y.; Yao, J.; Zhang, Y. *Org. Lett.* **2013**, *15*, 3206. b) Yang, Y.; Xie, C.; Xie, Y.; Zhang, Y. *Org. Lett.* **2012**, *14*, 957. c) Šmejkal, T.; Breit, B. *Angew. Chem. Int. Ed.* **2008**, *47*, 3946.
16. For recent approaches to 5-substituted pyridines by derivatization of the pyridine core, see: a) Ye, M.; Gao, G.-L.; Edmunds, A. J. F.; Worthington, P. A.; Morris, J. A.; Yu, J.-Q. *J. Am. Chem. Soc.* **2011**, *133*, 19090. b) Ye, M.; Gao, G.-L.; Yu, J.-Q. *J. Am. Chem. Soc.* **2011**, *133*, 6964. c) Li, B.-J.; Shi, Z.-J. *Chem. Sci.* **2011**, *2*, 488.
17. Rh(I)-catalyzed coupling of unsaturated oximes and terminal alkynes favors formation of 5-substituted pyridines with selectivities that range from 1.6 to >20:1 5-/6-substituted products. See: Martin, R. M.; Bergman, R. G.; Ellman, J. A. *J. Org. Chem.* **2012**, *77*, 2501.
18. Neely, J. M.; Rovis, T. *J. Am. Chem. Soc.* **2014**, *136*, 2735.
19. Yvon, K.; Bezinge, A.; Tissot, P.; Fischer, P. *J. Solid State Chem.* **1986**, *65*, 225.
20. Ye, B.; Cramer, N. *Science* **2012**, *338*, 504.



21. a) Reference 15c. b) Szymanski, W.; Wu, B.; Weiner, B.; de Wildeman, S.; Feringa, B. L.; Janssen, D. B. *J. Org. Chem.* **2009**, *74*, 9152.
22. For a recent example, see: Liu, X.; Wang, Z.; Cheng, X.; Li, C. *J. Am. Chem. Soc.* **2012**, *134*, 14330.
23. a) Citterio, A.; Minisci, F.; Franchi, F. *J. Org. Chem.* **1980**, *45*, 4752. b) Anderson, J. M.; Kochi, J. K. *J. Am. Chem. Soc.* **1970**, *92*, 1651.
24. Thermal ellipsoids drawn at the 50% probability level.

## APPENDIX ONE

### Rhodium(III)–Catalyzed Coupling of $\alpha,\beta$ –Unsaturated Oxime Esters and Alkenes: Selective Synthesis of 6–Substituted Pyridines

A.1.1 General Methods .....	70
A.1.2 Synthesis of Oxime Ester Precursors .....	71
A.1.3 General Procedure for Oxime Ester Synthesis.....	71
A.1.4 General Procedure for Pyridine Synthesis .....	75
A.1.5 Mechanistic Experiments .....	89
A.1.6 $^1\text{H}$ and $^{13}\text{C}$ NMR Spectra of New Compounds .....	91
A.1.7 References .....	142

### A.1.1 General Methods

All reactions were carried out in oven-dried glassware under an atmosphere of argon with magnetic stirring. ACS grade acetic acid and 2,2,2-trifluoroethanol and reagent grade silver acetate were purchased from Sigma-Aldrich Co. and used without further purification. 1,2-Dichloroethane was distilled from calcium hydride under an atmosphere of argon. Alkenes **15k-m**, **15o-q**, **15t**, **15w**, **32a**, (*E*)-**32b**, **32c-f**, (*E*)-**32g** and **32h** were purchased and used without further purification. Substrates **15v**,<sup>1</sup> *trans*- and *cis*-**15x**,<sup>2</sup> (*Z*)-**32b**<sup>3</sup> and (*Z*)-**32g**<sup>4</sup> were prepared as previously reported. Alkenes **15r**, **15s** and **15u** were distilled and alkenes **15a-j** and **15n** were distilled under reduced pressure prior to use. [RhCp\*Cl<sub>2</sub>]<sub>2</sub> was prepared as previously reported.<sup>5</sup> Column chromatography was performed on Silicycle® SilicaFlash® P60 (230-400 mesh). Thin layer chromatography was performed on Silicycle® 250µm silica gel 60A plates. Visualization was accomplished with UV light (254 nm) or potassium permanganate.

<sup>1</sup>H NMR and <sup>13</sup>C NMR spectra were collected at ambient temperature in CDCl<sub>3</sub> on a Varian 400 MHz. Chemical shifts are expressed as parts per million (δ, ppm) and are referenced to 7.26 (CHCl<sub>3</sub>) for <sup>1</sup>H NMR and 77.16 (CDCl<sub>3</sub>) for <sup>13</sup>C NMR. Proton signal data uses the following abbreviations: s = singlet, d = doublet, t = triplet, q = quartet, m = multiplet and J = coupling constant. Mass spectra were obtained on a Fisons VG Autospec (HRMS) or an Agilent Technologies 6130 Quadrupole Mass Spec (LRMS). Infrared spectra were collected on a Bruker Tensor 27 FT-IR spectrometer.

Regioisomeric ratios were determined by integration of <sup>1</sup>H NMR spectra of product mixtures collected with first relaxation delay (d1) = 15 seconds. The major product of the reaction of **24f** and **32d** was identified as **33fd** by <sup>1</sup>H-<sup>13</sup>C HSQC and <sup>1</sup>H-<sup>13</sup>C HMBC.

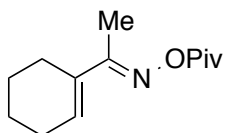
### A.1.2 Synthesis of Oxime Ester Precursors

The  $\alpha,\beta$ -unsaturated ketone precursors of **24a-c**, **24h**, and **24i** as well as **24f** were purchased from Sigma-Aldrich Co. and Tokyo Chemical Industry Co., respectively. Enone precursors corresponding to **24d** and **24e** were prepared as previously reported.<sup>6</sup> The precursors of **24g** and **24i-k** were obtained by methylenation of the appropriate ketones by the following procedure, adapted from the literature.<sup>7</sup> A solution of the ketone (20 mmol), aqueous formaldehyde (4.9 mL, 3 equiv) and morpholine (0.86 mL, 0.5 equiv) in 18 mL acetic acid was heated at 120 °C for 20 hours. After cooling, the mixture was neutralized with 3M NaOH and extracted with diethyl ether three times. The combined organic layers were washed with saturated NaHCO<sub>3</sub> and brine, dried over MgSO<sub>4</sub>, filtered and concentrated *in vacuo*. The crude product was purified by flash column chromatography.

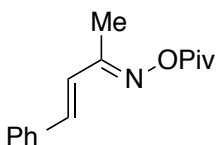
### A.1.3 General Procedure for Oxime Ester Synthesis

All *O*-pivaloyl oxime esters **24** were generated from the corresponding  $\alpha,\beta$ -unsaturated ketones according to the following procedure, adapted from the literature.<sup>8</sup> Hydroxylamine hydrochloride (347 mg, 7 mmol, 1.4 equiv) and Na<sub>2</sub>CO<sub>3</sub> (742 mg, 7 mmol, 1.4 equiv) were added to the enone (5 mmol) in 15 mL MeOH and the mixture was stirred at 65 °C for 1 hour (or room temperature for 4 hours for **24i** and **24l**). The solvent was removed *in vacuo* and the resulting residue was dissolved in 10 mL CH<sub>2</sub>Cl<sub>2</sub> and cooled to 0 °C. After the addition of Et<sub>3</sub>N (1.74 mL, 12.5 mmol, 2.5 equiv), a solution of pivaloyl chloride (1.23 mL, 10 mmol, 2 equiv) in 5 mL DCM was added dropwise at 0 °C. The mixture was stirred at room temperature overnight and quenched with water. The aqueous layer was extracted with CH<sub>2</sub>Cl<sub>2</sub> three times and the combined organic layers were washed with saturated NaHCO<sub>3</sub> and brine, dried over MgSO<sub>4</sub>,

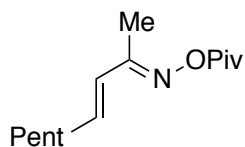
filtered and concentrated in vacuo. The crude product was purified by flash column chromatography.



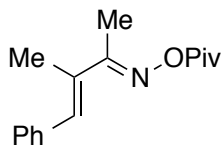
**(E)-1-(cyclohex-1-en-1-yl)ethanone O-pivaloyl oxime (24a).** White solid.  $R_f = 0.25$  (10:1 hexanes/EtOAc).  $^1\text{H NMR}$  (400 MHz,  $\text{CDCl}_3$ )  $\delta$  6.35 (m, 1H), 2.40 (m, 2H), 2.20 (m, 2H), 2.07 (s, 3H), 1.63 (m, 4H), 1.29 (s, 9H).  $^{13}\text{C NMR}$  (100 MHz,  $\text{CDCl}_3$ )  $\delta$  175.3, 164.1, 134.6, 133.5, 38.9, 27.4, 26.3, 24.6, 22.2, 22.0, 12.0. IR (NaCl, thin film)  $\nu$  2936, 1759, 1638, 1590, 1480, 1294, 1114, 917, 804  $\text{cm}^{-1}$ . HRMS (ESI)  $m/z$  [2M+Na] calcd 469.3042, found 469.3046.



**(2E,3E)-4-phenylbut-3-en-2-one O-pivaloyl oxime (24b).** Pale yellow viscous liquid.  $R_f = 0.21$  (10:1 hexanes/EtOAc).  $^1\text{H NMR}$  (400 MHz,  $\text{CDCl}_3$ )  $\delta$  7.48 (d,  $J = 7.2$  Hz, 2H), 7.38-7.30 (m, 3H), 7.08 (d,  $J = 17.2$  Hz, 1H), 7.04 (d,  $J = 16.8$  Hz, 1H), 2.23 (s, 3H), 1.33 (s, 9H).  $^{13}\text{C NMR}$  (100 MHz,  $\text{CDCl}_3$ )  $\delta$  175.1, 162.9, 137.3, 135.8, 129.3, 129.0, 127.3, 124.7, 38.9, 27.4, 11.7. IR (NaCl, thin film)  $\nu$  2974, 1749, 1633, 1587, 1479, 1272, 1112, 904, 751  $\text{cm}^{-1}$ . HRMS (ESI)  $m/z$  [2M+Na] calcd 513.2729, found 513.2732.

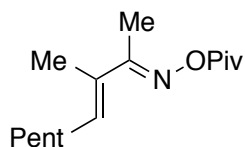


**(2E,3E)-non-3-en-2-one O-pivaloyl oxime (24c).** Pale yellow viscous liquid.  $R_f = 0.24$  (10:1 hexanes/EtOAc).  $^1\text{H NMR}$  (400 MHz,  $\text{CDCl}_3$ )  $\delta$  6.35-6.25 (m, 2H), 2.22-2.17 (m, 2H), 2.07 (s, 3H), 1.47-1.40 (m, 2H), 1.34-1.24 (m, 4H), 1.29 (s, 9H), 0.88 (t,  $J = 6.8$  Hz, 3H).  $^{13}\text{C NMR}$  (100 MHz,  $\text{CDCl}_3$ )  $\delta$  175.2, 163.0, 141.2, 126.5, 38.9, 33.0, 31.4, 28.4, 27.4, 22.6, 14.1, 11.7. IR (NaCl, thin film)  $\nu$  2931, 1761, 1649, 1481, 1271, 1110, 899, 758  $\text{cm}^{-1}$ . HRMS (ESI)  $m/z$  [2M+Na] calcd 501.3668, found 501.3681.



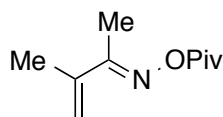
**(2E,3E)-3-methyl-4-phenylbut-3-en-2-one O-pivaloyl oxime (24d).**

Pale yellow viscous liquid.  $R_f = 0.28$  (10:1 hexanes/EtOAc).  $^1\text{H NMR}$  (300 MHz,  $\text{CDCl}_3$ )  $\delta$  7.41-7.29 (m, 5H), 7.05 (bs, 1H), 2.25 (s, 3H), 2.19 (s, 3H), 1.33 (s, 9H).



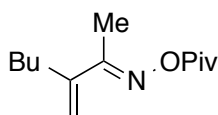
**(2E,3E)-3-methylnon-3-en-2-one O-pivaloyl oxime (24e).**

Pale yellow viscous liquid.  $R_f = 0.35$  (10:1 hexanes/EtOAc).  $^1\text{H NMR}$  (300 MHz,  $\text{CDCl}_3$ )  $\delta$  6.07 (t,  $J = 7.2$  Hz, 1H), 2.21 (q,  $J = 7.2$  Hz, 2H), 2.10 (s, 3H), 1.94 (s, 3H), 1.47-1.38 (m, 2H), 1.34-1.26 (m, 4H), 1.30 (s, 9H), 0.89 (t,  $J = 6.9$  Hz, 3H).



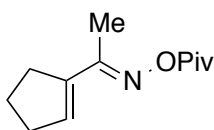
**(E)-3-methylbut-3-en-2-one O-pivaloyl oxime (24f).**

Colorless liquid.  $R_f = 0.43$  (10:1 hexanes/EtOAc).  $^1\text{H NMR}$  (400 MHz,  $\text{CDCl}_3$ )  $\delta$  5.54 (m, 1H), 5.43 (m, 1H), 2.12 (s, 3H), 2.05 (s, 3H), 1.30 (s, 9H).  $^{13}\text{C NMR}$  (100 MHz,  $\text{CDCl}_3$ )  $\delta$  175.2, 163.7, 141.0, 120.6, 38.9, 27.4, 19.3, 12.2. IR (NaCl, thin film)  $\nu$  2976, 1762, 1480, 1270, 1108, 921  $\text{cm}^{-1}$ . HRMS (ESI)  $m/z$   $[M+H]$  calcd 184.1338, found 184.1331.



**(E)-3-methyleneheptan-2-one O-pivaloyl oxime (24g).**

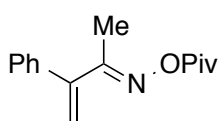
Colorless liquid.  $R_f = 0.45$  (10:1 hexanes/EtOAc).  $^1\text{H NMR}$  (400 MHz,  $\text{CDCl}_3$ )  $\delta$  5.53 (s, 1H), 5.38 (m, 1H), 2.44 (td,  $J = 7.6, 1.2$  Hz, 2H), 2.10 (s, 3H), 1.50 (m, 2H), 1.34 (m, 2H), 1.30 (s, 9H), 0.90 (t,  $J = 7.2$  Hz, 3H).  $^{13}\text{C NMR}$  (100 MHz,  $\text{CDCl}_3$ )  $\delta$  175.1, 163.5, 145.4, 119.1, 38.9, 32.0, 30.6, 27.4, 22.6, 14.1, 12.8. IR (NaCl, thin film)  $\nu$  2960, 1763, 1480, 1270, 1107, 920  $\text{cm}^{-1}$ . HRMS (ESI)  $m/z$   $[M+Na]$  calcd 248.1626, found 248.1622.



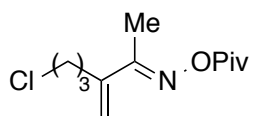
**(E)-1-(cyclopent-1-en-1-yl)ethanone O-pivaloyl oxime (27h).**

Colorless liquid.  $R_f = 0.33$  (10:1 hexanes/EtOAc).  $^1\text{H NMR}$  (400 MHz,  $\text{CDCl}_3$ )  $\delta$  6.35 (m, 1H), 2.68 (m, 2H), 2.48 (m, 2H), 2.14 (s, 3H), 1.94 (m, 2H), 1.29 (s, 9H).  $^{13}\text{C NMR}$  (100 MHz,  $\text{CDCl}_3$ )  $\delta$  175.2, 161.1, 140.8, 138.0, 39.0, 33.4, 31.5, 27.4, 23.4,

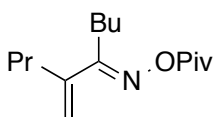
13.3. IR (NaCl, thin film)  $\nu$  2971, 1760, 1480, 1272, 1113, 891  $\text{cm}^{-1}$ . HRMS (ESI)  $m/z$  [M+H] calcd 210.1494, found 210.1495.



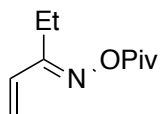
**(E)-3-phenylbut-3-en-2-one O-pivaloyl oxime (24i).** White solid.  $R_f = 0.26$  (10:1 hexanes/EtOAc).  $^1\text{H}$  NMR (400 MHz,  $\text{CDCl}_3$ )  $\delta$  7.38-7.30 (m, 5H), 5.70 (d,  $J = 0.8$  Hz, 1H), 5.58 (d,  $J = 0.4$  Hz, 1H), 2.09 (s, 3H), 1.33 (s, 9H).  $^{13}\text{C}$  NMR (100 MHz,  $\text{CDCl}_3$ )  $\delta$  175.1, 165.4, 145.2, 137.5, 128.6, 128.4, 127.9, 119.4, 39.0, 27.5, 15.6. IR (NaCl, thin film)  $\nu$  2980, 1752, 1584, 1367, 1267, 1110, 1031, 947, 896, 776, 695  $\text{cm}^{-1}$ . HRMS (ESI)  $m/z$  [M+Na] calcd 268.1313, found 268.1312.



**(E)-6-chloro-3-methylenehexan-2-one O-pivaloyl oxime (24j).** Colorless liquid.  $R_f = 0.33$  (10:1 hexanes/EtOAc).  $^1\text{H}$  NMR (400 MHz,  $\text{CDCl}_3$ )  $\delta$  5.62 (s, 1H), 5.49 (m, 1H), 3.55 (t,  $J = 6.4$  Hz, 2H), 2.62 (td,  $J = 7.6, 1.2$  Hz, 2H), 2.12 (s, 3H), 2.04 (m, 2H), 1.30 (s, 9H).  $^{13}\text{C}$  NMR (100 MHz,  $\text{CDCl}_3$ )  $\delta$  175.2, 162.7, 143.6, 120.9, 44.7, 39.0, 31.4, 30.0, 27.4, 12.6. IR (NaCl, thin film)  $\nu$  2971, 1761, 1480, 1270, 1106, 1027, 921  $\text{cm}^{-1}$ . LRMS (ESI + APCI)  $m/z$  [M+H] calcd 246.1, found 246.1.



**(E)-4-methylenenonan-5-one O-pivaloyl oxime (24k).** Colorless liquid.  $R_f = 0.26$  (10:1 hexanes/EtOAc).  $^1\text{H}$  NMR (400 MHz,  $\text{CDCl}_3$ )  $\delta$  5.53 (s, 1H), 5.38 (m, 1H), 2.55 (t,  $J = 8.0$  Hz, 2H), 2.40 (td,  $J = 7.2, 1.2$  Hz, 2H), 1.57-1.35 (m, 6H), 1.29 (s, 9H), 0.92 (t,  $J = 7.2$  Hz, 6H).  $^{13}\text{C}$  NMR (100 MHz,  $\text{CDCl}_3$ )  $\delta$  175.2, 167.3, 144.2, 119.1, 38.9, 34.7, 29.5, 27.4, 26.8, 23.1, 21.5, 13.9. IR (NaCl, thin film)  $\nu$  2962, 1763, 1462, 1110, 1026, 916  $\text{cm}^{-1}$ . HRMS (ESI)  $m/z$  [M+Na] calcd 276.1939, found 276.1935.



**Pent-1-en-3-one O-pivaloyl oxime (24I).** Pale yellow liquid, 5.1:1

mixture of isomers.  $R_f = 0.46$  (5:1 hexanes/EtOAc).  $^1\text{H NMR}$  (400 MHz,

$\text{CDCl}_3$ )  $\delta$  6.9 (dd,  $J = 18.0, 11.2$  Hz, 1H), 6.52 (dd,  $J = 18.0, 11.2$  Hz, 1H),

5.80 (dd,  $J = 18.0, 0.8$  Hz, 1H), 5.79 (d,  $J = 18.0$  Hz, 1H), 5.67 (dd,  $J = 11.2, 0.8$  Hz, 1H), 5.64

(d,  $J = 10.8$  Hz, 1H), 2.56 (m, 2H), 1.29 (s, 9H), 1.28 (s, 9H), 1.20 (t,  $J = 7.6$  Hz, 3H), 1.13 (t,  $J =$

7.6 Hz, 3H).  $^{13}\text{C NMR}$  (100 MHz,  $\text{CDCl}_3$ )  $\delta$  175.1, 167.5, 164.4, 132.2, 125.3, 125.2, 122.7,

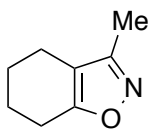
38.9, 27.4, 27.3, 24.1, 18.9, 12.3, 11.4. IR (NaCl, thin film)  $\nu$  2977, 1762, 1481, 1271, 1110,

1027, 899  $\text{cm}^{-1}$ . LRMS (ESI + APCI)  $m/z$  [M+H] calcd 184.1, found 184.2.

#### A.1.4 General Procedure for Pyridine Synthesis

A 0.5 dram vial was charged with oxime ester **24** (0.21 mmol) and AgOAc (73.6 mg, 0.441 mmol, 2.1 equiv) and a solution of  $[\text{RhCp}^*\text{Cl}_2]_2$  (3.3 mg, 0.005 mmol, 0.025 equiv) and alkene **15** or **32** (0.252 mmol, 1.2 equiv) in 0.7 mL 2:1 DCE/AcOH was added. The vial was flushed with argon, sealed and heated at 85 °C in an aluminum heating block for 14 hours. The solids were filtered and the mixture was diluted with  $\text{CH}_2\text{Cl}_2$  and washed with 15% aqueous  $\text{Na}_2\text{CO}_3$ . The aqueous layer was extracted twice with  $\text{CH}_2\text{Cl}_2$  and the combined organic layers were dried over  $\text{MgSO}_4$ , filtered and concentrated *in vacuo*. The crude product was purified by flash column chromatography.

Compounds **13fh**,<sup>9</sup> **13fu** and **14fu**,<sup>10</sup> **29**<sup>11</sup> and **30**<sup>12</sup> were previously characterized.



**3-Methyl-4,5,6,7-tetrahydrobenzo[d]isoxazole (23).** Colorless

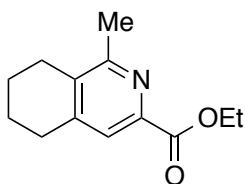
viscous liquid.  $R_f = 0.34$  (10:1 hexanes/EtOAc).  $^1\text{H NMR}$  (400

MHz,  $\text{CDCl}_3$ )  $\delta$  2.64 (tt,  $J = 6.4, 1.6$  Hz, 2H), 2.33 (tt,  $J = 6.0, 1.6$

Hz, 2H), 2.19 (s, 3H), 1.86-1.71 (m, 4H).  $^{13}\text{C NMR}$  (100 MHz,  $\text{CDCl}_3$ )  $\delta$  167.7, 158.3, 112.1,



22.7, 22.6, 22.3, 19.3, 10.1. IR (NaCl, thin film)  $\nu$  2938, 2856, 1642, 1466, 1321, 1201, 869, 740  $\text{cm}^{-1}$ . LRMS (ESI + APCI)  $m/z$  [M+H] calcd 138.1, found 138.2.



**Ethyl 1-methyl-5,6,7,8-tetrahydroisoquinoline-3-carboxylate**

**(13aa).** Pale yellow viscous liquid.  $R_f = 0.13$  (3:1

hexanes/EtOAc).  $^1\text{H}$  NMR (400 MHz,  $\text{CDCl}_3$ )  $\delta$  7.69 (s, 1H), 4.44

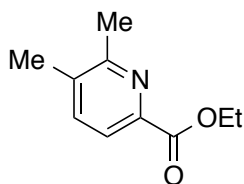
(q,  $J = 7.2$  Hz, 2H), 2.79 (t,  $J = 6.0$  Hz), 2.66 (t,  $J = 6.4$  Hz, 2H), 2.53 (s, 3H), 1.87 (m, 2H), 1.76

(m, 2H), 1.42 (t,  $J = 7.2$  Hz, 3H).  $^{13}\text{C}$  NMR (100 MHz,  $\text{CDCl}_3$ )  $\delta$  166.0, 157.8, 147.0, 144.1,

135.4, 124.0, 61.8, 29.6, 26.4, 22.8, 22.6, 22.0, 14.5. IR (NaCl, thin film)  $\nu$  2944, 1708, 1589,

1372, 1317, 1261, 1212, 1028, 789  $\text{cm}^{-1}$ . HRMS (ESI)  $m/z$  [M+H] calcd 220.1338, found

220.1339.



**Ethyl 5,6-dimethylpicolinate (13fa).** Pale yellow viscous liquid.

$R_f = 0.15$  (3:1 hexanes/EtOAc).  $^1\text{H}$  NMR (400 MHz,  $\text{CDCl}_3$ )  $\delta$

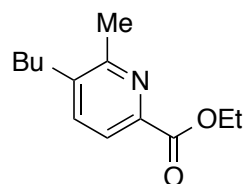
7.85 (d,  $J = 7.6$  Hz, 1H), 7.50 (d,  $J = 7.6$  Hz, 1H), 4.43 (q,  $J = 7.2$

Hz, 2H), 2.57 (s, 3H), 2.32 (s, 3H), 1.40 (t,  $J = 7.2$  Hz, 3H).  $^{13}\text{C}$  NMR (100 MHz,  $\text{CDCl}_3$ )  $\delta$

165.7, 157.9, 145.4, 137.7, 135.9, 123.0, 61.8, 23.0, 19.5, 14.4. IR (NaCl, thin film)  $\nu$  2983,

1716, 1460, 1369, 1312, 1249, 1188, 1135, 1025, 783, 718  $\text{cm}^{-1}$ . HRMS (ESI)  $m/z$  [M+H] calcd

180.1025, found 180.1025.



**Ethyl 5-butyl-6-methylpicolinate (13ga).** Yellow viscous liquid.

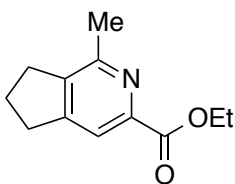
$R_f = 0.26$  (3:1 hexanes/EtOAc).  $^1\text{H}$  NMR (400 MHz,  $\text{CDCl}_3$ )  $\delta$

7.87 (d,  $J = 8.0$  Hz, 1H), 7.51 (d,  $J = 7.6$  Hz, 1H), 4.44 (q,  $J = 7.2$

Hz, 2H), 2.64 (t,  $J = 7.6$  Hz, 2H), 2.61 (s, 3H), 1.56 (m, 2H), 1.43-1.34 (m, 5H), 0.94 (t,  $J = 5.4$ ,

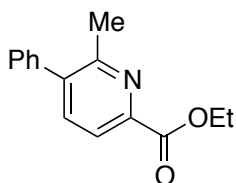
3H).  $^{13}\text{C}$  NMR (100 MHz,  $\text{CDCl}_3$ )  $\delta$  165.7, 157.4, 145.3, 140.3, 136.9, 123.0, 61.8, 32.6, 31.7,

22.6, 22.5, 14.4, 14.0. IR (NaCl, thin film)  $\nu$  2959, 1717, 1574, 1458, 1369, 1313, 1180, 1138, 1028  $\text{cm}^{-1}$ . HRMS (ESI)  $m/z$  [M+H] calcd 222.1494, found 222.1489.



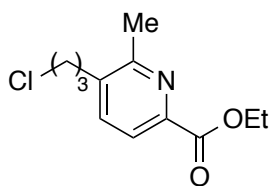
**Ethyl 1-methyl-6,7-dihydro-5H-cyclopenta[c]pyridine-3-carboxylate (13ha).** Pale yellow viscous liquid.  $R_f = 0.12$  (3:1 hexanes/EtOAc).  $^1\text{H}$  NMR (400 MHz,  $\text{CDCl}_3$ )  $\delta$  7.84 (s, 1H), 4.44

(q,  $J = 7.2$  Hz, 2H), 2.97 (t,  $J = 7.6$  Hz, 2H), 2.91 (t,  $J = 7.2$  Hz, 2H), 2.55 (s, 3H), 2.14 (dd,  $J = 7.6, 7.6$  Hz, 2H), 1.41 (t,  $J = 7.2$  Hz, 3H).  $^{13}\text{C}$  NMR (100 MHz,  $\text{CDCl}_3$ )  $\delta$  166.0, 154.5, 146.0, 142.5, 119.6, 61.8, 33.0, 31.0, 24.3, 22.4, 14.5. IR (NaCl, thin film)  $\nu$  2960, 1716, 1594, 1376, 1329, 1224, 1030, 791  $\text{cm}^{-1}$ . HRMS (ESI)  $m/z$  [M+H] calcd 206.1181, found 206.1175.



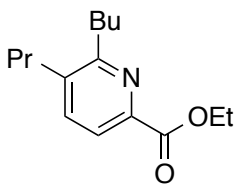
**Ethyl 6-methyl-5-phenylpicolinate (13ia).** Yellow viscous liquid.  $R_f = 0.23$  (5:1 hexanes/EtOAc).  $^1\text{H}$  NMR (400 MHz,  $\text{CDCl}_3$ )  $\delta$  8.01 (d,  $J = 7.6$  Hz, 1H), 7.64 (d,  $J = 8.0$  Hz, 1H), 7.43

(m, 3H), 7.32 (m, 2H), 4.49 (q,  $J = 7.2$  Hz, 2H), 2.60 (s, 3H), 1.45 (t,  $J = 7.2$  Hz, 3H).  $^{13}\text{C}$  NMR (100 MHz,  $\text{CDCl}_3$ )  $\delta$  165.5, 156.7, 146.6, 140.5, 139.2, 138.0, 128.9, 128.7, 128.1, 122.7, 62.0, 23.9, 14.5. IR (NaCl, thin film)  $\nu$  2982, 1716, 1561, 1446, 1369, 1309, 1200, 1142, 1027, 861, 763, 703  $\text{cm}^{-1}$ . HRMS (ESI)  $m/z$  [M+H] calcd 242.1181, found 242.1179.

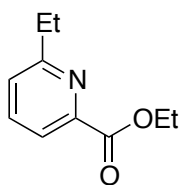


**Ethyl 5-(3-chloropropyl)-6-methylpicolinate (13ja).** Pale yellow viscous liquid.  $R_f = 0.17$  (3:1 hexanes/EtOAc).  $^1\text{H}$  NMR (400 MHz,  $\text{CDCl}_3$ )  $\delta$  7.90 (d,  $J = 7.6$  Hz, 1H), 7.56 (d,  $J = 8.0$  Hz, 1H),

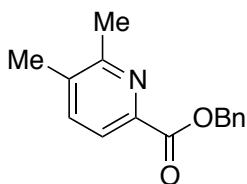
4.45 (q,  $J = 7.2$  Hz, 2H), 3.56 (t,  $J = 6.0$  Hz, 2H), 2.85 (t,  $J = 7.6$  Hz, 2H), 2.64 (s, 3H), 2.06 (m, 2H), 1.42 (t,  $J = 7.2$  Hz, 3H).  $^{13}\text{C}$  NMR (100 MHz,  $\text{CDCl}_3$ )  $\delta$  165.5, 157.5, 145.9, 138.3, 137.2, 123.1, 61.9, 44.2, 32.1, 30.0, 22.6, 14.5. IR (NaCl, thin film)  $\nu$  2960, 1716, 1573, 1445, 1369, 1312, 1184, 1138, 1028  $\text{cm}^{-1}$ . LRMS (ESI + APCI)  $m/z$  [M+H] calcd 242.1, found 242.1.



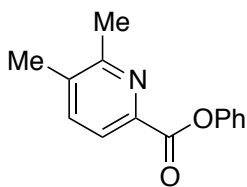
**Ethyl 6-butyl-5-propylpicolinate (13ka).** Pale yellow viscous liquid.  $R_f = 0.47$  (3:1 hexanes/EtOAc).  $^1\text{H NMR}$  (400 MHz,  $\text{CDCl}_3$ )  $\delta$  7.78 (d,  $J = 8.0$  Hz, 1H), 7.45 (d,  $J = 8.0$  Hz, 1H), 4.37 (q,  $J = 7.2$  Hz, 2H), 2.81 (t,  $J = 8.0$  Hz, 2H), 2.58 (t,  $J = 8.0$  Hz, 2H), 1.66-1.52 (m, 4H), 1.36 (m, 2H), 1.34 (t,  $J = 7.2$  Hz, 3H), 0.92 (t,  $J = 7.2$  Hz, 3H), 0.88 (t,  $J = 7.2$  Hz, 3H).  $^{13}\text{C NMR}$  (100 MHz,  $\text{CDCl}_3$ )  $\delta$  165.8, 161.2, 145.6, 139.4, 137.3, 122.7, 61.7, 35.0, 34.4, 32.0, 23.7, 23.0, 14.5, 14.1. IR (NaCl, thin film)  $\nu$  2960, 1717, 1572, 1456, 1369, 1312, 1178, 1138, 1024  $\text{cm}^{-1}$ . HRMS (ESI)  $m/z$  [M+H] calcd 250.1807, found 250.1809.



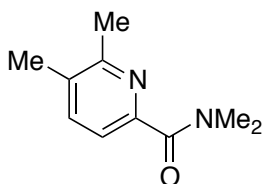
**Ethyl 6-ethylpicolinate (13la).** Colorless viscous liquid.  $R_f = 0.07$  (10:1 hexanes/EtOAc).  $^1\text{H NMR}$  (400 MHz,  $\text{CDCl}_3$ )  $\delta$  7.93 (dd,  $J = 7.6, 0.8$  Hz, 1H), 7.73 (t,  $J = 7.6$  Hz, 1H), 7.34 (dd,  $J = 7.6, 0.8$  Hz, 1H), 4.46 (q,  $J = 7.2$  Hz, 2H), 2.93 (q,  $J = 7.6$  Hz, 2H), 1.42 (t,  $J = 7.2$  Hz, 3H), 1.32 (t,  $J = 7.6$  Hz, 3H).  $^{13}\text{C NMR}$  (100 MHz,  $\text{CDCl}_3$ )  $\delta$  165.7, 164.3, 148.0, 137.3, 125.4, 122.6, 61.9, 31.6, 14.5, 14.2. IR (NaCl, thin film)  $\nu$  2976, 1718, 1591, 1463, 1368, 1235, 1139, 761  $\text{cm}^{-1}$ . LRMS (ESI + APCI)  $m/z$  [M+H] calcd 180.1, found 180.1.



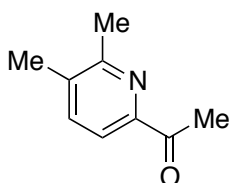
**Benzyl 5,6-dimethylpicolinate (13fb).** Yellow viscous liquid.  $R_f = 0.21$  (3:1 hexanes/EtOAc).  $^1\text{H NMR}$  (400 MHz,  $\text{CDCl}_3$ )  $\delta$  7.87 (d,  $J = 7.6$  Hz, 1H), 7.50 (d,  $J = 8.0$  Hz, 1H), 7.48 (m, 2H), 7.38-7.30 (m, 3H), 5.43 (s, 2H), 2.59 (s, 3H), 2.34 (s, 3H).  $^{13}\text{C NMR}$  (100 MHz,  $\text{CDCl}_3$ )  $\delta$  165.4, 158.1, 145.1, 137.7, 136.1, 128.6, 128.5, 128.3, 123.2, 67.3, 23.0, 19.6. IR (NaCl, thin film)  $\nu$  2954, 1716, 1587, 1456, 1398, 1308, 1255, 1185, 1131, 1002, 782, 698  $\text{cm}^{-1}$ . HRMS (ESI)  $m/z$  [M+H] calcd 242.1181, found 242.1173.



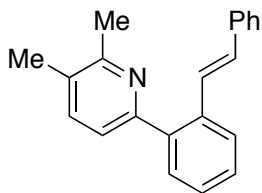
**Phenyl 5,6-dimethylpicolinate (13fc).** Off-white solid.  $R_f = 0.24$  (3:1 hexanes/EtOAc).  $^1\text{H NMR}$  (400 MHz,  $\text{CDCl}_3$ )  $\delta$  8.03 (d,  $J = 8.0$  Hz, 1H), 7.59 (d,  $J = 7.6$  Hz, 1H), 7.42 (m, 2H), 7.26 (m, 3H), 2.64 (s, 3H), 2.39 (s, 3H).  $^{13}\text{C NMR}$  (100 MHz,  $\text{CDCl}_3$ )  $\delta$  164.3, 158.3, 151.3, 144.7, 137.9, 136.7, 129.5, 126.1, 123.9, 122.0, 23.1, 19.7. IR (NaCl, thin film)  $\nu$  2923, 1732, 1591, 1493, 1309, 1196, 1109, 746  $\text{cm}^{-1}$ . LRMS (ESI + APCI)  $m/z$  [M+H] calcd 228.1, found 228.1.



***N,N*,5,6-Tetramethylpicolinamide (13fd).** Pale yellow viscous liquid.  $R_f = 0.21$  (EtOAc).  $^1\text{H NMR}$  (400 MHz,  $\text{CDCl}_3$ )  $\delta$  7.49 (d,  $J = 8.0$  Hz, 1H), 7.35 (d,  $J = 7.6$  Hz, 1H), 3.11 (s, 3H), 3.07 (s, 3H), 2.52 (s, 3H), 2.30 (s, 3H).  $^{13}\text{C NMR}$  (100 MHz,  $\text{CDCl}_3$ )  $\delta$  169.4, 156.0, 151.3, 138.1, 132.7, 121.1, 39.2, 35.9, 22.5, 19.3. IR (NaCl, thin film)  $\nu$  2926, 1637, 1575, 1441, 1397, 1274, 1175, 1104, 843  $\text{cm}^{-1}$ . LRMS (ESI + APCI)  $m/z$  [M+H] calcd 179.1, found 179.1.

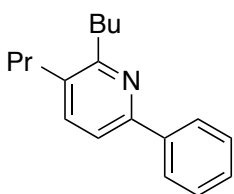


**1-(5,6-Dimethylpyridin-2-yl)ethanone (13fe).** Pale yellow viscous liquid.  $R_f = 0.26$  (5:1 hexanes/EtOAc).  $^1\text{H NMR}$  (400 MHz,  $\text{CDCl}_3$ )  $\delta$  7.78 (d,  $J = 7.6$ , 1H), 7.51 (d,  $J = 8.0$ , 1H), 2.70 (s, 3H), 2.55 (s, 3H), 2.34 (s, 3H).  $^{13}\text{C NMR}$  (100 MHz,  $\text{CDCl}_3$ )  $\delta$  200.7, 156.8, 151.2, 137.7, 136.0, 119.5, 25.9, 22.9, 19.6. IR (NaCl, thin film)  $\nu$  2926, 1696, 1573, 1459, 1355, 1301, 1177, 1122, 956, 839  $\text{cm}^{-1}$ . LRMS (ESI + APCI)  $m/z$  [M+H] calcd 150.1, found 150.2.



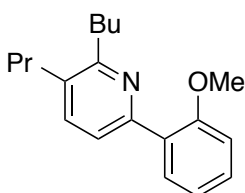
**(*E*)-2,3-Dimethyl-6-(2-styrylphenyl)pyridine (31h).** Pale yellow viscous liquid.  $R_f = 0.66$  (20:1 DCM/EtOAc).  $^1\text{H NMR}$  (400 MHz,  $\text{CDCl}_3$ )  $\delta$  7.75 (dd,  $J = 7.6, 1.6$  Hz, 1H), 7.55 (dd,  $J = 7.2, 2.0$  Hz, 1H), 7.46 (d,  $J = 7.6$  Hz, 1H), 7.41-7.19 (m, 9H), 7.04 (d,  $J = 16.4$  Hz, 1H), 2.60 (s, 3H), 2.36 (s, 3H).  $^{13}\text{C NMR}$  (100 MHz,  $\text{CDCl}_3$ )  $\delta$  156.9, 155.6, 137.9,

137.3, 135.9, 130.4, 129.7, 128.7, 128.4, 128.1, 127.8, 127.5, 126.7, 126.3, 122.7, 22.9, 19.1. IR (NaCl, thin film)  $\nu$  2922, 1737, 1589, 1462, 1236, 1129, 961, 836, 761, 692  $\text{cm}^{-1}$ . LRMS (ESI + APCI)  $m/z$  [M+H] calcd 286.2, found 286.2.



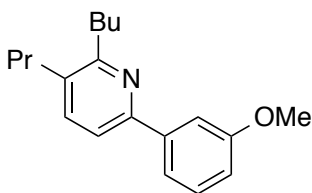
**2-Butyl-6-phenyl-3-propylpyridine (13kh).** Pale yellow viscous liquid.  $R_f = 0.11$  (1:1 hexanes/DCM).  $^1\text{H}$  NMR (400 MHz,  $\text{CDCl}_3$ )  $\delta$  8.02 (m, 2H), 7.50-7.35 (m, 5H), 2.87 (t,  $J = 8.0$  Hz, 2H),

2.64 (t,  $J = 8.0$  Hz, 2H), 1.82 (m, 2H), 1.66 (m, 2H), 1.48 (m, 2H), 1.02 (t,  $J = 7.2$  Hz, 3H), 1.00 (t,  $J = 7.6$  Hz, 3H).  $^{13}\text{C}$  NMR (100 MHz,  $\text{CDCl}_3$ )  $\delta$  160.1, 154.2, 137.4, 133.8, 128.7, 128.4, 126.8, 117.7, 34.8, 34.2, 31.7, 23.9, 23.0, 14.3, 14.2. IR (NaCl, thin film)  $\nu$  2959, 2871, 1585, 1564, 1457, 1379, 833, 758, 693  $\text{cm}^{-1}$ . LRMS (ESI + APCI)  $m/z$  [M+H] calcd 254.2, found 254.2.



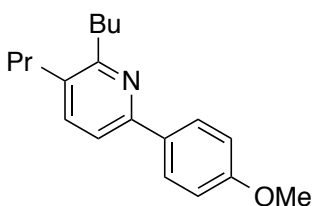
**2-Butyl-6-(2-methoxyphenyl)-3-propylpyridine (13ki).**

Colorless viscous liquid.  $R_f = 0.20$  (10:1 hexanes/EtOAc).  $^1\text{H}$  NMR (400 MHz,  $\text{CDCl}_3$ )  $\delta$  7.80 (dd,  $J = 7.6, 1.6$  Hz, 1H), 7.57 (d,  $J = 8.0$  Hz, 1H), 7.43 (d,  $J = 8.0$  Hz, 1H), 7.33 (ddd,  $J = 6.8, 6.8, 1.6$  Hz, 1H), 7.07 (ddd,  $J = 7.6, 7.6, 0.8$  Hz, 1H), 6.98 (dd,  $J = 8.0, 0.8$  Hz, 1H), 3.85 (s, 3H), 2.86 (t,  $J = 8.0$  Hz, 2H), 2.63 (t,  $J = 8.0, 2\text{H}$ ), 1.77 (m, 2H), 1.66 (m, 2H), 1.47 (m, 2H), 1.03 (t,  $J = 7.6$  Hz, 3H), 0.98 (t,  $J = 7.6$  Hz, 3H).  $^{13}\text{C}$  NMR (100 MHz,  $\text{CDCl}_3$ )  $\delta$  159.9, 157.1, 152.7, 136.4, 133.2, 131.4, 129.4, 122.3, 121.2, 111.5, 55.7, 34.9, 34.2, 32.1, 24.0, 23.1, 14.3. IR (NaCl, thin film)  $\nu$  2958, 1585, 1493, 1461, 1240, 1027, 752  $\text{cm}^{-1}$ . HRMS (ESI)  $m/z$  [M+H] calcd 284.2014, found 284.2013.



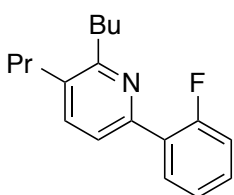
**2-Butyl-6-(3-methoxyphenyl)-3-propylpyridine (13kj).**

Colorless viscous liquid.  $R_f = 0.45$  (10:1 hexanes/EtOAc).  $^1\text{H}$  NMR (400 MHz,  $\text{CDCl}_3$ )  $\delta$  7.62 (dd,  $J = 2.8, 1.6$  Hz, 1H), 7.56 (ddd, 7.6, 1.6, 1.2 Hz, 1H), 7.47 (d,  $J = 8.0$  Hz, 1H), 7.45 (d,  $J = 8.0$  Hz, 1H), 7.36 (dd,  $J = 8.0, 8.0$  Hz, 1H), 6.92 (ddd,  $J = 8.0, 2.8, 0.8$  Hz, 1H), 3.89 (s, 3H), 2.86 (t,  $J = 8.0$  Hz, 2H), 2.63 (t,  $J = 8.0$  Hz, 2H), 1.80 (m, 2H), 1.65 (m, 2H), 1.47 (m, 2H), 1.01 (t,  $J = 5.4$ , 3H), 0.99 (t,  $J = 5.4$ , 3H).  $^{13}\text{C}$  NMR (100 MHz,  $\text{CDCl}_3$ )  $\delta$  160.1, 153.9, 141.6, 137.4, 134.0, 130.0, 119.3, 117.8, 114.2, 112.3, 55.4, 34.8, 34.2, 31.6, 23.9, 23.0, 14.3, 14.2. IR (NaCl, thin film)  $\nu$  2958, 2871, 1566, 1463, 1222, 1048, 826, 782  $\text{cm}^{-1}$ . HRMS (ESI)  $m/z$   $[\text{M}+\text{H}]$  calcd 284.2014, found 284.2015.



**2-Butyl-6-(4-methoxyphenyl)-3-propylpyridine (13kk).**

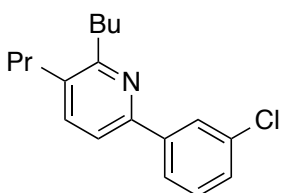
Colorless viscous liquid.  $R_f = 0.43$  (10:1 hexanes/EtOAc).  $^1\text{H}$  NMR (400 MHz,  $\text{CDCl}_3$ )  $\delta$  7.96 (m, 2H), 7.43 (d,  $J = 8.0$  Hz, 1H), 7.41 (d,  $J = 8.0$  Hz, 1H), 6.98 (m, 2H), 3.86 (s, 3H), 2.85 (t,  $J = 7.6$  Hz, 2H), 2.61 (t,  $J = 7.6$  Hz, 2H), 1.80 (m, 2H), 1.64 (m, 2H), 1.47 (m, 2H), 1.00 (t,  $J = 7.2$  Hz, 3H), 0.99 (t,  $J = 7.2$  Hz, 3H).  $^{13}\text{C}$  NMR (100 MHz,  $\text{CDCl}_3$ )  $\delta$  160.1, 160.0, 153.9, 137.4, 133.0, 128.1, 117.0, 114.1, 55.5, 34.8, 34.1, 31.7, 24.0, 23.0, 14.3, 14.2. IR (NaCl, thin film)  $\nu$  2958, 1609, 1585, 1513, 1456, 1249, 1181, 1032, 825  $\text{cm}^{-1}$ . LRMS (ESI + APCI)  $m/z$   $[\text{M}+\text{H}]$  calcd 284.2, found 284.2.



**2-Butyl-6-(2-fluorophenyl)-3-propylpyridine (13kl).**

Colorless viscous liquid.  $R_f = 0.16$  (1:1 hexanes/DCM).  $^1\text{H}$  NMR (400 MHz,  $\text{CDCl}_3$ )  $\delta$  8.04 (ddd,  $J = 8.0, 8.0, 2.0$  Hz, 1H), 7.55 (dd,  $J = 8.0, 2.4$  Hz, 1H), 7.47 (d,  $J = 8.0$  Hz, 1H), 7.33 (m, 1H), 7.25 (ddd,  $J = 7.6, 7.6, 1.2$  Hz, 1H), 7.13 (ddd,  $J = 11.6, 8.0, 1.2$  Hz, 1H), 2.87 (t,  $J = 8.0$  Hz, 2H), 2.64 (t,  $J = 7.6$  Hz, 2H), 1.79 (m,

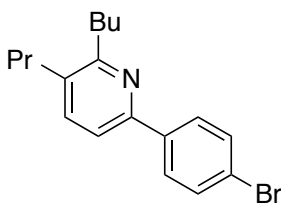
2H), 1.66 (m, 2H), 1.47 (m, 2H), 1.02 (t,  $J = 7.2$ , 3H), 0.99 (t,  $J = 7.2$ , 3H).  $^{13}\text{C}$  NMR (100 MHz,  $\text{CDCl}_3$ )  $\delta$  160.7 (d,  $J = 247.7$  Hz), 160.4, 151.1 (d,  $J = 2.2$ ), 137.0, 134.2, 131.2 (d,  $J = 3.1$ ), 129.8 (d,  $J = 8.4$ ), 124.5 (d,  $J = 3.4$ ), 121.8 (d,  $J = 9.2$ ), 116.3, 116.0, 34.8, 34.2, 31.8, 23.9, 23.0, 14.2. IR (NaCl, thin film)  $\nu$  2959, 2872, 1585, 1491, 1455, 1387, 1212, 1109, 816, 757  $\text{cm}^{-1}$ . LRMS (ESI + APCI)  $m/z$  [M+H] calcd 272.2, found 272.2.



**2-Butyl-6-(3-chlorophenyl)-3-propylpyridine (13km).** Colorless

viscous liquid.  $R_f = 0.38$  (1:1 hexanes/DCM).  $^1\text{H}$  NMR (400 MHz,  $\text{CDCl}_3$ )  $\delta$  8.03 (ddd,  $J = 2.0, 1.6, 0.4$  Hz, 1H), 7.88 (ddd,  $J =$

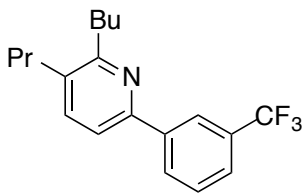
7.2, 1.6, 1.6 Hz, 1H), 7.47 (d,  $J = 8.0$  Hz, 1H), 7.45 (d,  $J = 8.0$  Hz, 1H), 7.37 (ddd,  $J = 8.0, 7.2, 0.4$  Hz, 1H), 7.33 (ddd,  $J = 8.0, 2.0, 1.6$  Hz, 1H), 2.86 (t,  $J = 8.0$  Hz, 2H), 2.63 (t,  $J = 8.0$  Hz, 2H), 1.80 (m, 2H), 1.65 (m, 2H), 1.48 (m, 2H), 1.01 (t,  $J = 7.2$  Hz, 3H), 1.00 (t,  $J = 7.6$  Hz, 3H).  $^{13}\text{C}$  NMR (100 MHz,  $\text{CDCl}_3$ )  $\delta$  160.4, 152.6, 141.9, 137.5, 134.8, 134.5, 129.9, 128.4, 127.0, 124.9, 117.7, 34.8, 34.2, 31.6, 23.9, 23.0, 14.2. IR (NaCl, thin film)  $\nu$  2959, 2871, 1561, 1454, 1379, 1078, 784  $\text{cm}^{-1}$ . LRMS (ESI + APCI)  $m/z$  [M+H] calcd 288.2, found 288.2.



**6-(4-Bromophenyl)-2-butyl-3-propylpyridine (13kn).** Colorless

viscous liquid.  $R_f = 0.63$  (10:1 hexanes/EtOAc).  $^1\text{H}$  NMR (400 MHz,  $\text{CDCl}_3$ )  $\delta$  7.89 (m, 2H), 7.56 (m, 2H), 7.46 (d,  $J = 8.0$  Hz,

1H), 7.44 (d,  $J = 7.6$  Hz, 1H), 2.85 (t,  $J = 7.6$  Hz, 2H), 2.62 (t,  $J = 7.6$  Hz, 2H), 1.78 (m, 2H), 1.64 (m, 2H), 1.46 (m, 2H), 1.01 (t,  $J = 7.6$  Hz, 3H), 0.98 (t,  $J = 7.6$  Hz, 3H).  $^{13}\text{C}$  NMR (100 MHz,  $\text{CDCl}_3$ )  $\delta$  160.4, 152.9, 138.9, 137.5, 134.3, 131.8, 128.4, 122.8, 117.4, 34.8, 34.2, 31.6, 23.9, 23.0, 14.3, 14.2. IR (NaCl, thin film)  $\nu$  2958, 2930, 2871, 1586, 1454, 1377, 1072, 1009, 818  $\text{cm}^{-1}$ . LRMS (ESI + APCI)  $m/z$  [M+H] calcd 332.1, found 332.1.



**2-Butyl-3-propyl-6-(3-(trifluoromethyl)phenyl)pyridine (13ko).**

Colorless viscous liquid.  $R_f = 0.29$  (10:1 hexanes/EtOAc).  $^1\text{H}$

NMR (400 MHz,  $\text{CDCl}_3$ )  $\delta$  8.27 (s, 1H), 8.20 (d,  $J = 7.6$  Hz, 1H),

7.62 (d,  $J = 8.0$  Hz, 1H), 7.57 (t,  $J = 8.0$  Hz, 1H), 7.51 (d,  $J = 8.0$  Hz, 1H), 7.49 (d,  $J = 8.0$ , 1H),

2.87 (t,  $J = 8.0$  Hz, 2H), 2.64 (t,  $J = 8.0$  Hz, 2H), 1.84-1.76 (m, 2H), 1.70-1.61 (m, 2H), 1.52-

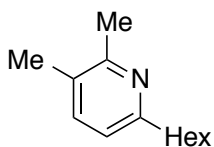
1.43 (m, 2H), 1.01 (q,  $J = 7.6$ , 6H).  $^{13}\text{C}$  NMR (100 MHz,  $\text{CDCl}_3$ )  $\delta$  160.6, 152.5, 140.8, 137.6,

134.7, 131.1 (q,  $J = 32.3$  Hz), 130.0, 129.2, 125.0 (q,  $J = 3.7$  Hz), 124.5 (q,  $J = 270.9$  Hz), 123.7

(q,  $J = 4.0$  Hz), 117.7, 34.8, 34.2, 31.6, 23.9, 23.0, 14.2, 14.2. IR (NaCl, thin film)  $\nu$  2960, 2932,

2873, 1570, 1458, 1442, 1380, 1336, 1270, 1166, 1127, 1072, 921, 835, 800, 697  $\text{cm}^{-1}$ . LRMS

(ESI + APCI)  $m/z$   $[\text{M}+\text{H}]$  calcd 322.2, found 322.2.



**6-Hexyl-2,3-dimethylpyridine (13fr).** Pale yellow viscous liquid.

$R_f = 0.52$  (5:1 hexanes/EtOAc).  $^1\text{H}$  NMR (400 MHz,  $\text{CDCl}_3$ )  $\delta$

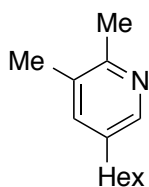
7.29 (d,  $J = 7.6$  Hz, 1H), 6.87 (d,  $J = 8.0$  Hz), 2.70 (t,  $J = 7.6$  Hz,

2H), 2.47 (s, 3H), 2.23 (s, 3H), 1.67 (m, 2H), 1.37-1.25 (m, 6H), 0.87 (m, 3H).  $^{13}\text{C}$  NMR (100

MHz,  $\text{CDCl}_3$ )  $\delta$  159.1, 156.1, 137.4, 128.1, 119.8, 38.1, 31.7, 30.2, 29.1, 22.6, 22.5, 18.7, 14.1.

IR (NaCl, thin film)  $\nu$  2926, 2857, 1578, 1467, 1397, 824  $\text{cm}^{-1}$ . LRMS (ESI + APCI)  $m/z$

$[\text{M}+\text{H}]$  calcd 192.2, found 192.2.



**5-Hexyl-2,3-dimethylpyridine (14fr).** Pale yellow viscous liquid.

$R_f = 0.26$  (5:1 hexanes/EtOAc).  $^1\text{H}$  NMR (400 MHz,  $\text{CDCl}_3$ )  $\delta$

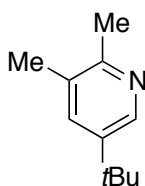
8.13 (d,  $J = 2.0$  Hz, 1H), 7.20 (d,  $J = 1.6$  Hz, 1H), 2.52 (t,  $J = 7.6$

Hz, 2H), 2.45 (s, 3H), 2.24 (s, 3H), 1.57 (m, 2H), 1.28 (m, 6H), 0.87 (m, 3H).  $^{13}\text{C}$  NMR (100

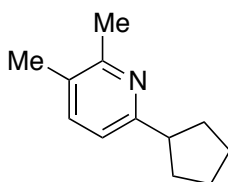
MHz,  $\text{CDCl}_3$ )  $\delta$  154.3, 146.5, 137.3, 135.5, 130.9, 32.6, 31.8, 31.4, 29.0, 22.7, 22.2, 19.2, 14.2.



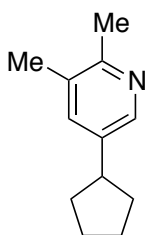
IR (NaCl, thin film)  $\nu$  2928, 2857, 1474, 1412, 1139, 1020, 899, 727  $\text{cm}^{-1}$ . LRMS (ESI + APCI)  $m/z$  [M+H] calcd 192.2, found 192.2.



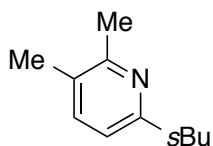
**5-(*tert*-Butyl)-2,3-dimethylpyridine (14fs).** Yellow viscous liquid.  $R_f = 0.10$  (3:1 hexanes/EtOAc).  $^1\text{H}$  NMR (400 MHz,  $\text{CDCl}_3$ )  $\delta$  8.35 (d,  $J = 2.4$  Hz, 1H), 7.39 (d,  $J = 2.4$  Hz, 1H), 2.46 (s, 3H), 2.26 (s, 3H), 1.31 (s, 9H).  $^{13}\text{C}$  NMR (100 MHz,  $\text{CDCl}_3$ )  $\delta$  154.0, 143.7, 143.6, 134.6, 130.6, 33.2, 31.2, 22.0, 19.5. IR (NaCl, thin film)  $\nu$  2962, 1481, 1397, 1167, 733  $\text{cm}^{-1}$ . LRMS (ESI + APCI)  $m/z$  [M+H] calcd 164.1439, found 164.2.



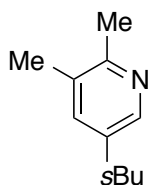
**6-Cyclopentyl-2,3-dimethylpyridine (13ft).** Pale yellow viscous liquid.  $R_f = 0.60$  (5:1 hexanes/EtOAc).  $^1\text{H}$  NMR (400 MHz,  $\text{CDCl}_3$ )  $\delta$  7.30 (d,  $J = 8.0$ , 1H), 6.93 (d,  $J = 8.0$  Hz, 1H), 3.11 (m, 1H), 2.47 (s, 3H), 2.23 (s, 3H), 2.07 (m, 2H), 1.81-1.66 (m, 6H).  $^{13}\text{C}$  NMR (100 MHz,  $\text{CDCl}_3$ )  $\delta$  162.6, 156.1, 137.5, 128.3, 118.3, 48.0, 33.9, 25.8, 22.8, 18.9. IR (NaCl, thin film)  $\nu$  2952, 2868, 1578, 1465, 1400, 1127, 825  $\text{cm}^{-1}$ . LRMS (ESI + APCI)  $m/z$  [M+H] calcd 176.1, found 176.2.



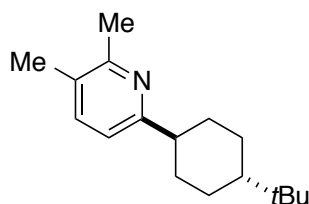
**5-Cyclopentyl-2,3-dimethylpyridine (14ft).** Pale yellow viscous liquid.  $R_f = 0.19$  (5:1 hexanes/EtOAc).  $^1\text{H}$  NMR (400 MHz,  $\text{CDCl}_3$ )  $\delta$  8.19 (d,  $J = 2.0$  Hz, 1H), 7.25 (d,  $J = 2.0$  Hz, 1H), 2.93 (m, 1H), 2.45 (s, 3H), 2.25 (s, 3H), 2.05 (m, 2H), 1.82-1.50 (m, 6H).  $^{13}\text{C}$  NMR (100 MHz,  $\text{CDCl}_3$ )  $\delta$  154.4, 145.6, 139.1, 135.8, 130.9, 43.0, 34.6, 25.6, 22.2, 19.4. IR (NaCl, thin film)  $\nu$  2953, 2869, 1475, 1242, 1020, 892, 732  $\text{cm}^{-1}$ . LRMS (ESI + APCI)  $m/z$  [M+H] calcd 176.1, found 176.1.



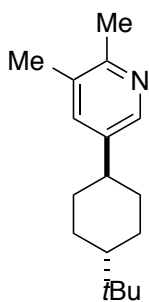
**6-(*sec*-Butyl)-2,3-dimethylpyridine (13fw).** Pale yellow viscous liquid.  $R_f = 0.65$  (5:1 hexanes/EtOAc).  $^1\text{H}$  NMR (400 MHz,  $\text{CDCl}_3$ )  $\delta$  7.32 (d,  $J = 7.6$  Hz, 1H), 6.87 (d,  $J = 7.6$  Hz, 1H), 2.75 (m, 2H), 2.47 (s, 3H), 2.23 (s, 3H), 1.72 (m, 1H), 1.57 (m, 1H), 1.24 (d,  $J = 7.2$  Hz, 3H), 0.85 (t,  $J = 7.2$  Hz, 3H).  $^{13}\text{C}$  NMR (100 MHz,  $\text{CDCl}_3$ )  $\delta$  163.5, 156.1, 137.6, 128.4, 118.2, 43.4, 30.2, 22.7, 20.7, 18.9, 12.3. IR (NaCl, thin film)  $\nu$  2962, 2927, 1741, 1578, 1467, 1377, 1107, 827  $\text{cm}^{-1}$ . LRMS (ESI + APCI)  $m/z$  [M+H] calcd 164.1, found 164.2.



**5-(*sec*-Butyl)-2,3-dimethylpyridine (14fw).** Pale yellow viscous liquid.  $R_f = 0.23$  (5:1 hexanes/EtOAc).  $^1\text{H}$  NMR (400 MHz,  $\text{CDCl}_3$ )  $\delta$  8.14 (bs, 1H), 7.22 (bs, 1H), 2.56 (m, 1H), 2.47 (s, 3H), 2.26 (s, 3H), 1.58 (m, 2H), 1.22 (d,  $J = 7.2$  Hz, 3H), 0.82 (t,  $J = 7.2$  Hz, 3H).  $^{13}\text{C}$  NMR (100 MHz,  $\text{CDCl}_3$ )  $\delta$  154.3, 145.3, 140.1, 135.7, 131.0, 38.6, 30.9, 21.9, 21.6, 19.2, 12.1. IR (NaCl, thin film)  $\nu$  2963, 2926, 2875, 1740, 1459, 1376, 1240, 1111, 1019, 898, 733  $\text{cm}^{-1}$ . LRMS (ESI + APCI)  $m/z$  [M+H] calcd 164.1, found 164.2.



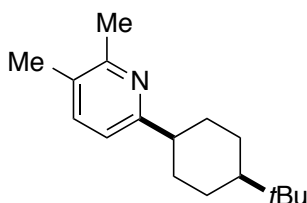
**6-(*trans*-4-(*tert*-butyl)cyclohexyl)-2,3-dimethylpyridine (13fx).** Pale yellow viscous liquid.  $R_f = 0.44$  (5:1 hexanes/EtOAc).  $^1\text{H}$  NMR (400 MHz,  $\text{CDCl}_3$ )  $\delta$  7.30 (d,  $J = 8.0$  Hz, 1H), 6.88 (d,  $J = 8.0$  Hz, 1H), 2.58 (tt,  $J = 12.4, 3.2$  Hz, 1H), 2.46 (s, 3H), 2.26 (s, 3H), 2.03-1.99 (m, 2H), 1.90-1.86 (m, 2H), 1.45 (q,  $J = 12.8$  Hz, 2H), 1.22-1.05 (m, 3H), 0.87 (s, 9H).  $^{13}\text{C}$  NMR (100 MHz,  $\text{CDCl}_3$ )  $\delta$  163.2, 155.9, 137.4, 128.3, 117.6, 47.7, 46.3, 33.6, 32.4, 27.4, 22.6, 18.8. IR (NaCl, thin film)  $\nu$  2937, 2856, 1577, 1465, 1449, 1364  $\text{cm}^{-1}$ . LRMS (ESI + APCI)  $m/z$  [M+H] calcd 246.2, found 246.2.



**5-(*trans*-4-(*tert*-butyl)cyclohexyl)-2,3-dimethylpyridine** (*trans*-**14fx**). Pale yellow viscous liquid.  $R_f = 0.09$  (5:1 hexanes/EtOAc).

$^1\text{H}$  NMR (400 MHz,  $\text{CDCl}_3$ )  $\delta$  8.17 (d,  $J = 2.0$  Hz, 1H), 7.22 (d,  $J = 1.6$  Hz, 1H), 2.45 (s, 3H), 2.40 (tt,  $J = 12.0, 3.2$  Hz, 1H), 2.25 (s, 3H), 1.93-1.88 (m, 4H), 1.42 (q,  $J = 12.4$  Hz, 2H), 1.20-1.04 (m,

3H), 0.88 (s, 9H).  $^{13}\text{C}$  NMR (100 MHz,  $\text{CDCl}_3$ )  $\delta$  154.4, 145.2, 140.2, 135.5, 130.8, 47.6, 41.5, 34.6, 32.5, 27.6, 22.0, 19.2. IR (NaCl, thin film)  $\nu$  2938, 2855, 1475, 1448, 1365  $\text{cm}^{-1}$ . LRMS (ESI + APCI)  $m/z$  [M+H] calcd 246.2, found 246.2.

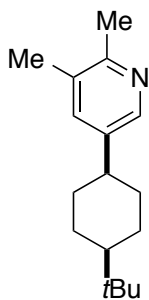


**6-(*cis*-4-(*tert*-butyl)cyclohexyl)-2,3-dimethylpyridine** (*cis*-**13fx**).

As 4.4:1 mixture with *trans*-**13fx**. Pale yellow viscous liquid.  $R_f =$

0.42 (5:1 hexanes/EtOAc).  $^1\text{H}$  NMR (400 MHz,  $\text{CDCl}_3$ )  $\delta$  7.30 (d,  $J = 7.6$  Hz, 1H), 7.04 (d,  $J = 7.6$  Hz, 1H), 3.04 (bs, 1H), 2.47 (s,

3H), 2.39-2.36 (m, 2H), 2.23 (s, 3H), 1.78-1.69 (m, 2H), 1.59-1.55 (m, 2H), 1.25-1.06 (m, 3H), 0.80 (s, 9H).  $^{13}\text{C}$  NMR (100 MHz,  $\text{CDCl}_3$ )  $\delta$  161.2, 156.0, 137.0, 127.5, 118.9, 48.2, 38.8, 33.6, 32.6, 30.0, 27.5, 22.9, 18.7. IR (NaCl, thin film)  $\nu$  2937, 2864, 1575, 1465, 1365  $\text{cm}^{-1}$ . LRMS (ESI + APCI)  $m/z$  [M+H] calcd 246.2, found 246.2.

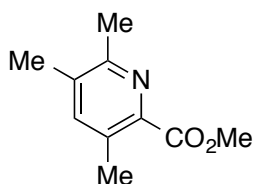


**5-(*cis*-4-(*tert*-butyl)cyclohexyl)-2,3-dimethylpyridine** (*cis*-**14fx**).

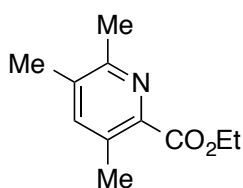
Pale yellow viscous liquid.  $R_f = 0.12$  (5:1 hexanes/EtOAc).  $^1\text{H}$

NMR (400 MHz,  $\text{CDCl}_3$ )  $\delta$  8.32 (d,  $J = 1.6$  Hz, 1H), 7.35 (d,  $J = 0.8$  Hz, 1H), 3.00 (bs, 1H), 2.46 (s, 3H), 2.27 (s, 3H), 2.22-2.19 (m, 2H), 1.80-1.73 (m, 2H), 1.61-1.58 (m, 2H), 1.20-1.07 (m, 3H), 0.80

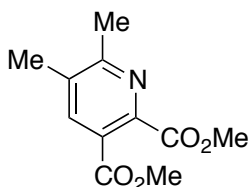
(s, 9H).  $^{13}\text{C}$  NMR (100 MHz,  $\text{CDCl}_3$ )  $\delta$  153.6, 145.9, 137.6, 136.8, 130.5, 48.2, 34.2, 32.6, 30.4, 27.5, 22.6, 19.3. IR (NaCl, thin film)  $\nu$  2938, 2865, 1477, 1449, 1366, 1240  $\text{cm}^{-1}$ . LRMS (ESI + APCI)  $m/z$  [M+H] calcd 246.2, found 246.2.



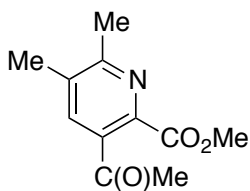
**Methyl 3,5,6-trimethylpicolinate (33fa).** White solid.  $R_f = 0.18$  (3:1 hexanes/EtOAc).  $^1\text{H}$  NMR (400 MHz,  $\text{CDCl}_3$ )  $\delta$  7.32 (s, 1H), 3.96 (s, 3H), 2.52 (s, 6H), 2.30 (s, 3H).  $^{13}\text{C}$  NMR (100 MHz,  $\text{CDCl}_3$ )  $\delta$  166.9, 154.7, 143.8, 141.1, 135.0, 133.3, 52.6, 22.4, 19.6, 19.2. IR (NaCl, thin film)  $\nu$  2947, 2925, 1704, 1598, 1552, 1445, 1382, 1316, 1241, 1186, 1154, 1065, 1041, 1022, 999, 910, 832, 803, 713  $\text{cm}^{-1}$ . LRMS (ESI + APCI)  $m/z$  [M+H] calcd 180.1, found 180.1.



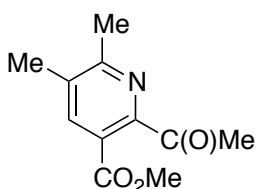
**Ethyl 3,5,6-trimethylpicolinate (33fb).** Pale yellow viscous liquid.  $R_f = 0.23$  (3:1 hexanes/EtOAc).  $^1\text{H}$  NMR (400 MHz,  $\text{CDCl}_3$ )  $\delta$  7.29 (s, 1H), 4.42 (q,  $J = 7.2$  Hz, 2H), 2.50 (s, 3H), 2.47 (s, 3H), 2.27 (s, 3H), 1.41 (t,  $J = 7.2$  Hz, 3H).  $^{13}\text{C}$  NMR (100 MHz,  $\text{CDCl}_3$ )  $\delta$  166.8, 154.7, 144.7, 140.8, 134.6, 132.4, 61.5, 22.4, 19.5, 19.1, 14.4. IR (NaCl, thin film)  $\nu$  2981, 1719, 1462, 1310, 1237, 1155, 1062, 713  $\text{cm}^{-1}$ . LRMS (ESI + APCI)  $m/z$  [M+H] calcd 194.1, found 194.1.



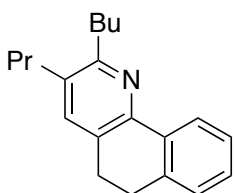
**Dimethyl 5,6-dimethylpyridine-2,3-dicarboxylate (33fc).** White solid.  $R_f = 0.19$  (3:1 hexanes/EtOAc).  $^1\text{H}$  NMR (400 MHz,  $\text{CDCl}_3$ )  $\delta$  7.88 (s, 1H), 3.96 (s, 3H), 3.89 (s, 3H), 2.57 (s, 3H), 2.35 (s, 3H).  $^{13}\text{C}$  NMR (100 MHz,  $\text{CDCl}_3$ )  $\delta$  167.3, 166.1, 160.9, 148.2, 138.2, 133.7, 123.7, 53.1, 52.8, 22.9, 19.1. IR (NaCl, thin film)  $\nu$  2955, 1732, 1597, 1428, 1309, 1151, 1046, 797  $\text{cm}^{-1}$ . LRMS (ESI + APCI)  $m/z$  [M+H] calcd 224.1, found 224.1.



**Methyl 3-acetyl-5,6-dimethylpicolinate (33fd).** White solid.  $R_f$  = 0.11 (3:1 hexanes/EtOAc).  $^1\text{H}$  NMR (400 MHz,  $\text{CDCl}_3$ )  $\delta$  7.54 (s, 1H), 3.97 (s, 3H), 2.59 (s, 3H), 2.53 (s, 3H), 2.37 (s, 3H).  $^{13}\text{C}$  NMR (100 MHz,  $\text{CDCl}_3$ )  $\delta$  200.5, 166.8, 159.7, 144.1, 136.2, 135.1, 134.8, 53.2, 29.7, 22.9, 19.4. IR (NaCl, thin film)  $\nu$  2954, 1744, 1692, 1591, 1552, 1429, 1365, 1301, 1261, 1161, 1137, 1019  $\text{cm}^{-1}$ . LRMS (ESI + APCI)  $m/z$  [M+H] calcd 208.1, found 208.1.



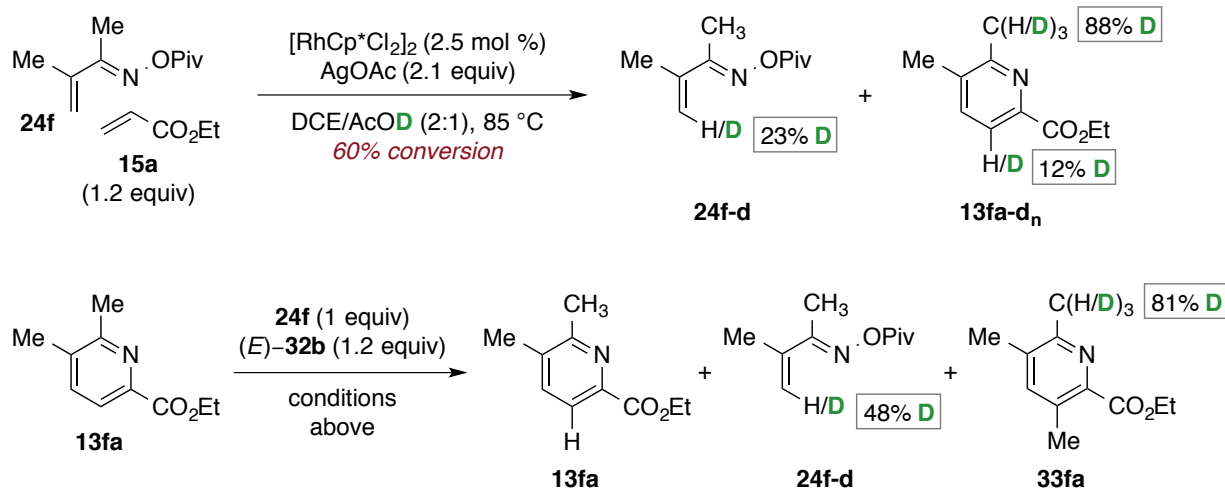
**Methyl 2-acetyl-5,6-dimethylnicotinate (34fd).** White solid.  $R_f$  = 0.34 (3:1 hexanes/EtOAc).  $^1\text{H}$  NMR (400 MHz,  $\text{CDCl}_3$ )  $\delta$  7.71 (s, 1H), 3.89 (s, 3H), 2.65 (s, 3H), 2.56 (s, 3H), 2.35 (s, 3H).  $^{13}\text{C}$  NMR (100 MHz,  $\text{CDCl}_3$ )  $\delta$  201.0, 167.9, 159.4, 152.6, 137.6, 134.0, 124.4, 52.9, 27.5, 22.8, 19.2. IR (NaCl, thin film)  $\nu$  2955, 1733, 1595, 1432, 1356, 1301, 1272, 1161, 1131, 1022  $\text{cm}^{-1}$ . LRMS (ESI + APCI)  $m/z$  [M+H] calcd 208.1, found 208.1.



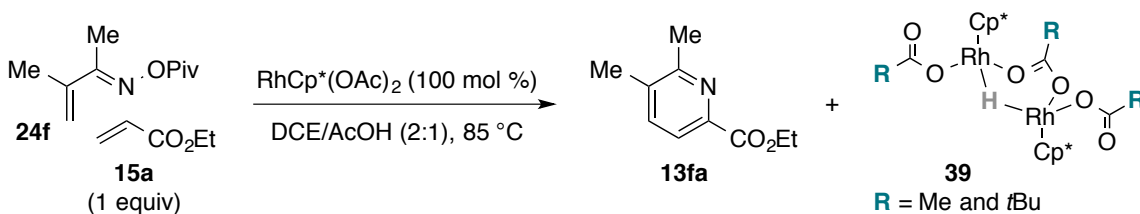
**2-Butyl-3-propyl-5,6-dihydrobenzo[h]quinoline (33kh).** Colorless viscous liquid.  $R_f$  = 0.14 (3:1 hexanes/DCM).  $^1\text{H}$  NMR (400 MHz,  $\text{CDCl}_3$ )  $\delta$  8.34 (d,  $J$  = 7.6 Hz, 1H), 7.36-7.19 (m, 4H), 2.94-2.81 (m, 6H), 2.60 (t,  $J$  = 7.6 Hz, 2H), 1.80 (m, 2H), 1.64 (m, 2H), 1.47 (m, 2H), 1.01 (t,  $J$  = 5.7, 3H), 0.99 (t,  $J$  = 5.4, 3H).  $^{13}\text{C}$  NMR (100 MHz,  $\text{CDCl}_3$ )  $\delta$  158.2, 149.3, 137.9, 136.3, 135.2, 134.0, 128.8, 128.4, 127.7, 127.1, 124.8, 34.4, 34.2, 31.7, 28.5, 27.8, 24.0, 23.0, 14.3. IR (NaCl, thin film)  $\nu$  2957, 2931, 2870, 1553, 1461, 1438, 1377, 915, 740  $\text{cm}^{-1}$ . LRMS (ESI + APCI)  $m/z$  [M+H] calcd 280.2, found 280.2.

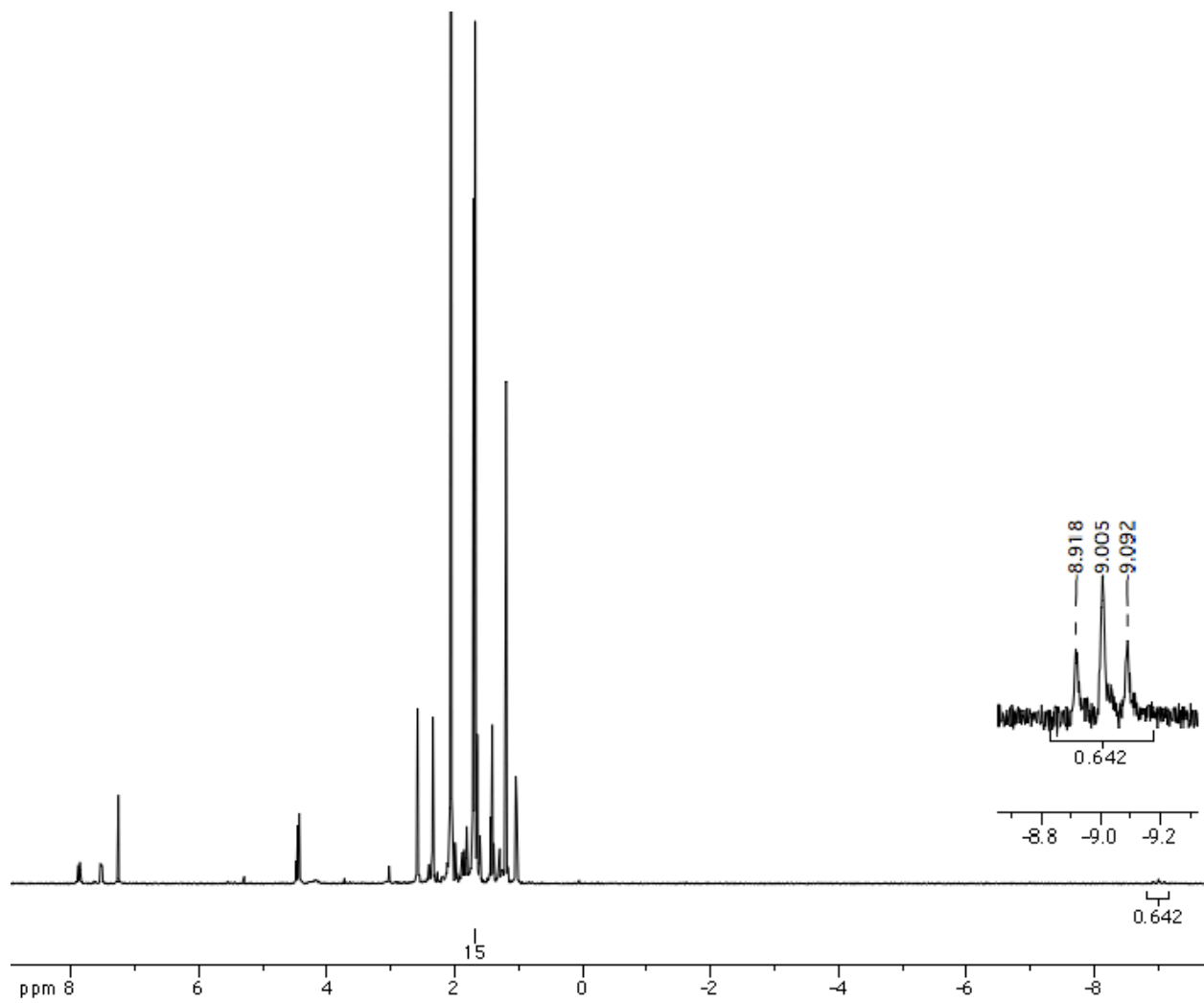
### A.1.5 Mechanistic Experiments

Isotope experiments were conducted with AcOD (purchased from Sigma-Aldrich Co. and used as received) according to the reaction procedure described above for the length of time indicated. Deuterium incorporation was determined by integration of the  $^1\text{H}$  NMR spectra collected with first relaxation delay ( $d_1$ ) = 15 seconds of the crude reaction mixtures.

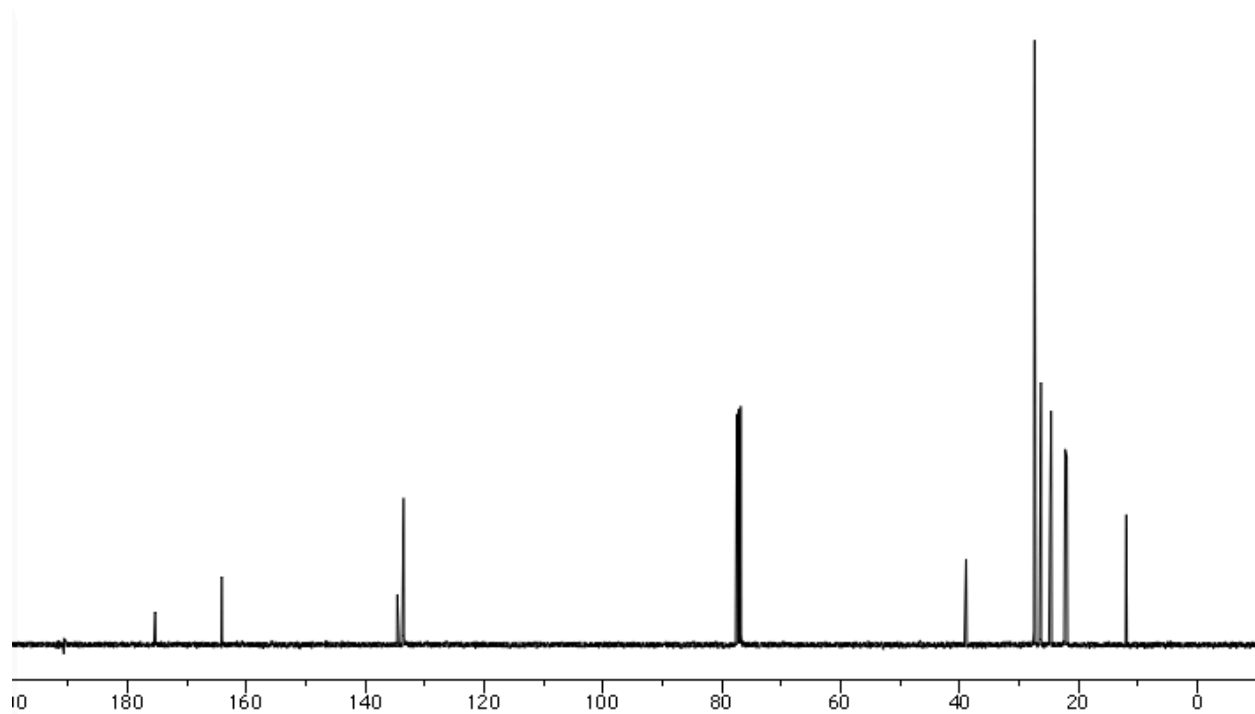
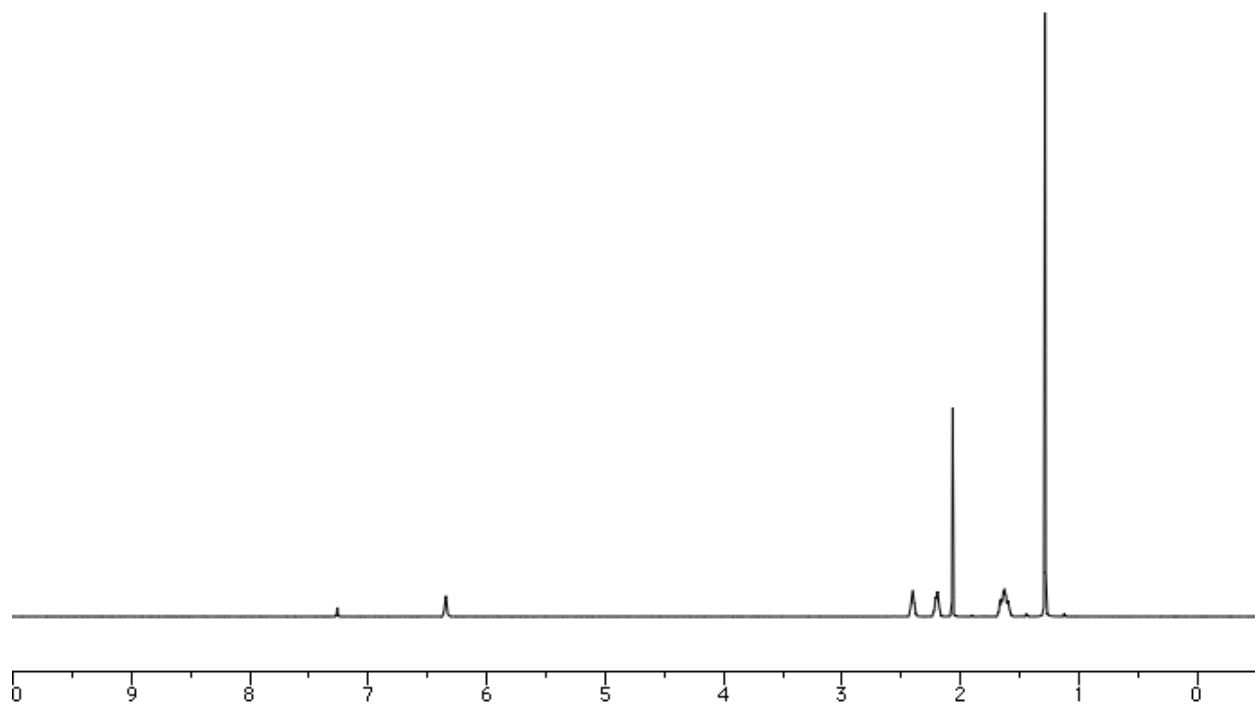
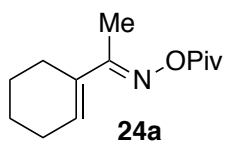


A stoichiometric experiment was performed according to the following procedure. A 0.5 dram vial was charged with  $\text{RhCp}^*(\text{OAc})_2$  (9.6 mg, 100 mol %)<sup>9</sup> and a solution of **24f** (0.027 mmol) and **15a** (2.7 mg, 1 equiv) in 0.09 mL 2:1 DCE/AcOH was added. The vial was flushed with argon, sealed and heated at 85 °C in an aluminum heating block for 20 minutes. The solvent was removed and the reaction mixture was analyzed by  $^1\text{H}$  NMR (300 MHz,  $\text{CDCl}_3$ ). The upfield signal at -9.005 ppm consistent with a Rh-H is highlighted in the spectrum provided below.

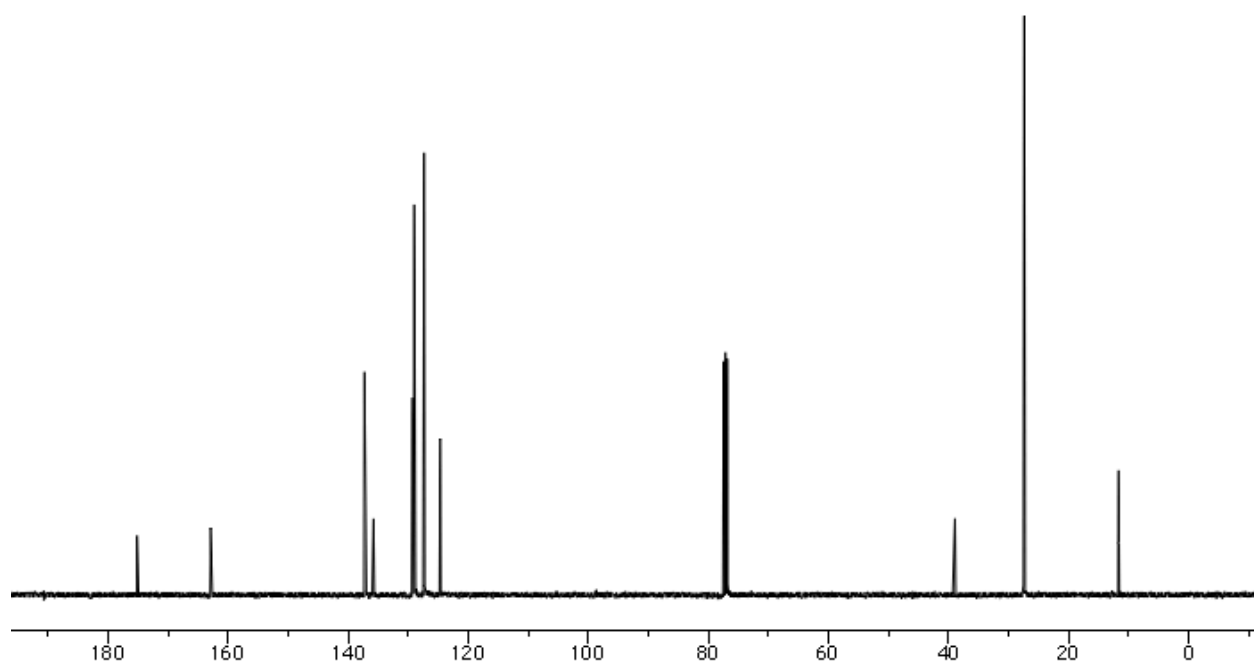
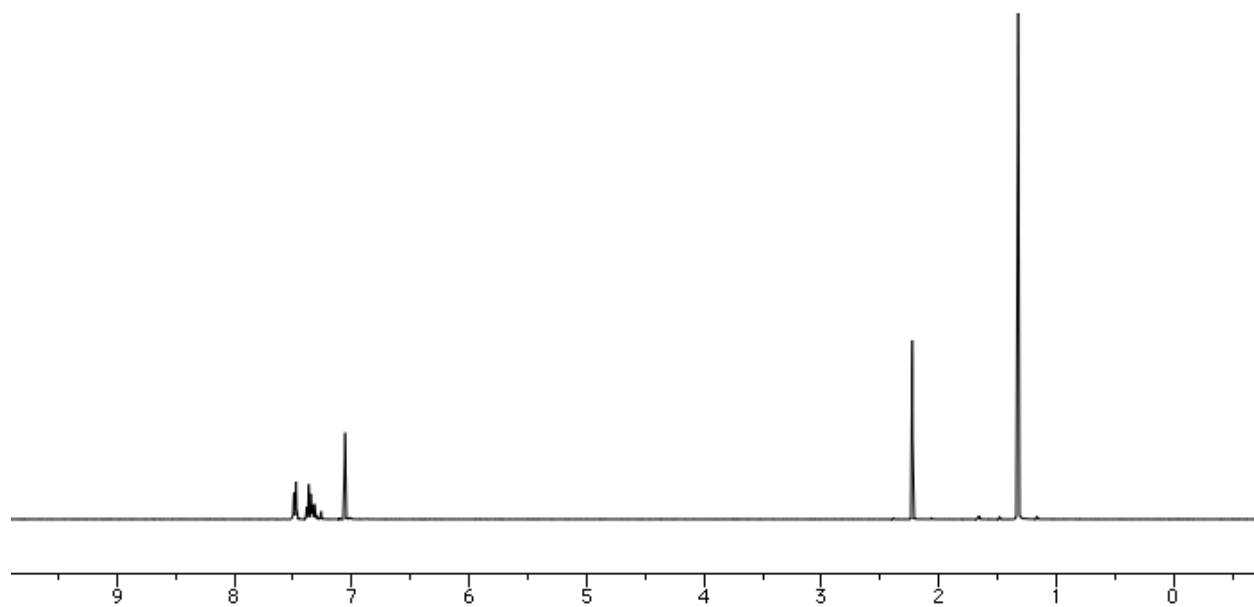
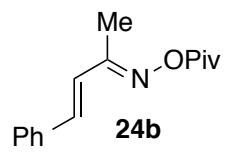


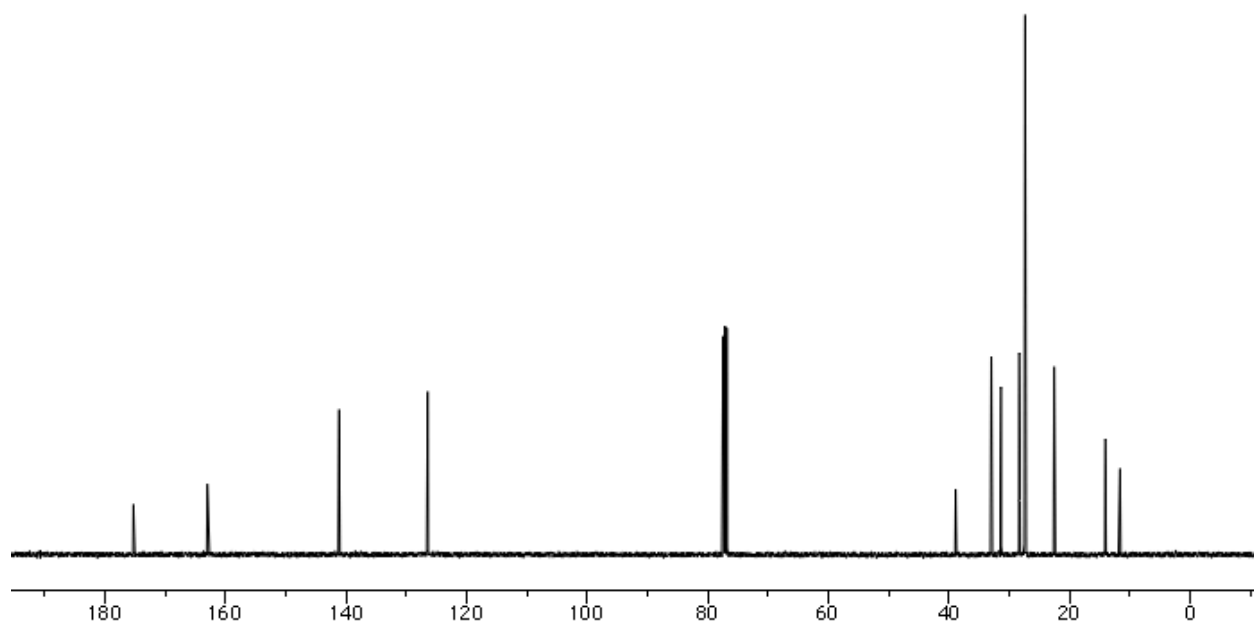
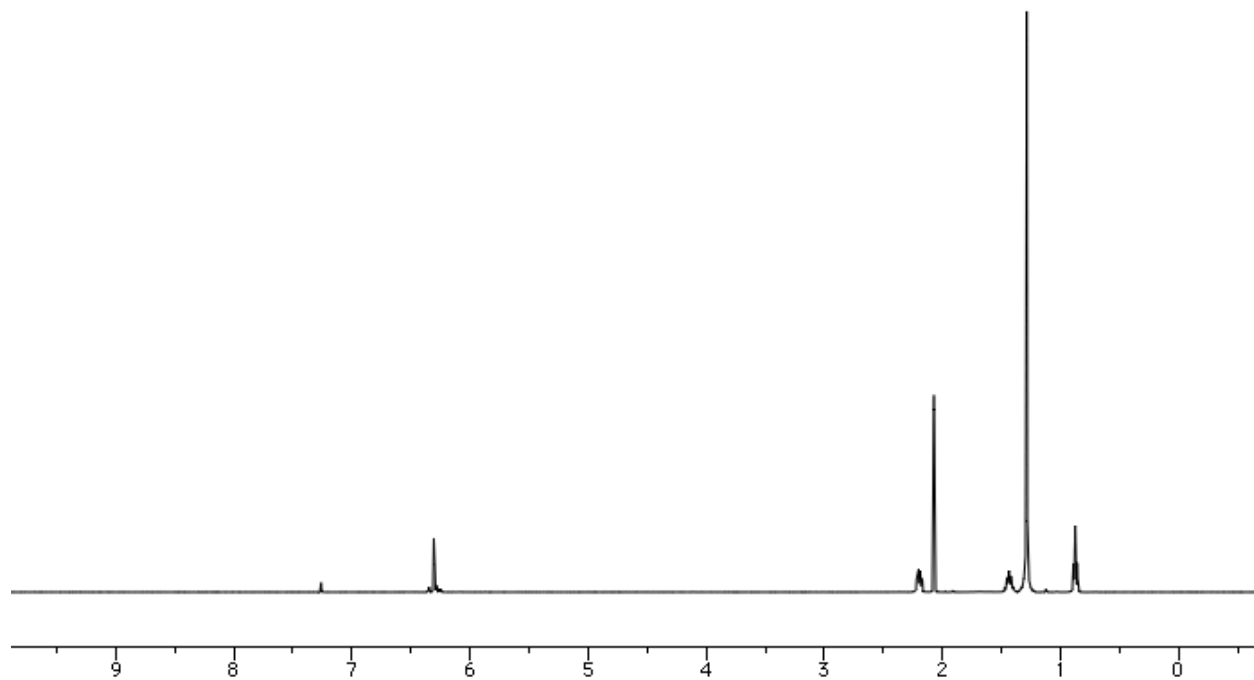
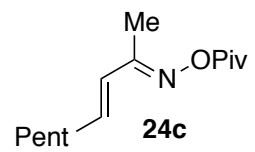


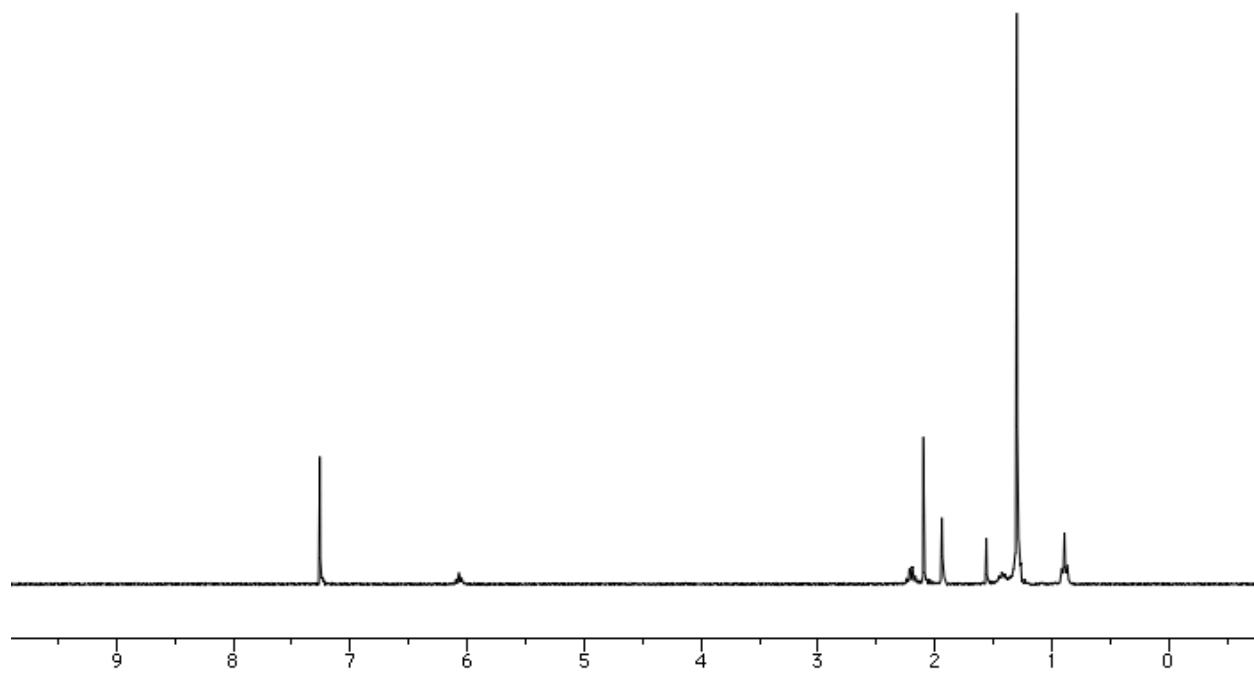
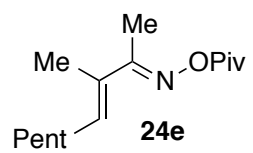
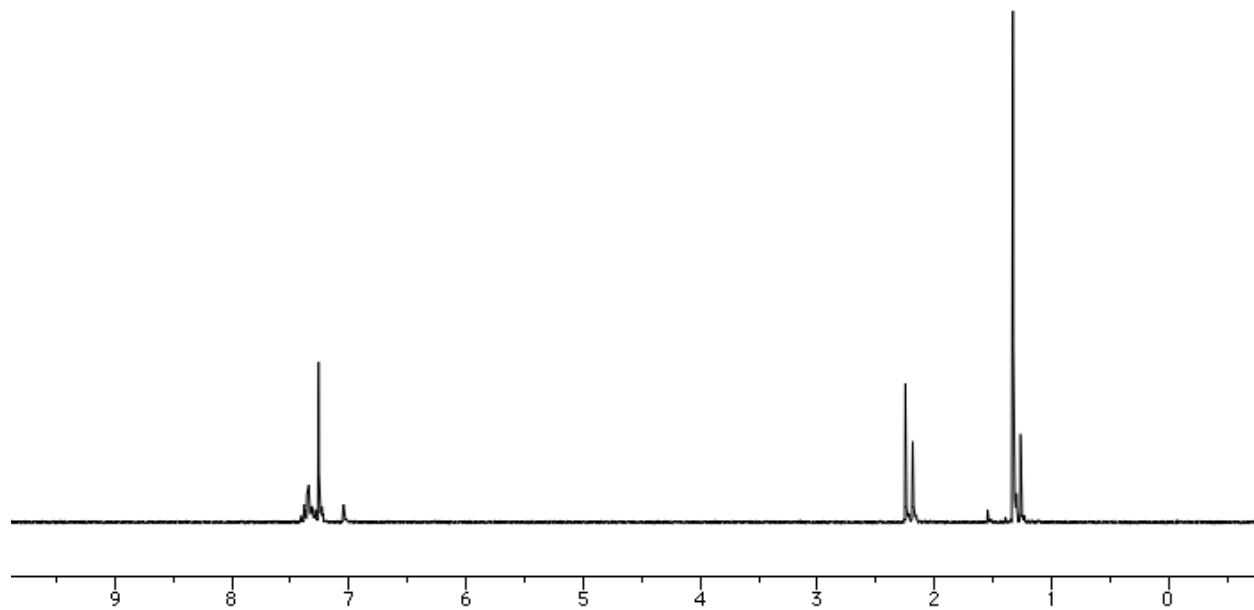
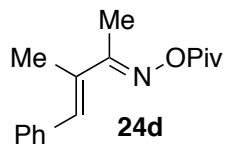
A.1.6  $^1\text{H}$  and  $^{13}\text{C}$  NMR Spectra of New Compounds

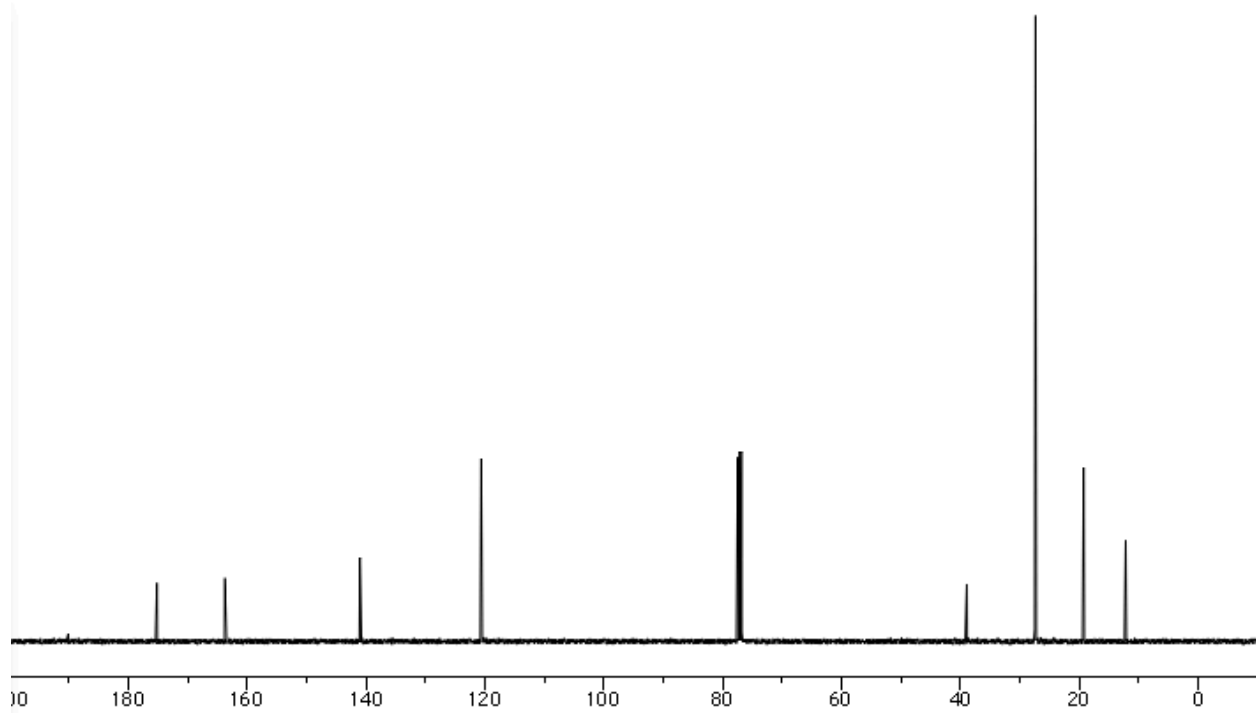
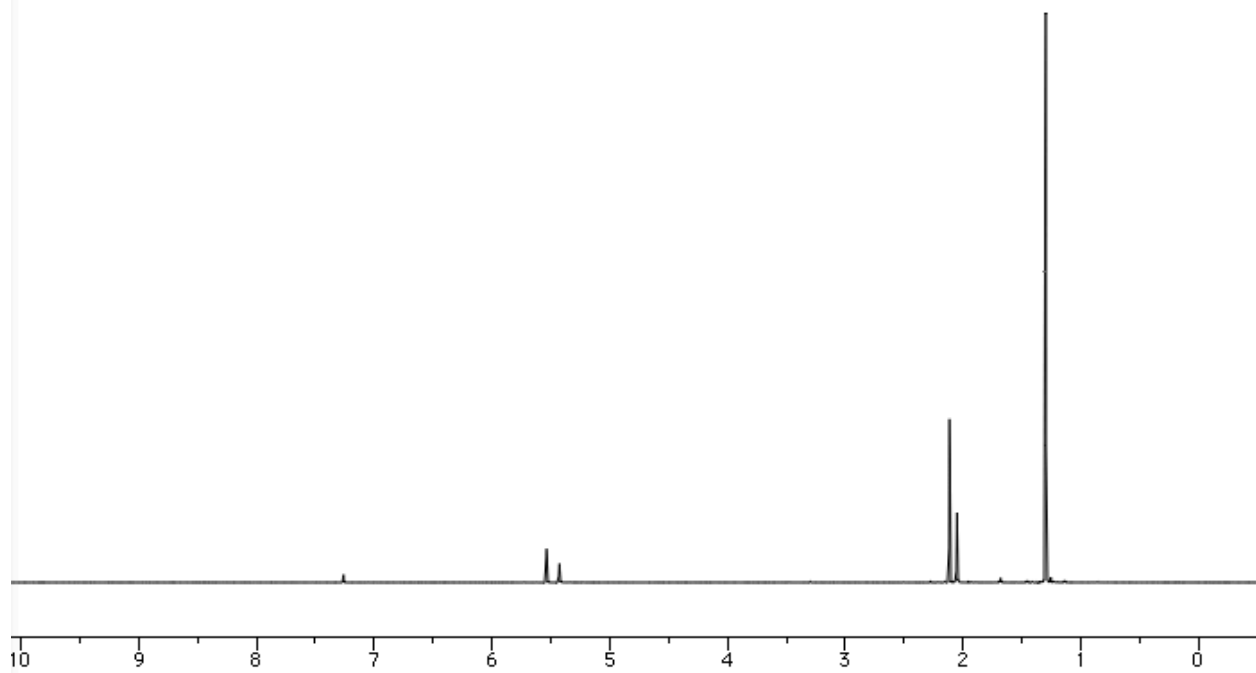
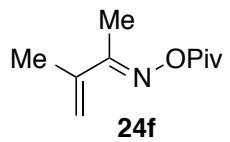


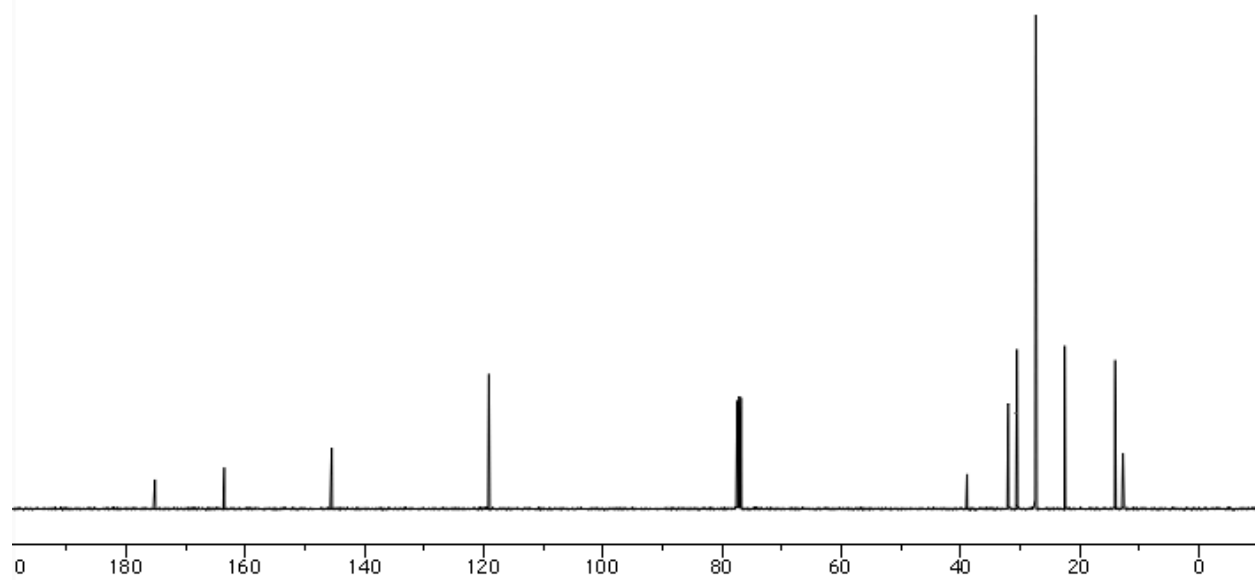
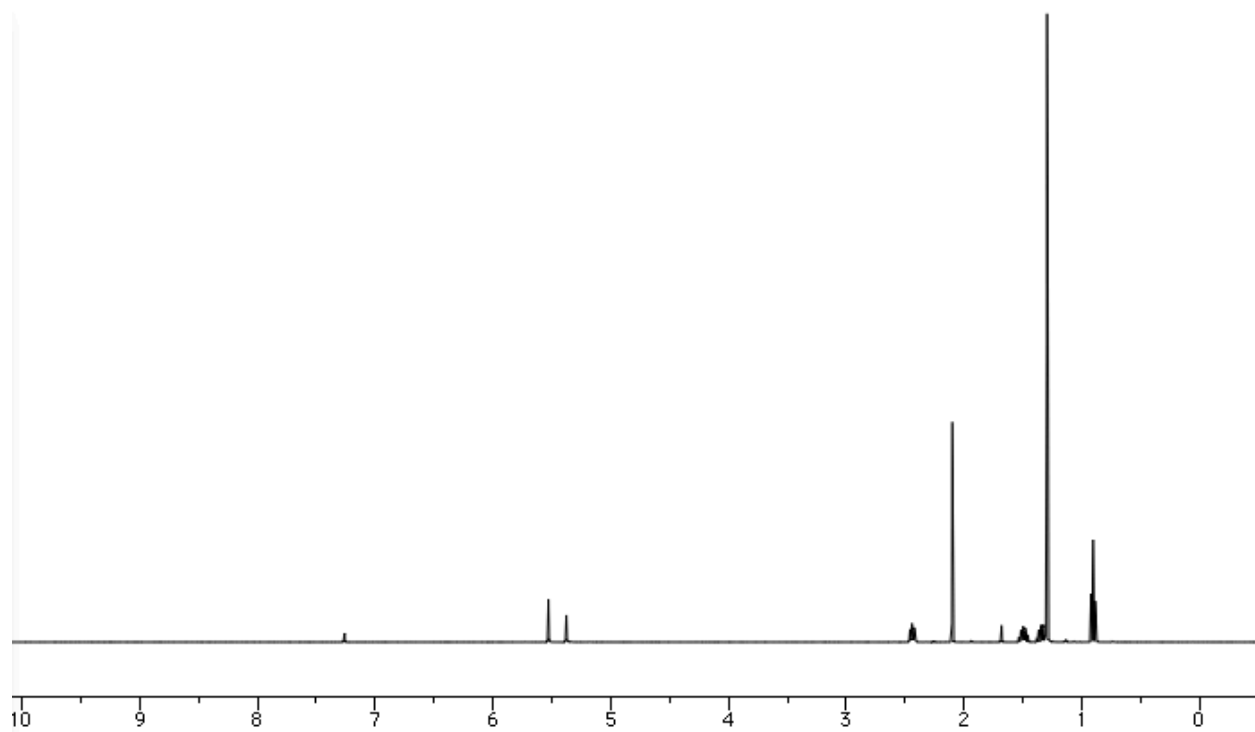
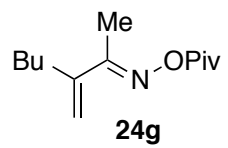


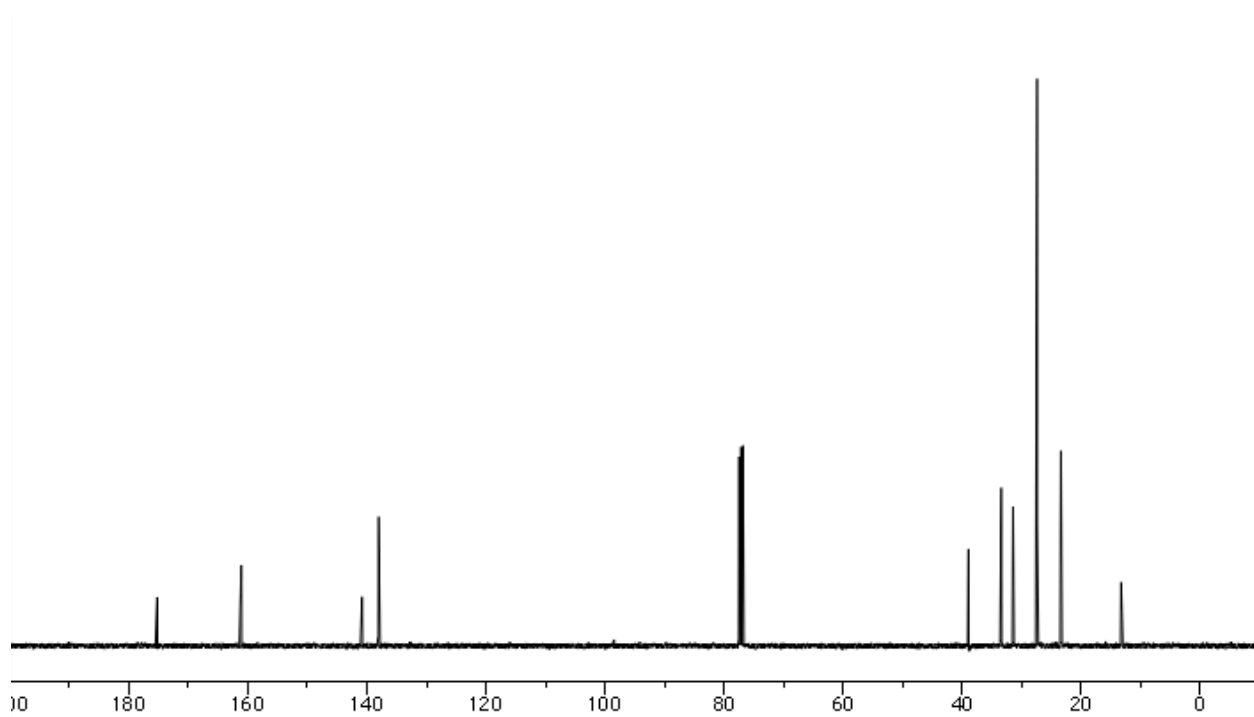
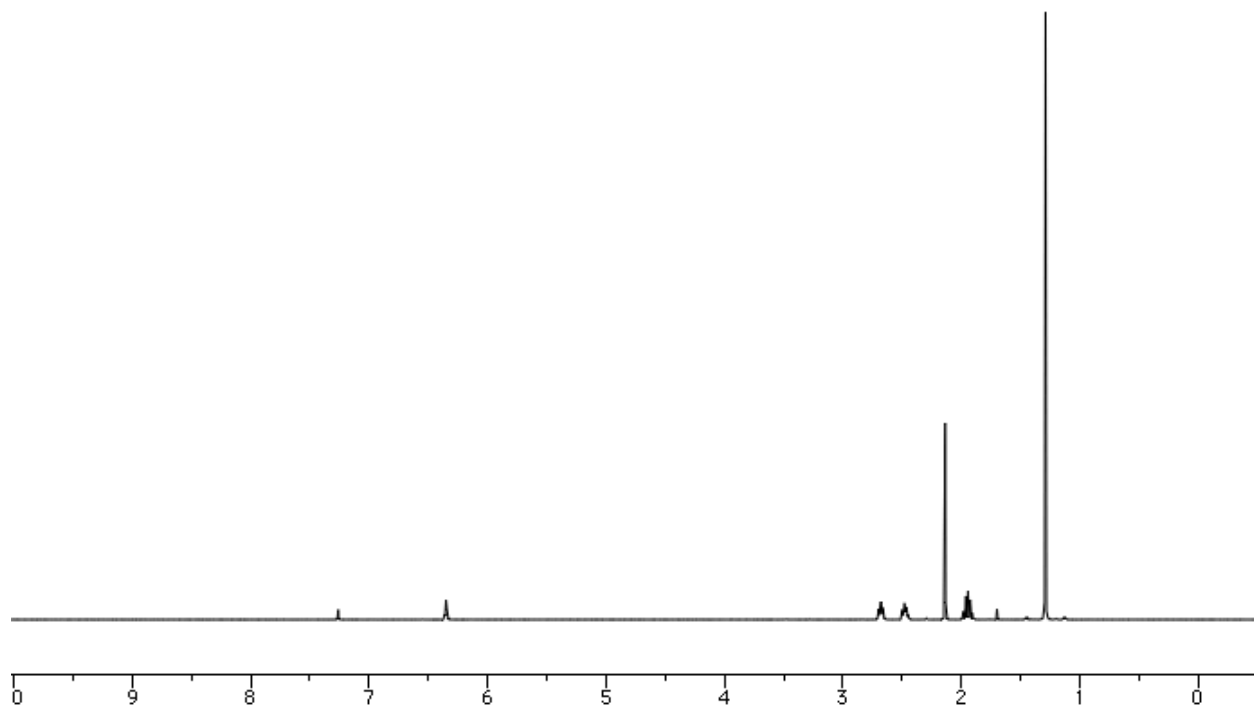
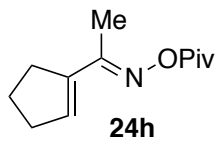


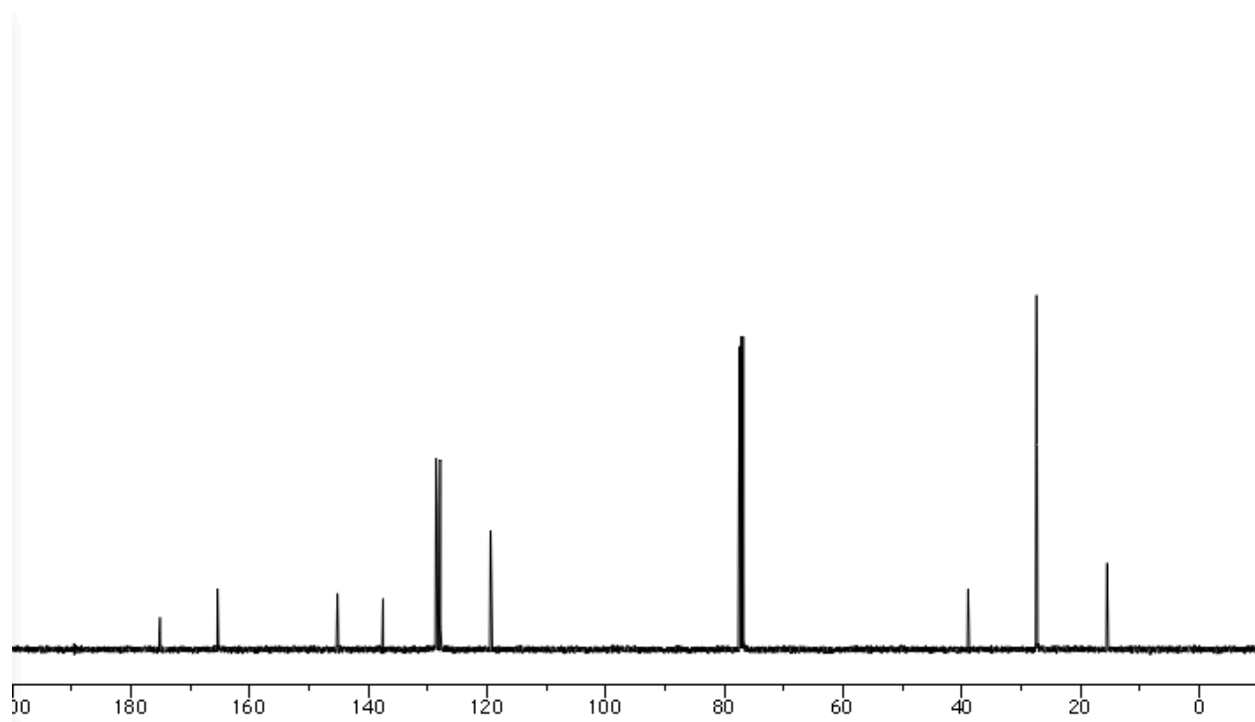
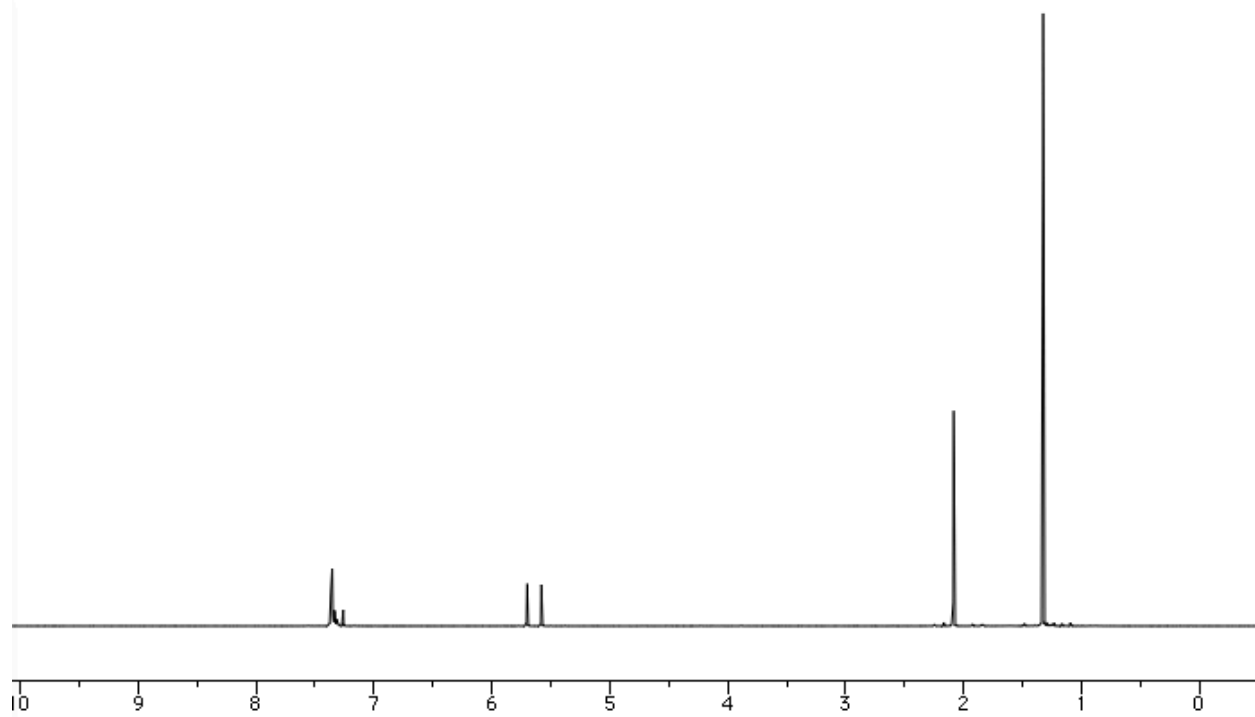
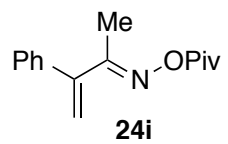


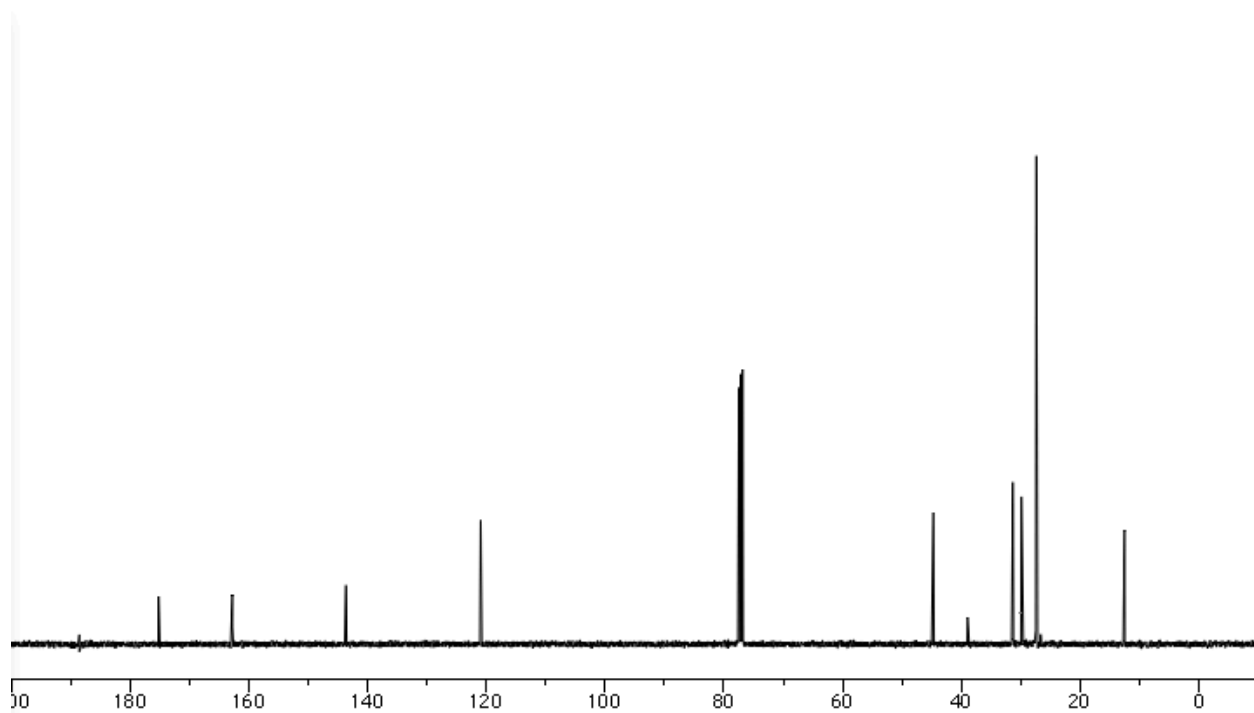
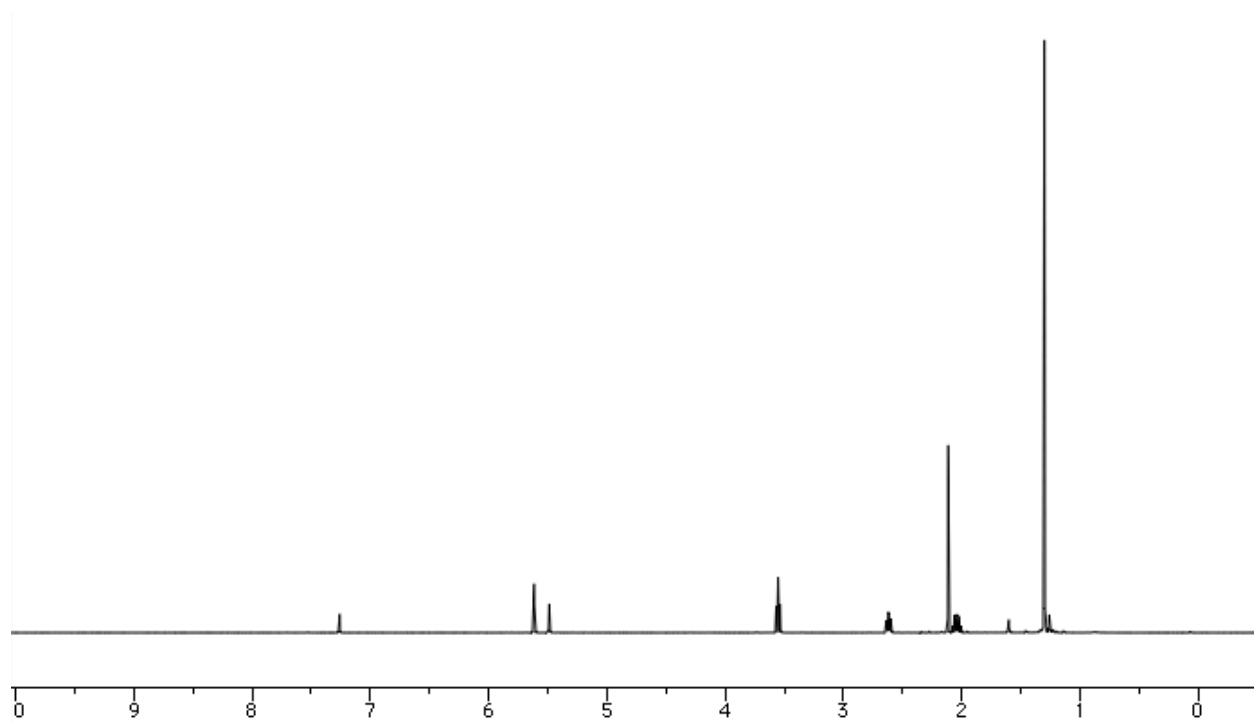
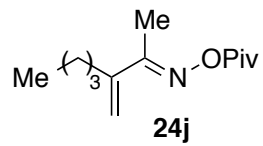




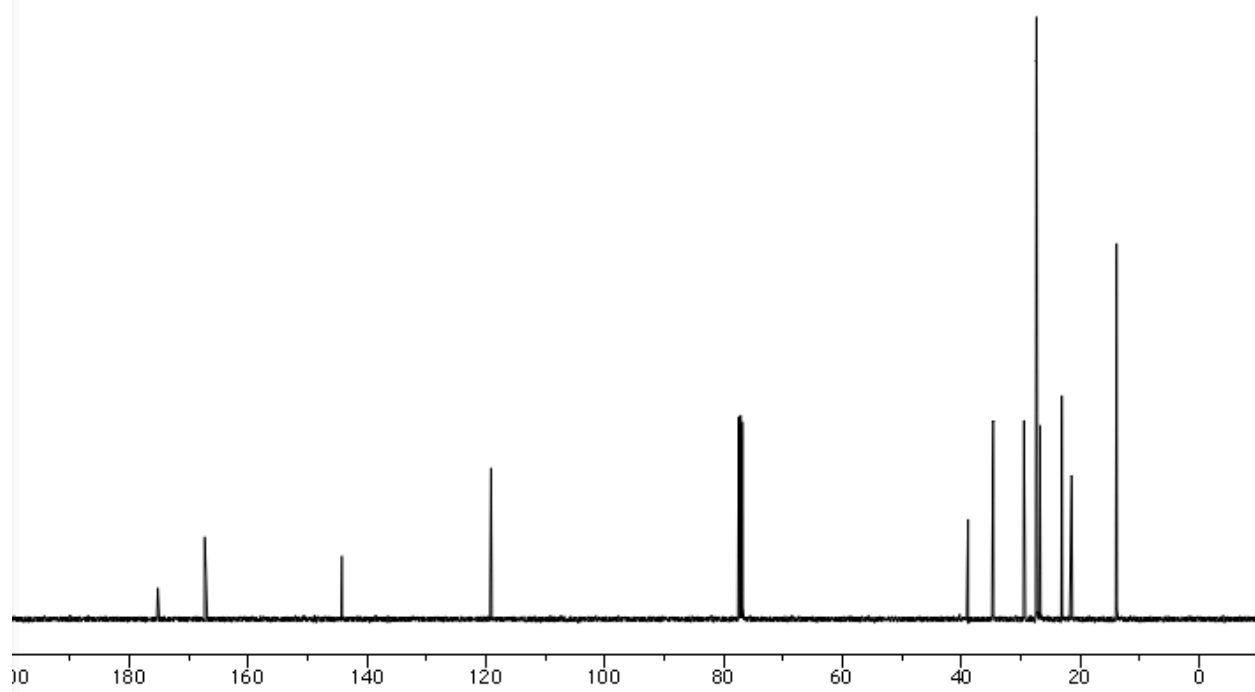
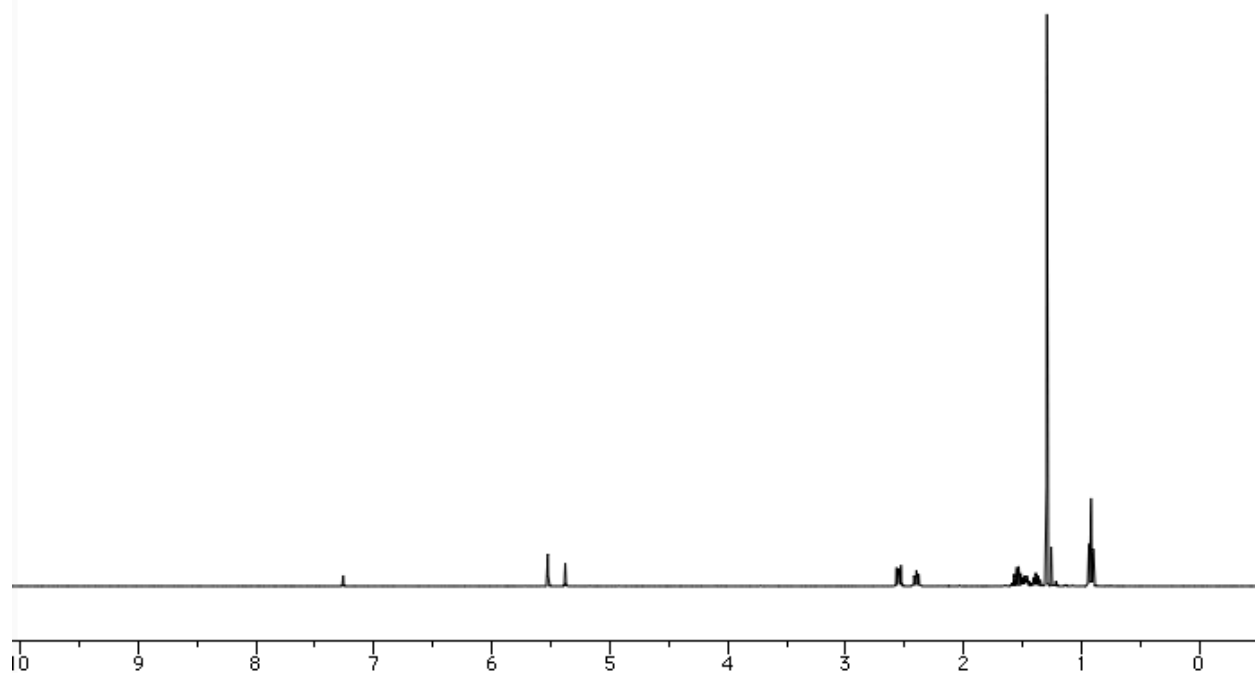
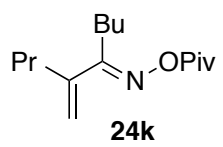


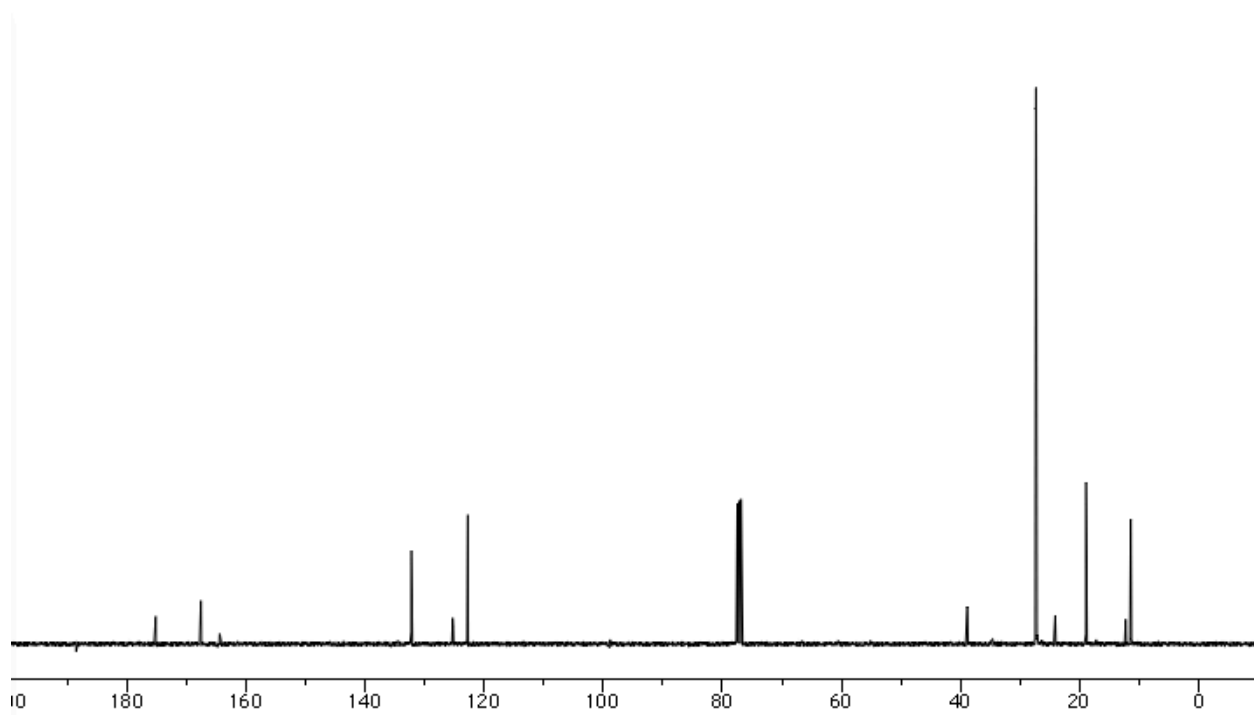
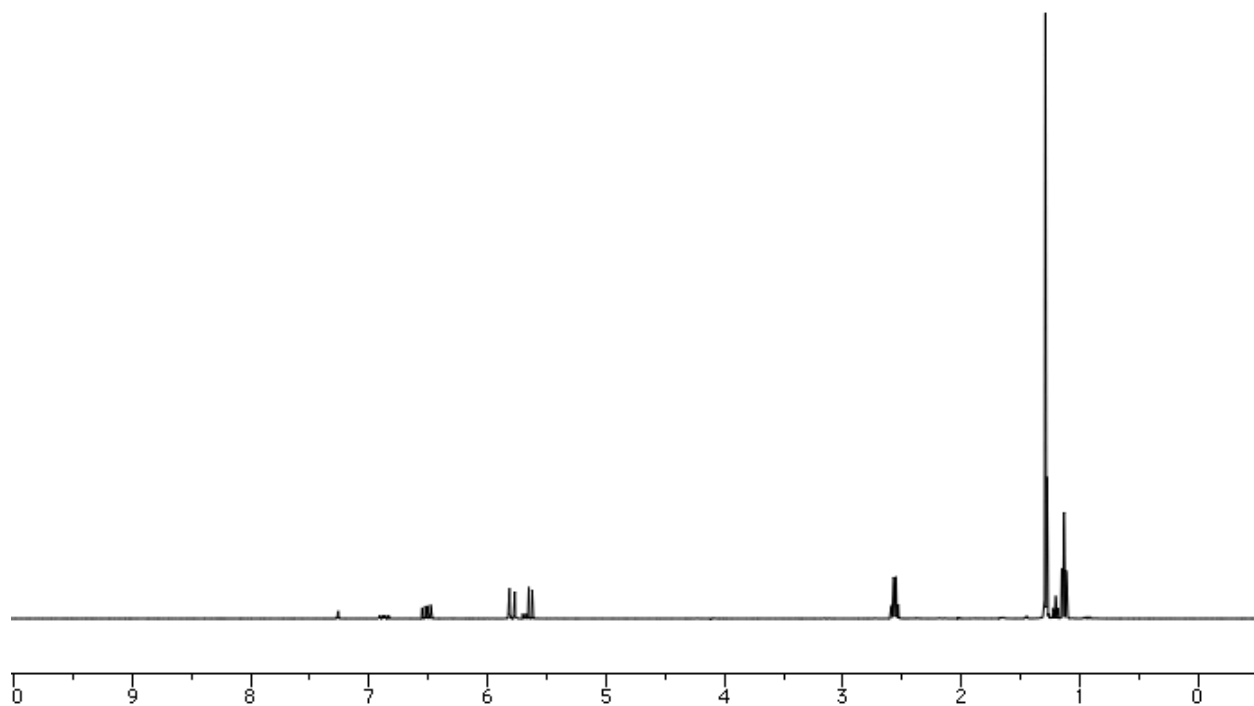
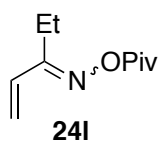


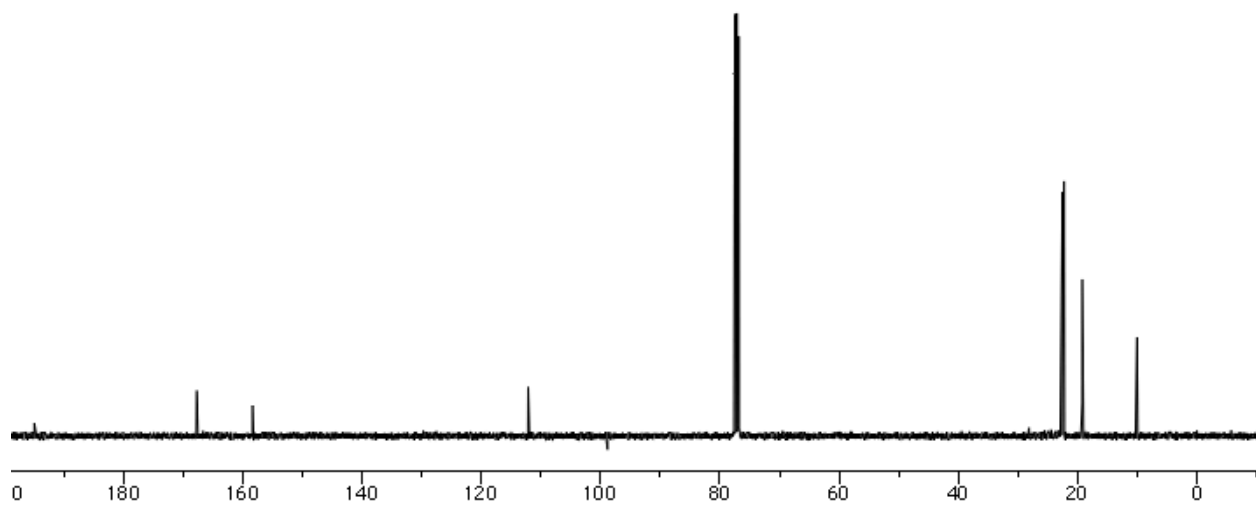
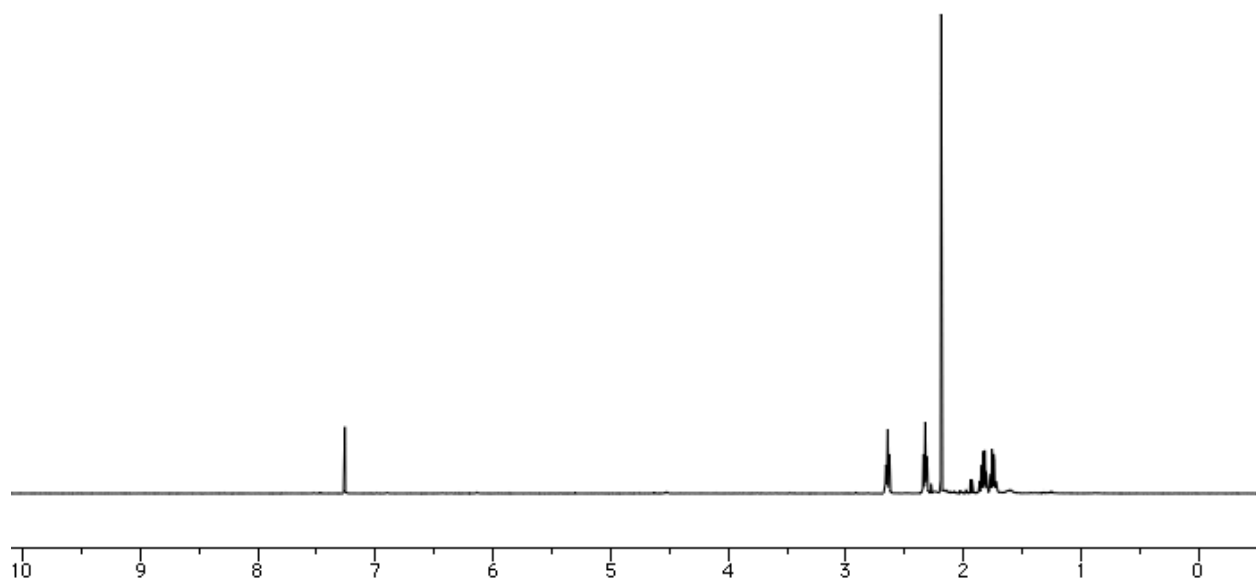
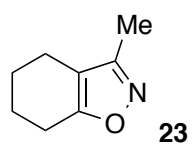


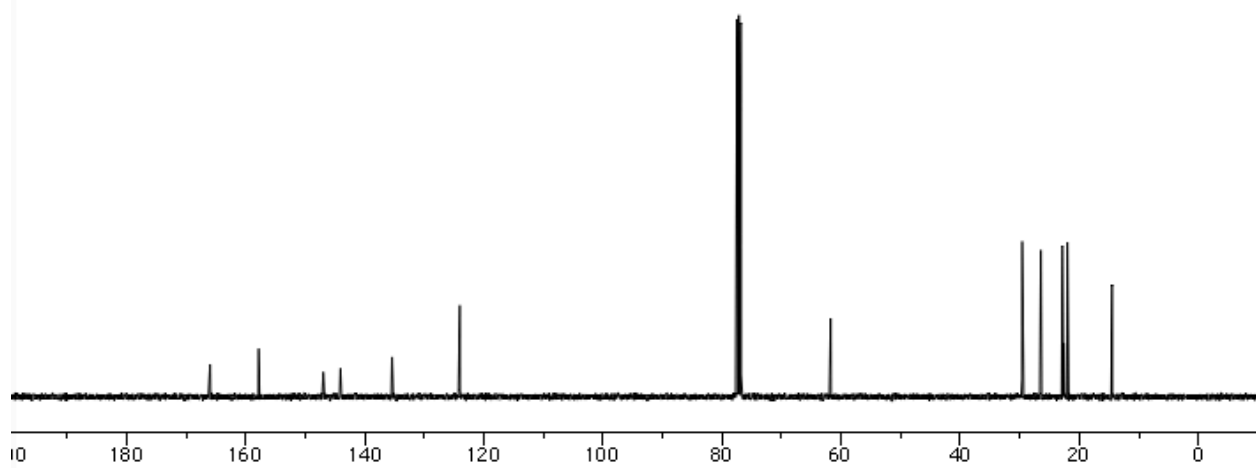
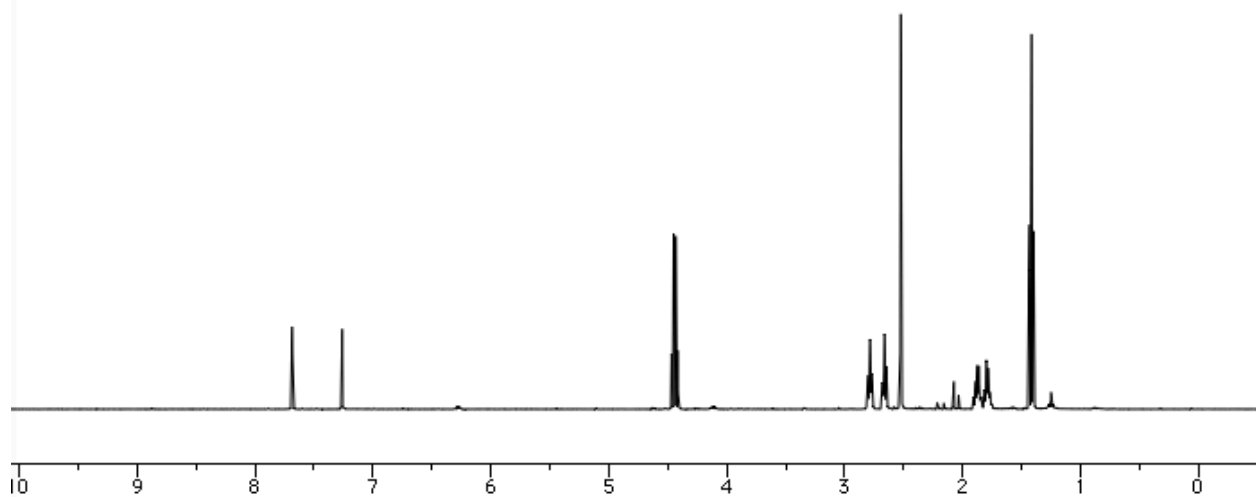
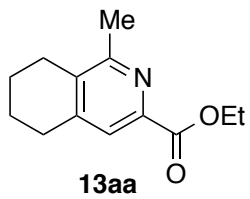


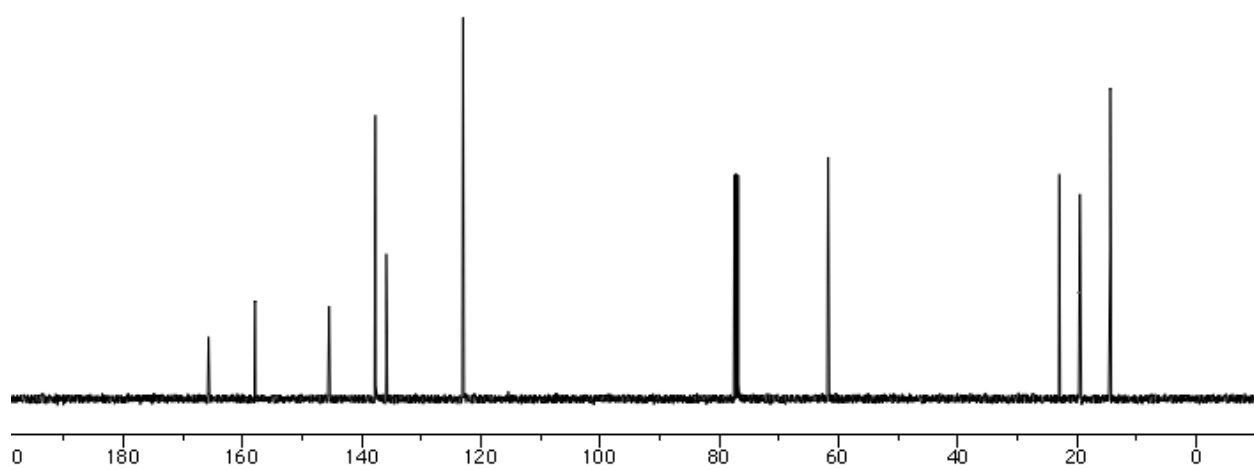
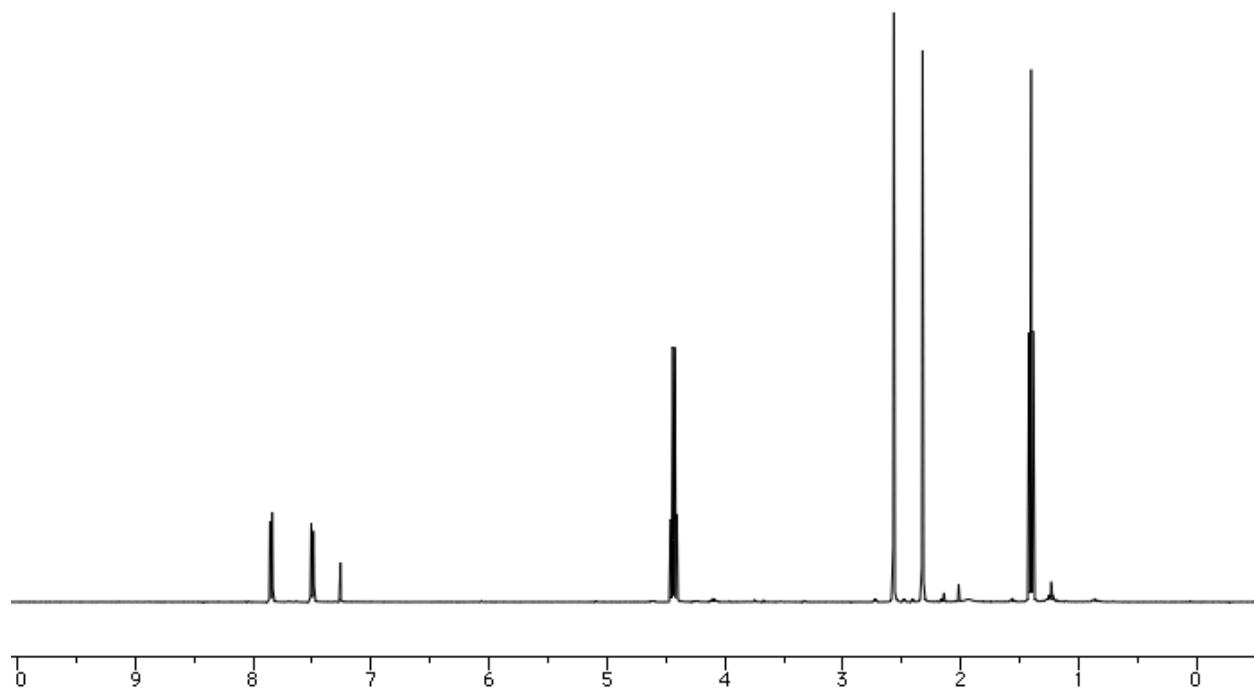
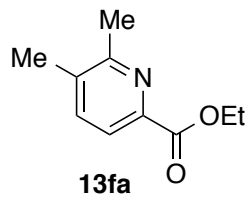


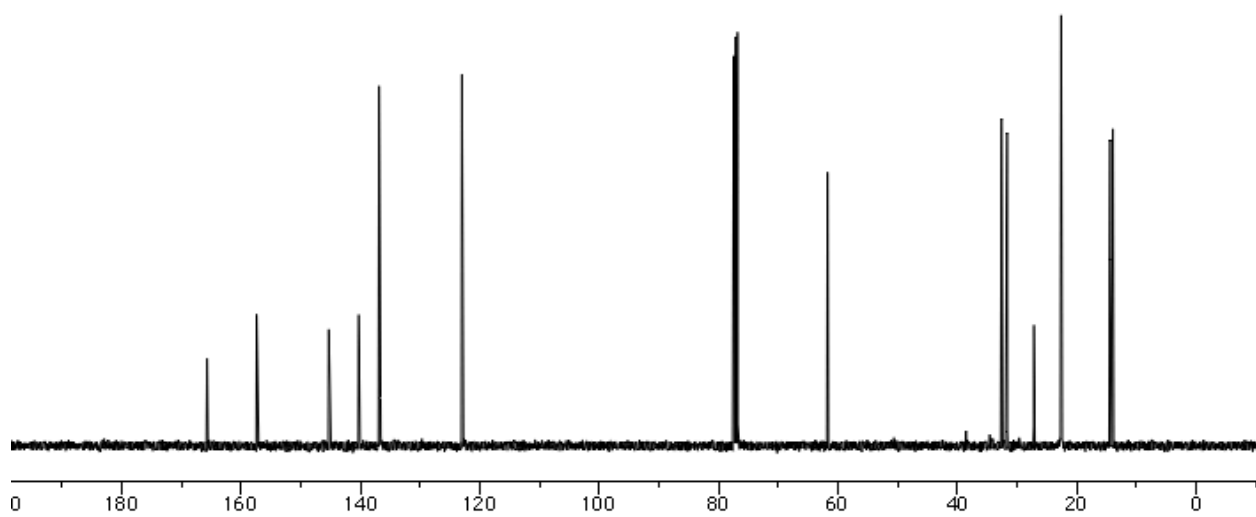
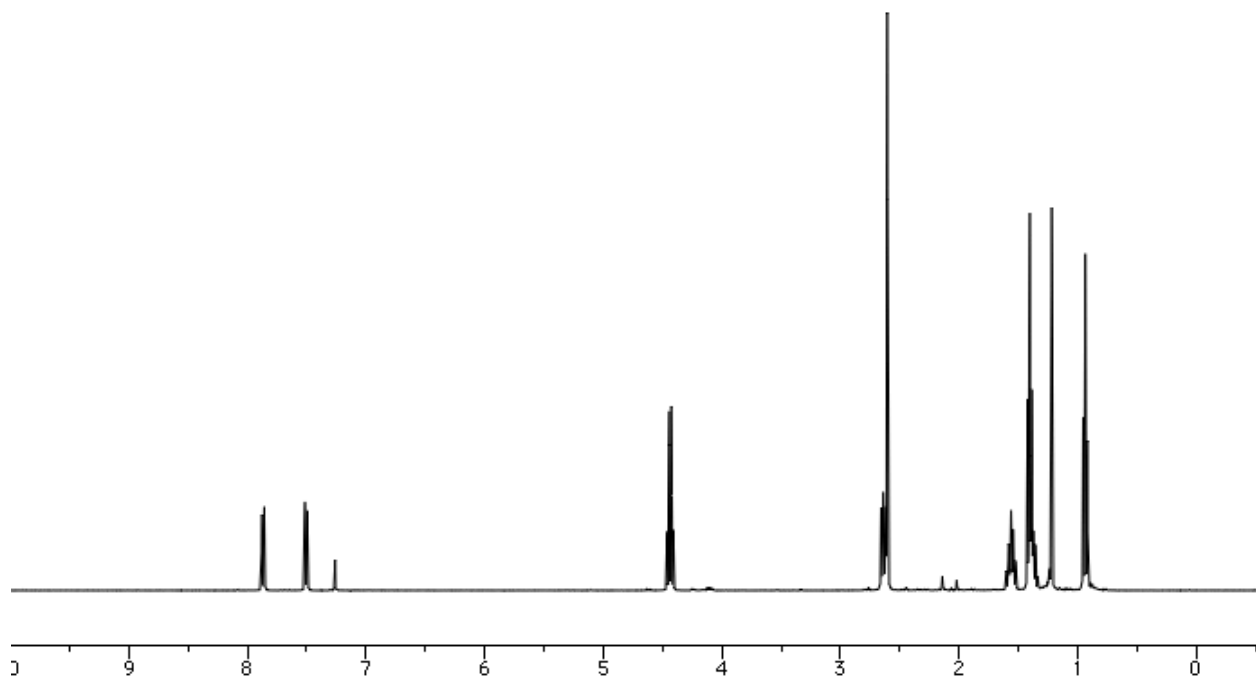
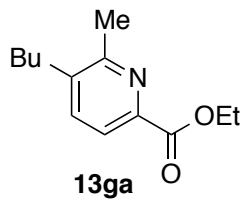


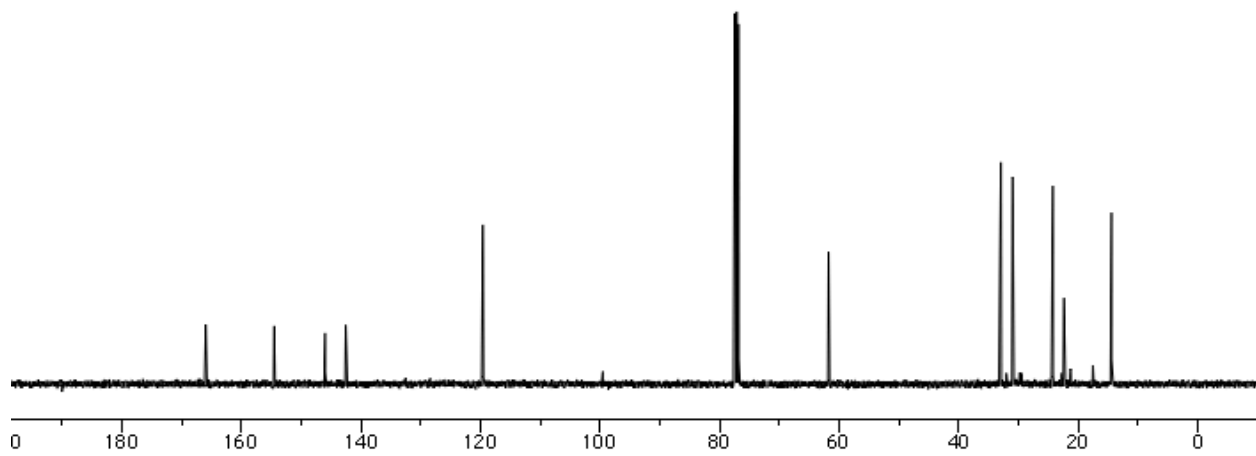
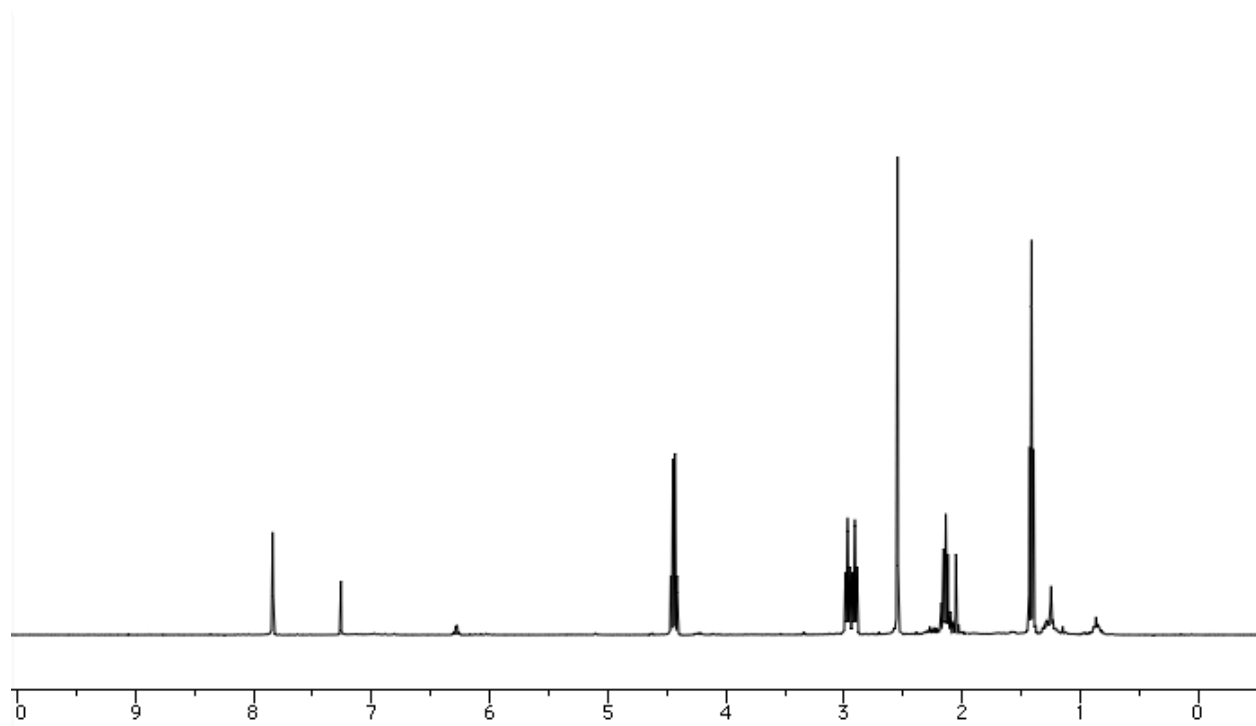
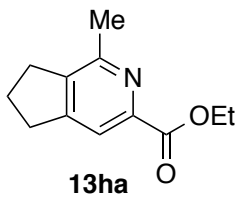


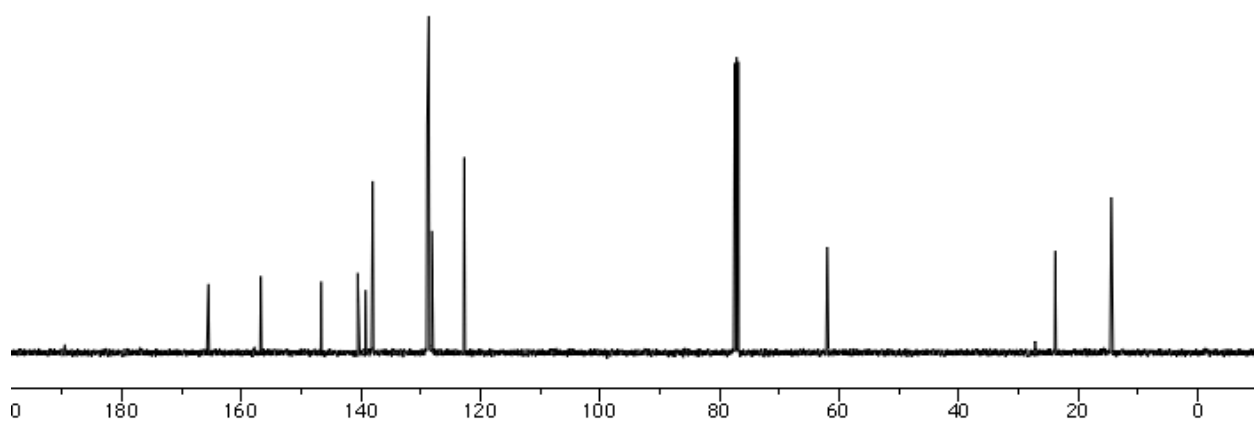
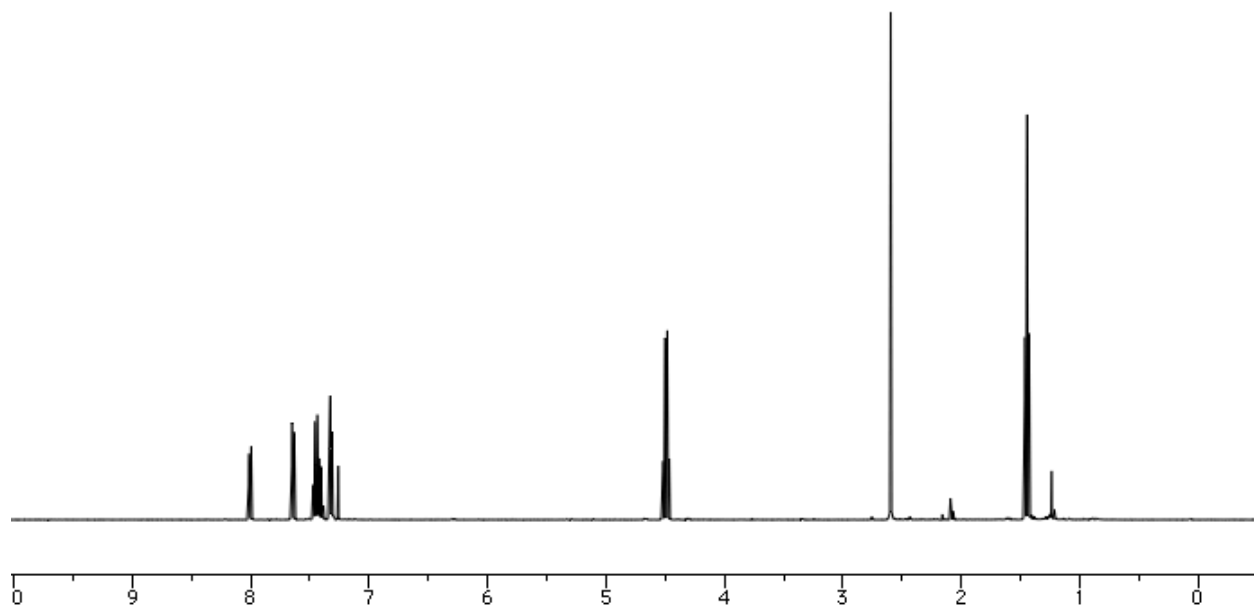
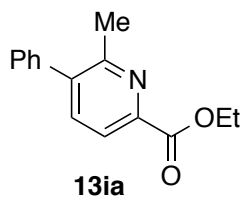




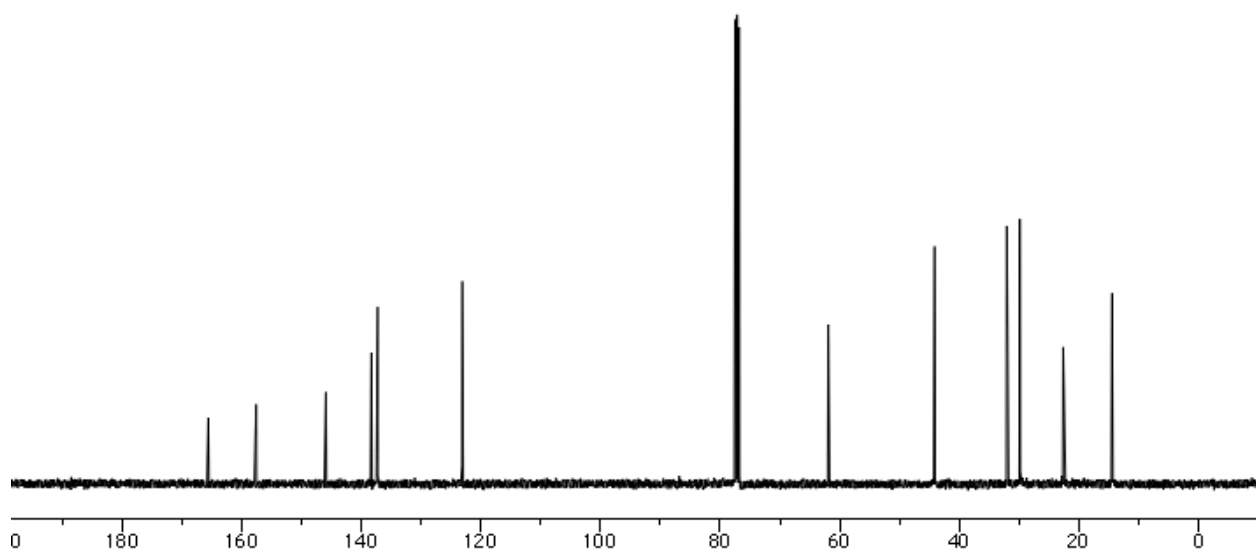
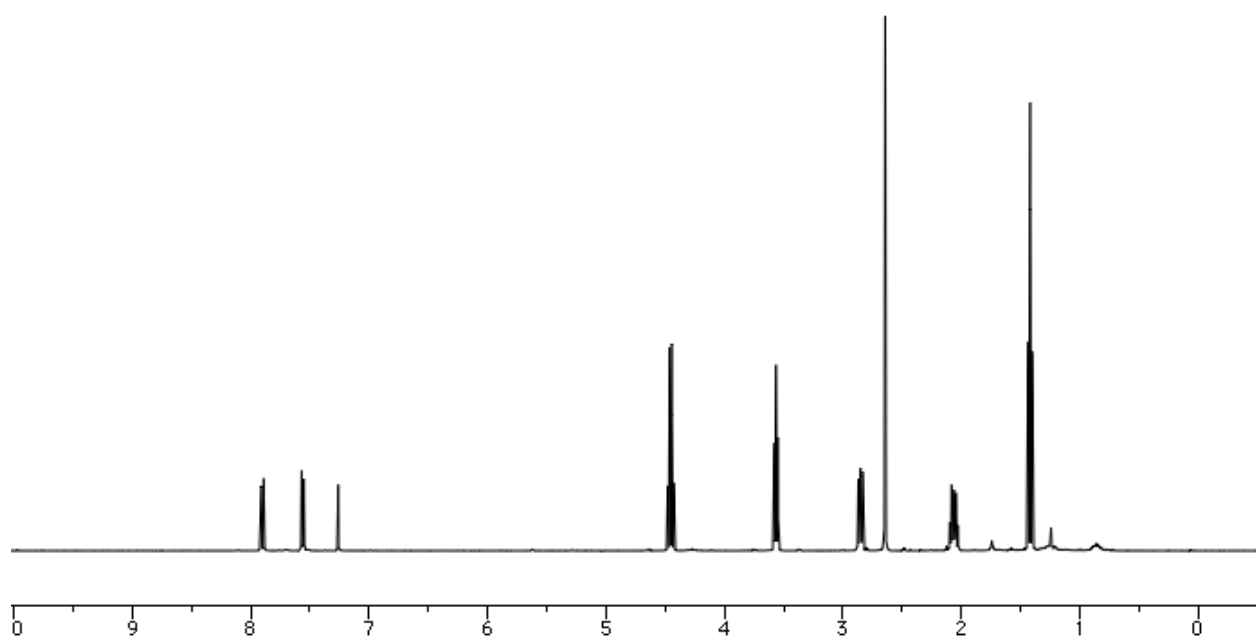
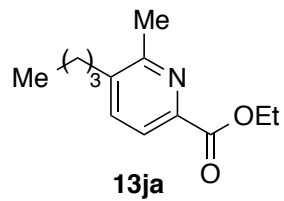


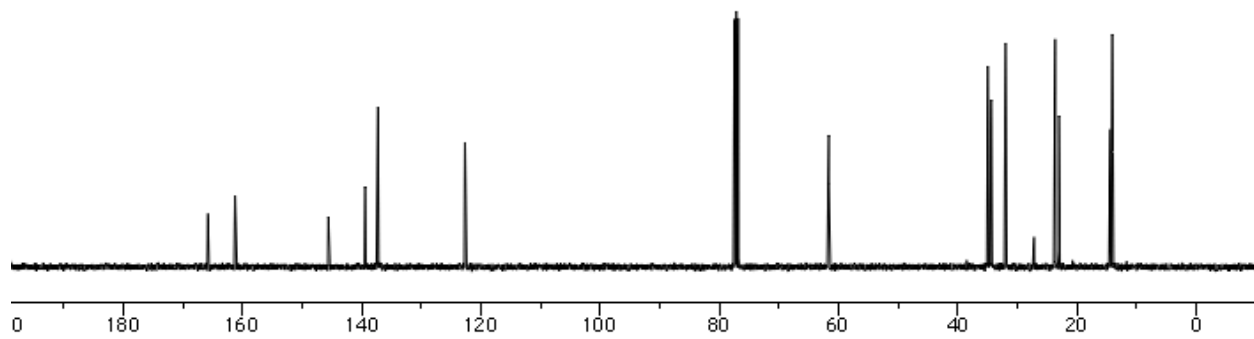
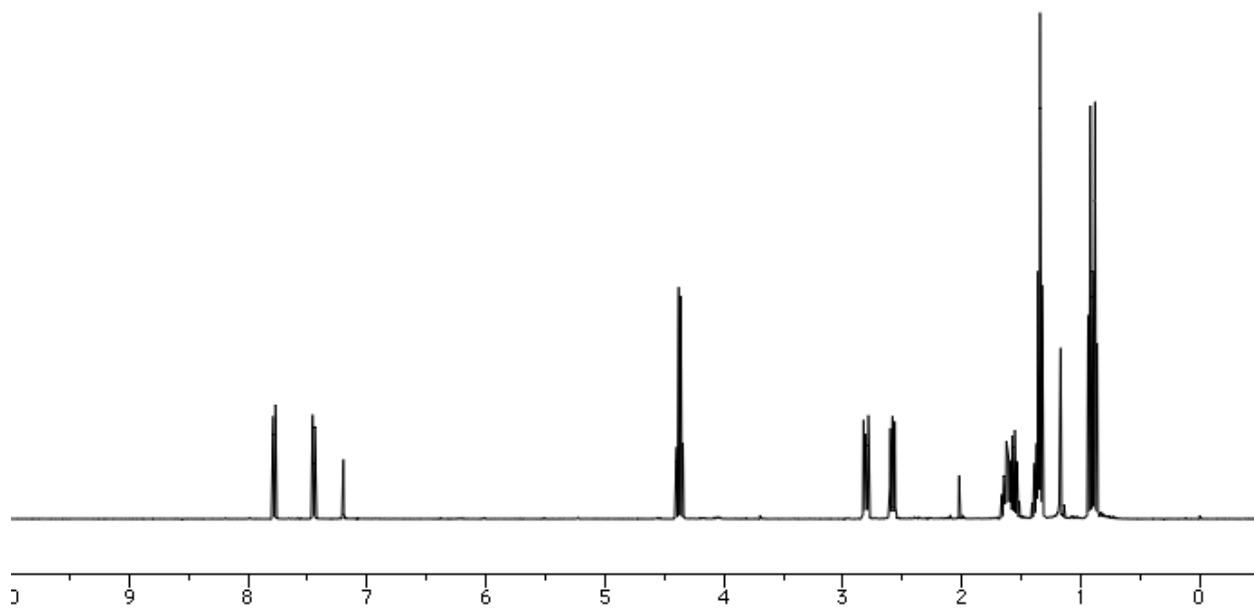
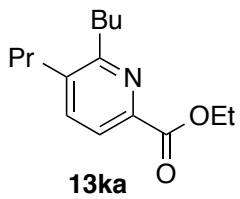


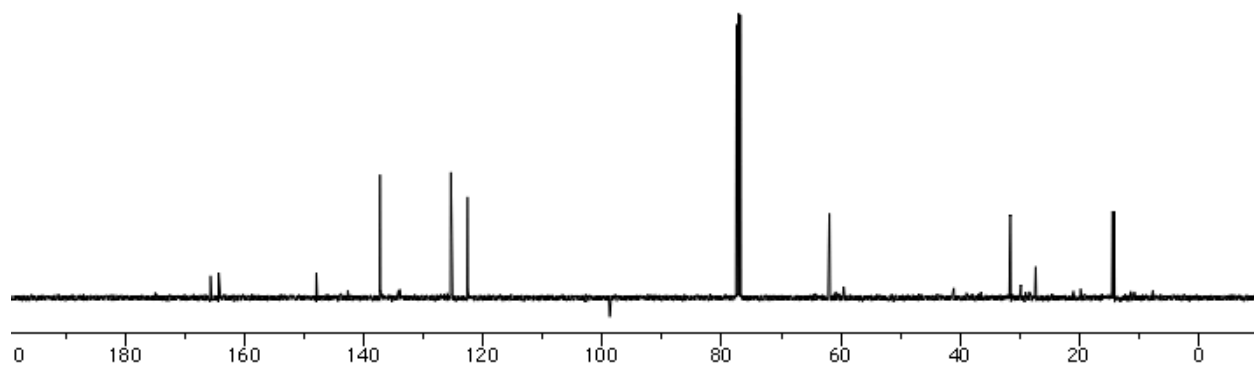
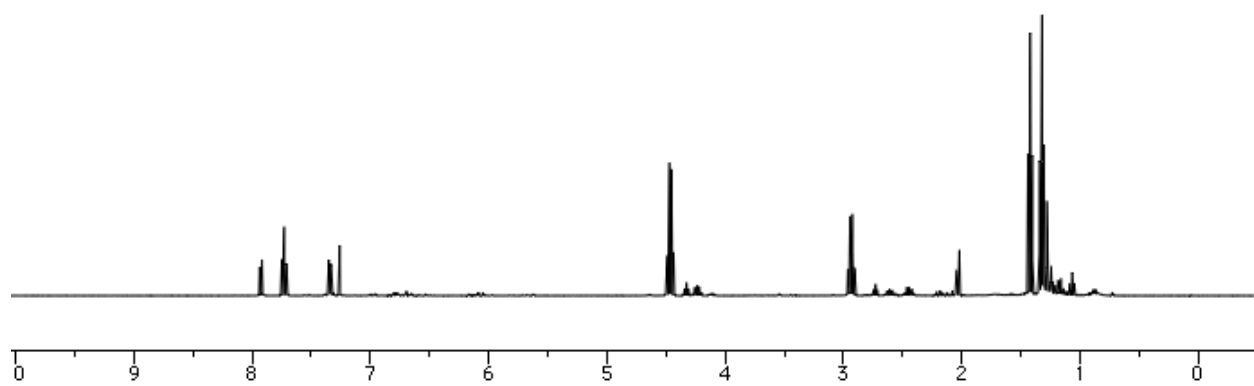
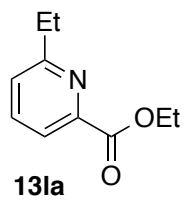


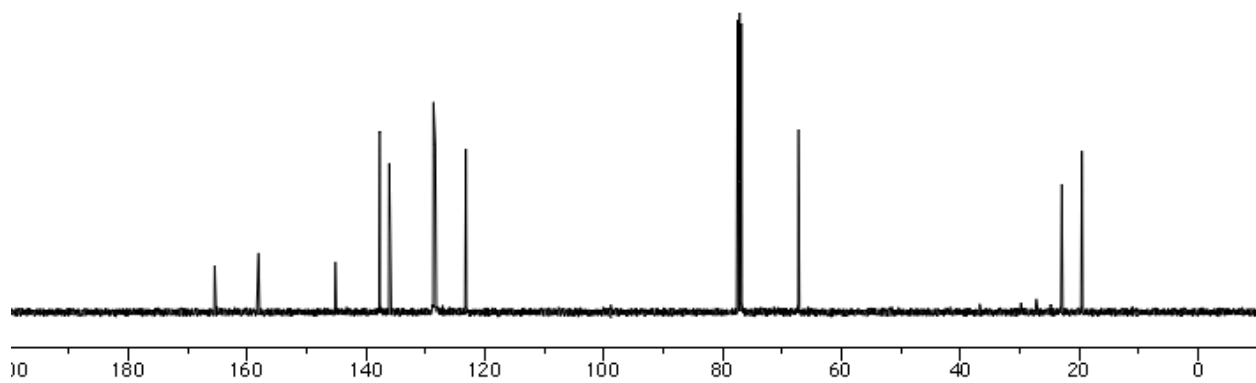
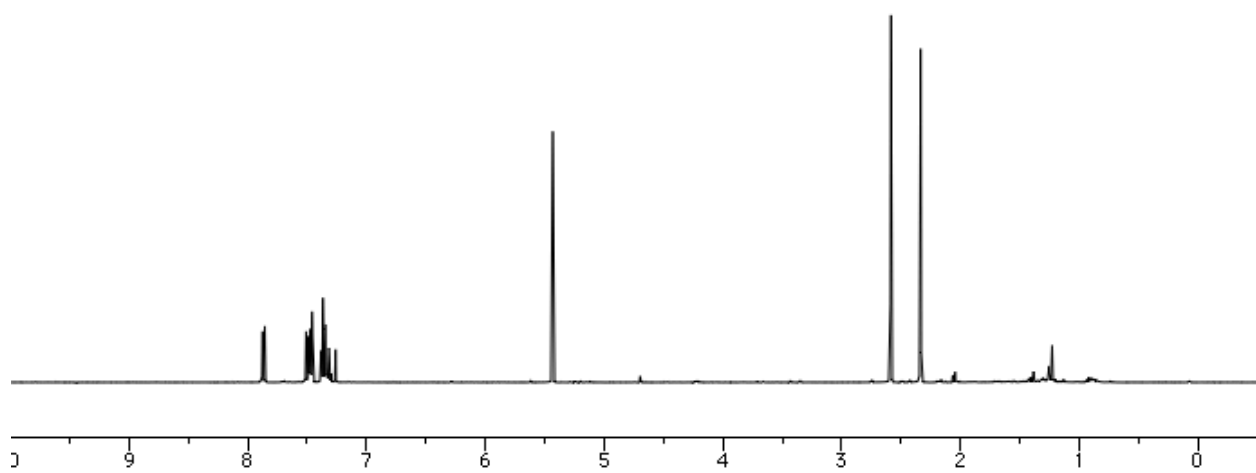
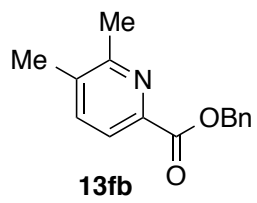


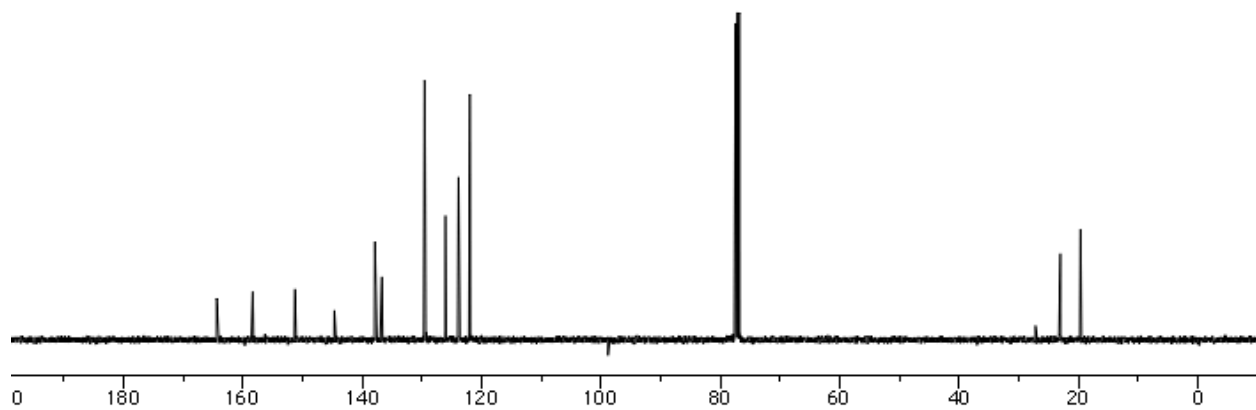
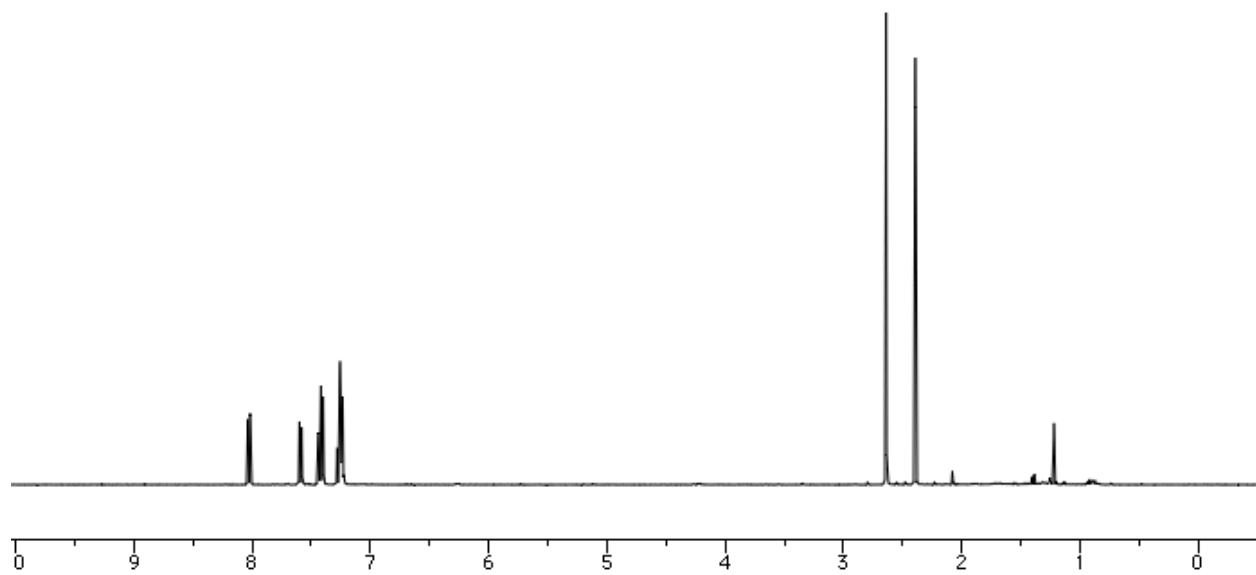
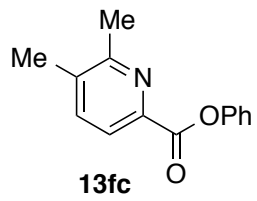


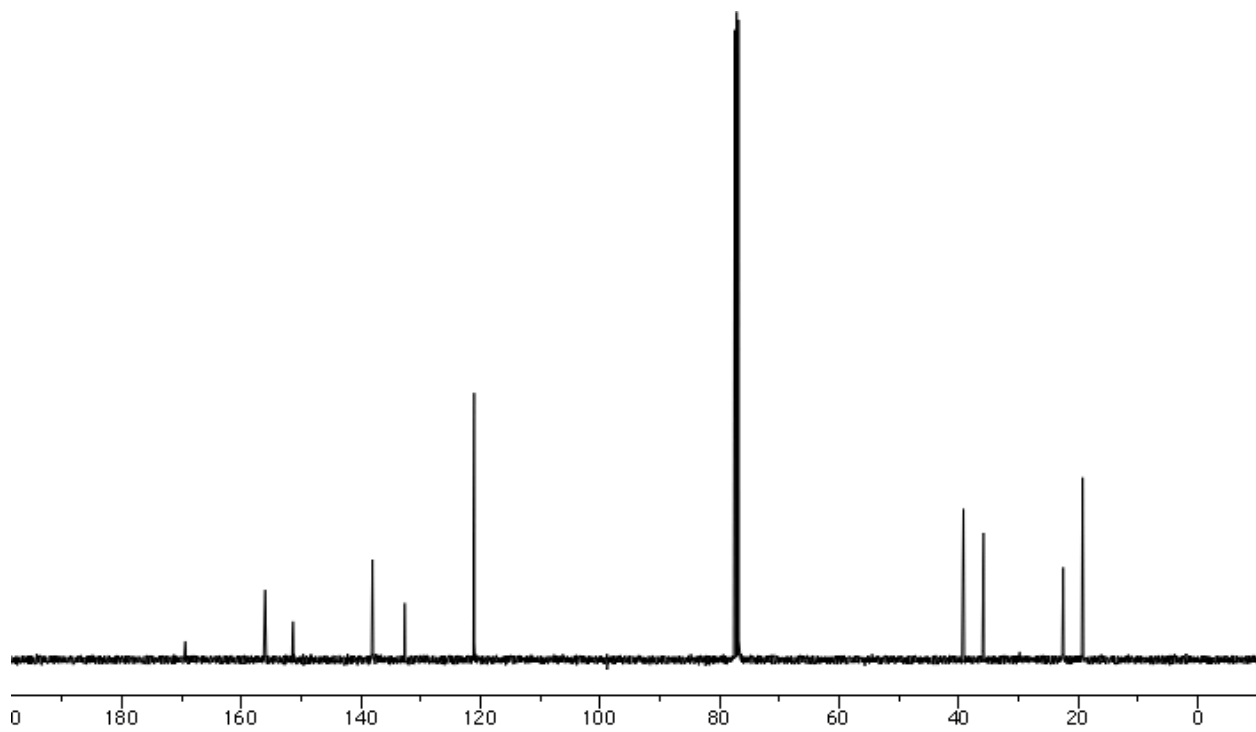
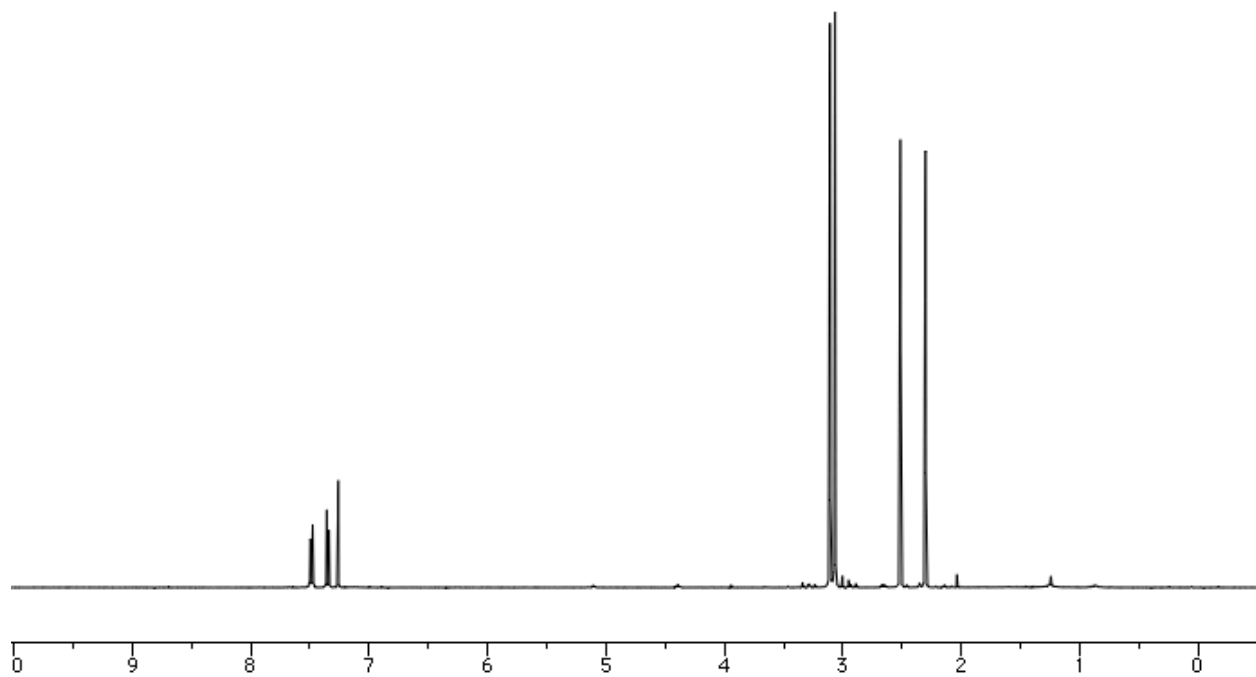
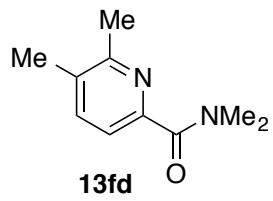


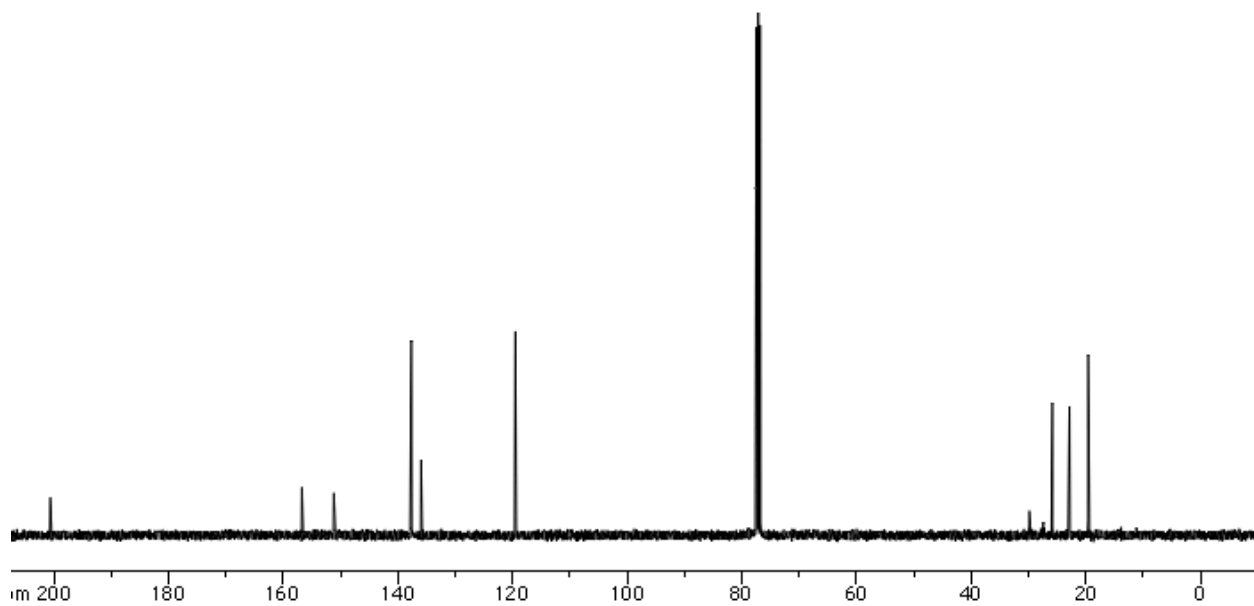
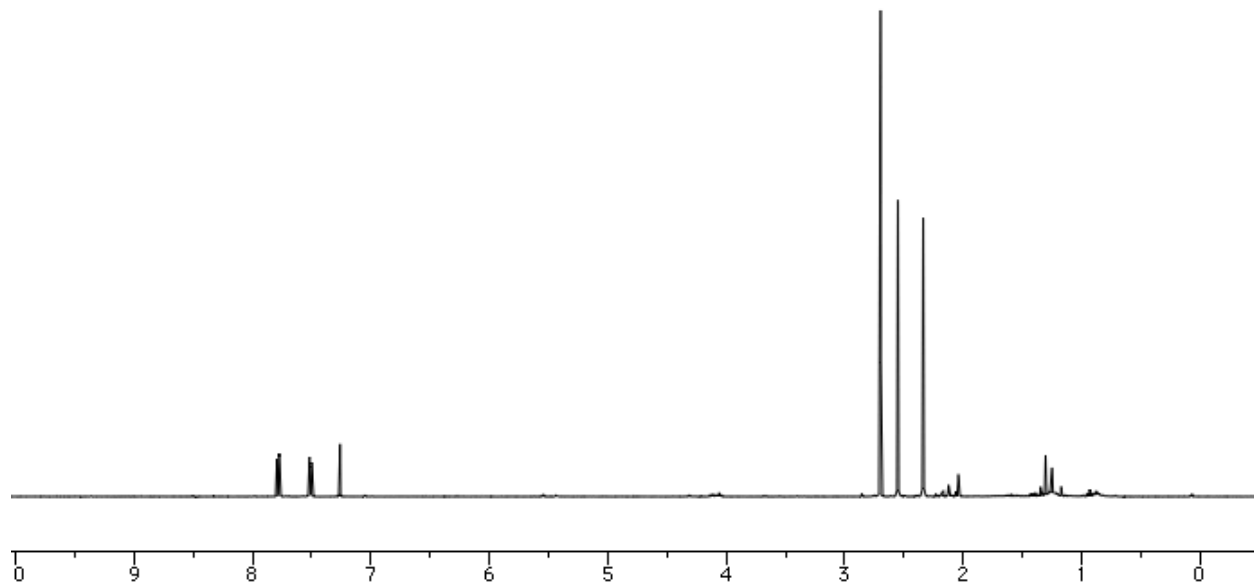
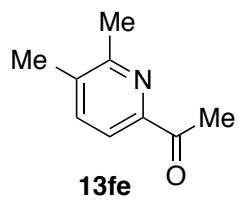


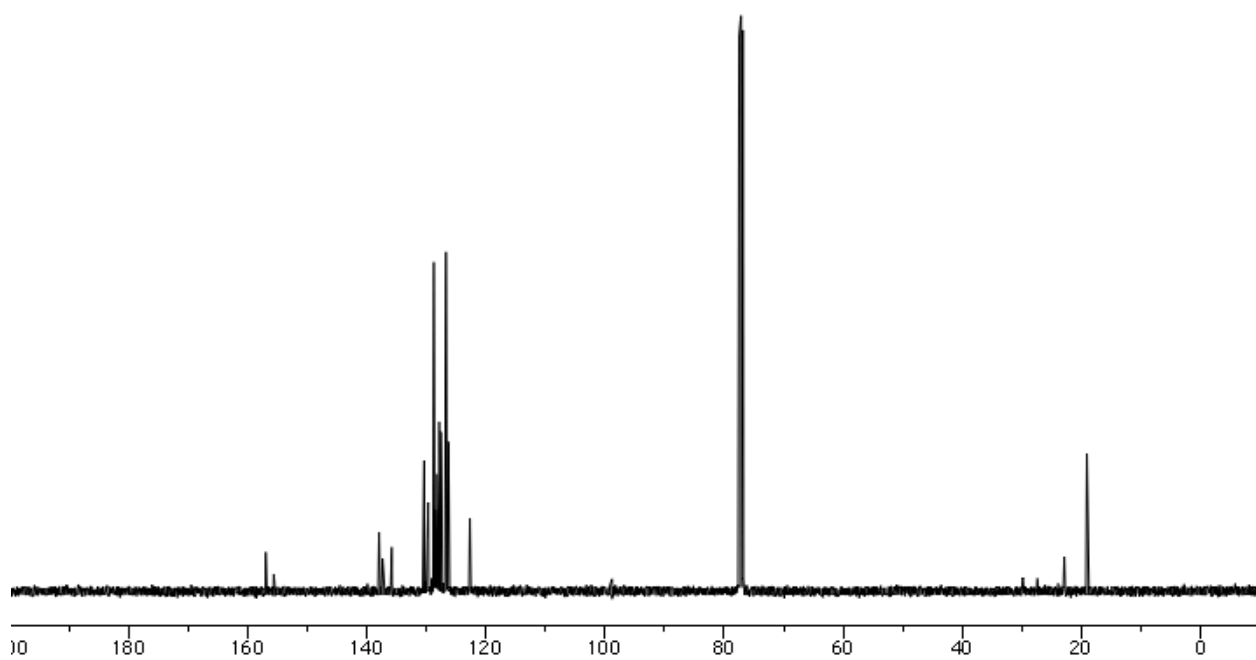
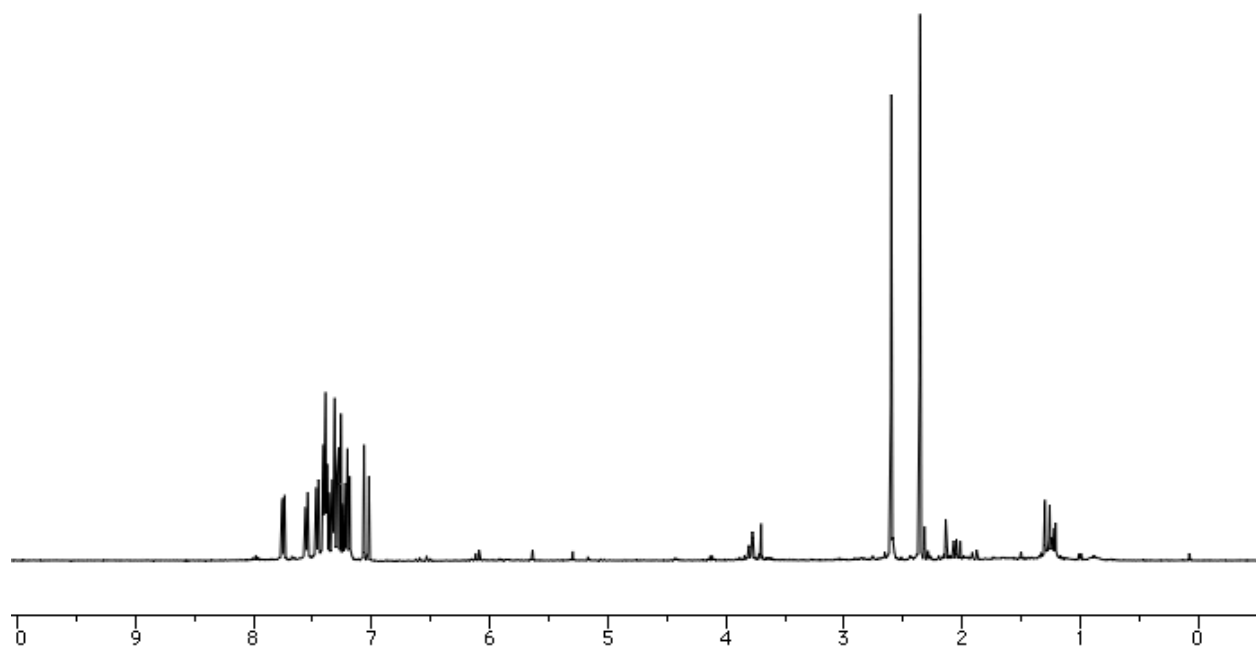
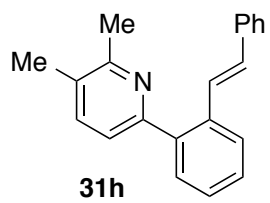




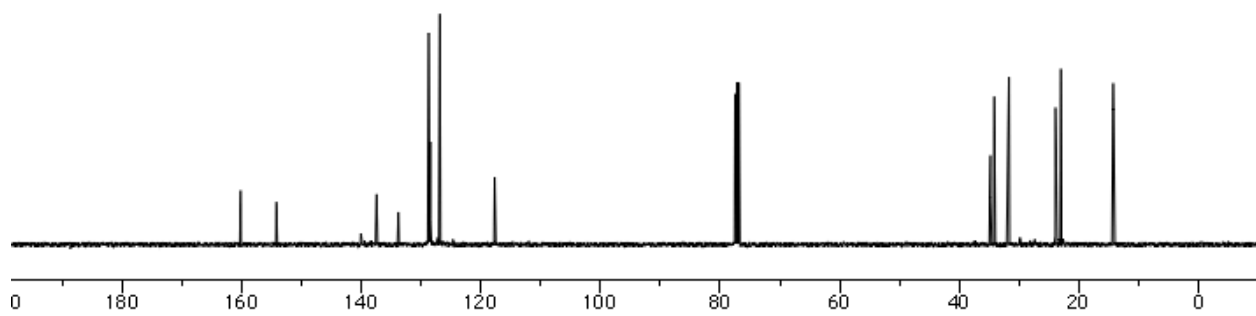
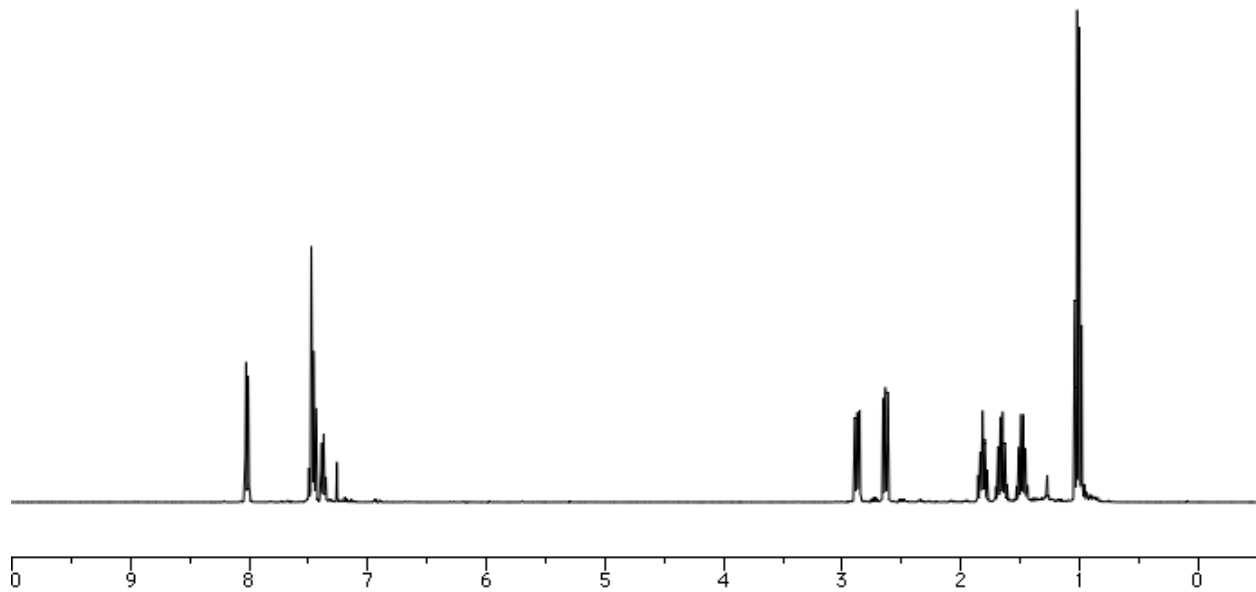
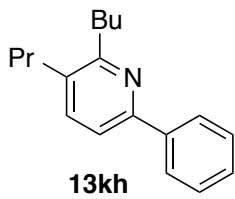


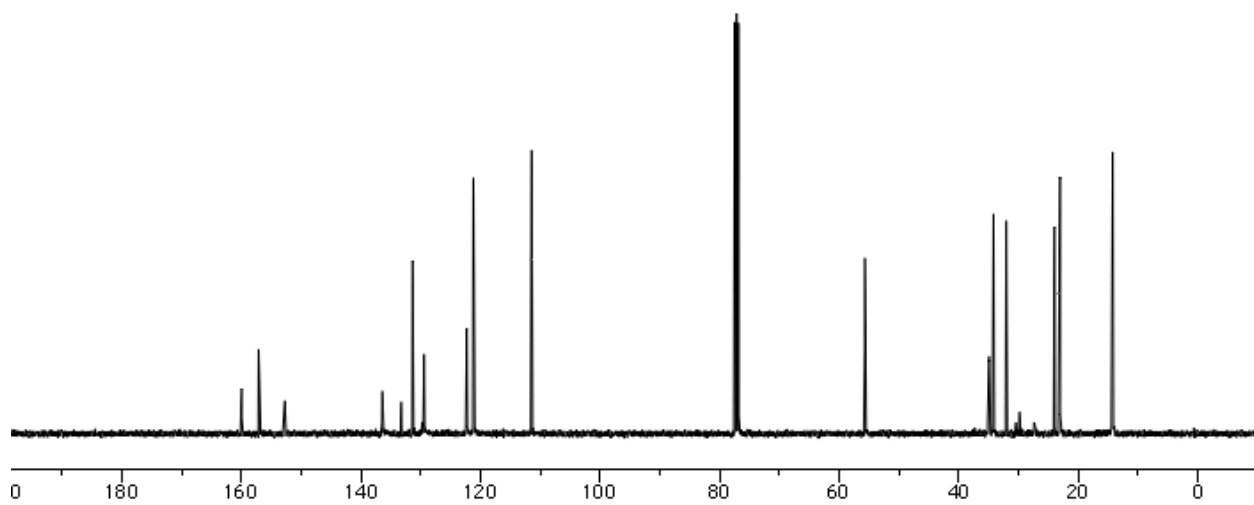
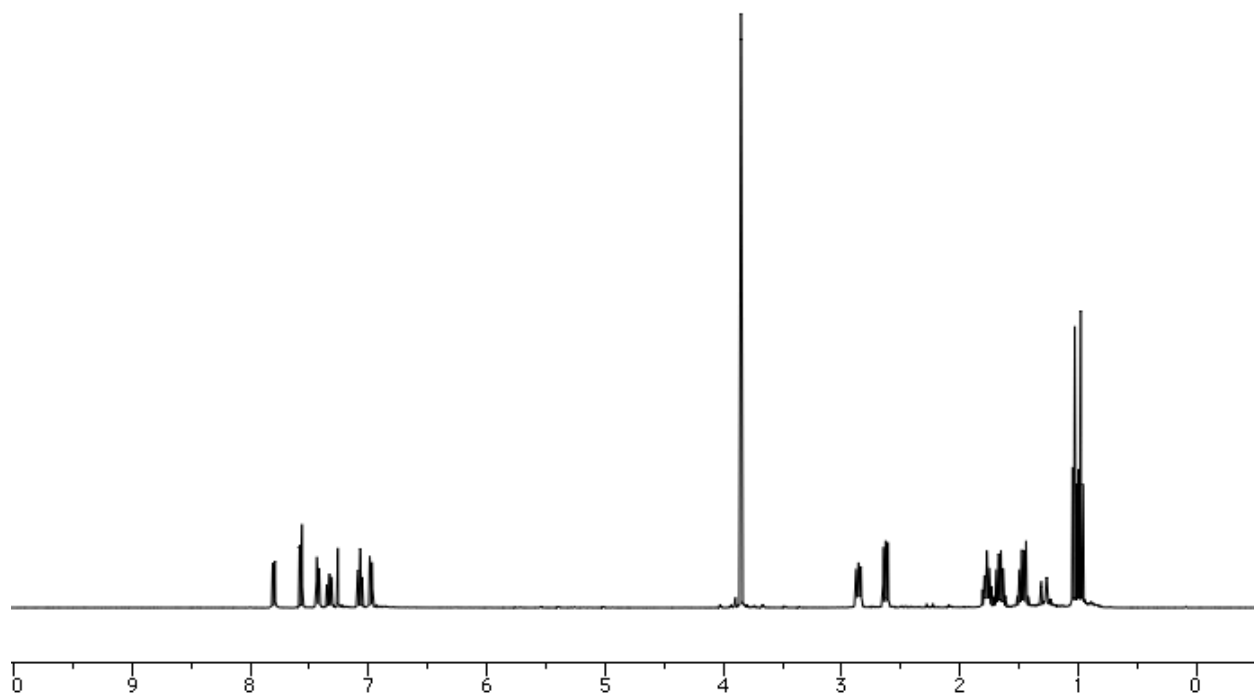
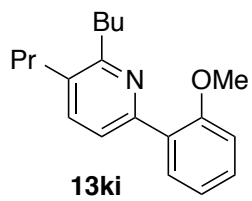


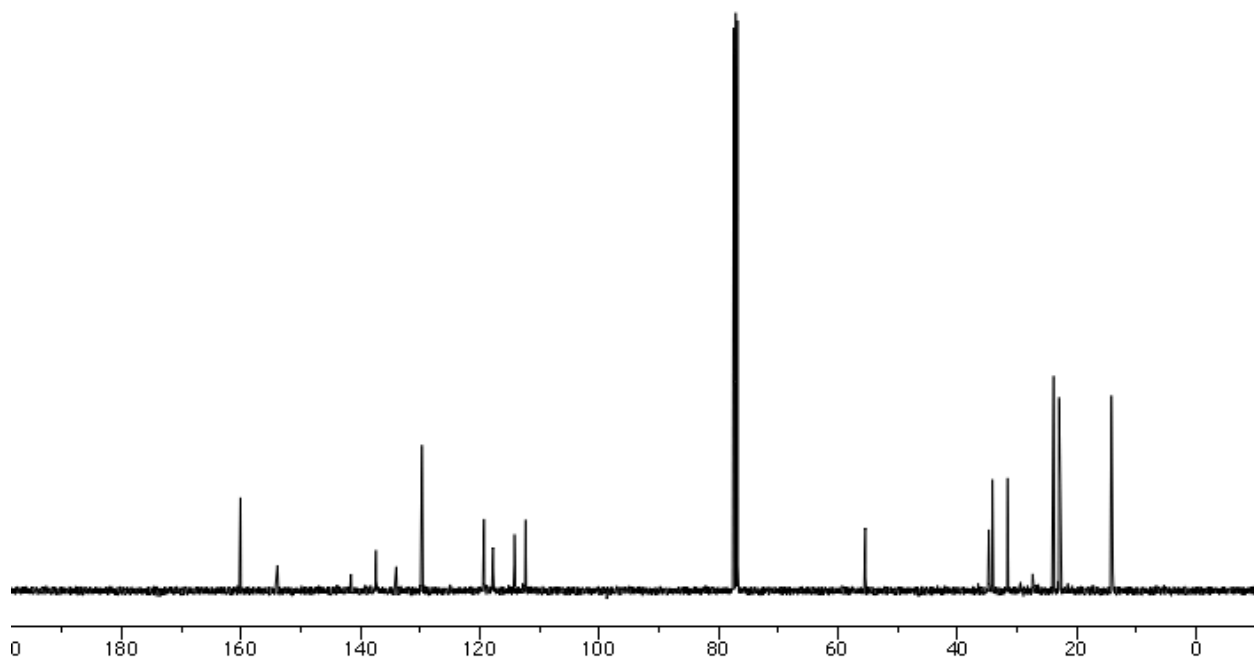
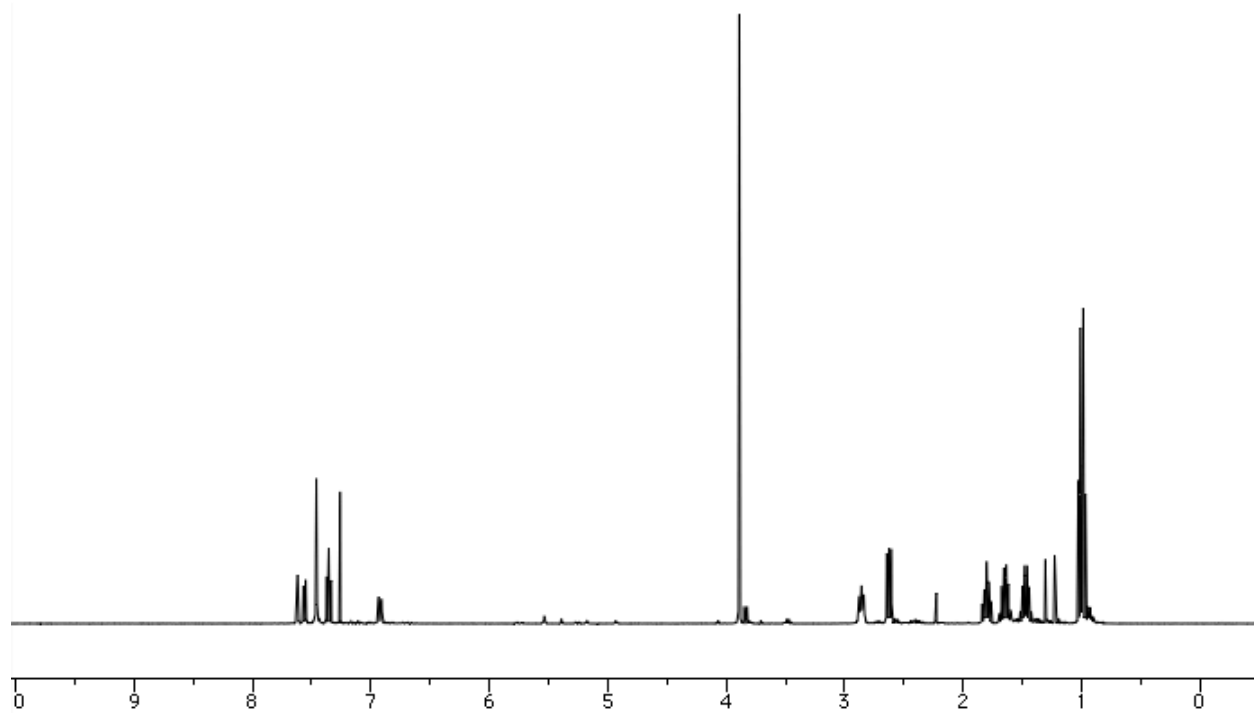
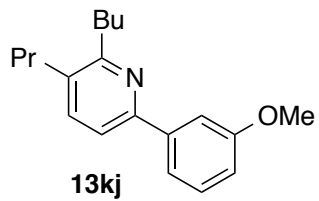


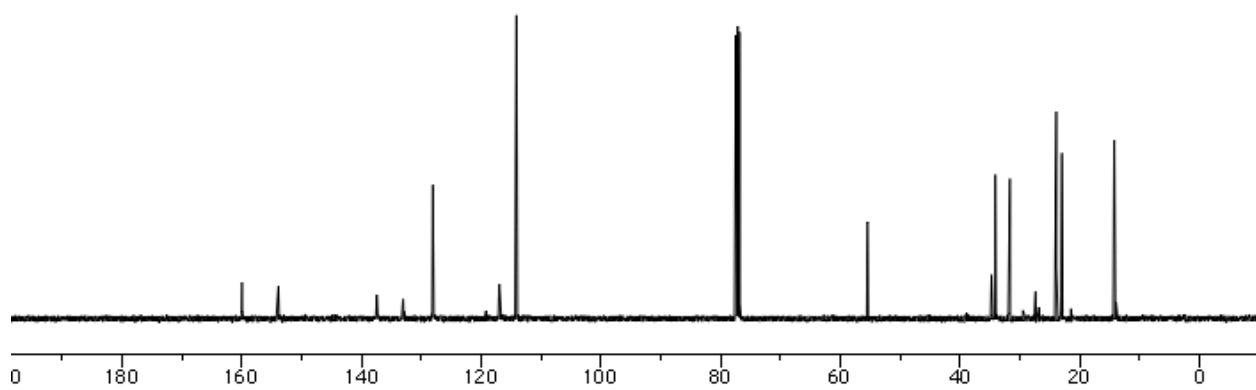
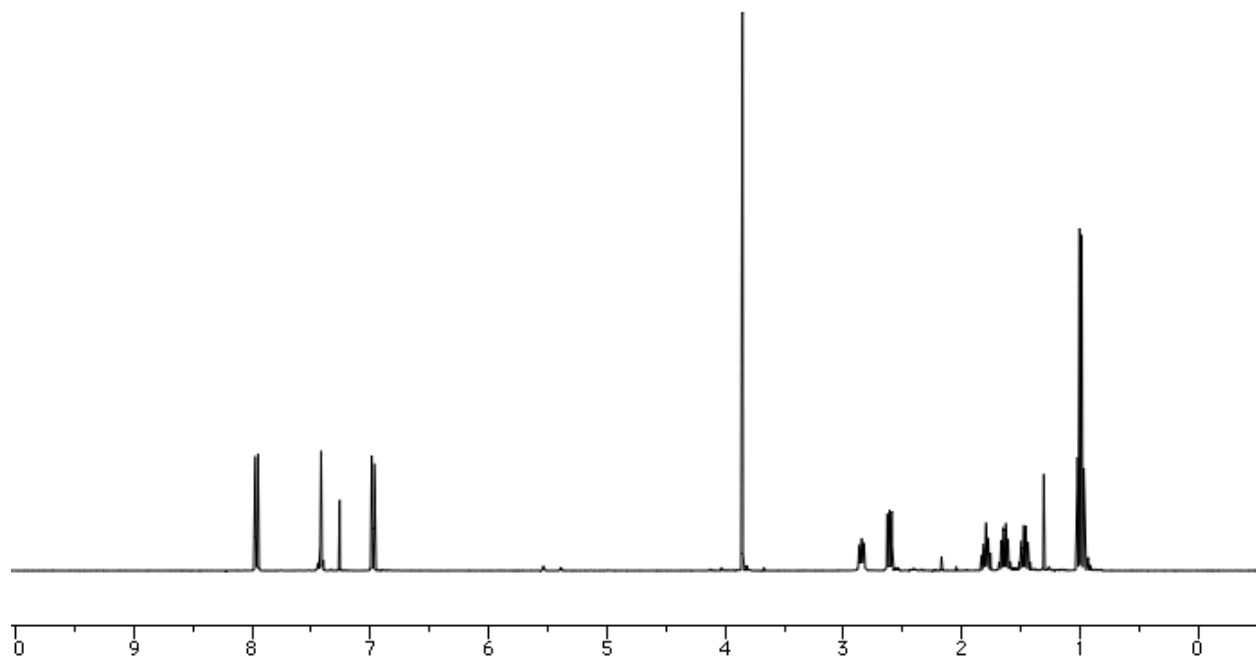
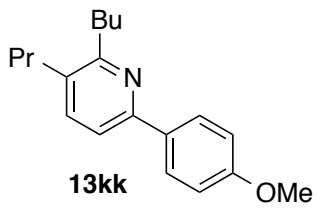


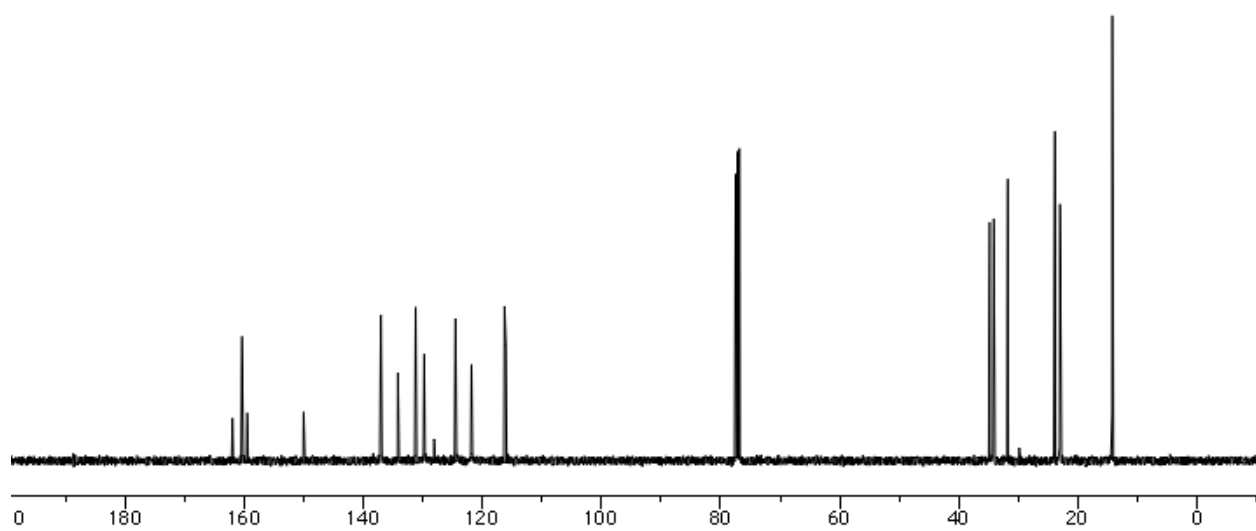
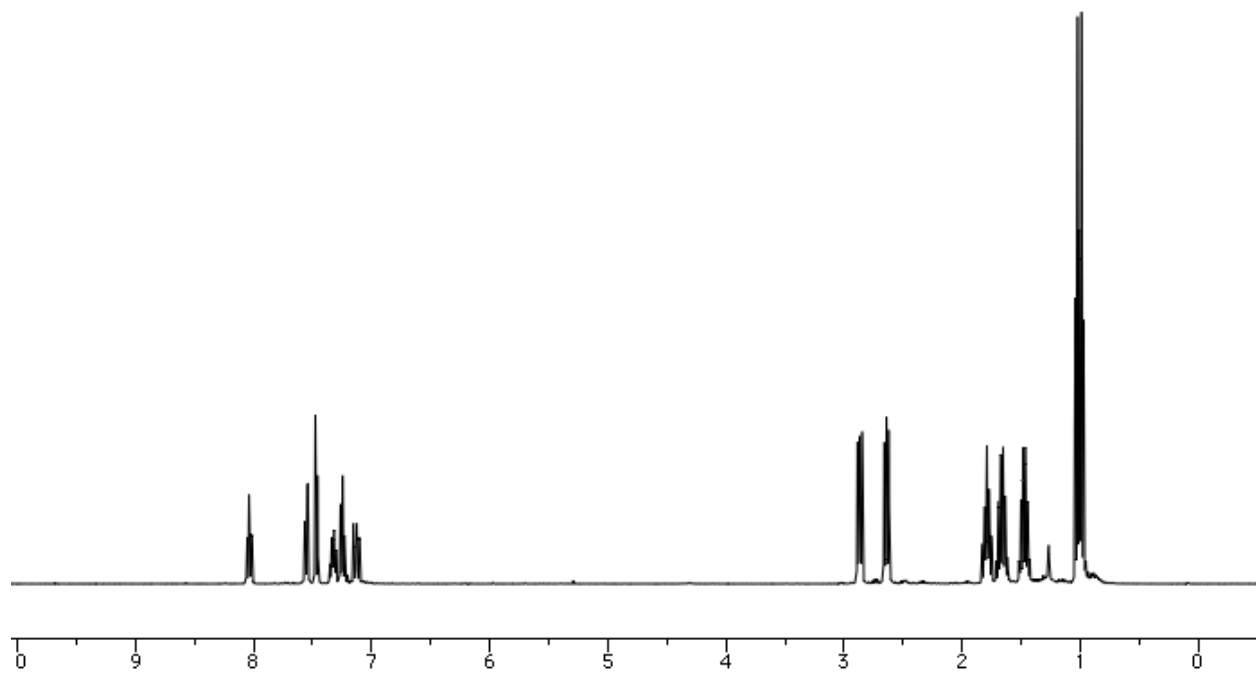
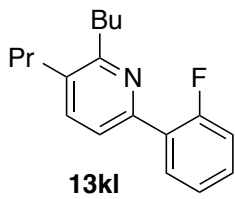


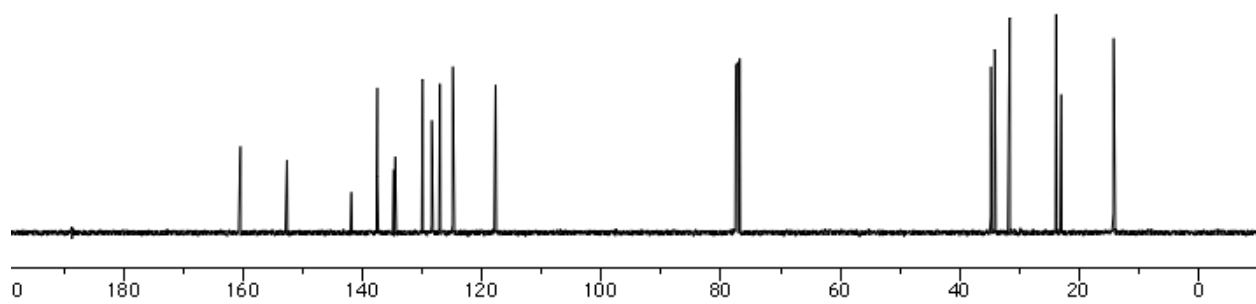
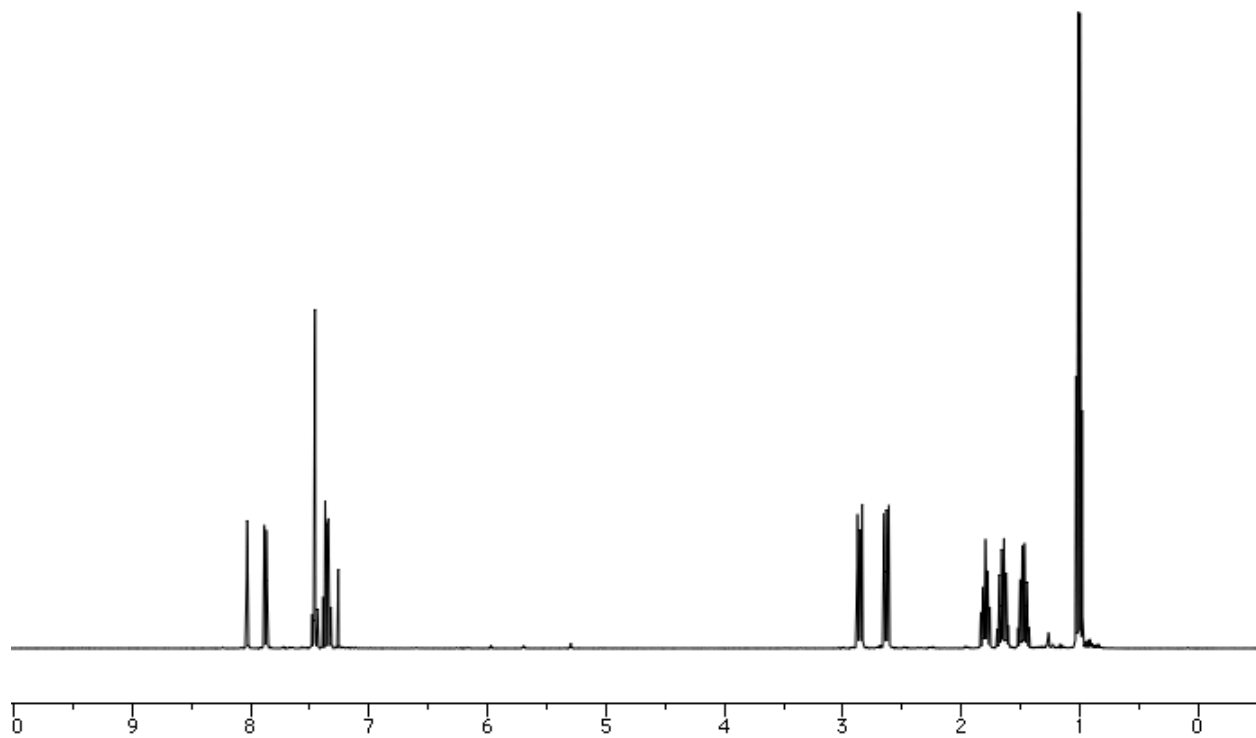
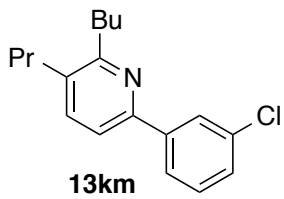


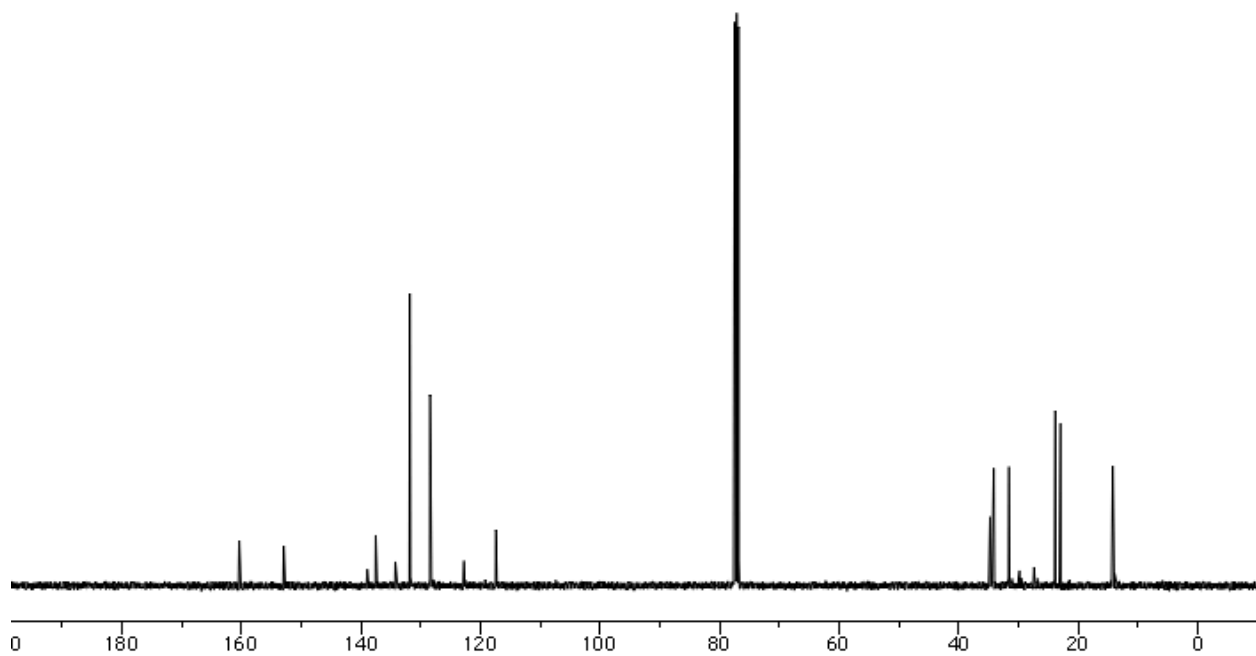
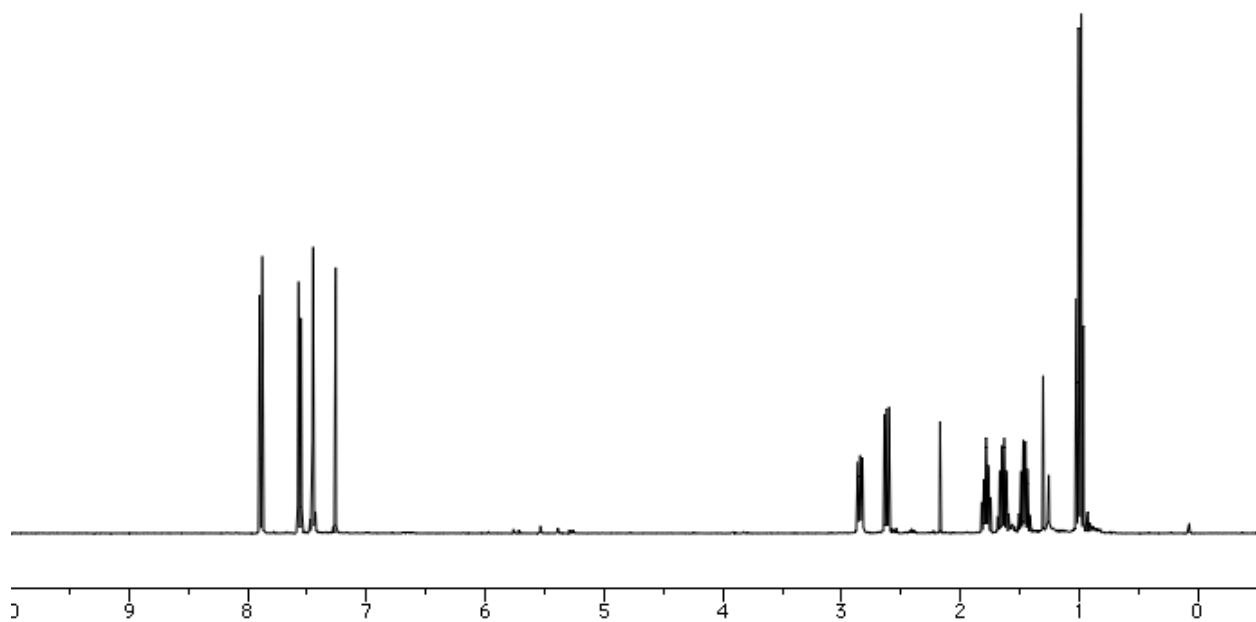
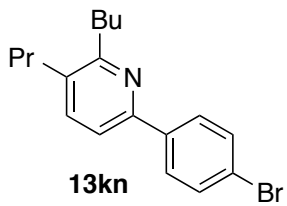


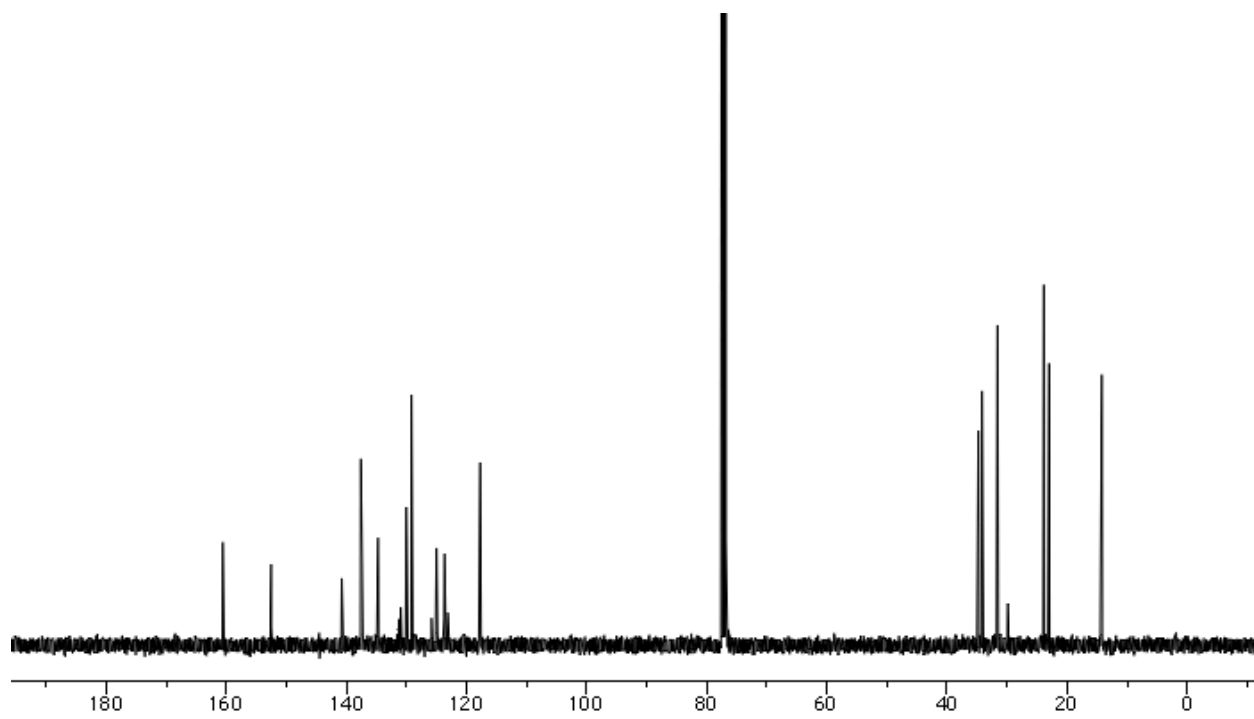
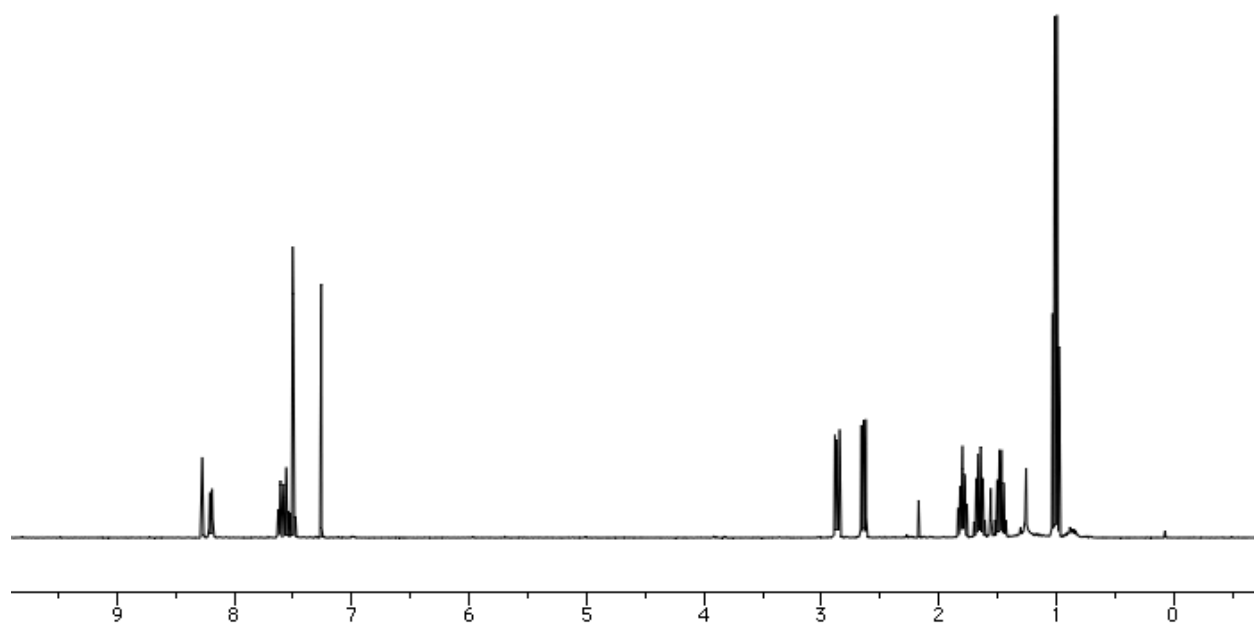
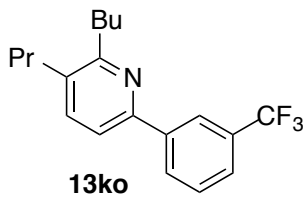




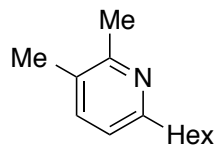




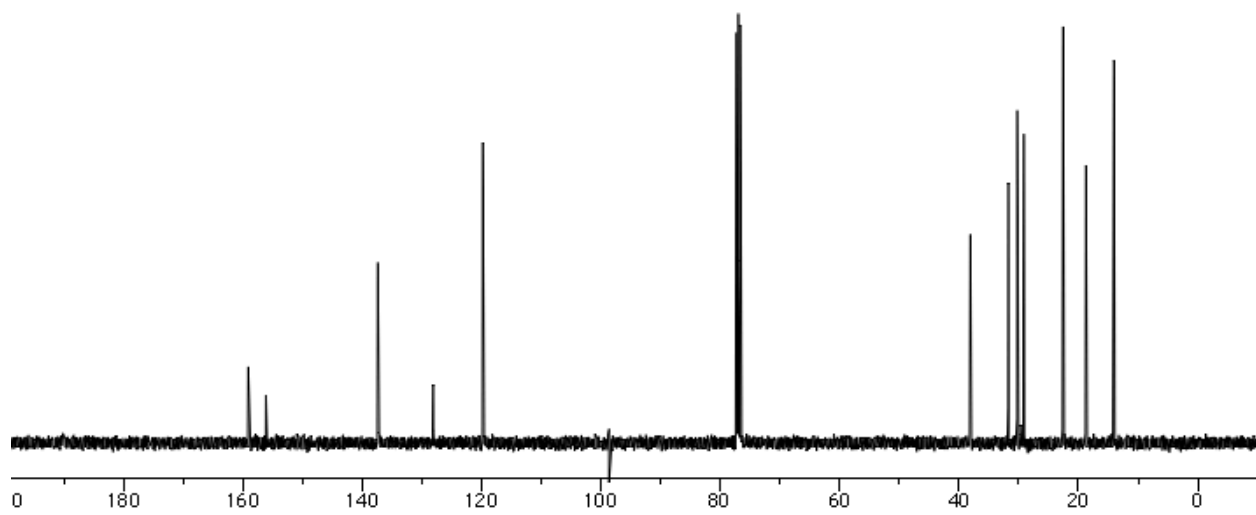
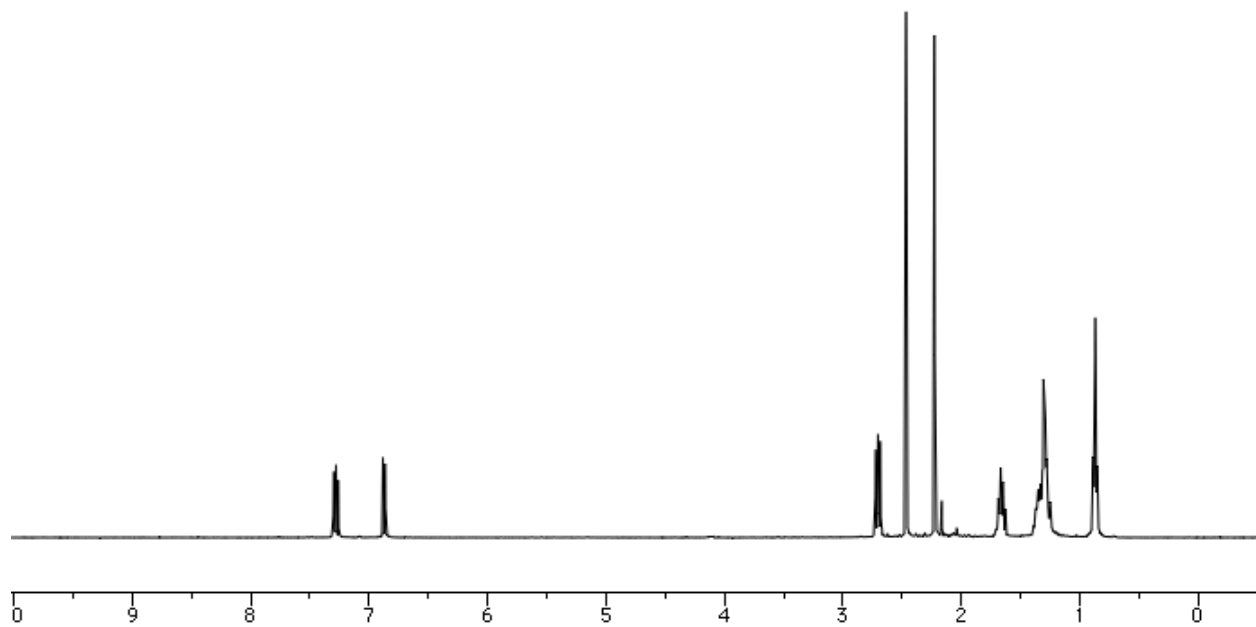


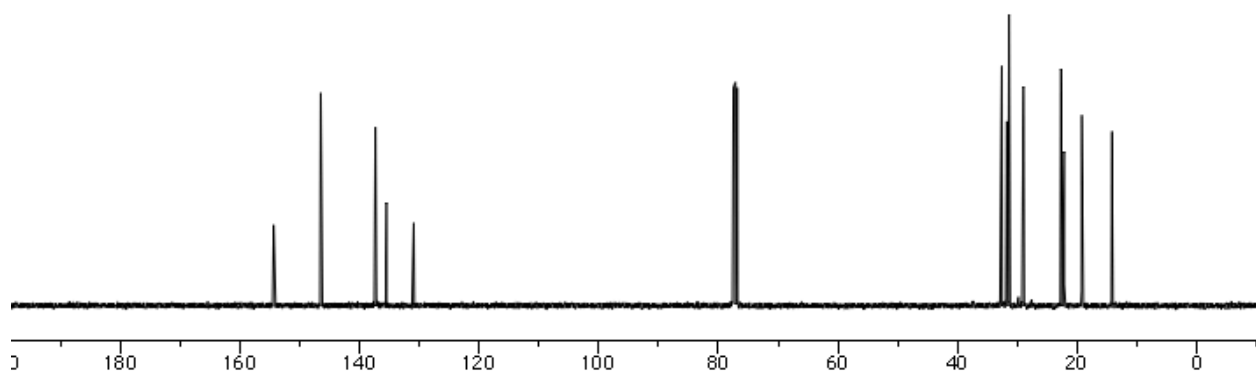
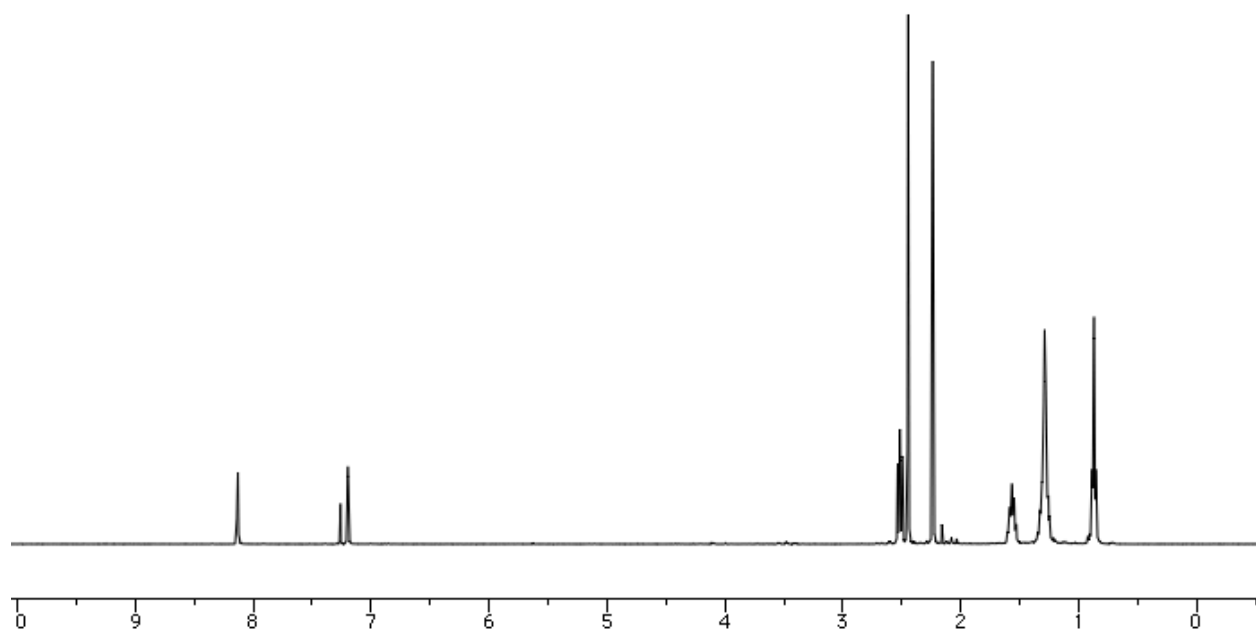
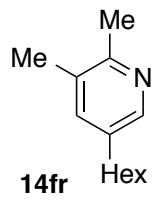


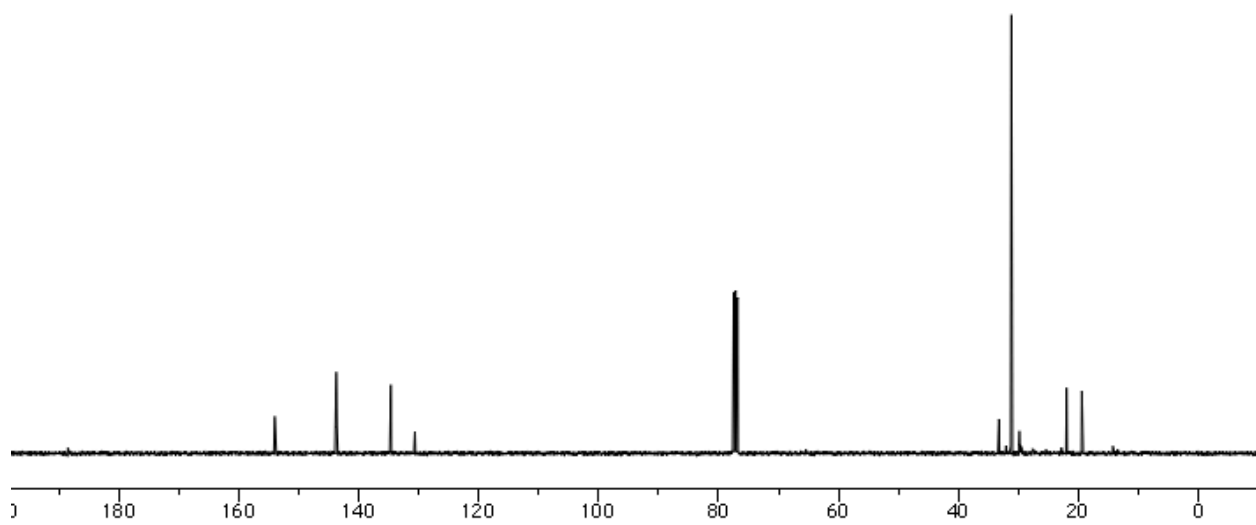
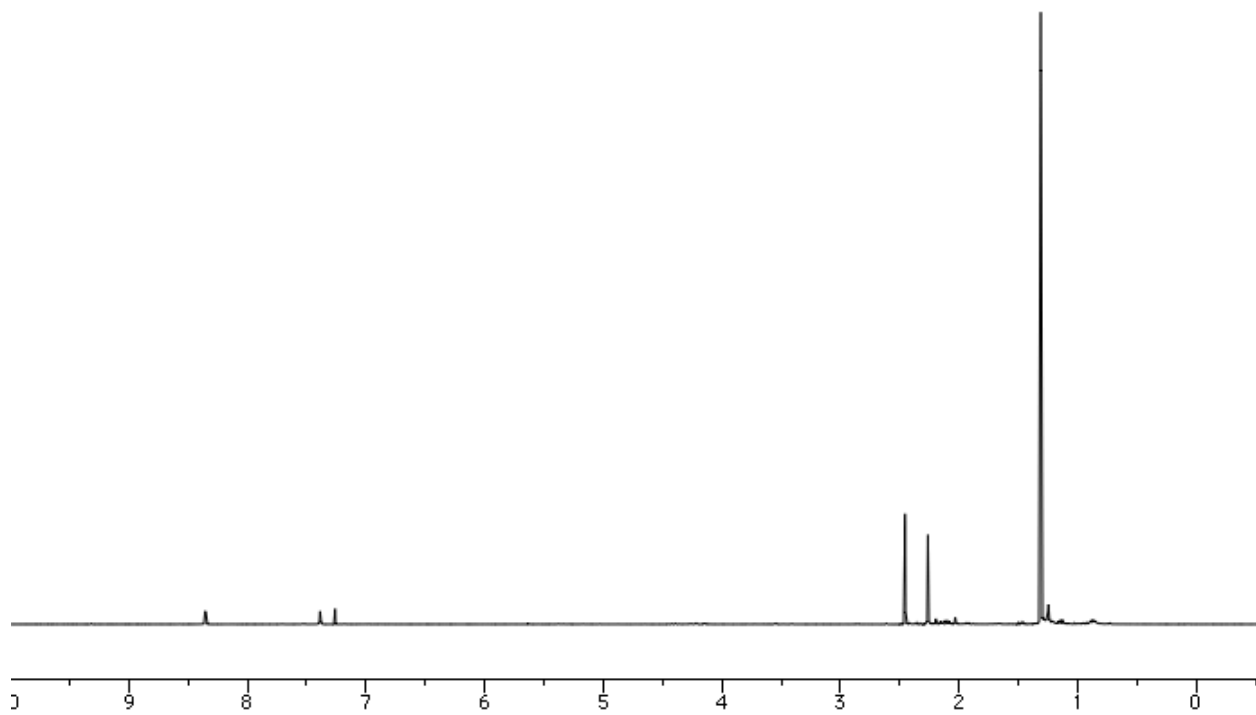
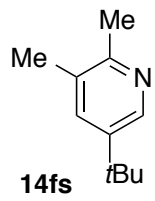


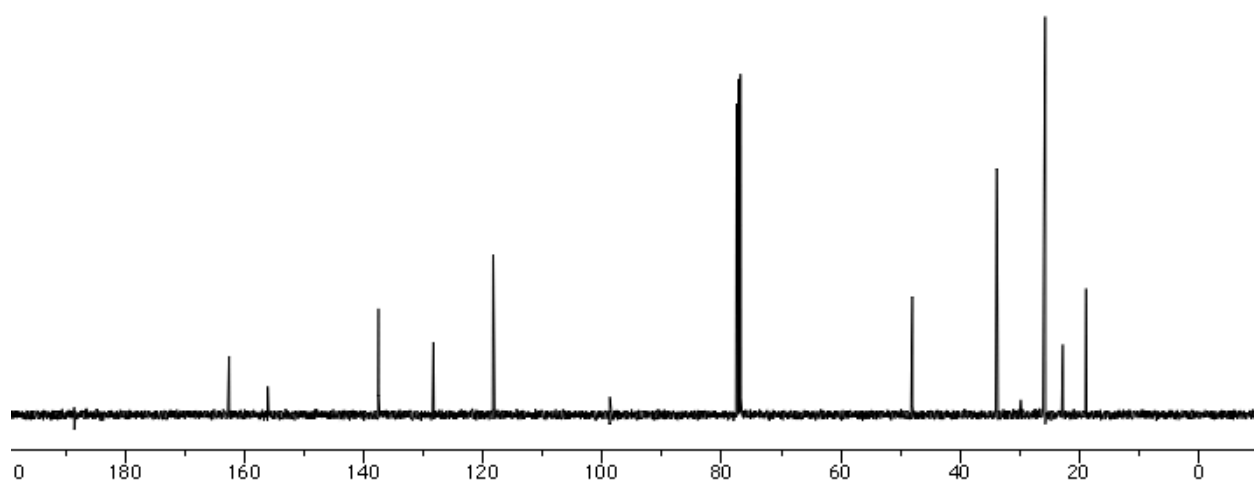
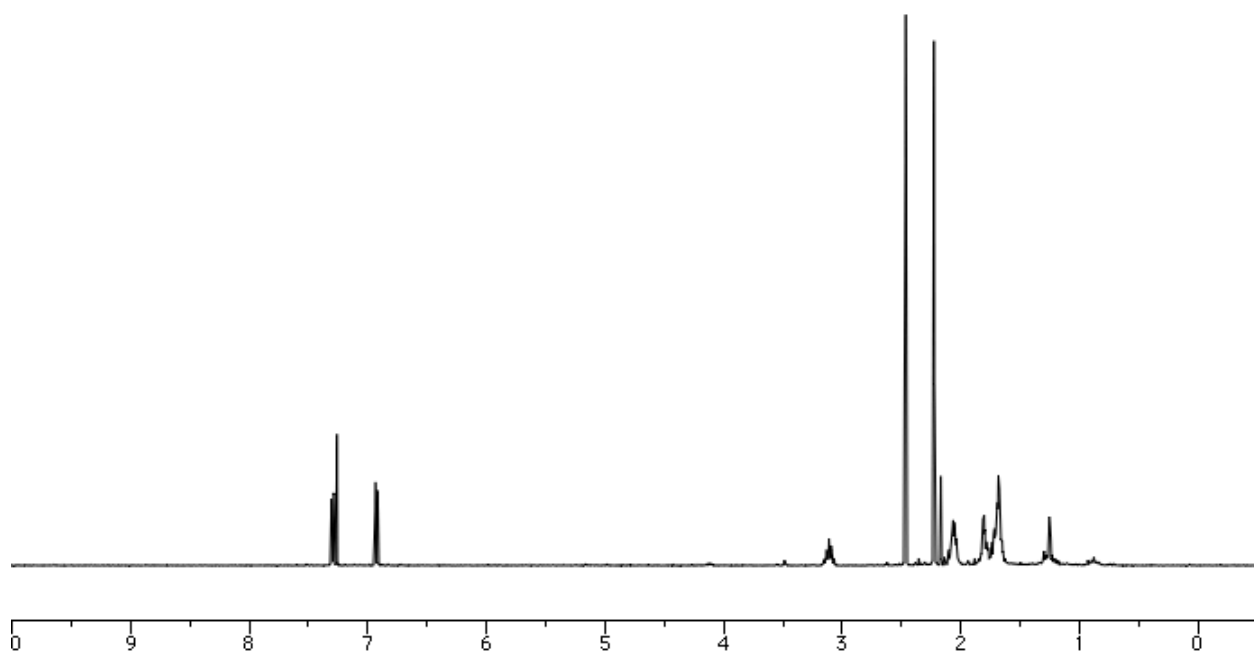
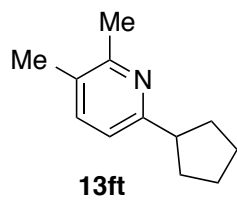


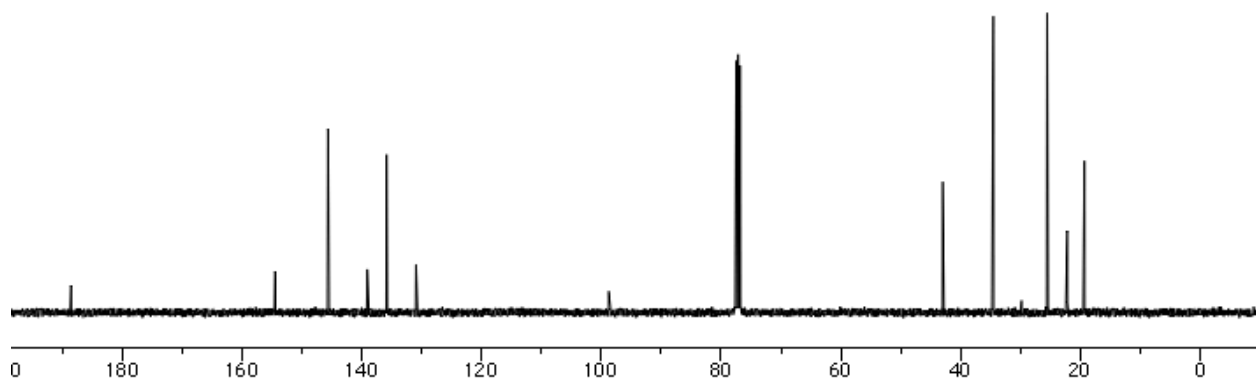
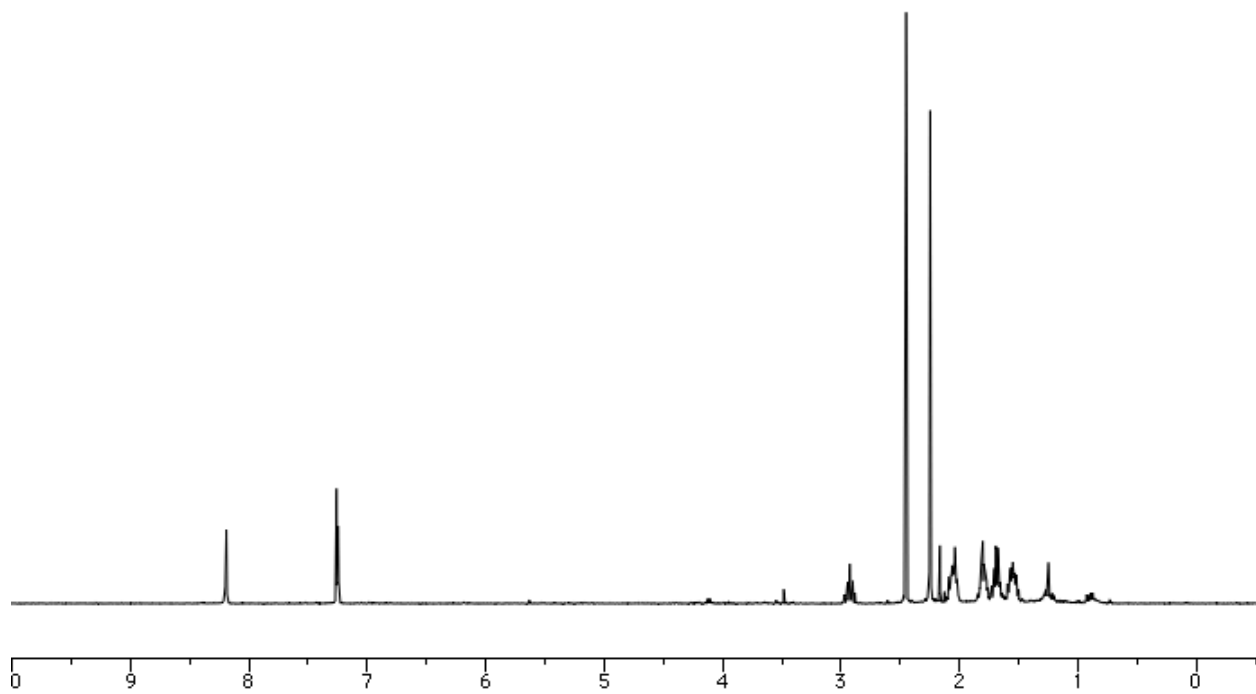
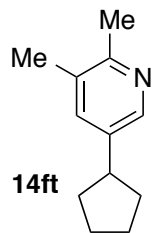
13fr

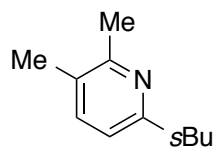




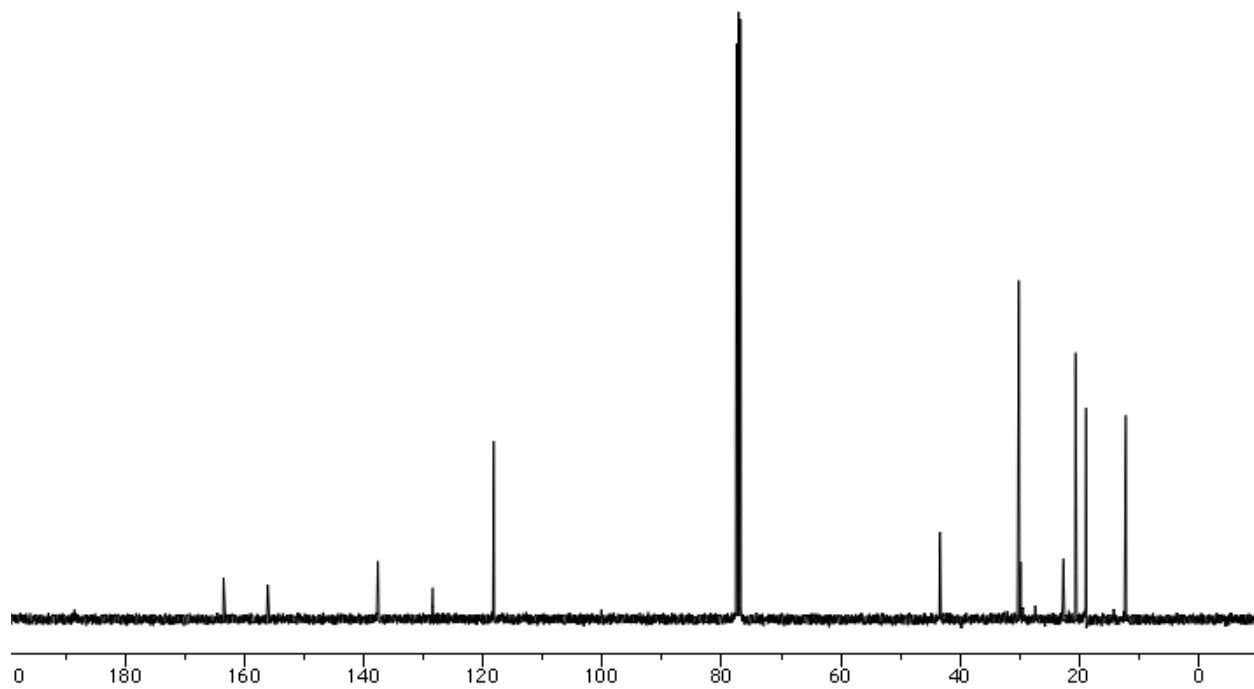
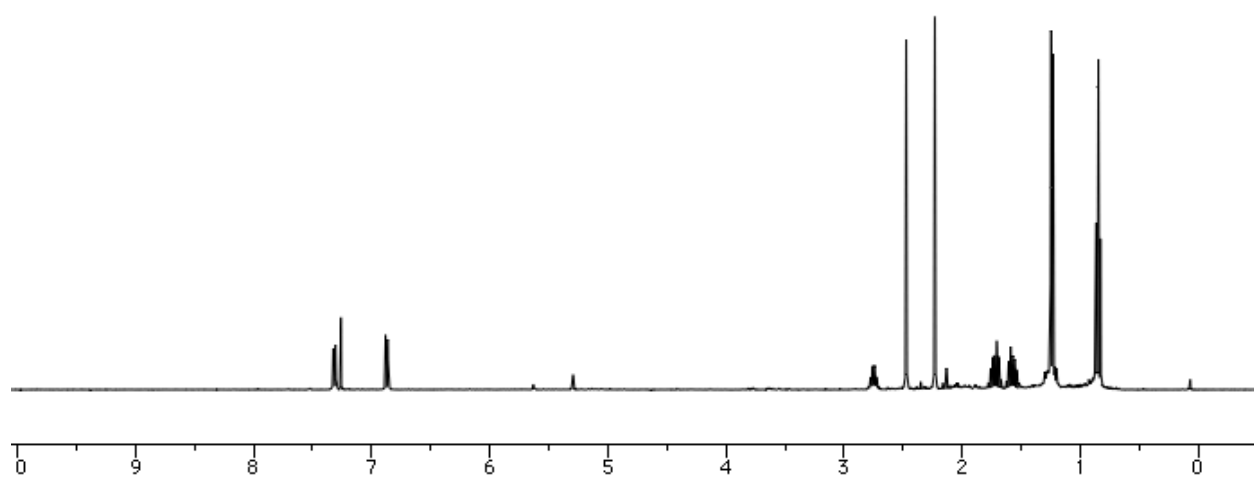


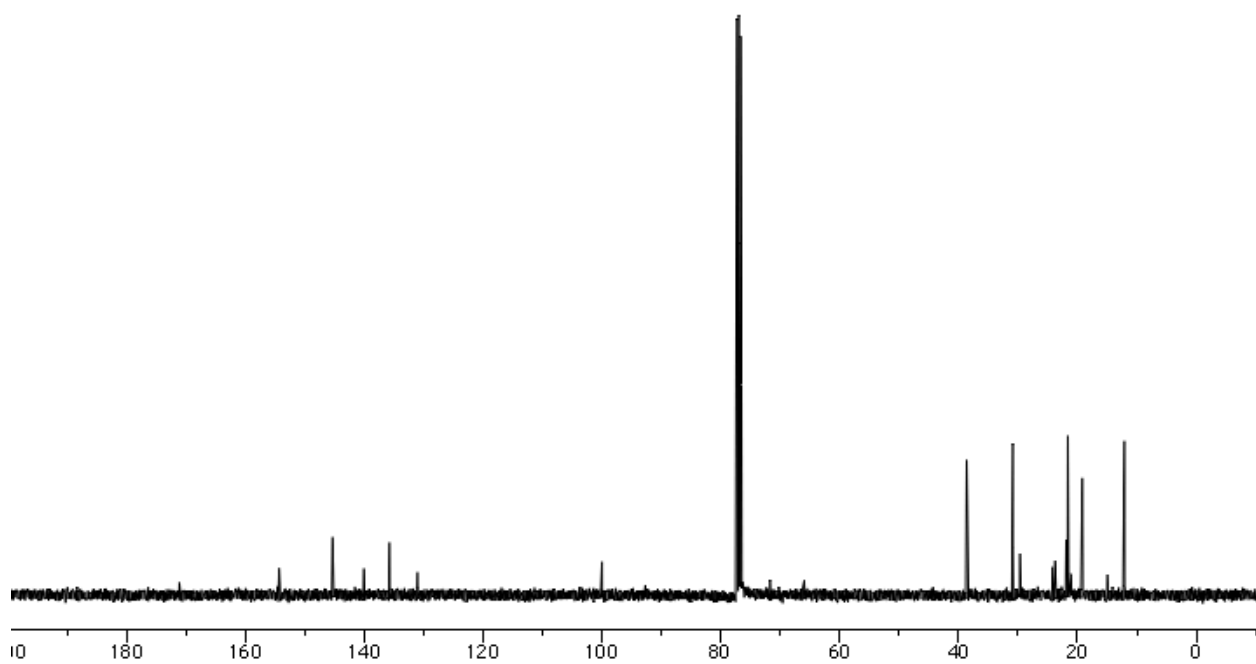
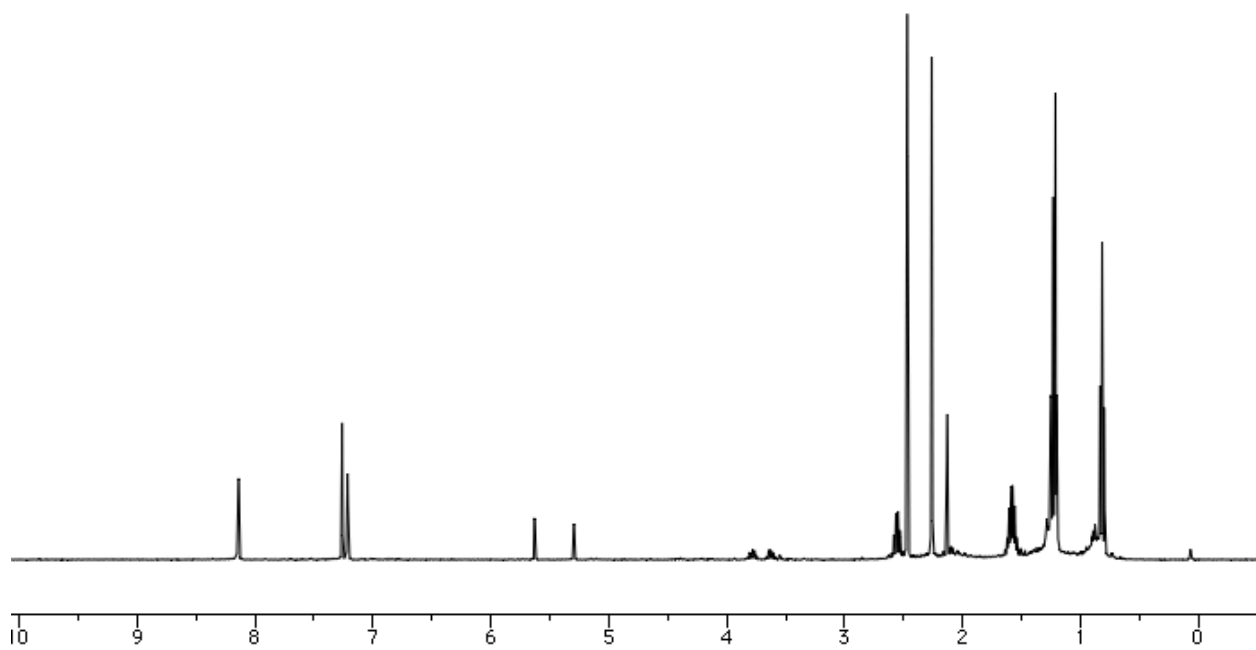
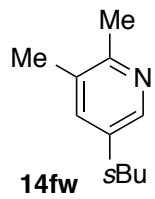


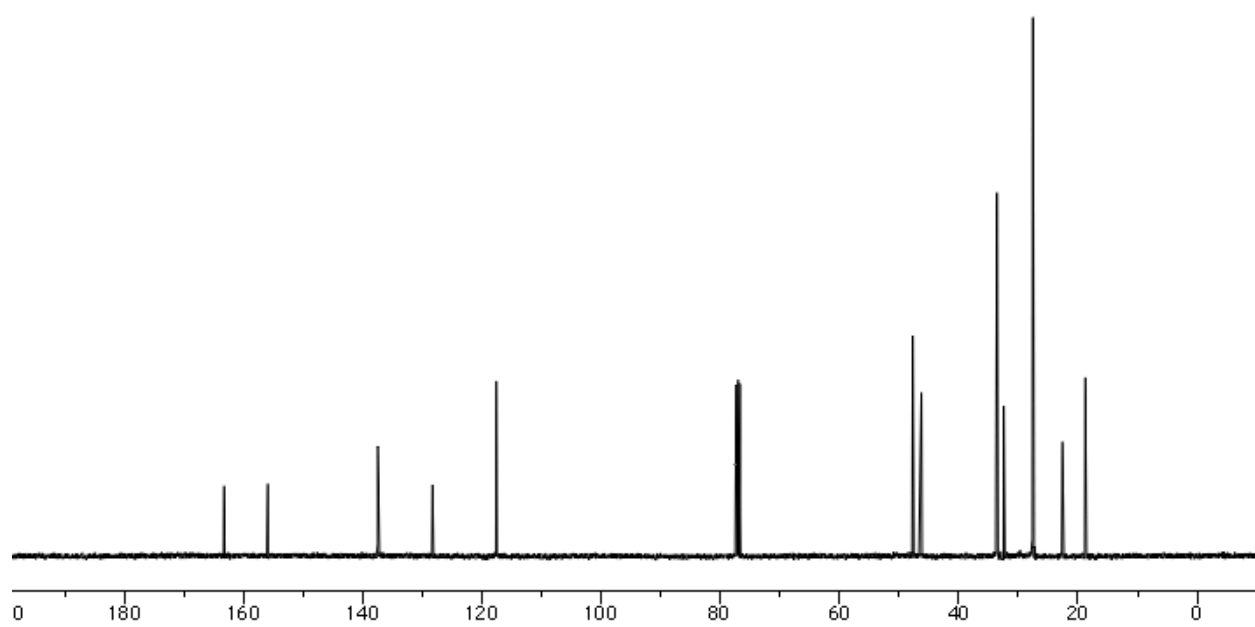
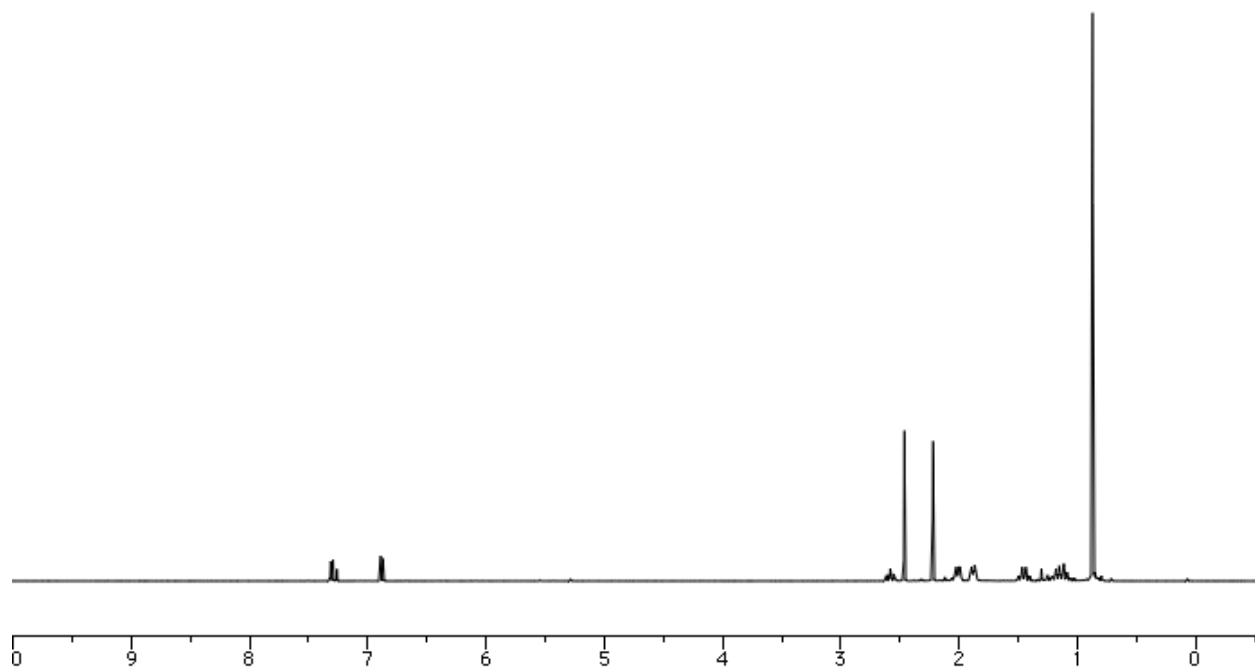
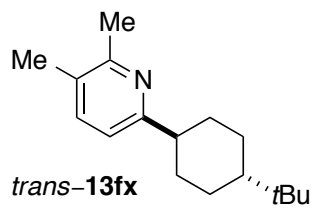




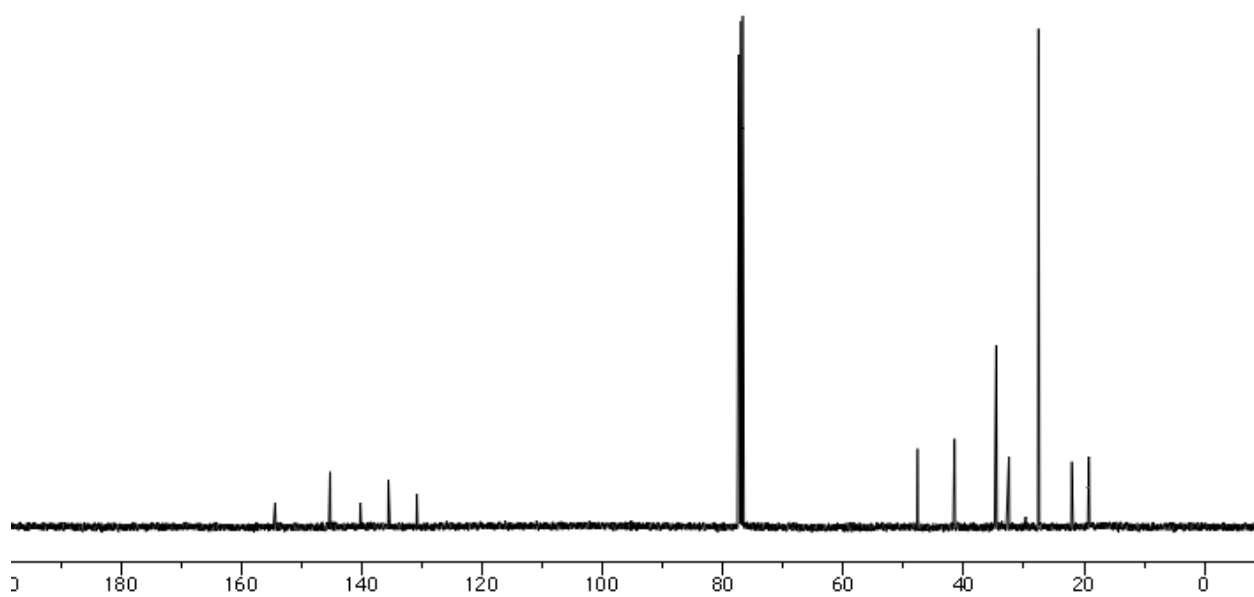
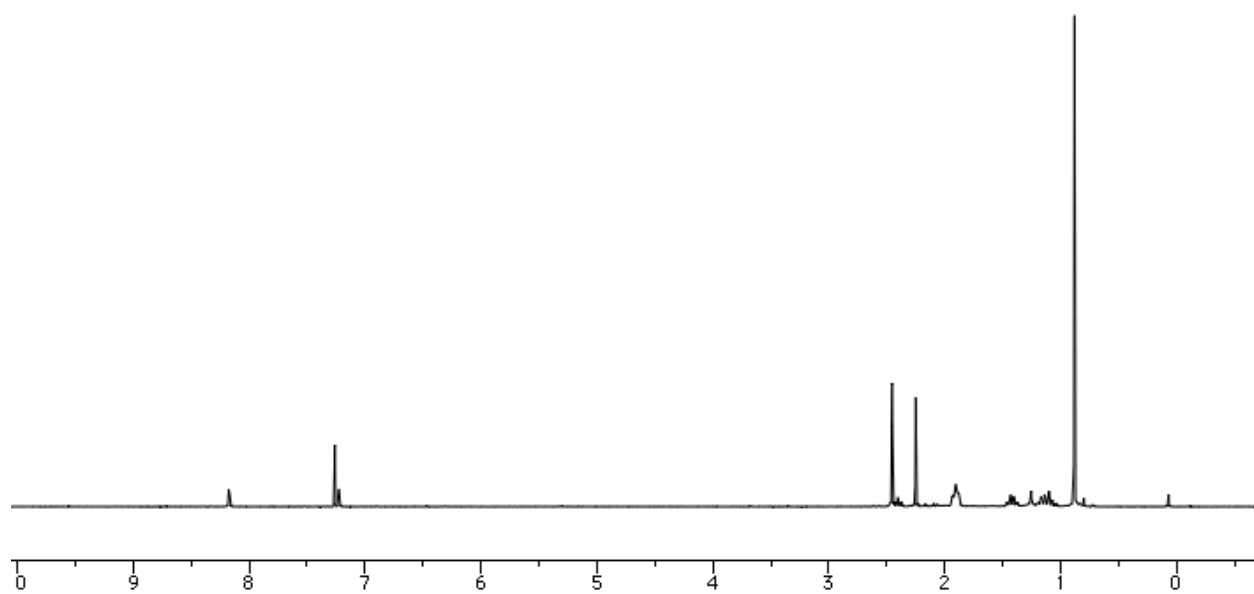
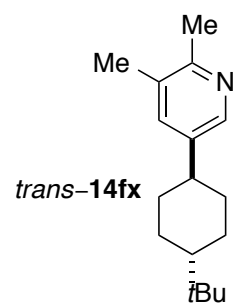
13fw

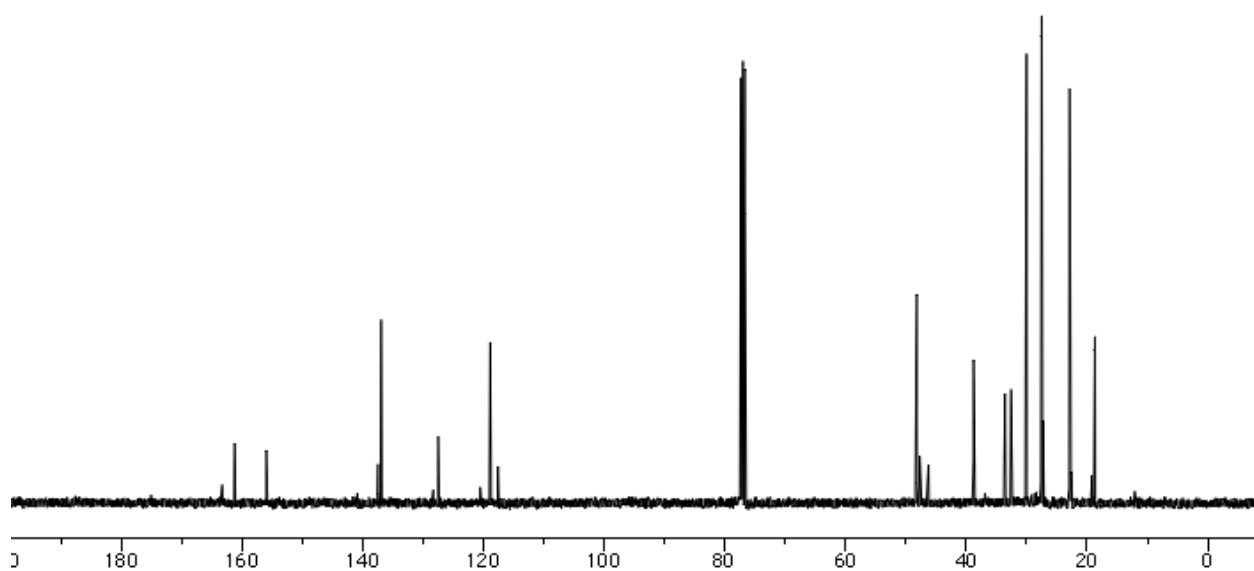
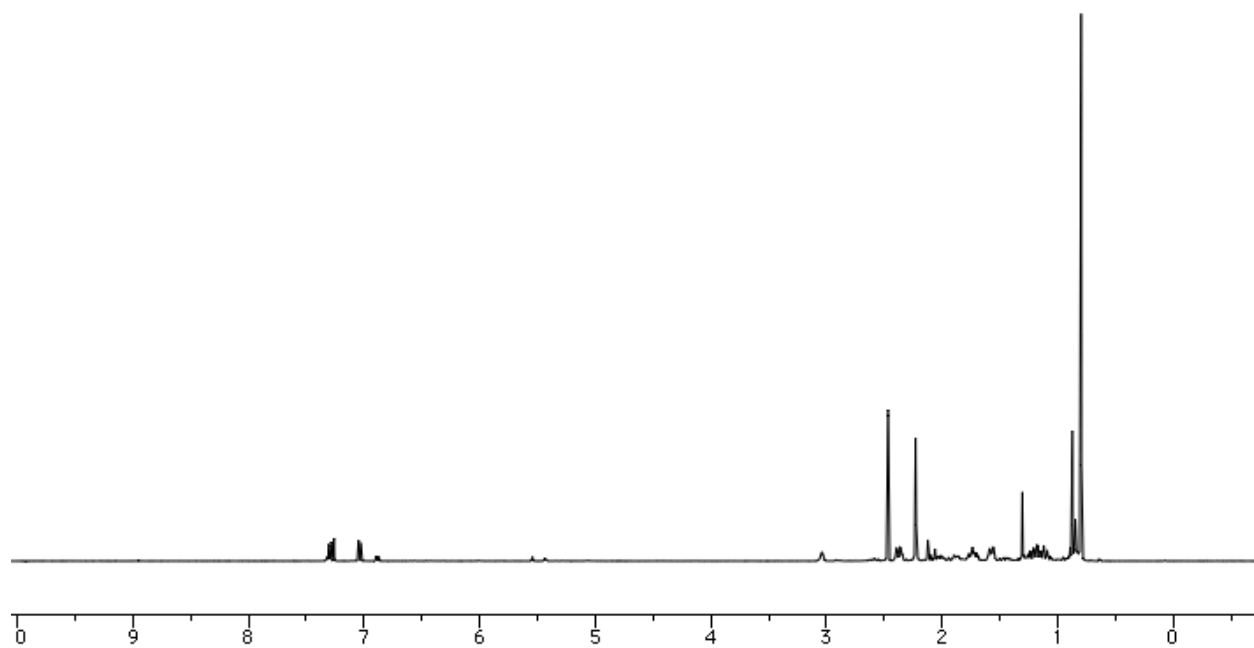
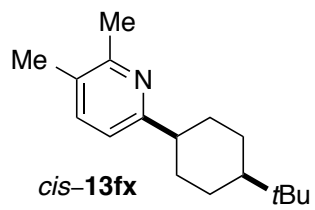


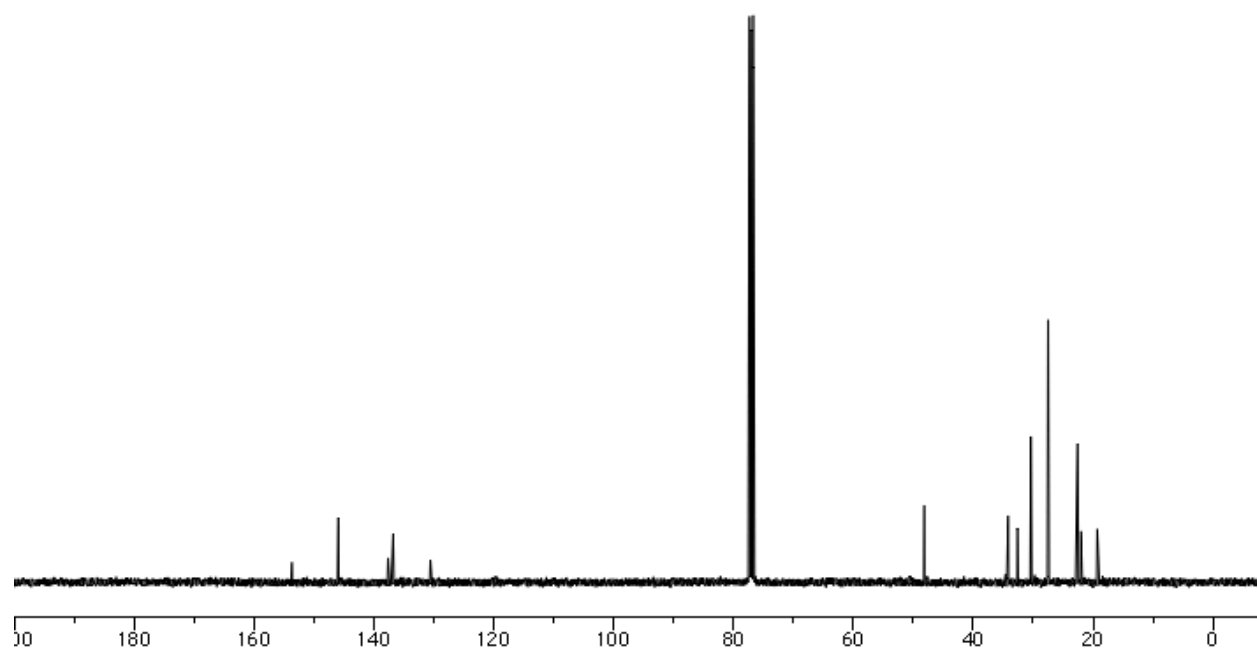
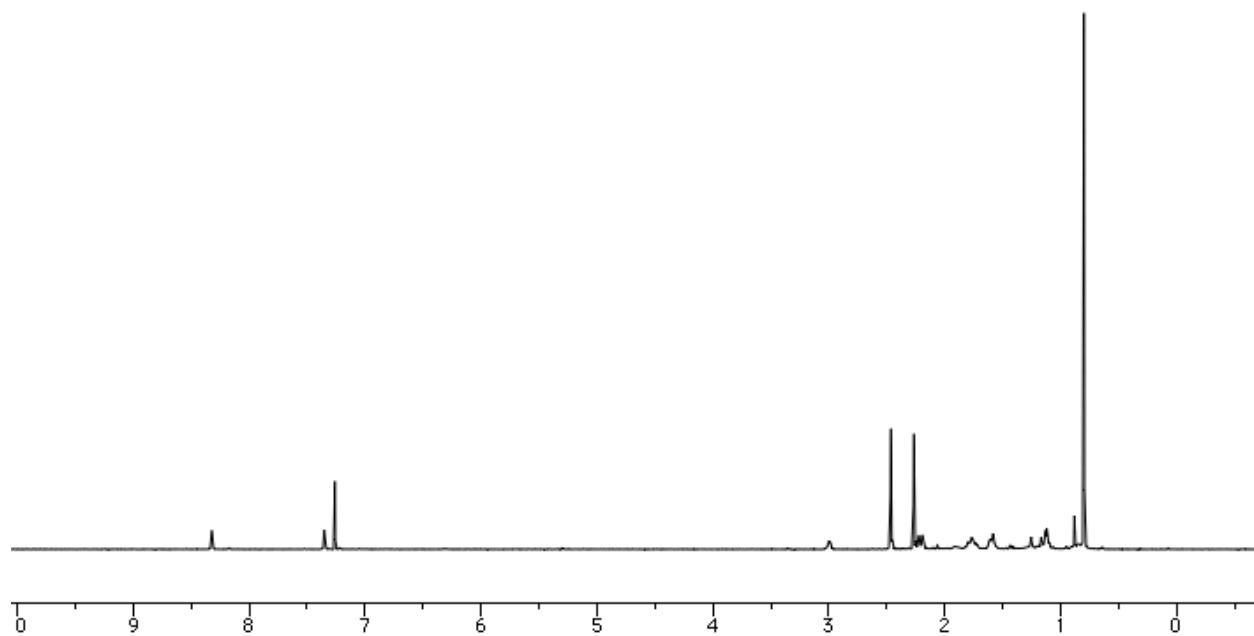
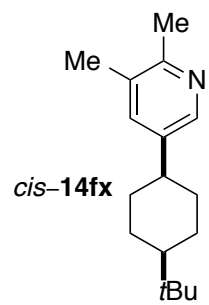


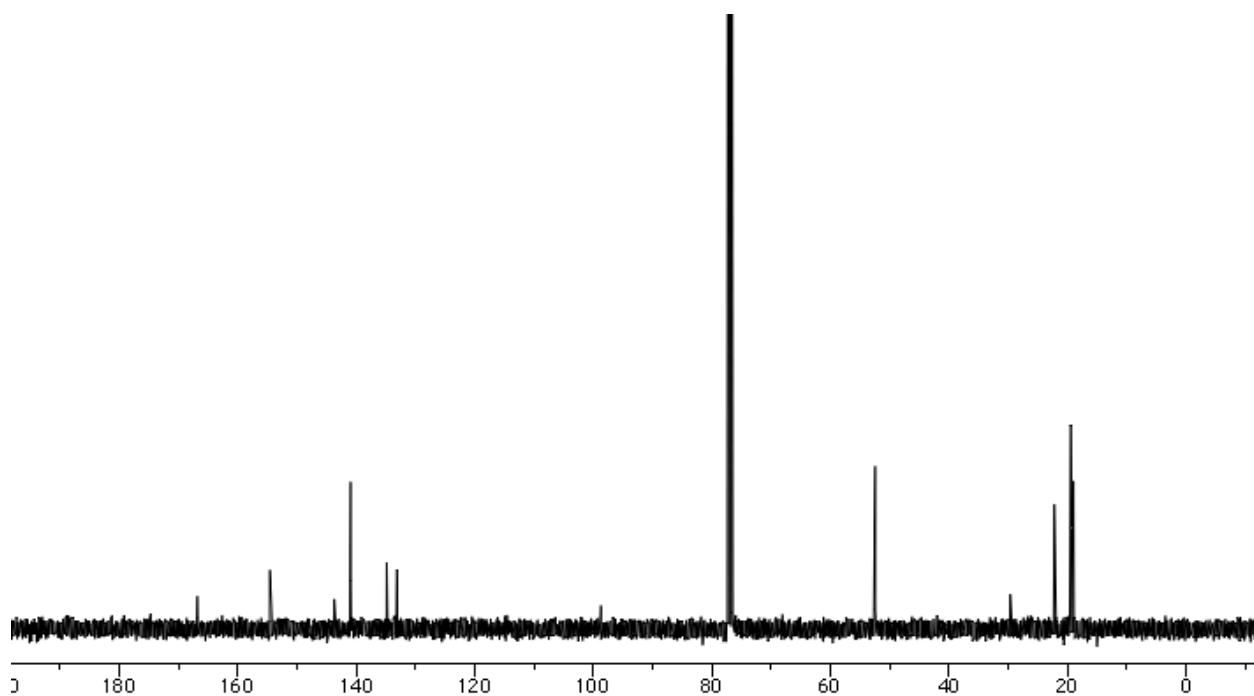
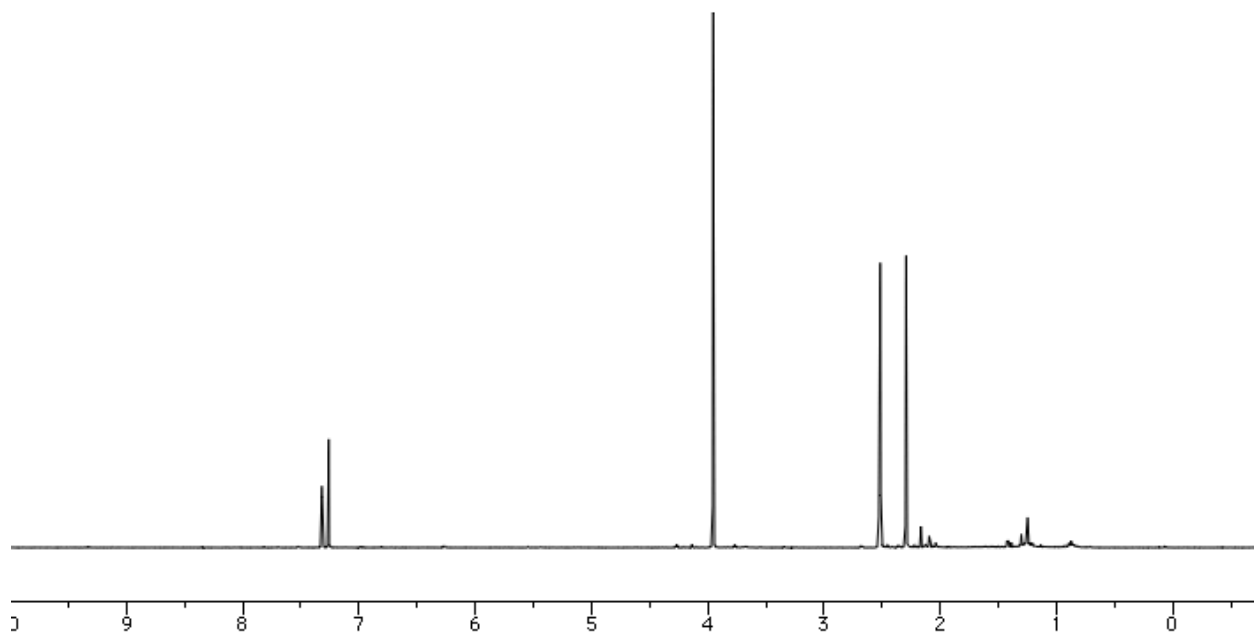
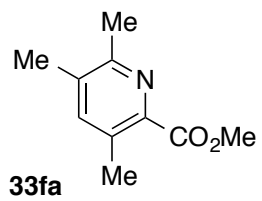


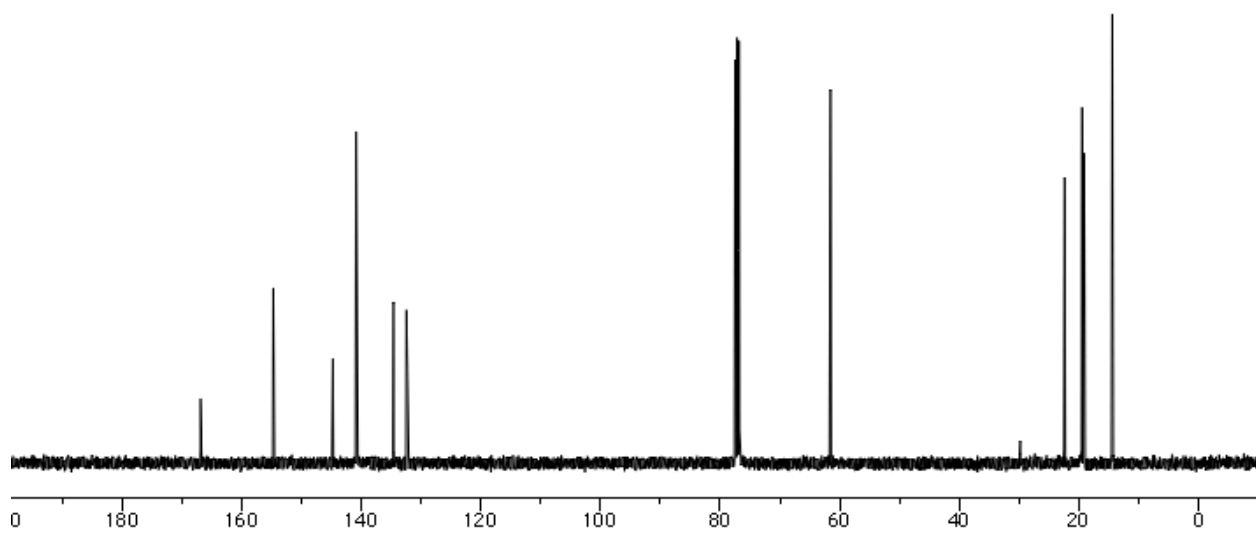
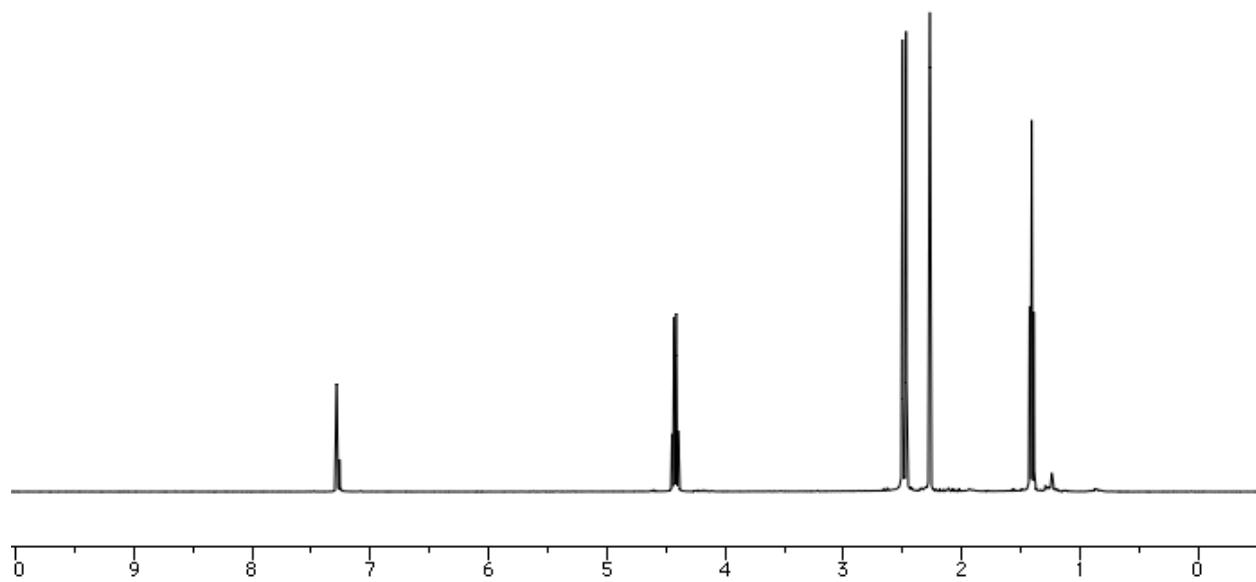
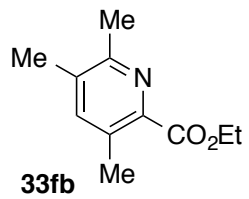


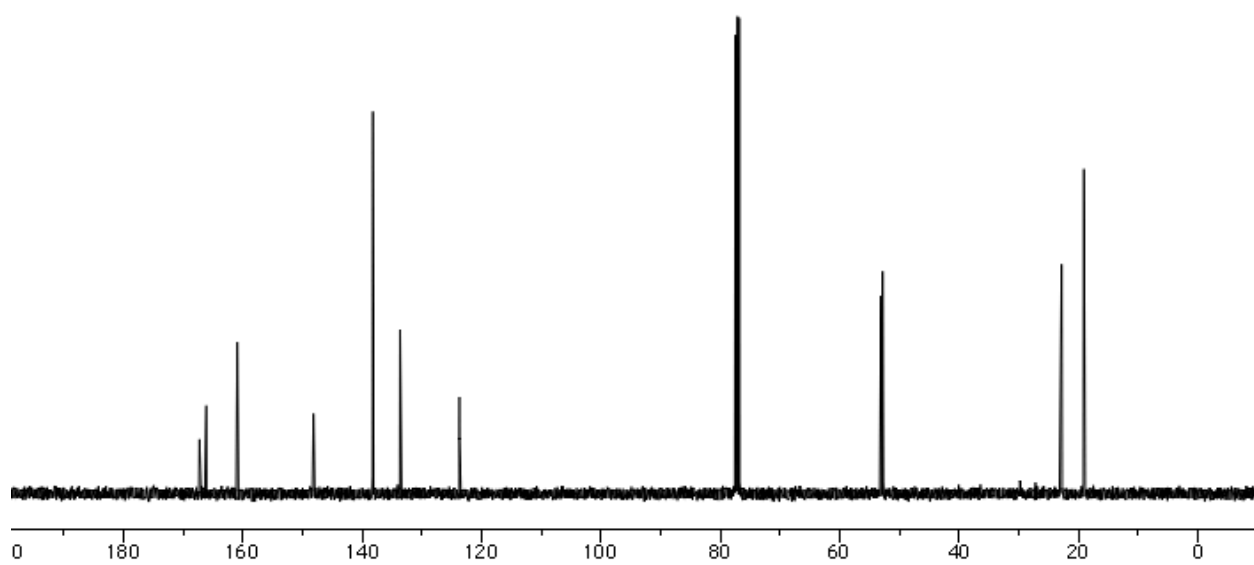
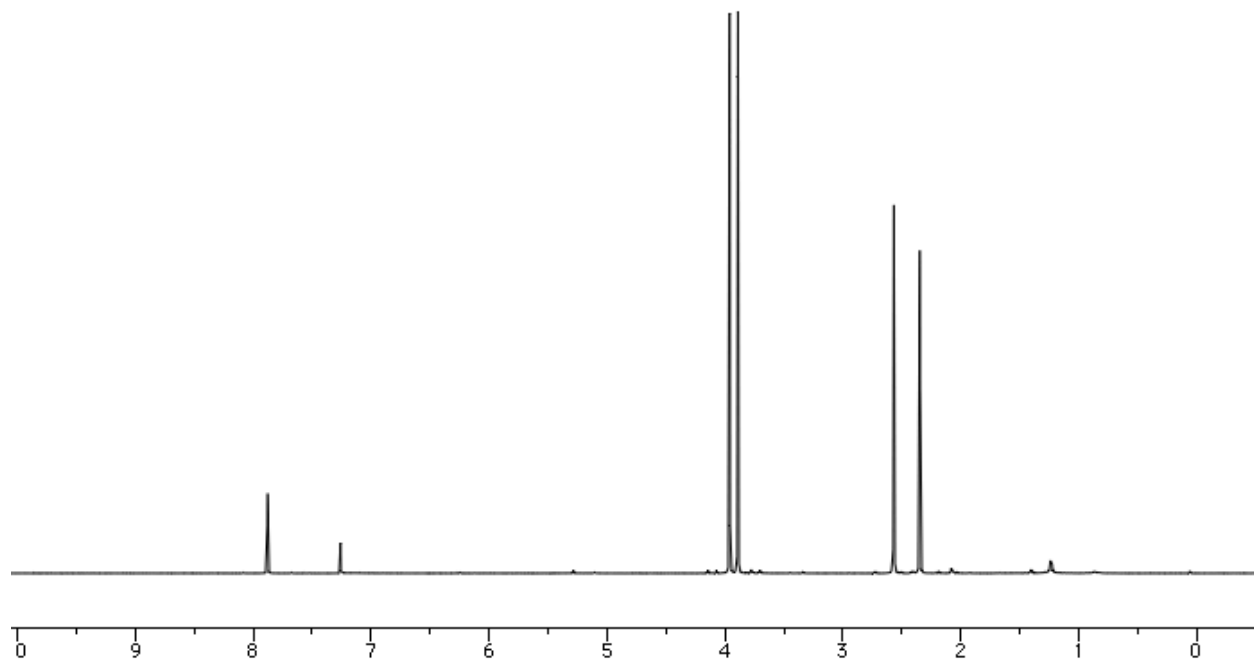
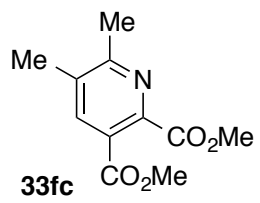


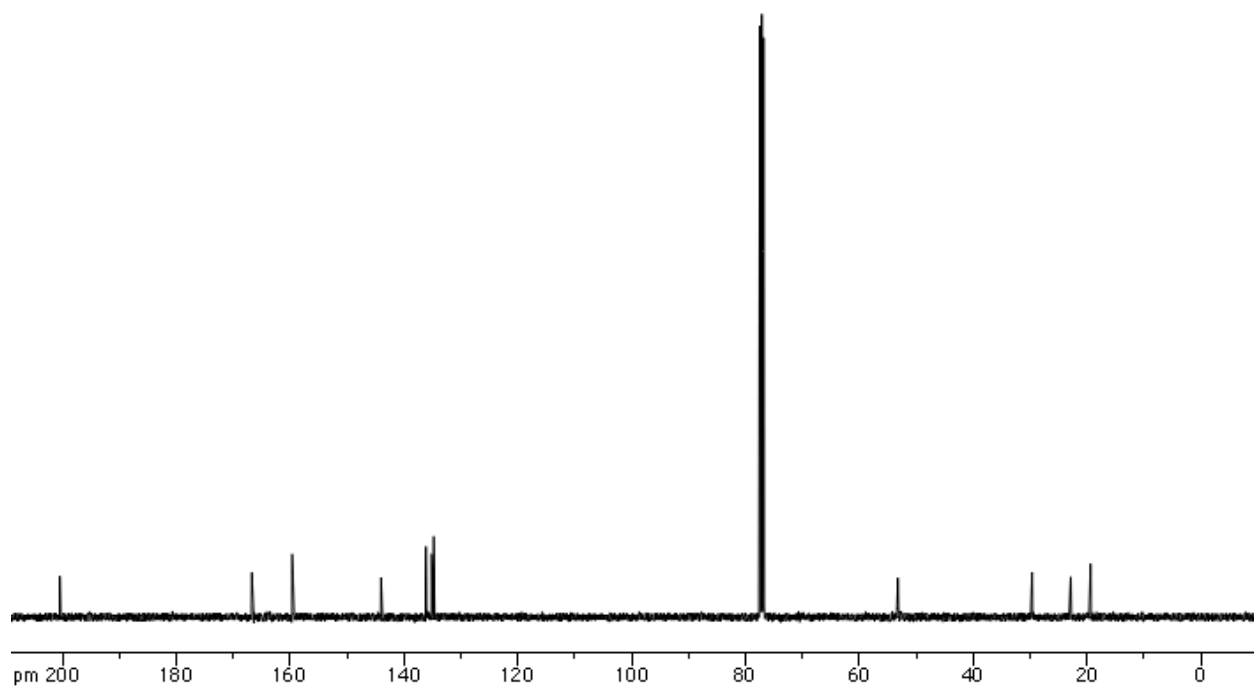
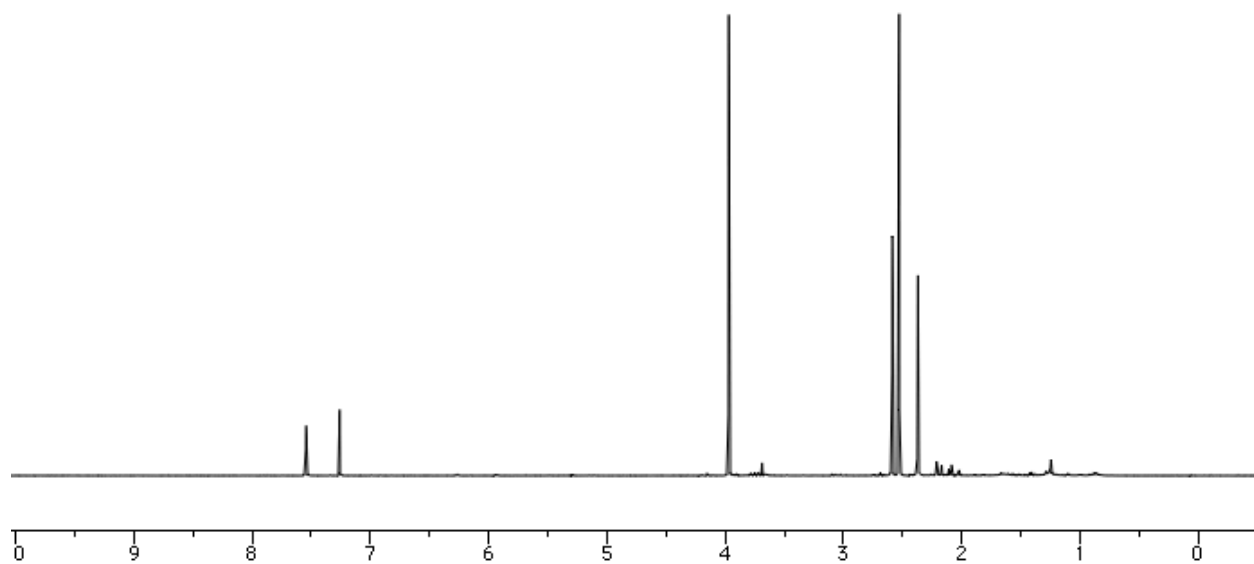
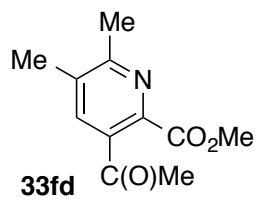


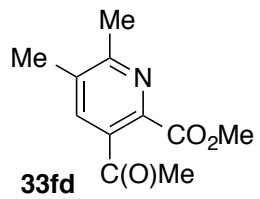




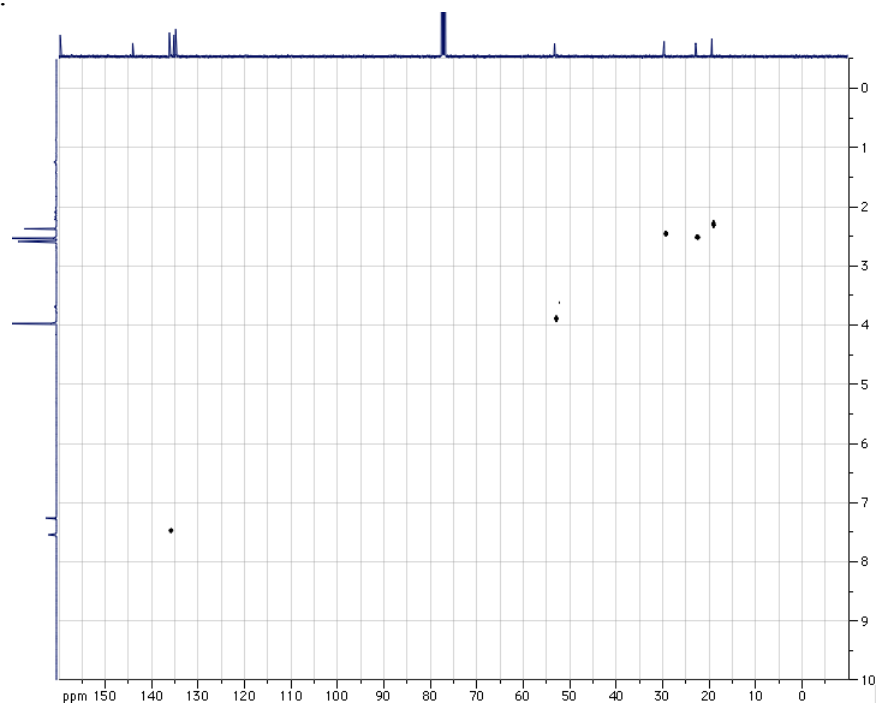




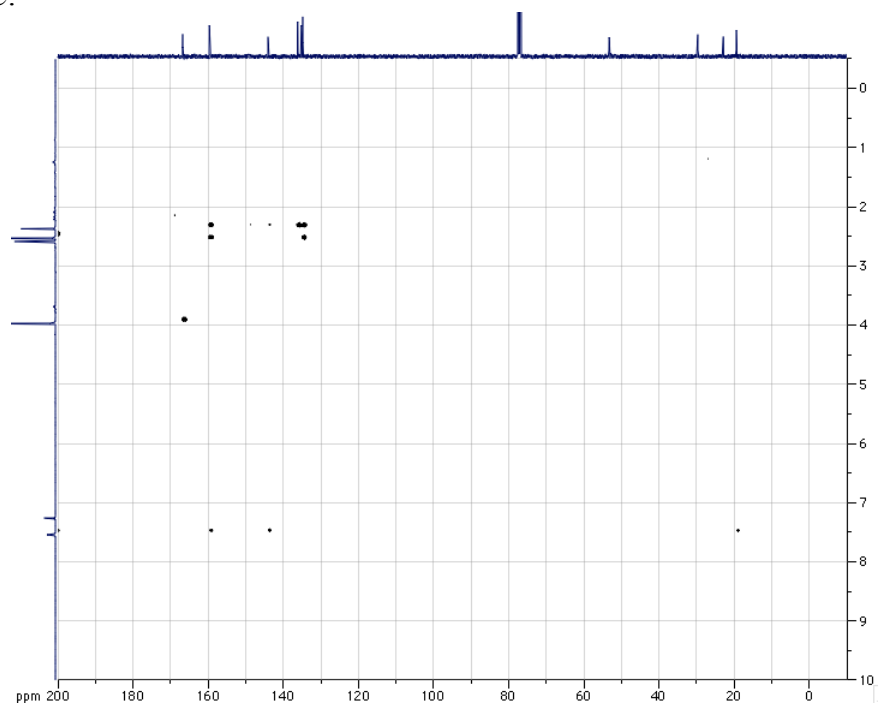




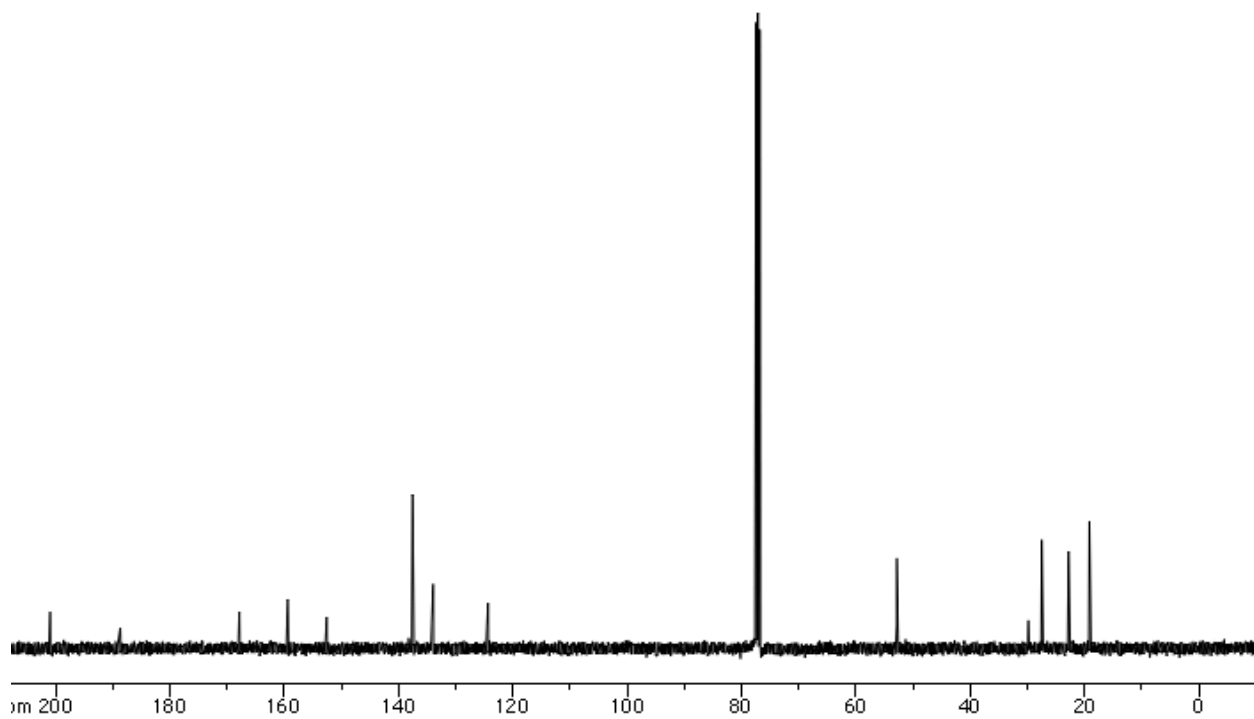
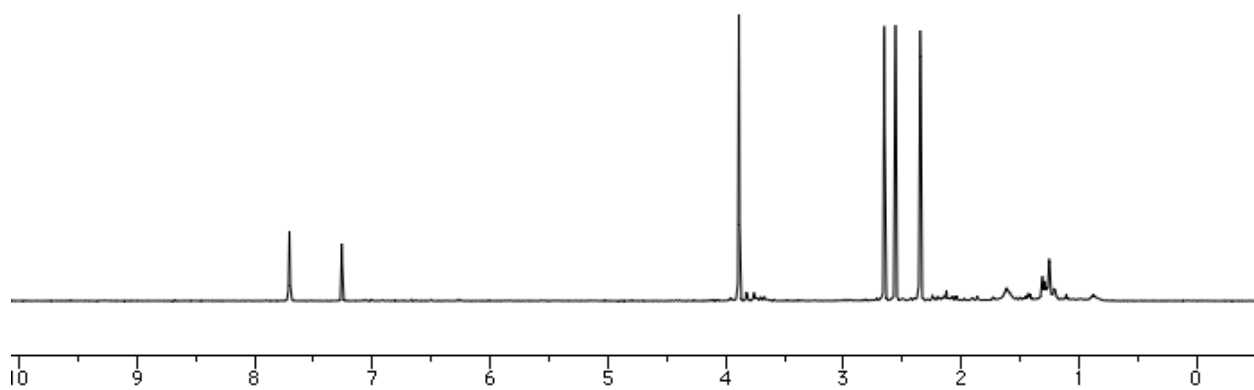
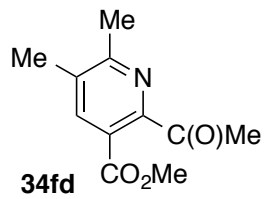
$^1\text{H}$ - $^{13}\text{C}$  HSQC:

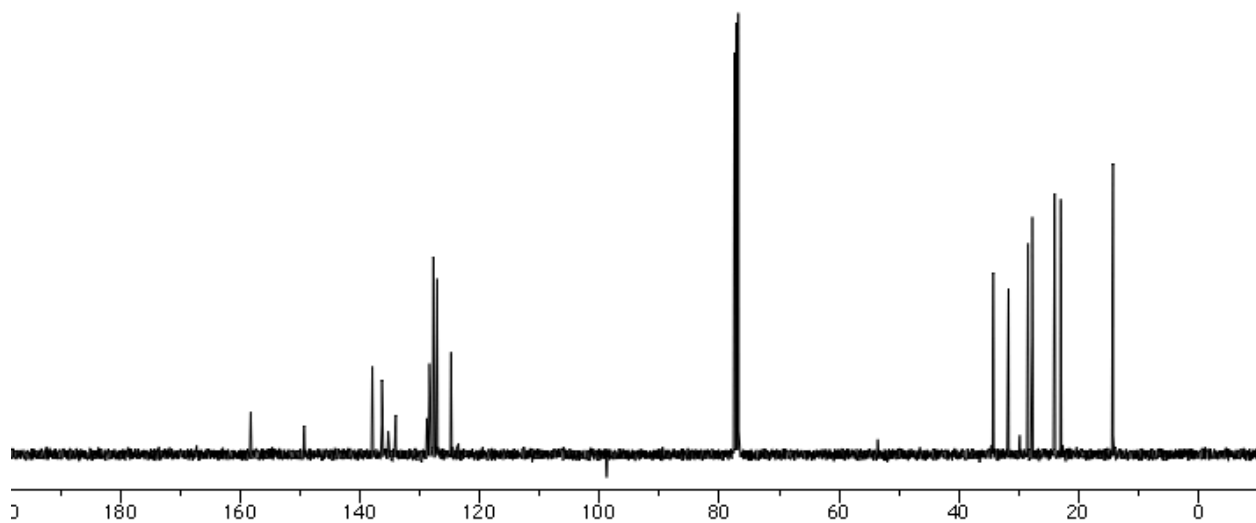
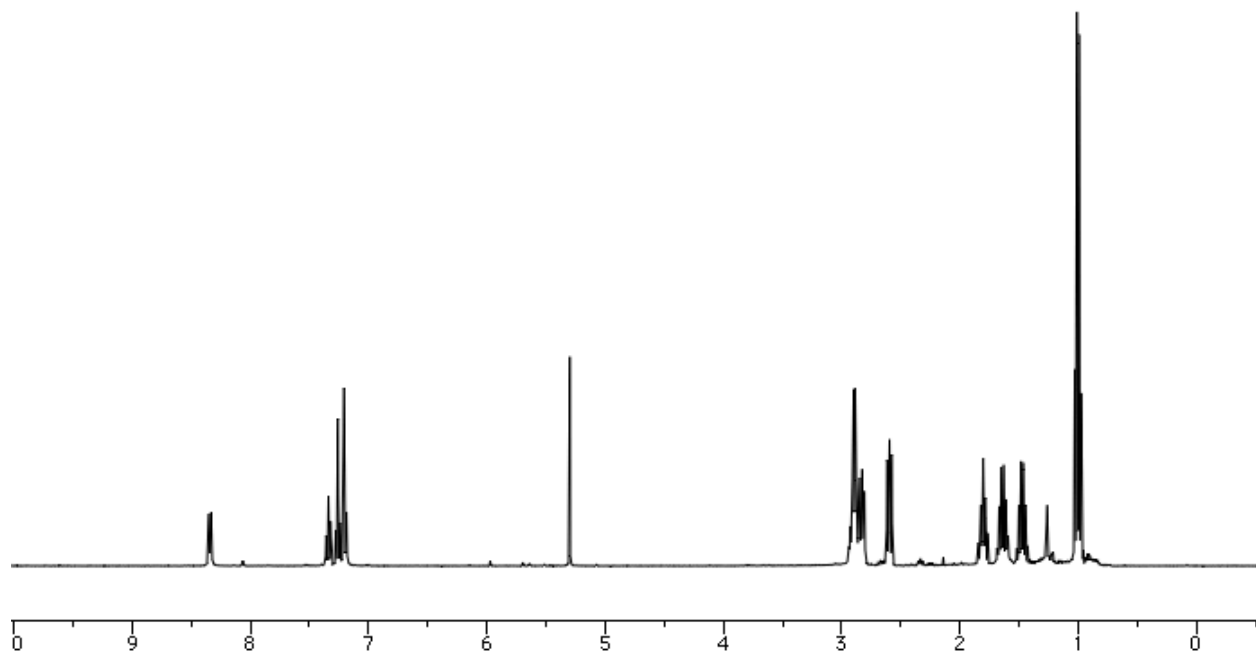
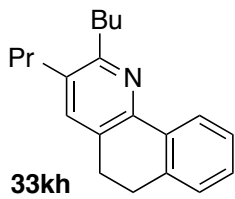


$^1\text{H}$ - $^{13}\text{C}$  HMBC:









### A.1.7 References

- 1) Cahiez, G.; Duplais, C.; Moyeux, A. *Org. Lett.* **2007**, *9*, 3253.
- 2) a) DiLabio, G. A.; Ingold, K. U.; Roydhouse, M. D.; Walton, J. C. *Org. Lett.* **2004**, *6*, 4319.  
b) Halterman, R. L.; Chen, Z.; Khan, M. A. *Organometallics* **1996**, *15*, 3957.
- 3) Rosen, T.; Taschner, M. J.; Thomas, J. A.; Heathcock, C. H. *J. Org. Chem.* **1985**, *50*, 1190.
- 4) Lewis, F. D.; Oxman, J. D.; Gibson, L. L.; Hampsch, H. L.; Quillen, S. L. *J. Am. Chem. Soc.* **1986**, *108*, 3005.
- 5) Fujita, K.; Takahashi, Y.; Owaki, M.; Yamamoto, K.; Yamaguchi, R. *Org. Lett.* **2004**, *6*, 2785.
- 6) Moser, R.; Bošković, Ž. V.; Crowe, C. S.; Lipshutz, B. H. *J. Am. Chem. Soc.* **2010**, *132*, 7852.
- 7) Ezequias, S. F. P.; Rodrigues, J. A. R.; Moran, P. J. S. *Tetrahedron-Asymmetr.* **2001**, *12*, 847.
- 8) Tan, Y.; Hartwig, J. F. *J. Am. Chem. Soc.* **2010**, *132*, 3676.
- 9) Ohashi, M.; Takeda, I.; Ikawa, M.; Ogoshi, S. *J. Am. Chem. Soc.* **2011**, *133*, 18018.
- 10) Martin, R. M.; Bergman, R. G.; Ellman, J. A. *J. Org. Chem.* **2012**, *77*, 2501.
- 11) Fujita, M.; Kim, W. H.; Fujiwara, K.; Okuyama, T. *J. Org. Chem.* **2005**, *70*, 480.
- 12) Harada, S.; Yano, H.; Obora, Y. *ChemCatChem* **2013**, *5*, 121.
- 13) RhCp\*(OAc)<sub>2</sub> was prepared by previously reported conditions with the following modifications: dichloromethane was used as the solvent at a concentration of 0.05 M for a reaction time of 48 hours. See: Boyer, P. M.; Roy, C. P.; Bielski, J. M.; Merola, J. S. *Inorg. Chim. Acta* **1996**, *245*, 7.

## APPENDIX TWO

### Rhodium(III)–Catalyzed Decarboxylative Coupling of $\alpha,\beta$ –Unsaturated Oxime Esters and Acrylic Acids: Selective Synthesis of 5–Substituted Pyridines

A.2.1 General Methods .....	144
A.2.2 General Procedure for Oxime Ester Synthesis.....	145
A.2.3 General Procedure for Pyridine Synthesis .....	146
A.2.4 Preparation of Picolinic Acid <b>22aa</b> .....	150
A.2.5 Deuterium Incorporation Study .....	151
A.2.6 Preparation and Reactions of Rhodium Complexes <b>31</b> and <b>32</b> .....	152
A.2.7 $^1\text{H}$ and $^{13}\text{C}$ NMR Spectra of New Compounds.....	154
A.2.8 Crystallographic Data for Rhodium Complex <b>29</b> .....	170
A.2.9 References.....	179

### A.2.1 General Methods

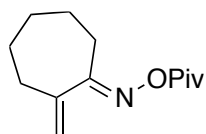
All reactions were carried out in oven-dried glassware under an atmosphere of argon with magnetic stirring. Reagent grade silver acetate and silver tosylate and ACS grade acetic acid were purchased from Sigma-Aldrich Co. and used without further purification. ACS grade potassium persulfate was purchased from Mallinckrodt Chemicals and used as received. 1,1,1,3,3,3-Hexafluoro-2-propanol was distilled from 3Å molecular sieves and dichloroethane was distilled from calcium hydride under an atmosphere of argon. 2-Pentenoic acid (**14b**) and cinnamic acid (**14e**) were purchased from Sigma-Aldrich Co. and Alfa Aesar, respectively, and used without further purification. Crotonic acid (**14a**) and acrylic acid (**16**) were distilled under reduced pressure prior to use. Methoxycinnamic acids **14f** and **14i** were recrystallized from methanol prior to use. Alkyl acrylic acids<sup>1</sup> **14c**, **14d**, **14j-n**, and **14v**, (hetero)aryl acrylic acids<sup>2</sup> **14g**, **14h**, and **14o-t**, and substrate **14u**<sup>3</sup> were synthesized according to literature procedure.  $[\text{RhCp}^*\text{Cl}_2]_2$ ,<sup>4</sup>  $\text{RhCp}^*(\text{OAc})_2$ <sup>5</sup> and  $[\text{RhCp}^{\text{CF}_3}\text{Cl}_2]_2$ <sup>6</sup> were prepared as previously reported. Column chromatography was performed on Silicycle® SilicaFlash® P60 (230–400 mesh). Thin layer chromatography was performed on Silicycle® 250µm silica gel 60A plates. Visualization was accomplished with UV light (254 nm) or potassium permanganate.

<sup>1</sup>H NMR and <sup>13</sup>C NMR spectra were collected at ambient temperature in CDCl<sub>3</sub> or CD<sub>2</sub>Cl<sub>2</sub> on a Varian 400 MHz. Chemical shifts are expressed as parts per million (δ, ppm) and are referenced to 7.26 (CHCl<sub>3</sub>) or 5.29 (CH<sub>2</sub>Cl<sub>2</sub>) for <sup>1</sup>H NMR and 77.0 (CDCl<sub>3</sub>) or 53.5 (CD<sub>2</sub>Cl<sub>2</sub>) for <sup>13</sup>C NMR. Signal data uses the following abbreviations: s = singlet, d = doublet, t = triplet, q = quartet, m = multiplet and *J* = coupling constant. Mass spectra were obtained on an Agilent Technologies 6130 Quadropole Mass Spec (LRMS). Infrared spectra were collected on a Bruker Tensor 27 FT-IR spectrometer or a Nicolet SX-60 FT-IR spectrometer.

### A.2.2 General Procedure for Oxime Ester Synthesis

*O*-Pivaloyl oxime esters **11** were generated from the corresponding  $\alpha,\beta$ -unsaturated ketones according to the following representative procedure, adapted from the literature.<sup>7</sup> Hydroxylamine hydrochloride (347 mg, 7 mmol, 1.4 equiv) and Na<sub>2</sub>CO<sub>3</sub> (742 mg, 7 mmol, 1.4 equiv) were added to the enone (5 mmol) in 15 mL MeOH and the mixture was stirred at 65 °C for 1 hour (or room temperature for 3 hours in the case of **11c**). The solvent was removed *in vacuo* and the resulting residue was dissolved in 10 mL CH<sub>2</sub>Cl<sub>2</sub> and cooled to 0 °C. After the addition of Et<sub>3</sub>N (1.74 mL, 12.5 mmol, 2.5 equiv), a solution of pivaloyl chloride (1.23 mL, 10 mmol, 2 equiv) in 5 mL CH<sub>2</sub>Cl<sub>2</sub> was added dropwise at 0 °C. The mixture was stirred at room temperature overnight and quenched with water. The aqueous layer was extracted with CH<sub>2</sub>Cl<sub>2</sub> three times and the combined organic layers were washed with saturated NaHCO<sub>3</sub> and brine, dried over MgSO<sub>4</sub>, filtered and concentrated *in vacuo*. The crude product was purified by flash column chromatography.

Compounds **11a–c** and **11e** were characterized in our previous report.<sup>8</sup>



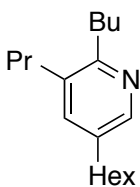
**(E)-2-methylenecycloheptanone O-pivaloyl oxime (11d).** Colorless liquid.

$R_f = 0.15$  (10:1 hexanes/EtOAc). <sup>1</sup>H NMR (400 MHz, CDCl<sub>3</sub>)  $\delta$  5.48 (d,  $J = 1.6$  Hz, 1H), 5.06 (d,  $J = 1.6$  Hz, 1H), 2.64 (m, 2H), 2.38 (m, 2H), 1.64 (m, 6H), 1.28 (s, 9H). <sup>13</sup>C NMR (100 MHz, CDCl<sub>3</sub>)  $\delta$  175.0, 170.9, 144.3, 117.2, 38.8, 34.9, 30.6, 29.4, 28.9, 27.3, 25.3. IR (NaCl, thin film)  $\nu$  2928, 1755, 1479, 1270, 1099, 1026, 882 cm<sup>-1</sup>. LRMS (ESI)  $m/z$  [M+H] calcd 447.3, found 447.6.

### A.2.3 General Procedure for Pyridine Synthesis

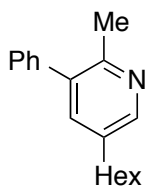
A 0.5 dram vial was charged with oxime ester **11** (0.21 mmol), AgOTs (52.7 mg, 0.189 mmol, 0.9 equiv) and K<sub>2</sub>S<sub>2</sub>O<sub>8</sub> (59.6 mg, 0.221 mmol, 1.05 equiv) and a solution of [RhCp<sup>CF<sub>3</sub></sup>Cl<sub>2</sub>]<sub>2</sub> (3.8 mg, 0.005 mmol, 0.025 equiv) and alkene **14** (0.252 mmol, 1.2 equiv) in 0.7 mL HFIP was added. The vial was flushed with argon, sealed and heated at 58 °C in an aluminum heating block for 12 hours. In the event that an observable amount of **11** remained after 12 hours, the mixture was heated at 100 °C until it was consumed. The mixture was diluted with CH<sub>2</sub>Cl<sub>2</sub> and washed with 1M aqueous NaOH. The aqueous layer was extracted twice with CH<sub>2</sub>Cl<sub>2</sub> and the combined organic layers were dried over MgSO<sub>4</sub>, filtered and concentrated *in vacuo*. The residue was dissolved in EtOAc and passed through a short plug of silica to provide analytically pure product.

Compounds **15bj** and **15bm** were characterized in our previous report.<sup>8</sup> Compounds **15bd** and **15be** were characterized by Ellman and coworkers.<sup>9</sup> Compound **17c** was characterized by Craig and coworkers.<sup>10</sup>



**2-Butyl-5-hexyl-3-propylpyridine (15aj).** Yellow viscous liquid.  $R_f = 0.61$  (3:1 hexanes/EtOAc). <sup>1</sup>H NMR (400 MHz, CDCl<sub>3</sub>)  $\delta$  8.17 (d,  $J = 2.0$  Hz, 1H), 7.21 (d,  $J = 1.6$  Hz, 1H), 2.74 (m, 2H), 2.54 (m, 4H), 1.69–1.53 (m, 6H), 1.41 (m, 2H), 1.34–1.25 (m, 6H), 0.96 (m, 6H), 0.87 (t,  $J = 6.4$  Hz, 3H).

<sup>13</sup>C NMR (100 MHz, CDCl<sub>3</sub>)  $\delta$  157.4, 146.4, 136.9, 135.1, 134.7, 34.2, 34.2, 32.6, 32.0, 31.6, 31.2, 28.9, 23.9, 22.9, 22.6, 14.0, 14.0. IR (NaCl, thin film)  $\nu$  2959, 1562, 1459, 1378, 1287, 1183, 1102 cm<sup>-1</sup>. LRMS (ESI + APCI)  $m/z$  [M+H] calcd 262.3, found 262.8.



**5-hexyl-2-methyl-3-phenylpyridine (15cj).** Yellow orange viscous

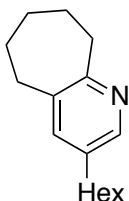
liquid.  $R_f = 0.42$  (3:1 hexanes/EtOAc).  $^1\text{H NMR}$  (400 MHz,  $\text{CDCl}_3$ )  $\delta$  8.32 (d,  $J = 2.0$  Hz, 1H), 7.45–7.31 (m, 6H), 2.61 (t,  $J = 7.6$  Hz, 2H), 2.47 (s, 3H),

1.62 (m, 2H), 1.37–1.26 (m, 6H), 0.88 (t,  $J = 6.8$  Hz, 3H).  $^{13}\text{C NMR}$  (100

MHz,  $\text{CDCl}_3$ )  $\delta$  152.9, 147.8, 140.1, 137.3, 136.5, 135.3, 129.0, 128.3, 127.3, 32.5, 31.6, 31.4,

28.8, 22.8, 22.5, 14.0. IR (NaCl, thin film)  $\nu$  2928, 2857, 1459, 1183, 1027, 909, 702  $\text{cm}^{-1}$ .

LRMS (ESI + APCI)  $m/z$  [M+H] calcd 254.2, found 254.7.



**3-Hexyl-6,7,8,9-tetrahydro-5H-cyclohepta[b]pyridine (15dj).** Yellow

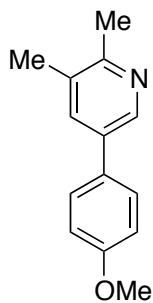
viscous liquid.  $R_f = 0.38$  (3:1 hexanes/EtOAc).  $^1\text{H NMR}$  (400 MHz,  $\text{CDCl}_3$ )

$\delta$  8.08 (d,  $J = 1.6$  Hz, 1H), 7.18 (d,  $J = 2.0$  Hz, 1H), 2.99 (m, 2H), 2.73 (m, 2H), 2.52 (t,  $J = 7.6$  Hz, 2H), 1.85 (m, 2H), 1.70–1.54 (m, 6H), 1.34–1.25

(m, 6H), 0.87 (t,  $J = 6.4$  Hz, 3H).  $^{13}\text{C NMR}$  (100 MHz,  $\text{CDCl}_3$ )  $\delta$  160.3, 145.5, 137.7, 136.8,

135.4, 38.7, 35.3, 32.5, 31.6, 31.1, 28.9, 28.0, 26.5, 22.6, 14.0. IR (NaCl, thin film)  $\nu$  2926,

2855, 1468, 1287, 1182, 958  $\text{cm}^{-1}$ . LRMS (ESI + APCI)  $m/z$  [M+H] calcd 232.2, found 232.7.



**5-(4-Methoxyphenyl)-2,3-dimethylpyridine (15bf).** Yellow orange

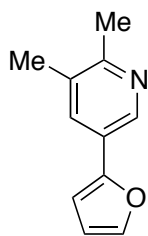
viscous liquid.  $R_f = 0.34$  (1:1 hexanes/EtOAc).  $^1\text{H NMR}$  (400 MHz,  $\text{CDCl}_3$ )  $\delta$  8.51 (s, 1H), 7.56 (s, 1H), 7.49 (d,  $J = 8.0$  Hz, 2H), 6.99 (d,  $J = 8.4$  Hz, 2H), 3.85 (s, 3H), 2.53 (s, 3H), 2.33 (s, 3H).  $^{13}\text{C NMR}$  (100 MHz,  $\text{CDCl}_3$ )  $\delta$

159.4, 155.2, 144.3, 135.3, 134.0, 131.2, 130.4, 128.0, 114.4, 55.3, 22.1,

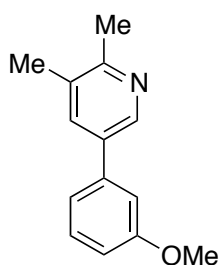
19.2. IR (NaCl, thin film)  $\nu$  2936, 1610, 1516, 1470, 1387, 1287, 1249, 1180, 1112, 1033, 830

$\text{cm}^{-1}$ . LRMS (ESI + APCI)  $m/z$  [M+H] calcd 214.1, found 214.1.

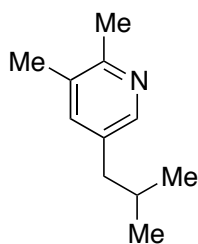




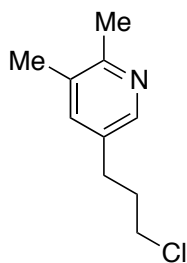
**5-(Furan-2-yl)-2,3-dimethylpyridine (15bh).** Yellow orange viscous liquid.  $R_f = 0.48$  (1:1 hexanes/EtOAc).  $^1\text{H NMR}$  (400 MHz,  $\text{CDCl}_3$ )  $\delta$  8.64 (d,  $J = 2.0$  Hz, 1H), 7.71 (d,  $J = 1.2$  Hz, 1H), 7.49 (d,  $J = 1.6$  Hz, 1H), 6.68 (d,  $J = 3.2$  Hz, 1H), 6.48 (dd,  $J = 3.2$  Hz, 1.6 Hz, 1H), 2.53 (s, 3H), 2.33 (s, 3H).  $^{13}\text{C NMR}$  (100 MHz,  $\text{CDCl}_3$ )  $\delta$  155.4, 151.1, 142.6, 141.3, 132.6, 131.7, 125.0, 111.7, 105.8, 21.9, 19.1. IR (NaCl, thin film)  $\nu$  2922, 1684, 1596, 1401, 1143, 1017, 885, 735  $\text{cm}^{-1}$ . LRMS (ESI + APCI)  $m/z$  [M+H] calcd 174.1, found 174.5.



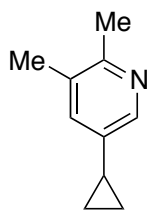
**5-(3-Methoxyphenyl)-2,3-dimethylpyridine (15bi).** Yellow viscous liquid.  $R_f = 0.37$  (1:1 hexanes/EtOAc).  $^1\text{H NMR}$  (400 MHz,  $\text{CDCl}_3$ )  $\delta$  8.55 (d,  $J = 2.0$  Hz, 1H), 7.59 (d,  $J = 2.0$  Hz, 1H), 7.36 (t,  $J = 8.0$  Hz, 1H), 7.14 (d,  $J = 7.6$  Hz, 1H), 7.08 (t,  $J = 2.4$  Hz, 1H), 6.91 (dd,  $J = 8.0$  Hz, 2.4 Hz, 1H), 3.86 (s, 3H), 2.54 (s, 3H), 2.34 (s, 3H).  $^{13}\text{C NMR}$  (100 MHz,  $\text{CDCl}_3$ )  $\delta$  160.0, 154.0, 144.6, 139.4, 135.7, 134.1, 131.3, 130.0, 119.4, 113.0, 112.7, 55.3, 22.2, 19.2. IR (NaCl, thin film)  $\nu$  2941, 1583, 1471, 1387, 1285, 1219, 1046, 870, 827, 781, 730, 697  $\text{cm}^{-1}$ . LRMS (ESI + APCI)  $m/z$  [M+H] calcd 214.1, found 214.6.



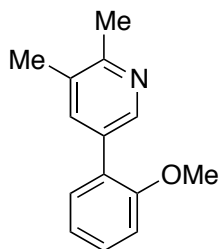
**5-Isobutyl-2,3-dimethylpyridine (15bk).** Pale yellow viscous liquid.  $R_f = 0.33$  (1:1 hexanes/EtOAc).  $^1\text{H NMR}$  (400 MHz,  $\text{CDCl}_3$ )  $\delta$  8.10 (d,  $J = 1.6$  Hz, 1H), 7.19 (d,  $J = 1.2$  Hz, 1H), 2.46 (s, 3H), 2.40 (d,  $J = 7.2$  Hz, 2H), 2.25 (s, 3H), 1.82 (m, 1H), 0.89 (d,  $J = 6.8$  Hz).  $^{13}\text{C NMR}$  (100 MHz,  $\text{CDCl}_3$ )  $\delta$  154.2, 146.7, 138.0, 134.2, 130.8, 41.8, 30.0, 22.2, 21.9, 19.1. IR (NaCl, thin film)  $\nu$  2957, 2870, 1475, 1412, 1214, 1001, 900, 723  $\text{cm}^{-1}$ . LRMS (ESI + APCI)  $m/z$  [M+H] calcd 164.1, found 164.5.



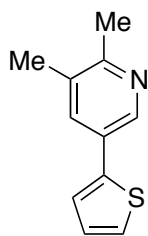
**5-(3-Chloropropyl)-2,3-dimethylpyridine (15bl).** Pale yellow viscous liquid.  $R_f = 0.25$  (1:1 hexanes/EtOAc).  $^1\text{H NMR}$  (400 MHz,  $\text{CDCl}_3$ )  $\delta$  8.16 (s, 1H), 7.24 (s, 1H), 3.51 (t,  $J = 6.4$  Hz, 2H), 2.71 (t,  $J = 7.2$  Hz, 2H), 2.46 (s, 3H), 2.25 (s, 3H), 2.05 (m, 2H).  $^{13}\text{C NMR}$  (100 MHz,  $\text{CDCl}_3$ )  $\delta$  154.8, 146.1, 137.5, 133.3, 131.2, 43.9, 33.7, 29.3, 22.0, 19.1. IR (NaCl, thin film)  $\nu$  2922, 1476, 1444, 1413, 1286, 1213, 1182, 731, 706  $\text{cm}^{-1}$ . LRMS (ESI + APCI)  $m/z$  [M+H] calcd 184.1, found 184.5.



**5-Cyclopropyl-2,3-dimethylpyridine (15bn).** Pale yellow viscous liquid.  $R_f = 0.34$  (1:1 hexanes/EtOAc).  $^1\text{H NMR}$  (400 MHz,  $\text{CDCl}_3$ )  $\delta$  8.11 (s, 1H), 7.04 (s, 1H), 2.44 (s, 3H), 2.22 (s, 3H), 1.82 (m, 1H), 0.96 (m, 2H), 0.65 (m, 2H).  $^{13}\text{C NMR}$  (100 MHz,  $\text{CDCl}_3$ )  $\delta$  153.7, 144.3, 136.8, 134.4, 131.1, 21.6, 19.1, 12.5, 8.6. IR (NaCl, thin film)  $\nu$  2922, 1480, 1460, 1286, 1224, 1183, 1101, 1020, 989, 729  $\text{cm}^{-1}$ . LRMS (ESI + APCI)  $m/z$  [M+H] calcd 148.1, found 148.4.



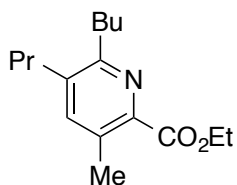
**5-(2-Methoxyphenyl)-2,3-dimethylpyridine (15br).** Yellow viscous liquid.  $R_f = 0.37$  (1:1 hexanes/EtOAc).  $^1\text{H NMR}$  (400 MHz,  $\text{CDCl}_3$ )  $\delta$  8.48 (d,  $J = 1.6$  Hz, 1H), 7.58 (d,  $J = 1.2$  Hz, 1H), 7.36–7.28 (m, 2H), 7.04 (t,  $J = 7.6$  Hz, 1H), 6.99 (d,  $J = 8.0$  Hz, 1H), 3.81 (s, 3H), 2.54 (s, 3H), 2.32 (s, 3H).  $^{13}\text{C NMR}$  (100 MHz,  $\text{CDCl}_3$ )  $\delta$  156.6, 155.3, 146.7, 138.0, 131.8, 130.5, 129.1, 127.2, 120.9, 111.2, 55.5, 22.2, 19.2. IR (NaCl, thin film)  $\nu$  2941, 1598, 1498, 1471, 1392, 1242, 1122, 1026, 754  $\text{cm}^{-1}$ . LRMS (ESI + APCI)  $m/z$  [M+H] calcd 214.1, found 214.6.



**2,3-Dimethyl-5-(thiophen-2-yl)pyridine (15bt).** Yellow orange viscous liquid.  $R_f = 0.51$  (1:1 hexanes/EtOAc).  $^1\text{H NMR}$  (400 MHz,  $\text{CDCl}_3$ )  $\delta$  8.59 (d,  $J = 2.0$  Hz, 1H), 7.62 (d,  $J = 1.2$  Hz, 1H), 7.31 (m, 2H), 7.10 (m, 1H), 2.52 (s, 3H), 2.33 (s, 3H).  $^{13}\text{C NMR}$  (100 MHz,  $\text{CDCl}_3$ )  $\delta$  155.8, 143.0, 140.5, 134.7, 131.7, 128.3, 128.1, 125.4, 123.7, 21.9, 19.1. IR (NaCl, thin film)  $\nu$  2920, 1474, 1402, 1231, 895, 843, 697  $\text{cm}^{-1}$ . LRMS (ESI + APCI)  $m/z$  [M+H] calcd 190.1, found 190.1.

#### A.2.4 Preparation of Picolinic Acid **20aa**

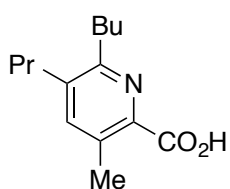
An oven-dried 20 mL vial was charged with  $[\text{RhCp}^*\text{Cl}_2]_2$  (27.8 mg, 0.025 equiv) and AgOAc (631 mg, 2.1 equiv) and a solution of oxime substrate **11a** (456 mg, 1.8 mmol) and ethyl acrylate **22** (0.27 mL, 1.2 equiv) in 0.7 mL 2:1 DCE/AcOH was added. The vial was flushed with argon, sealed and heated at 85 °C in a sand bath for 14 hours. The solids were filtered and the mixture was diluted with DCM and washed with 15%  $\text{Na}_2\text{CO}_3$ . The aqueous layer was extracted twice with DCM and the combined organic layers were dried over  $\text{MgSO}_4$ , filtered and concentrated *in vacuo*. The crude product was purified by flash column chromatography (5:1 hexanes/EtOAc) to afford **23** (168 mg, 35% yield).



**Ethyl 6-butyl-3-methyl-5-propylpicolinate (23).** Colorless liquid.  $R_f = 0.35$  (5:1 hexanes/EtOAc).  $^1\text{H NMR}$  (400 MHz,  $\text{CDCl}_3$ )  $\delta$  7.27 (s, 1H), 4.42 (q,  $J = 7.2$  Hz, 2H), 2.79 (m, 2H), 2.58 (m, 2H), 2.45 (s, 3H), 1.69–1.55 (m, 4H), 1.46–1.36 (m, 5H), 0.95 (m, 6H).  $^{13}\text{C NMR}$  (100 MHz,  $\text{CDCl}_3$ )  $\delta$  167.0, 157.9, 145.2, 140.0, 137.9, 131.3, 61.3, 34.3, 34.0, 31.8, 23.6, 22.8, 19.2, 14.3, 14.0. IR (NaCl, thin film)  $\nu$

2960, 2873, 1719, 1456, 1366, 1309, 1244, 1150, 1058  $\text{cm}^{-1}$ . LRMS (ESI + APCI)  $m/z$  [M+H] calcd 264.2, found 264.7.

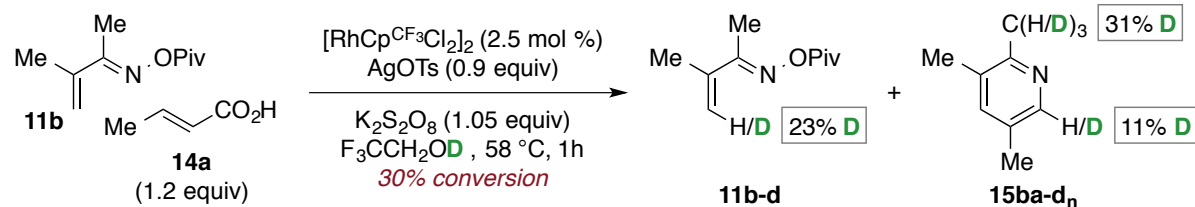
A solution of pyridine **23** (146 mg, 0.55 mmol) in 7.4 mL EtOH was added to LiOH (106 mg, 8 equiv) in 3.7 mL H<sub>2</sub>O and the mixture was stirred at room temperature overnight. The solution was acidified with 3M HCl and extracted with EtOAc. The organic layer was washed with H<sub>2</sub>O and brine, dried over MgSO<sub>4</sub>, filtered and concentrated *in vacuo* to provide **20aa** (107 mg, 83% yield).



**6-Butyl-3-methyl-5-propylpicolinic acid (20aa).** Colorless liquid.  $R_f = 0.24$  (1:1 hexanes/EtOAc).  $^1\text{H}$  NMR (400 MHz, CDCl<sub>3</sub>)  $\delta$  7.40 (s, 1H), 2.78 (m, 2H), 2.68 (s, 3H), 2.63 (m, 2H), 1.74–1.59 (m, 4H), 1.41 (m, 2H), 0.98 (m, 6H).  $^{13}\text{C}$  NMR (100 MHz, CDCl<sub>3</sub>)  $\delta$  164.7, 156.3, 142.0, 140.8, 139.8, 134.3, 33.8, 33.2, 30.9, 23.4, 22.6, 19.4, 14.0, 14.0. IR (NaCl, thin film)  $\nu$  3420, 2960, 2873, 1763, 1639, 1460, 1363  $\text{cm}^{-1}$ . LRMS (ESI + APCI)  $m/z$  [M+H] calcd 236.2, found 236.7.

#### A.2.5 Deuterium Incorporation Study

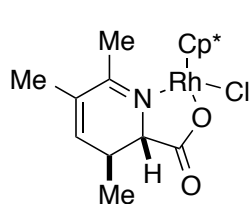
An isotope experiment was performed according to the procedure described above with **11b** and **14a** in 2,2,2-trifluoroethanol- $\text{d}_1$  (purchased from Sigma-Aldrich Co. and used as received) as the solvent for one hour. Deuterium incorporation was determined by integration of the  $^1\text{H}$  NMR spectrum collected with first relaxation delay ( $d_1$ ) = 25 seconds of the reaction mixture.



### A.2.6 Preparation and Reactions of Rhodium Complexes **29** and **30**

A 0.5 dram vial was charged with  $\text{RhCp}^*(\text{OAc})_2$ <sup>11</sup> (0.054 mmol, 100 mol %) and a solution of oxime ester **11b** (0.054 mmol) and crotonic acid **14a** (0.054 mmol, 1 equiv) in 0.18 mL HFIP was added. The vial was flushed with argon, sealed and heated at 58 °C in an aluminum heating block for 30 minutes. The mixture was transferred to a 1 dram vial, the solvents were removed and a solution of TMSCl (0.054 mmol, 1 equiv) in 1 mL Et<sub>2</sub>O was added. After 10 minutes stirring at room temperature, the heterogeneous mixture was filtered and the solid rinsed with Et<sub>2</sub>O. The solid was dissolved in DCM, the solution was filtered and the filtrate was concentrated to give **29** (16.2 mg, 68% yield) as an orange solid. A 0.5 dram vial was charged with a solution of complex **29** (7.5 mg, 0.017 mmol) in 0.06 mL HFIP, flushed with argon and heated for 24 hours in an aluminum heating block. The solvent was removed and the reaction mixture analyzed by <sup>1</sup>H NMR.

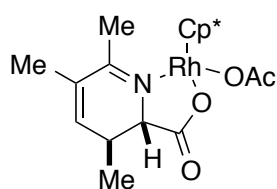
Slow evaporation of a concentrated solution of **29** in DCM afforded prismatic orange crystals suitable for X-ray diffraction analysis.



**Rhodium chloride complex 29.** <sup>1</sup>H NMR (400 MHz, CDCl<sub>3</sub>) δ 5.88 (bs, 1H), 3.59 (dq,  $J = 16.0$  Hz, 2.4 Hz, 1H), 2.71–2.61 (m, 1H), 2.52 (d,  $J = 2.4$  Hz, 3H), 1.89 (dd,  $J = 2.4$  Hz, 1.6 Hz, 3H), 1.66 (s, 15H), 1.34 (d,  $J = 6.8$

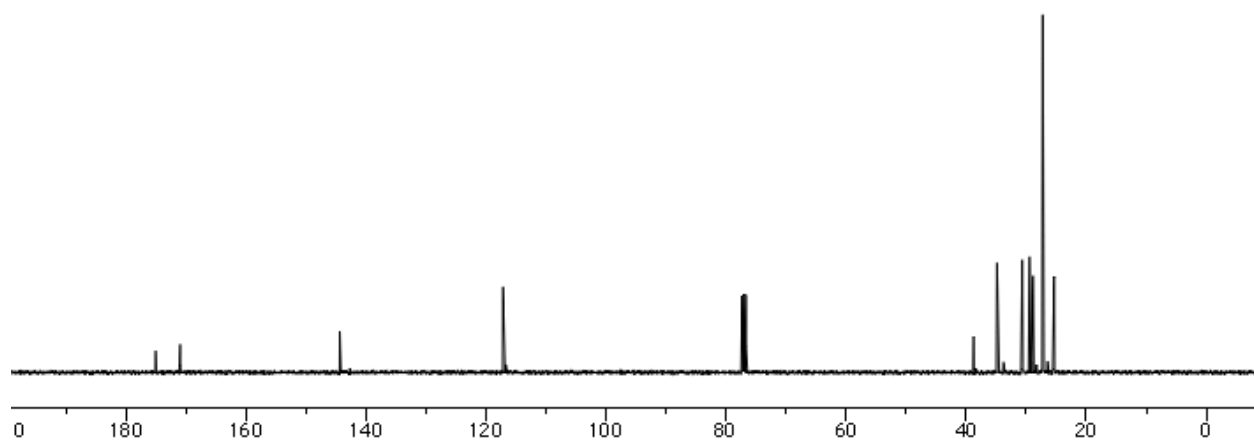
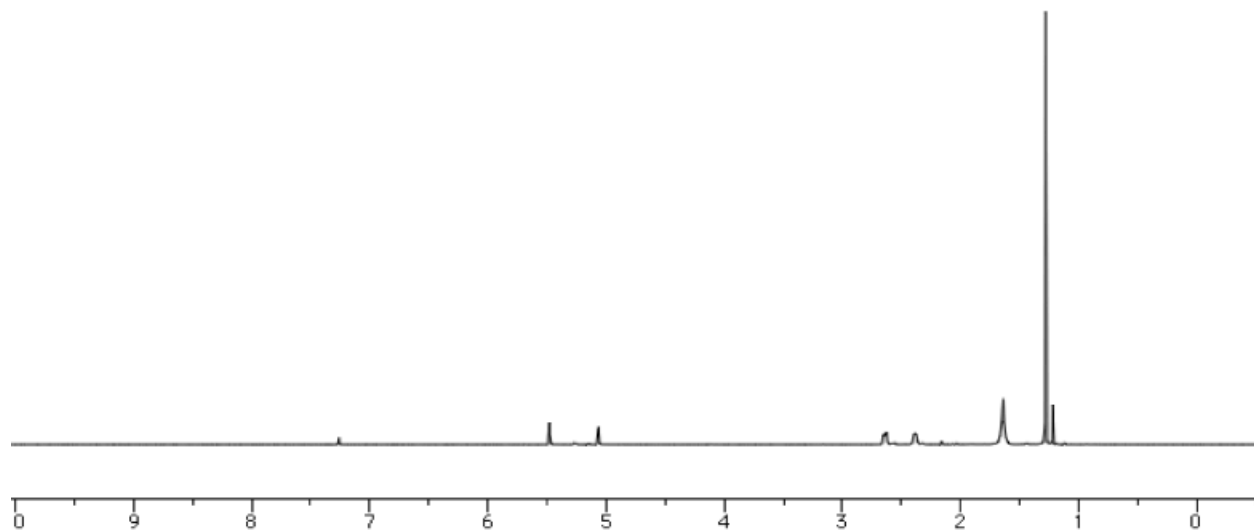
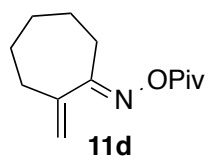
Hz, 3H).  $^{13}\text{C}$  NMR (100 MHz,  $\text{CDCl}_3$ )  $\delta$  176.8, 172.0, 141.7, 127.4, 93.5 (d,  $J = 8.6$  Hz), 70.3, 31.5, 26.9, 21.3, 19.3, 9.1. IR (thin film)  $\nu$  2922, 1639, 1587, 1448, 1323, 1089, 1025, 921, 809, 726  $\text{cm}^{-1}$ . LRMS (ESI + APCI)  $m/z$  [M–Cl] calcd 404.1, found 404.3.

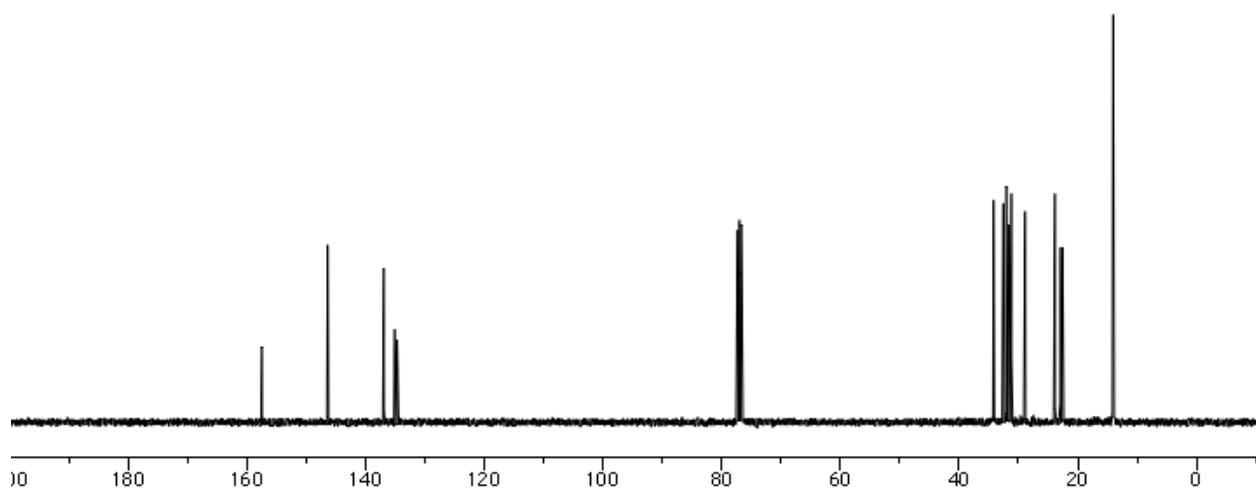
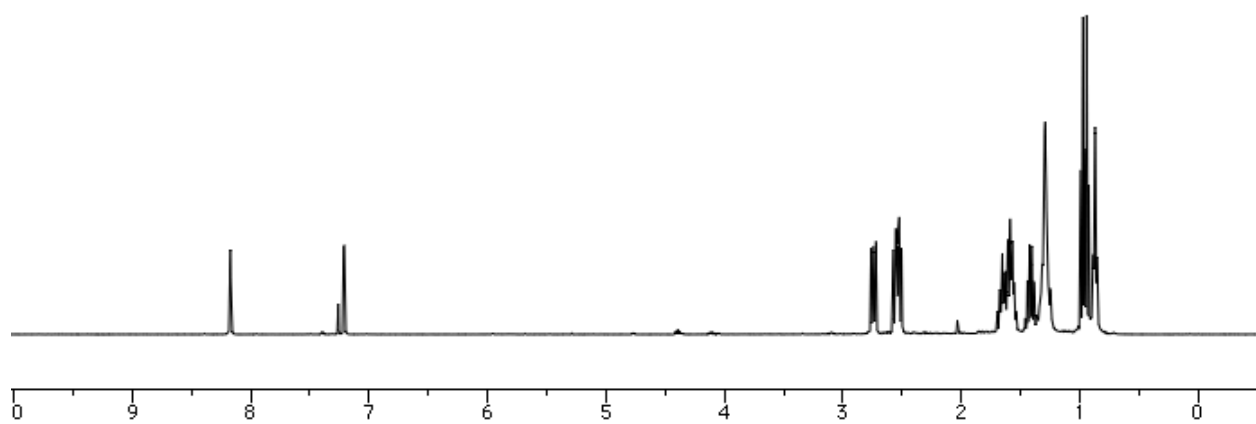
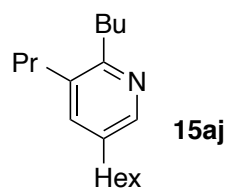
A 1 dram vial was charged with **29** (29.7 mg, 0.068 mmol) and AgOAc (0.068, 1 equiv) and 1.4 mL DCM was added. The vial was flushed with argon, sealed, wrapped in aluminum foil and stirred at room temperature overnight. The heterogeneous mixture was filtered and the filtrate concentrated to give **30** (25.0 mg, 80% yield) as an orange solid. A 0.5 dram vial was charged with a solution of complex **30** (12.7 mg, 0.027 mmol) in 0.09 mL HFIP, flushed with argon and heated for 24 hours in an aluminum heating block. The solvent was removed and the reaction mixture analyzed by  $^1\text{H}$  NMR. Alternately, a 0.5 dram vial was charged with AgOTs (0.029 mmol, 1 equiv) and a solution of **30** (13.4 mg, 0.029 mmol) in 0.1 mL HFIP was added. The vial was flushed with argon, sealed and heated at 58  $^\circ\text{C}$  in an aluminum heating block for 24 hours. The solvent was removed and the reaction mixture analyzed by  $^1\text{H}$  NMR.



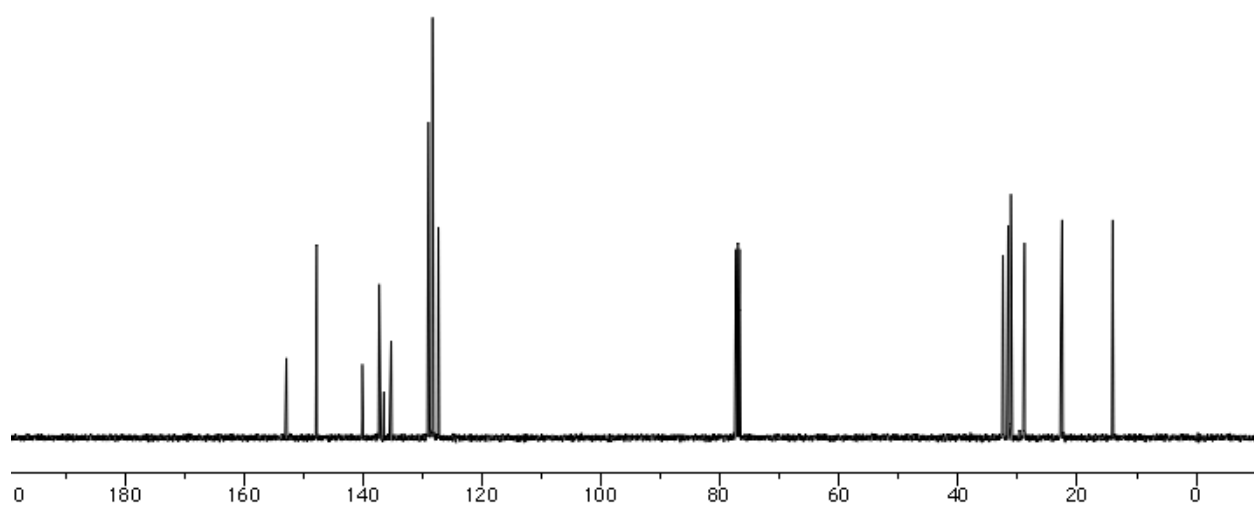
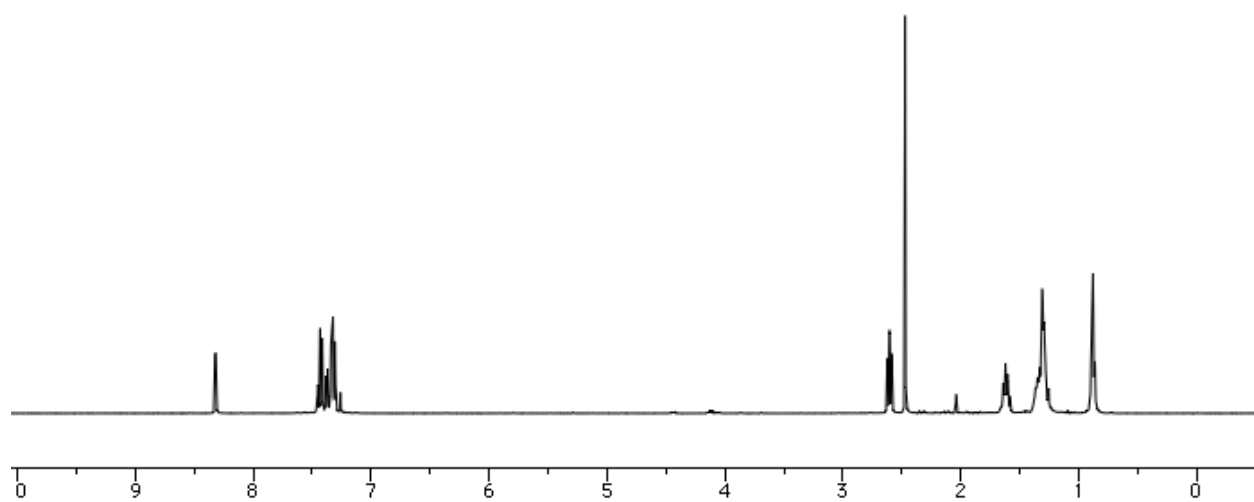
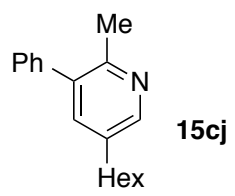
**Rhodium acetate complex 30.**  $^1\text{H}$  NMR (400 MHz,  $\text{CD}_2\text{Cl}_2$ )  $\delta$  5.84 (bs, 1H), 3.40 (dq,  $J = 15.6$  Hz, 2.4 Hz, 1H), 2.55–2.43 (m, 1H), 2.49 (d,  $J = 2.8$  Hz, 3H), 1.87 (dd,  $J = 2.4$  Hz, 1.6 Hz, 3H), 1.83 (s, 3H), 1.57 (s, 15H), 1.27 (d,  $J = 6.8$  Hz, 3H).  $^{13}\text{C}$  NMR (100 MHz,  $\text{CD}_2\text{Cl}_2$ )  $\delta$  176.8, 176.6, 171.4, 141.2, 127.8, 92.8 (d,  $J = 8.8$  Hz), 70.1, 31.6, 26.5, 24.3, 21.1, 19.1, 9.0. IR (thin film)  $\nu$  2922, 1640, 1613, 1448, 1359, 1315, 1160, 1090, 1026, 809, 727, 666  $\text{cm}^{-1}$ . LRMS (ESI + APCI)  $m/z$  [M–OAc] calcd 404.1, found 404.1.

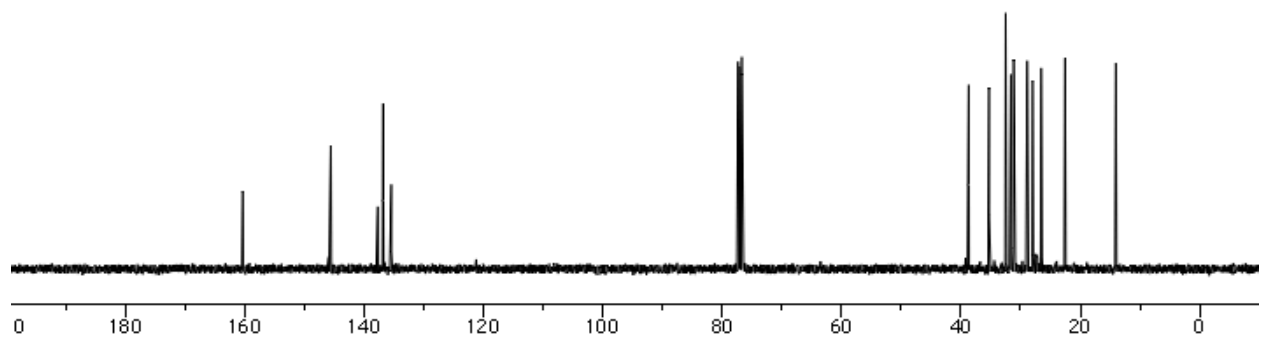
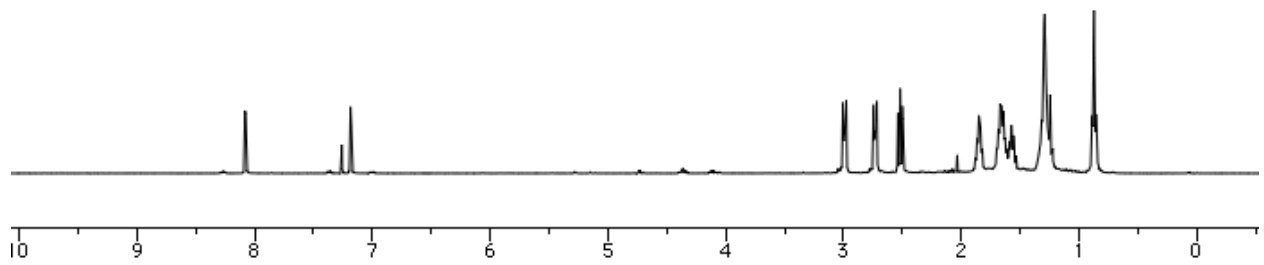
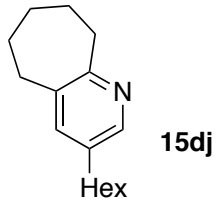
A.2.7  $^1\text{H}$  and  $^{13}\text{C}$  NMR Spectra of New Compounds

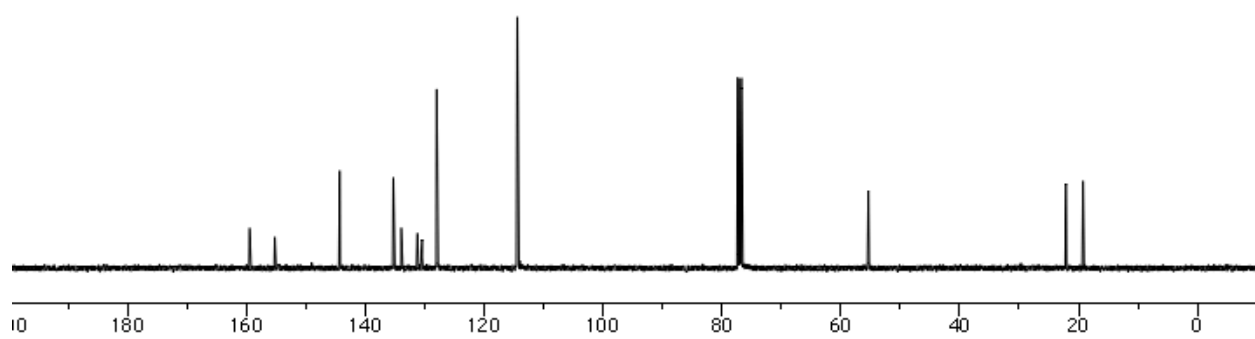
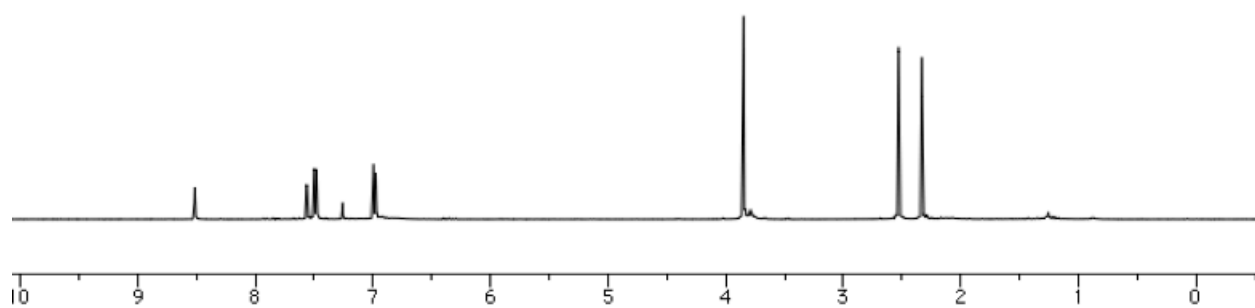
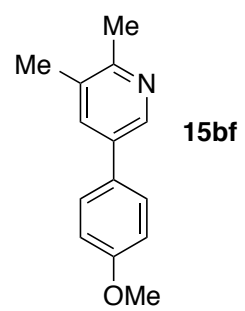


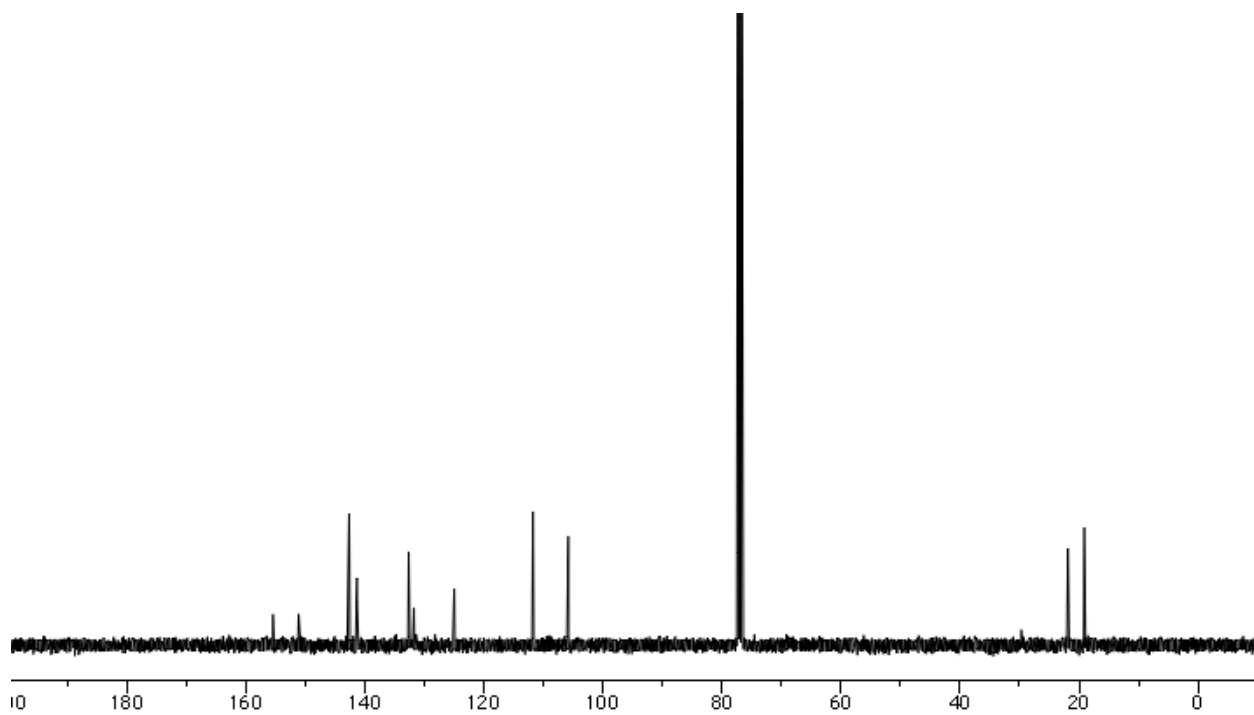
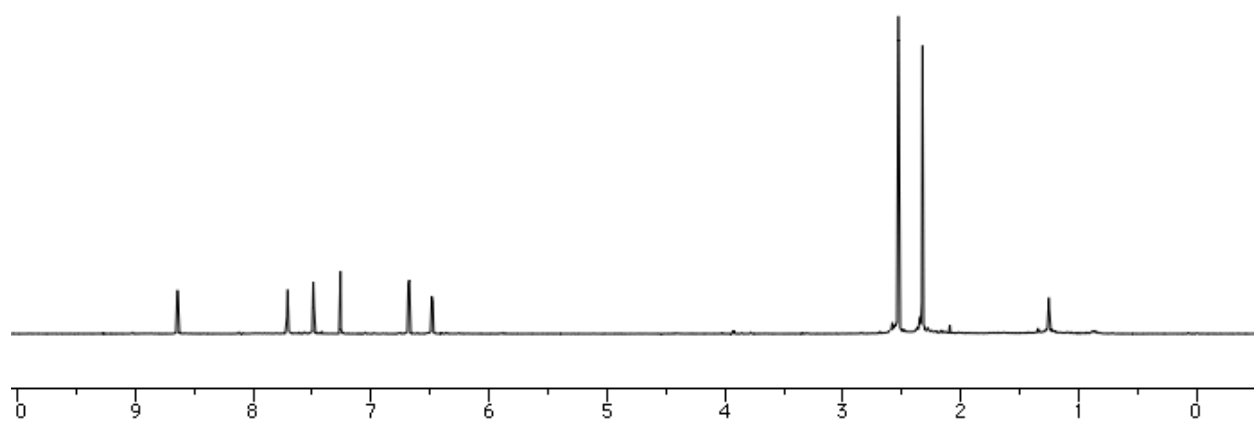
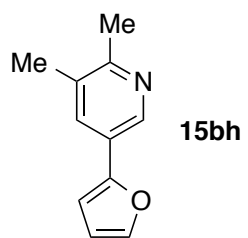


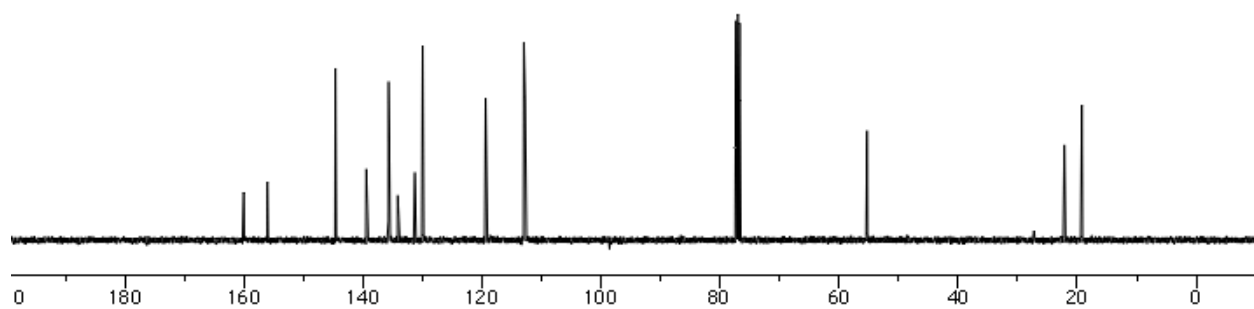
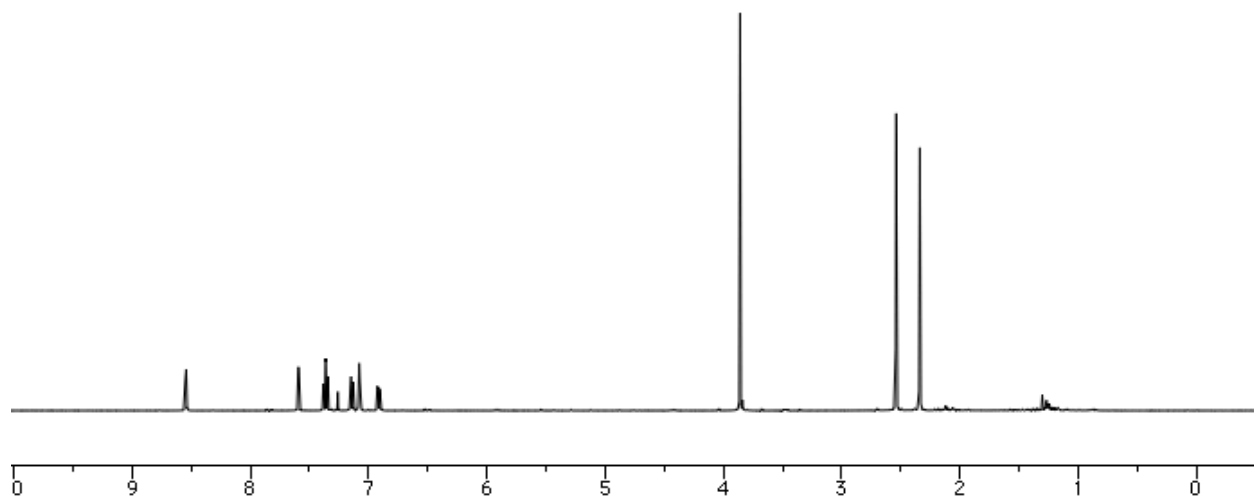
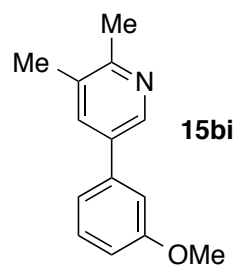


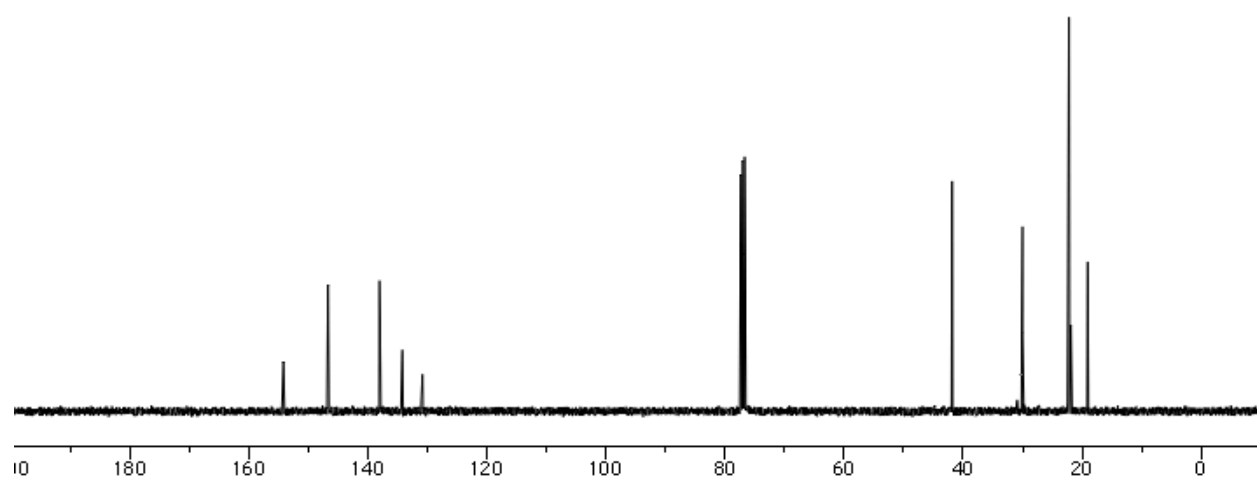
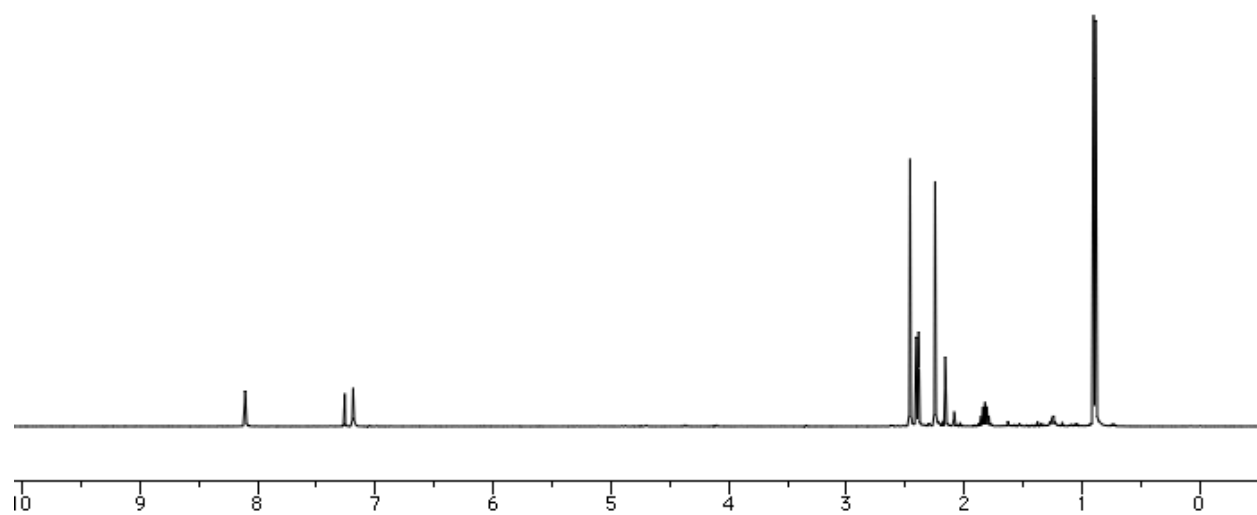
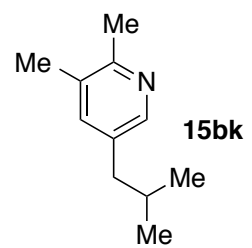


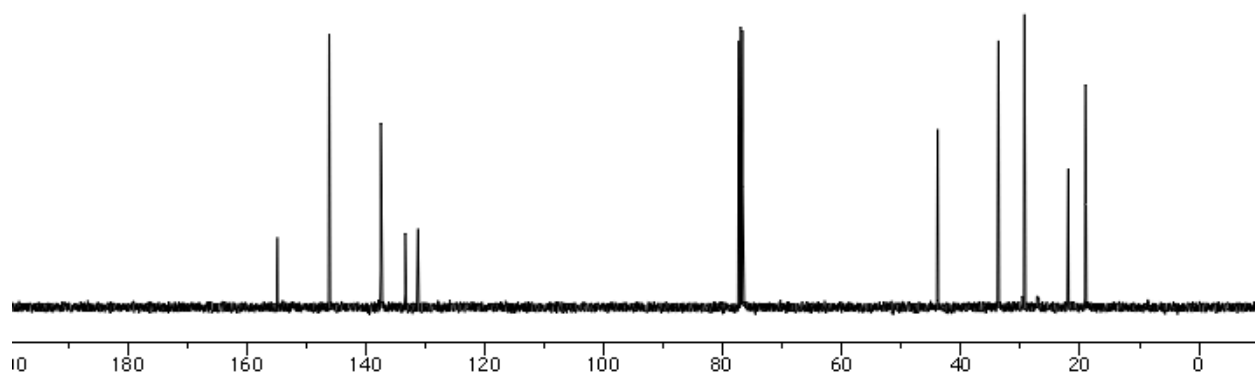
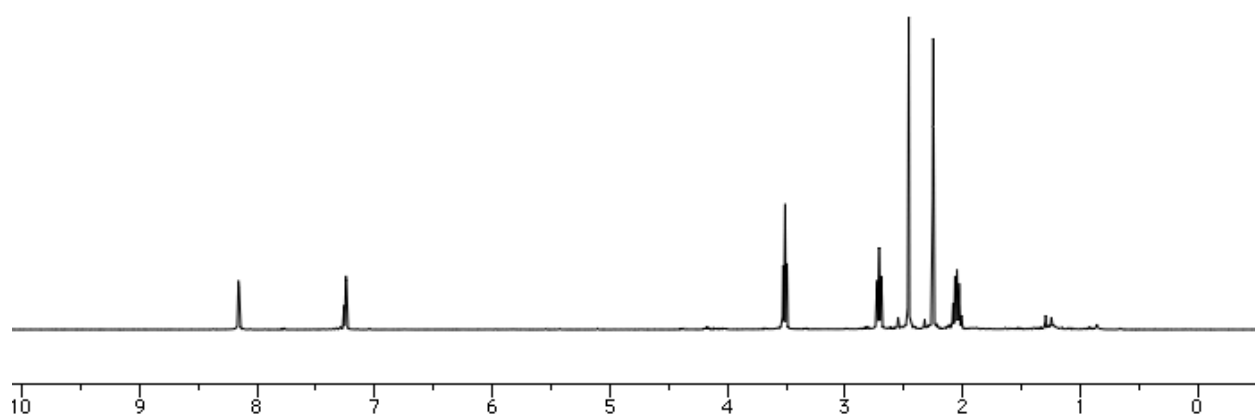
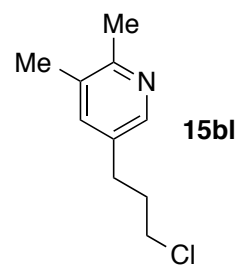


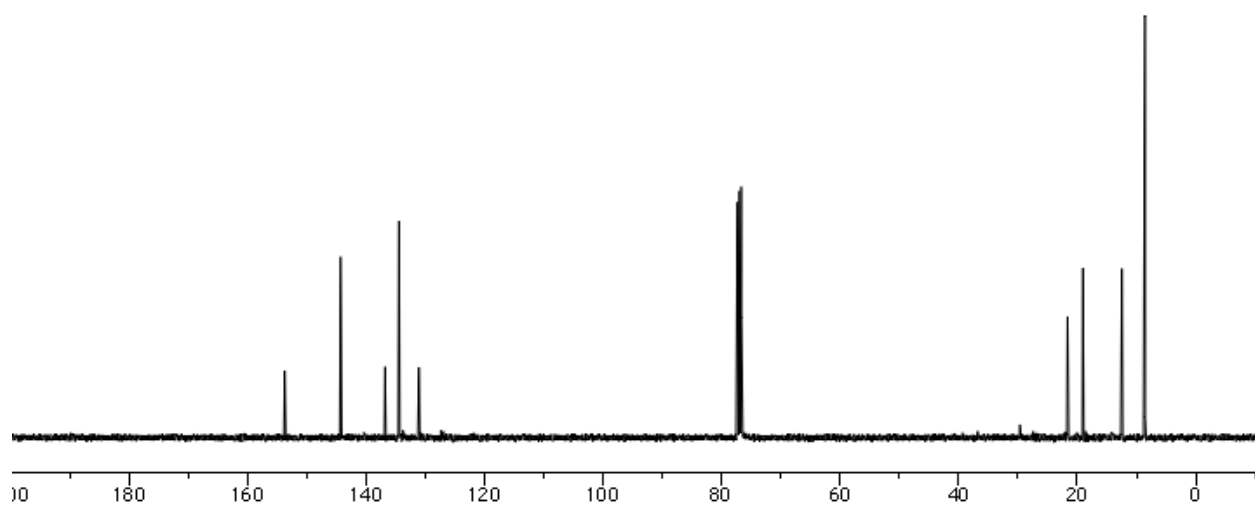
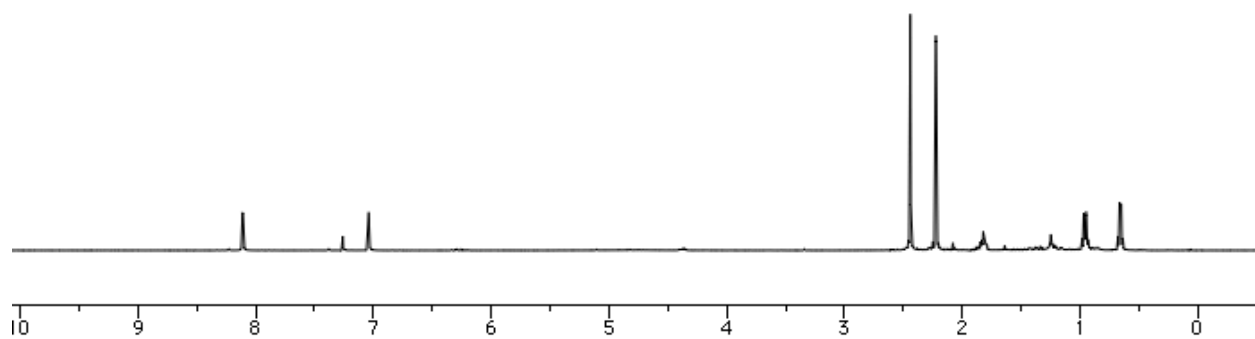
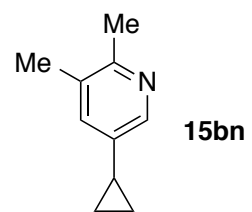




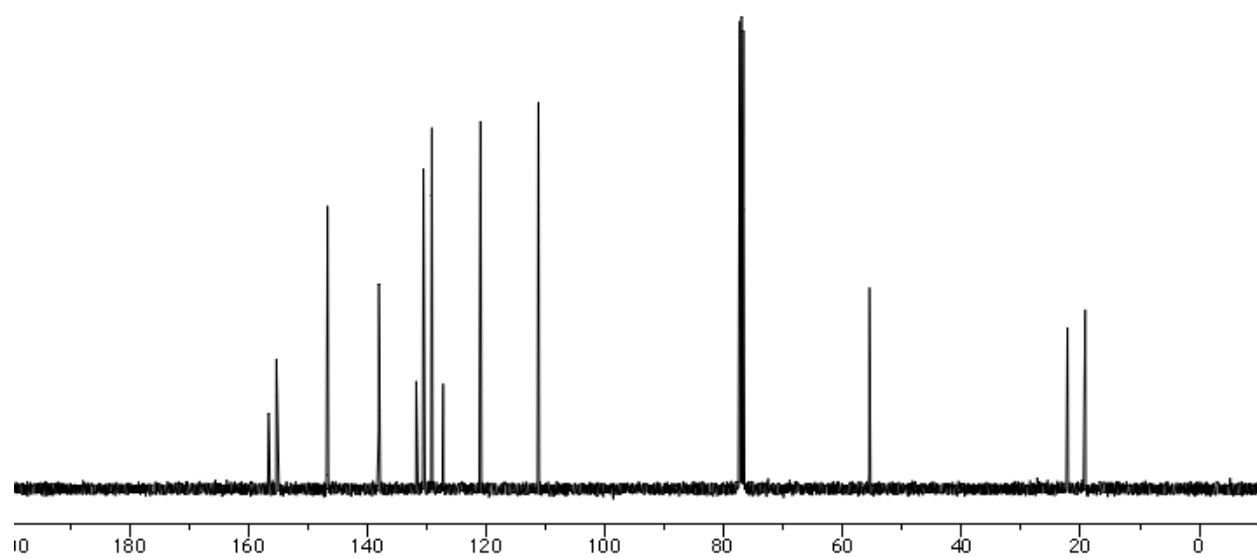
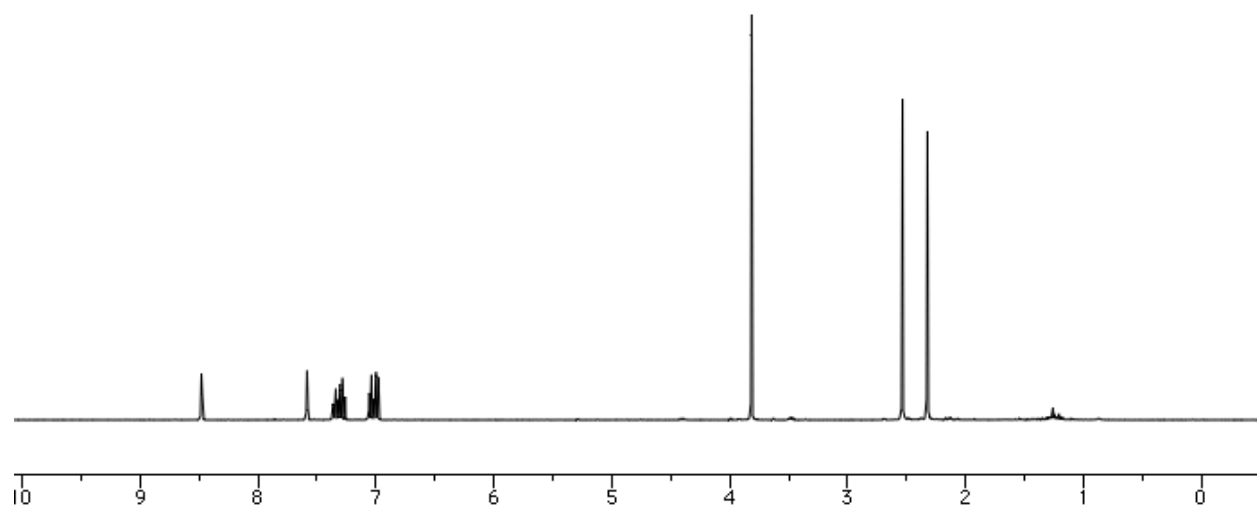
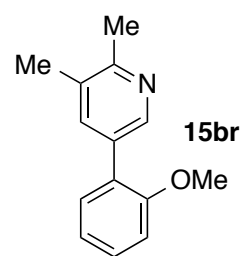


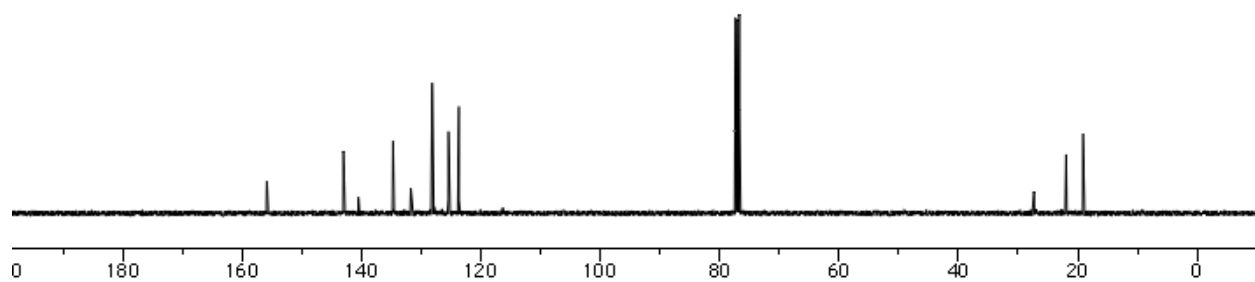
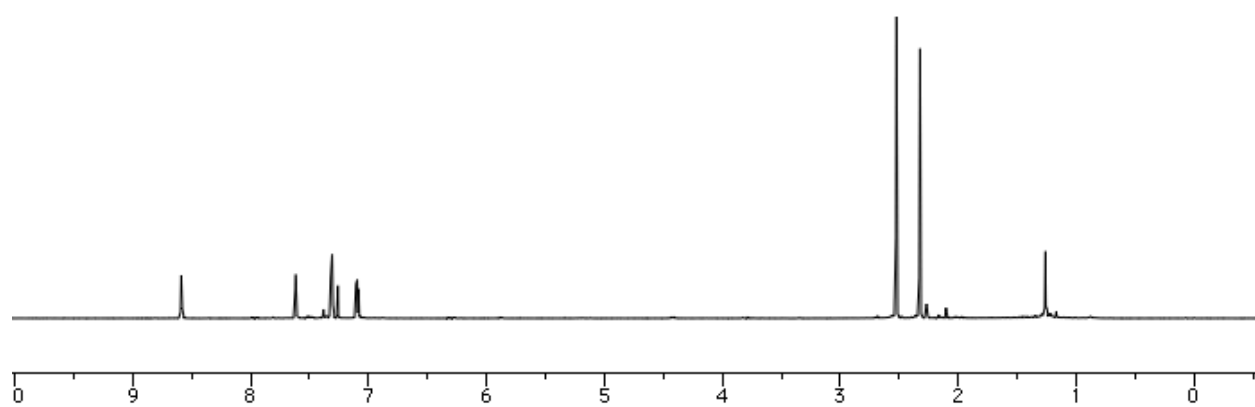
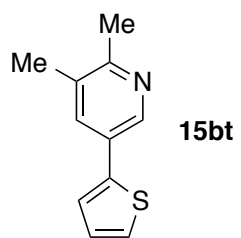


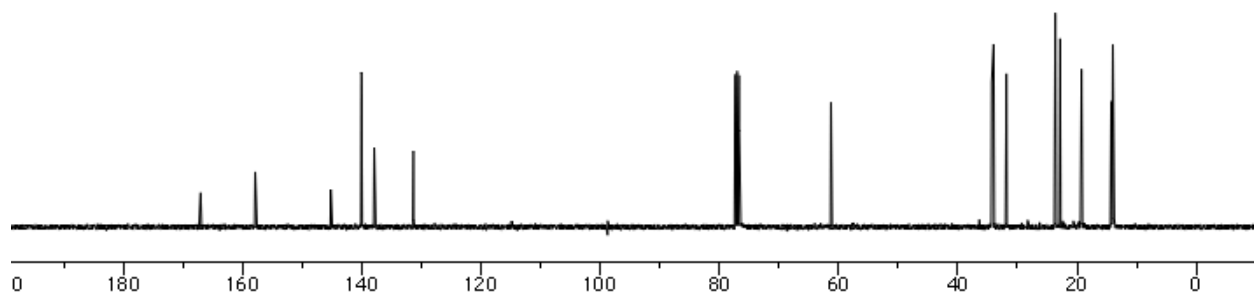
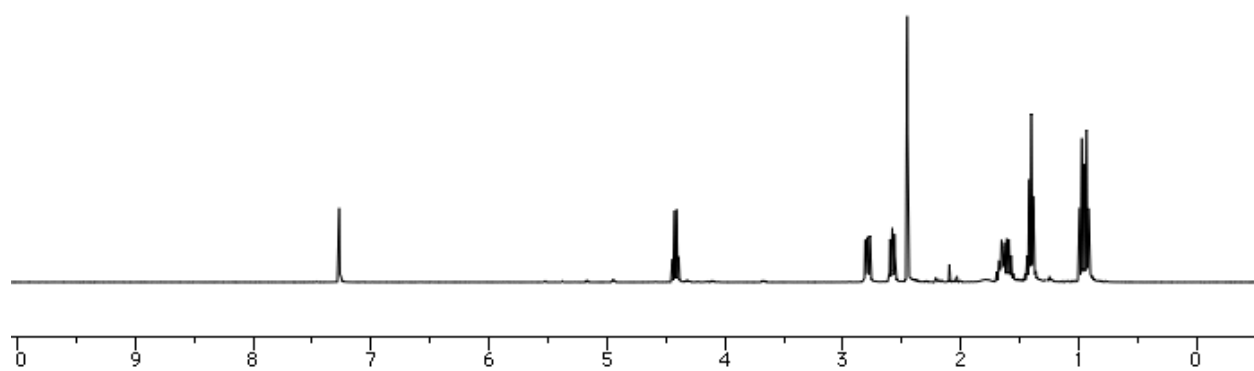
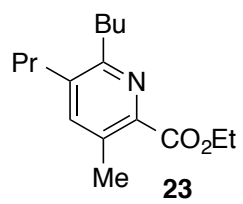


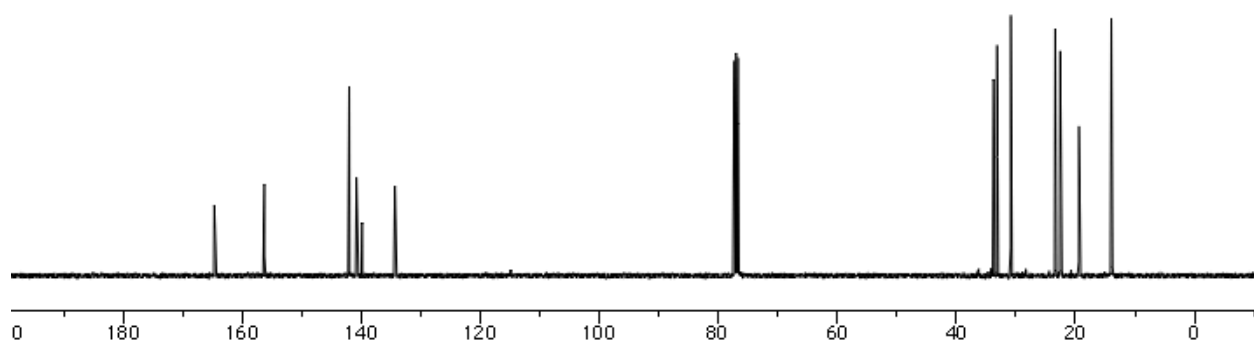
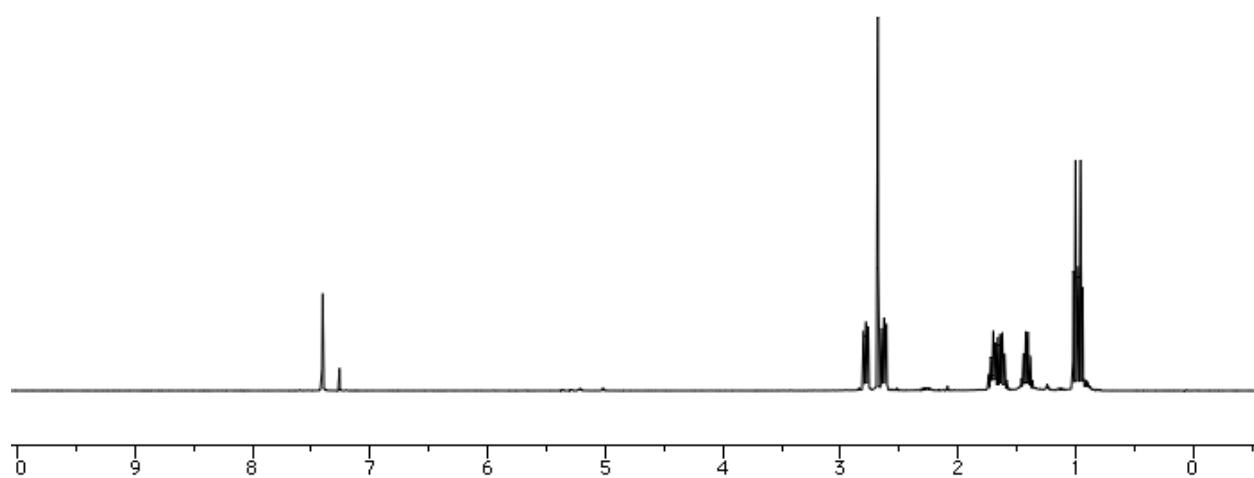
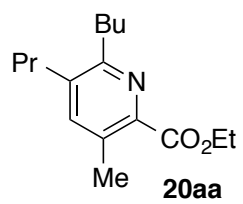


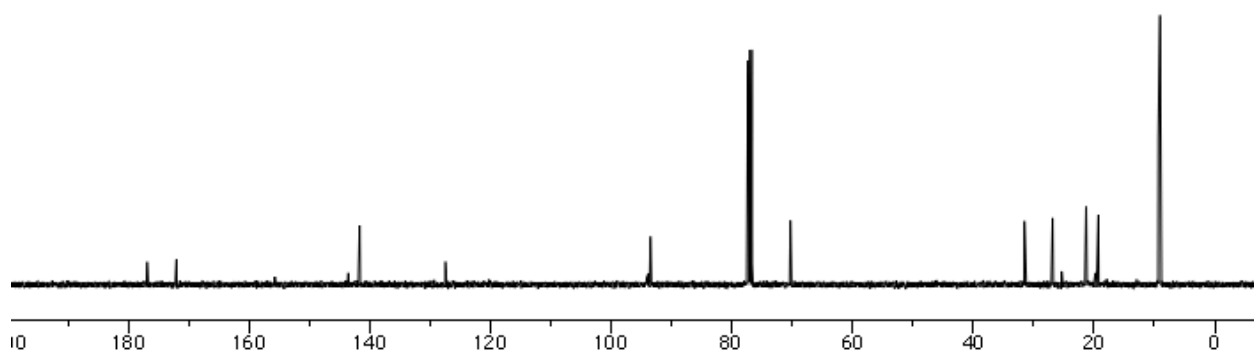
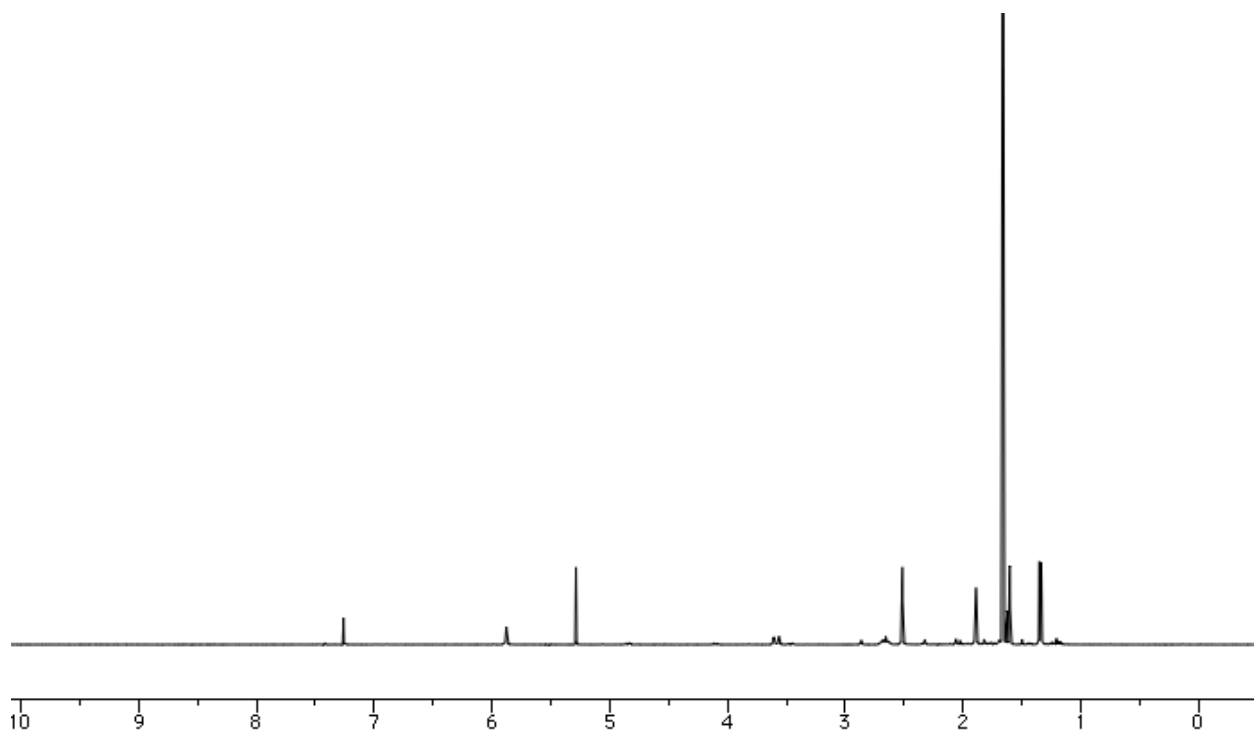
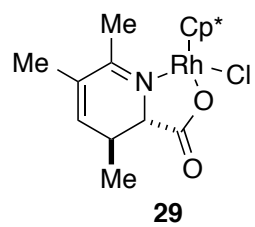


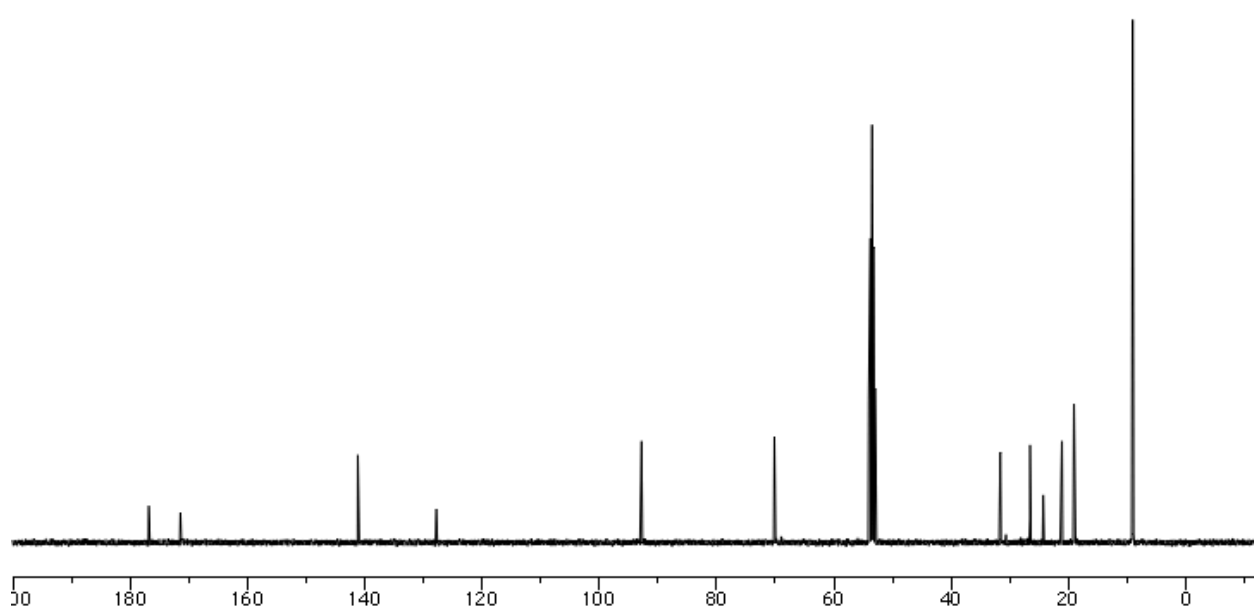
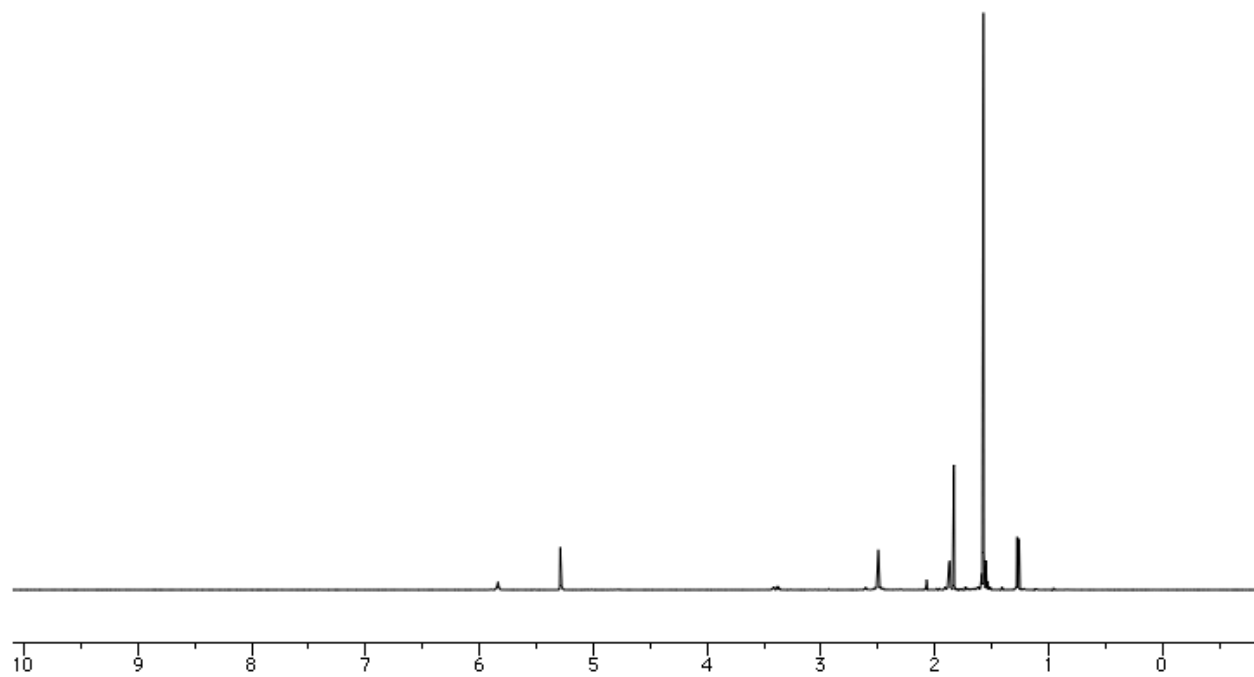
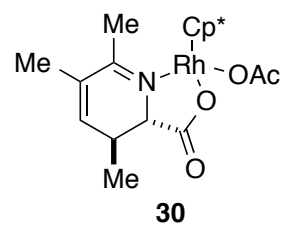












### A.2.8 Crystallographic Data for Rhodium Complex **29**

Prismatic orange crystals were obtained after slow evaporation of a concentrated solution of **29** in DCM in loosely sealed vial. A single crystal was coated in Paratone–N oil and mounted under a stream of nitrogen. X–ray diffraction data was collected on a Bruker Kappa Apex II CCD diffractometer with Mo K $\alpha$  radiation ( $\lambda = 0.71073 \text{ \AA}$ ) and a graphite monochromator. Data integration and Lorentz and polarization corrections were accomplished with Bruker APEX2 software and semiempirical absorption corrections were applied using SCALE with the aid of numerical face indexing.<sup>12</sup> The crystal structure was solved with SHELXTL software.<sup>13</sup> The thermal parameters of all non–hydrogen atoms were refined anisotropically and hydrogen atoms were added in idealized positions.

**Table 1.** Crystal data and structure refinement for **29**.

Identification code	rovis178	
Empirical formula	C <sub>19</sub> H <sub>27</sub> NO <sub>2</sub> RhCl	
Formula weight	439.78	
Temperature	120(2) K	
Wavelength	0.71073 $\text{\AA}$	
Crystal system	Monoclinic	
Space group	<i>P2<sub>1</sub>/n</i>	
Unit cell dimensions	$a = 10.0060(6) \text{ \AA}$	$\alpha = 90^\circ$ .
	$b = 12.4200(6) \text{ \AA}$	$\beta = 106.763(3)^\circ$ .
	$c = 15.5420(12) \text{ \AA}$	$\gamma = 90^\circ$ .
Volume	1849.4(2) $\text{\AA}^3$	
Z	4	
Density (calculated)	1.579 Mg/m <sup>3</sup>	
Absorption coefficient	1.079 mm <sup>-1</sup>	
F(000)	904	
Crystal size	0.35 x 0.13 x 0.11 mm <sup>3</sup>	
Theta range for data collection	2.14 to 26.41 $^\circ$ .	
Index ranges	$-12 \leq h \leq 12, -15 \leq k \leq 15, -19 \leq l \leq 19$	

Reflections collected	60907
Independent reflections	3791 [R(int) = 0.0479]
Completeness to theta = 26.41°	99.9 %
Absorption correction	Semi-empirical from equivalents
Max. and min. transmission	0.8887 and 0.7039
Refinement method	Full-matrix least-squares on F <sup>2</sup>
Data / restraints / parameters	3791 / 0 / 225
Goodness-of-fit on F <sup>2</sup>	1.056
Final R indices [I>2sigma(I)]	R1 = 0.0201, wR2 = 0.0439
R indices (all data)	R1 = 0.0282, wR2 = 0.0477
Largest diff. peak and hole	0.441 and -0.325 e.Å <sup>-3</sup>



**Table 2.** Atomic coordinates ( $\times 10^4$ ) and equivalent isotropic displacement parameters ( $\text{\AA}^2 \times 10^3$ ) for **29**.  $U(\text{eq})$  is defined as one third of the trace of the orthogonalized  $U^{ij}$  tensor.

	x	y	z	$U(\text{eq})$
Rh(1)	5817(1)	2969(1)	2469(1)	12(1)
C(1)	8845(2)	3809(2)	3093(1)	15(1)
C(2)	10154(2)	4189(2)	2928(1)	18(1)
C(3)	10348(2)	4010(2)	2130(2)	20(1)
C(4)	9311(2)	3467(2)	1366(1)	19(1)
C(5)	7866(2)	3434(2)	1514(1)	16(1)
C(6)	8750(2)	3865(2)	4034(1)	22(1)
C(7)	11201(2)	4768(2)	3674(2)	25(1)
C(8)	9231(2)	4020(2)	478(2)	27(1)
C(9)	6980(2)	2484(2)	1021(1)	19(1)
N(1)	7809(2)	3456(1)	2452(1)	14(1)
O(1)	7174(2)	2132(1)	329(1)	30(1)
O(2)	6066(1)	2111(1)	1378(1)	19(1)
C(10)	3796(2)	2905(2)	2710(1)	16(1)
C(11)	3635(2)	3255(2)	1814(1)	17(1)
C(12)	4431(2)	4230(2)	1847(1)	17(1)
C(13)	5038(2)	4501(2)	2778(1)	18(1)
C(14)	4677(2)	3680(2)	3312(1)	16(1)
C(15)	3146(2)	1944(2)	3008(2)	23(1)
C(16)	2850(2)	2698(2)	969(1)	24(1)
C(17)	4479(2)	4901(2)	1056(2)	28(1)
C(18)	5867(2)	5496(2)	3098(2)	27(1)
C(19)	5035(2)	3620(2)	4316(1)	23(1)
Cl(1)	6832(1)	1481(1)	3429(1)	21(1)

**Table 3.** Bond lengths [Å] and angles [°] for **29**.

---

Rh(1)–O(2)	2.0779(14)
Rh(1)–N(1)	2.0904(16)
Rh(1)–C(12)	2.1299(19)
Rh(1)–C(11)	2.1556(19)
Rh(1)–C(14)	2.1592(19)
Rh(1)–C(13)	2.162(2)
Rh(1)–C(10)	2.1618(19)
Rh(1)–Cl(1)	2.4089(5)
C(1)–N(1)	1.290(3)
C(1)–C(2)	1.483(3)
C(1)–C(6)	1.495(3)
C(2)–C(3)	1.328(3)
C(2)–C(7)	1.501(3)
C(3)–C(4)	1.493(3)
C(4)–C(8)	1.523(3)
C(4)–C(5)	1.529(3)
C(5)–N(1)	1.475(2)
C(5)–C(9)	1.540(3)
C(9)–O(1)	1.228(2)
C(9)–O(2)	1.285(2)
C(10)–C(11)	1.424(3)
C(10)–C(14)	1.450(3)
C(10)–C(15)	1.495(3)
C(11)–C(12)	1.442(3)
C(11)–C(16)	1.491(3)
C(12)–C(13)	1.439(3)
C(12)–C(17)	1.498(3)
C(13)–C(14)	1.426(3)
C(13)–C(18)	1.493(3)
C(14)–C(19)	1.499(3)
O(2)–Rh(1)–N(1)	78.40(6)
O(2)–Rh(1)–C(12)	102.84(7)
N(1)–Rh(1)–C(12)	106.29(7)
O(2)–Rh(1)–C(11)	92.42(7)

N(1)–Rh(1)–C(11)	141.83(7)
C(12)–Rh(1)–C(11)	39.32(8)
O(2)–Rh(1)–C(14)	156.05(7)
N(1)–Rh(1)–C(14)	124.22(7)
C(12)–Rh(1)–C(14)	65.56(8)
C(11)–Rh(1)–C(14)	65.11(7)
O(2)–Rh(1)–C(13)	140.23(7)
N(1)–Rh(1)–C(13)	98.92(7)
C(12)–Rh(1)–C(13)	39.17(8)
C(11)–Rh(1)–C(13)	65.11(8)
C(14)–Rh(1)–C(13)	38.53(8)
O(2)–Rh(1)–C(10)	117.45(7)
N(1)–Rh(1)–C(10)	162.92(7)
C(12)–Rh(1)–C(10)	65.58(8)
C(11)–Rh(1)–C(10)	38.51(7)
C(14)–Rh(1)–C(10)	39.21(7)
C(13)–Rh(1)–C(10)	65.06(8)
O(2)–Rh(1)–Cl(1)	89.06(4)
N(1)–Rh(1)–Cl(1)	89.77(5)
C(12)–Rh(1)–Cl(1)	161.53(5)
C(11)–Rh(1)–Cl(1)	127.42(6)
C(14)–Rh(1)–Cl(1)	98.04(6)
C(13)–Rh(1)–Cl(1)	130.71(6)
C(10)–Rh(1)–Cl(1)	96.47(6)
N(1)–C(1)–C(2)	121.91(18)
N(1)–C(1)–C(6)	120.53(17)
C(2)–C(1)–C(6)	117.55(17)
C(3)–C(2)–C(1)	118.79(19)
C(3)–C(2)–C(7)	122.93(19)
C(1)–C(2)–C(7)	118.27(18)
C(2)–C(3)–C(4)	124.29(18)
C(3)–C(4)–C(8)	111.16(18)
C(3)–C(4)–C(5)	111.31(17)
C(8)–C(4)–C(5)	110.06(17)
N(1)–C(5)–C(4)	117.08(16)
N(1)–C(5)–C(9)	108.98(16)

C(4)–C(5)–C(9)	112.34(16)
O(1)–C(9)–O(2)	124.2(2)
O(1)–C(9)–C(5)	119.67(19)
O(2)–C(9)–C(5)	116.14(17)
C(1)–N(1)–C(5)	121.20(16)
C(1)–N(1)–Rh(1)	130.20(13)
C(5)–N(1)–Rh(1)	108.39(12)
C(9)–O(2)–Rh(1)	115.78(13)
C(11)–C(10)–C(14)	107.79(18)
C(11)–C(10)–C(15)	127.55(19)
C(14)–C(10)–C(15)	124.61(18)
C(11)–C(10)–Rh(1)	70.51(11)
C(14)–C(10)–Rh(1)	70.30(11)
C(15)–C(10)–Rh(1)	126.52(14)
C(10)–C(11)–C(12)	108.40(17)
C(10)–C(11)–C(16)	127.02(19)
C(12)–C(11)–C(16)	124.51(19)
C(10)–C(11)–Rh(1)	70.98(11)
C(12)–C(11)–Rh(1)	69.38(11)
C(16)–C(11)–Rh(1)	122.98(14)
C(13)–C(12)–C(11)	107.51(17)
C(13)–C(12)–C(17)	126.2(2)
C(11)–C(12)–C(17)	125.94(19)
C(13)–C(12)–Rh(1)	71.61(11)
C(11)–C(12)–Rh(1)	71.30(11)
C(17)–C(12)–Rh(1)	127.64(14)
C(14)–C(13)–C(12)	108.32(18)
C(14)–C(13)–C(18)	127.46(19)
C(12)–C(13)–C(18)	124.21(19)
C(14)–C(13)–Rh(1)	70.63(11)
C(12)–C(13)–Rh(1)	69.22(11)
C(18)–C(13)–Rh(1)	126.99(14)
C(13)–C(14)–C(10)	107.91(17)
C(13)–C(14)–C(19)	128.08(19)
C(10)–C(14)–C(19)	123.90(19)
C(13)–C(14)–Rh(1)	70.83(11)

C(10)–C(14)–Rh(1)	70.49(11)
C(19)–C(14)–Rh(1)	127.04(14)

---

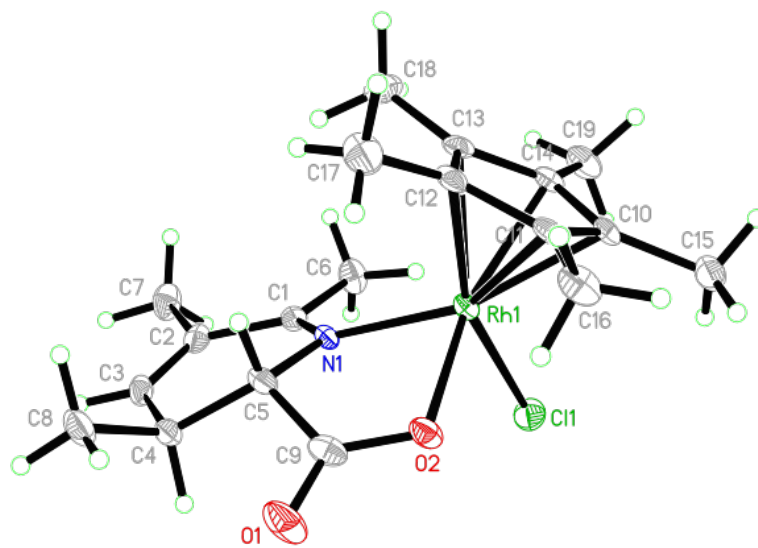
Symmetry transformations used to generate equivalent atoms:

**Table 4.** Anisotropic displacement parameters ( $\text{\AA}^2 \times 10^3$ ) for **29**. The anisotropic displacement factor exponent takes the form:  $-2\pi^2 [ h^2 a^{*2} U^{11} + \dots + 2 h k a^* b^* U^{12} ]$ .

	U <sup>11</sup>	U <sup>22</sup>	U <sup>33</sup>	U <sup>23</sup>	U <sup>13</sup>	U <sup>12</sup>
Rh(1)	10(1)	15(1)	11(1)	0(1)	3(1)	1(1)
C(1)	14(1)	15(1)	17(1)	3(1)	4(1)	2(1)
C(2)	13(1)	16(1)	24(1)	7(1)	4(1)	2(1)
C(3)	14(1)	18(1)	28(1)	7(1)	10(1)	2(1)
C(4)	20(1)	18(1)	23(1)	3(1)	12(1)	3(1)
C(5)	16(1)	19(1)	16(1)	1(1)	7(1)	4(1)
C(6)	18(1)	31(1)	17(1)	-2(1)	5(1)	-5(1)
C(7)	16(1)	29(1)	29(1)	4(1)	3(1)	-5(1)
C(8)	31(1)	31(1)	26(1)	6(1)	20(1)	7(1)
C(9)	16(1)	24(1)	16(1)	-1(1)	3(1)	7(1)
N(1)	13(1)	15(1)	13(1)	1(1)	6(1)	2(1)
O(1)	30(1)	44(1)	20(1)	-13(1)	12(1)	-3(1)
O(2)	16(1)	23(1)	18(1)	-7(1)	6(1)	0(1)
C(10)	10(1)	21(1)	18(1)	-1(1)	6(1)	3(1)
C(11)	10(1)	23(1)	16(1)	-1(1)	3(1)	6(1)
C(12)	13(1)	20(1)	18(1)	3(1)	6(1)	6(1)
C(13)	14(1)	17(1)	22(1)	-2(1)	6(1)	5(1)
C(14)	14(1)	20(1)	17(1)	-3(1)	6(1)	3(1)
C(15)	20(1)	26(1)	26(1)	-1(1)	10(1)	-2(1)
C(16)	18(1)	35(1)	17(1)	-3(1)	1(1)	4(1)
C(17)	26(1)	33(1)	27(1)	13(1)	10(1)	9(1)
C(18)	27(1)	16(1)	38(1)	-4(1)	9(1)	1(1)
C(19)	22(1)	34(1)	14(1)	-3(1)	6(1)	4(1)
Cl(1)	20(1)	19(1)	24(1)	6(1)	6(1)	3(1)

**Table 5.** Hydrogen coordinates ( $\times 10^4$ ) and isotropic displacement parameters ( $\text{\AA}^2 \times 10^{-3}$ ) for **29**.

	x	y	z	U(eq)
H(3)	11202	4242	2040	24
H(4)	9628	2709	1332	23
H(5)	7376	4100	1226	19
H(6A)	8771	4620	4222	33
H(6B)	9541	3480	4436	33
H(6C)	7875	3532	4062	33
H(7A)	12021	4952	3479	38
H(7B)	11484	4301	4204	38
H(7C)	10781	5428	3825	38
H(8A)	8949	4772	503	40
H(8B)	8543	3649	-11	40
H(8C)	10147	3993	369	40
H(15A)	2657	1515	2482	35
H(15B)	2481	2181	3324	35
H(15C)	3875	1504	3412	35
H(16A)	3503	2297	726	36
H(16B)	2354	3232	528	36
H(16C)	2175	2197	1098	36
H(17A)	3694	5407	910	42
H(17B)	4418	4433	539	42
H(17C)	5359	5304	1202	42
H(18A)	5245	6123	2979	41
H(18B)	6577	5580	2781	41
H(18C)	6324	5440	3746	41
H(19A)	5751	4158	4583	35
H(19B)	5391	2900	4518	35
H(19C)	4198	3763	4505	35



### A.2.9 References

1. Šmejkal, T. S.; Breit, B. *Angew. Chem. Int. Ed.* **2008**, *47*, 3946.
2. Szymanski, W.; Wu, B.; Weiner, B.; de Wildeman, S.; Feringa, B. L.; Janssen, D. B. *J. Org. Chem.* **2009**, *74*, 9152.
3. a) Tilley, D. S.; Reber, K. P.; Sorensen, E. J. *Org. Lett.* **2009**, *11*, 701. b) Marshall, J. A.; Garofalo, A. W. *J. Org. Chem.* **1996**, *61*, 8732.
4. Fujita, K.-I.; Takahashi, Y.; Owaki, M.; Yamamoto, K.; Yamaguchi, R. *Org. Lett.* **2004**, *6*, 2785.
5. RhCp\*(OAc)<sub>2</sub> was prepared as previously reported with the following modifications: CH<sub>2</sub>Cl<sub>2</sub> was used as the solvent at a concentration of 0.05 M for 48 hours. See: Boyer, P. M.; Roy, C. P.; Bielski, J. M.; Merola, J. S. *Inorg. Chim. Acta* **1996**, *245*, 7.
6. Gassman, P. G.; Mickelson, J. W.; Sowa, J. R. *J. Am. Chem. Soc.* **1992**, *114*, 6942.
7. Tan, Y.; Hartwig, J. F. *J. Am. Chem. Soc.* **2010**, *132*, 3676.
8. Neely, J. M.; Rovis, T. *J. Am. Chem. Soc.* **2013**, *135*, 66.
9. Martin, R. M.; Bergman, R. G.; Ellman, J. A. *J. Org. Chem.* **2012**, *77*, 2501.
10. Craig, D.; Paina, F.; Smith, S. C. *Chem. Commun.* **2008**, 3408.
11. The analogous reaction with [RhCp\*Cl<sub>2</sub>]<sub>2</sub> was also performed and only starting material was observed.
12. Sheldrick, G. *SADABS*; Bruker AXS: Madison, WI, 1997.
13. Sheldrick, G. *SHELXTL 6.14*; Bruker AXS: Madison, WI, 2004.